NASA CR-120813

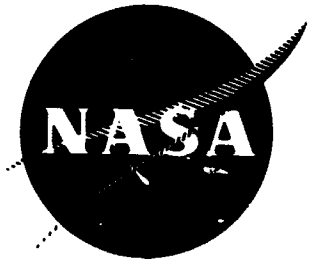

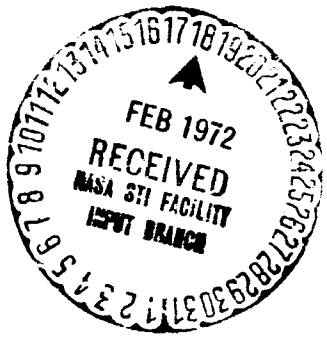

GENERATION OF FINITE LIFE DISTRIBUTIONAL GOODMAN DIAGRAMS FOR RELIABILITY PREDICTION

by Dimitri Kececioglu and William Neil Guerrieri

THE UNIVERSITY OF ARIZONA
College of Engineering
Engineering Experiment Station

prepared for

NATIONAL AERONAUTICS AND SPACE ADMINISTRATION

NASA Lewis Research Center
Contract NGR 03-002-044

(NASA-CR-120813) GENERATION OF FINITE LIFE DISTRIBUTIONAL GOODMAN DIAGRAMS FOR RELIABILITY PREDICTION D. Kececioglu, et al (Arizona Univ.) 31 Aug. 1971 258 p
CSCL 14D

N72-17456

G3/15 16450

NASA CR - 120813

TOPICAL REPORT

GENERATION OF FINITE LIFE DISTRIBUTIONAL GOODMAN DIAGRAMS FOR RELIABILITY PREDICTION

by

Dr. Dimitri Kececioglu and Lieutenant William Neil Guerrieri

prepared for

NATIONAL AERONAUTICS AND SPACE ADMINISTRATION

August 31, 1971

CONTRACT NGR 03-002-044

Technical Management

NASA Lewis Research Center
Cleveland, Ohio

Spacecraft Technology Division

Vincent R. Lalli

THE UNIVERSITY OF ARIZONA
College of Engineering
Engineering Experiment Station
Tucson, Arizona 85721

NOTICE

This report was prepared as an account of Government sponsored work. Neither the United States, nor the National Aeronautics and Space Administration (NASA), nor any person acting on behalf of NASA:

A). Makes any warranty or representation, expressed or implied, with respect to the accuracy, completeness, or usefulness of the information contained in this report, or that the use of any information, apparatus, method, or process disclosed in this report may not infringe privately owned rights; or

B). Assumes any liabilities with respect to the use of, or for damages resulting from the use of any information, apparatus, method or process disclossed in this report.

As used above, "person acting on behalf of NASA" includes any employee or contractor of NASA, or employee of such contractor, to the extent that such employee or contractor of NASA, or employee of such contractor prepares, disseminates, or provides access to, any information pursuant to his employment or contract with NASA, or his employment with such contractor.

Requests for copies of this report should be referred to

National Aeronautics and Space Administration
Office of Scientific and Technical Inforamtion
Attention: AFSS-A
Washington, D. C. 20546

ABSTRACT

The methodlogy of developing finite life distributional Goodman diagrams and surfaces is presented in this paper. The Goodman surface and diagram presents allowable combinations of alternating stress and mean stress to the design engineer. The combined stress condition presented in these surfaces and diagrams is that of an alternating bending stress and a constant shear stress. The finite life Goodman diagrams and surfaces are created from strength distributions developed at various ratios of alternating to mean stress at particular cycle life values.

The conclusions drawn in this report indicate that the Von-Mises Hencky ellipse, for cycle life values above 10^4 cycles, is an adequate model of the finite life Goodman diagram. In addition, suggestions are made which reduce the number of experimental data points required in a fatigue data acquisition program.

TABLE OF CONTENTS

TABLE OF CONTENTS (Continued).

TABLE OF CONTENTS (Continued).

TABLE OF CONTENTS (Continued)

LIST OF TABLES

LIST OF TABLES (Continued).

LIST OF ILLUSTRATIONS

LIST OF ILLUSTRATIONS (Continued).

LIST OF ILLUSTRATIONS (Continued).

LIST OF ILLUSTRATIONS (Continued).

CHAPTER I

INTRODUCTION

Presently in the United States and abroad fatigue data, to a large extent, is presented in the form of the conventional S-N diagram. The S-N diagram's purpose is to graphically present strength data as a function of cycle life. This is done by testing a few specimens to failure at incremented stress levels. The data is plotted on a graph of log stress versus log cycles, (see Figure 1.1). This method of presenting fatigue data does not take into account one of the fundamental and most important fatigue aspects: the variability of the fatigue mechanism; i.e., even high quality test specimens, subjected to tightly controlled test conditions will rarely, if ever, fail at precisely the same cycle of life at a given stress level.

Recently the American Society for Testing and Materials (ASTM) has suggested that a statistically significant number of specimens at each stress level be tested in order that a failure distribution be developed for each stress level (1, p. 9). The cycles-to-failure distributions which are developed can be used to construct a statistical S-N diagram. This particular diagram, as pictured in Figure 1.2, has a mean line as well as plus and minus three sigma lines.

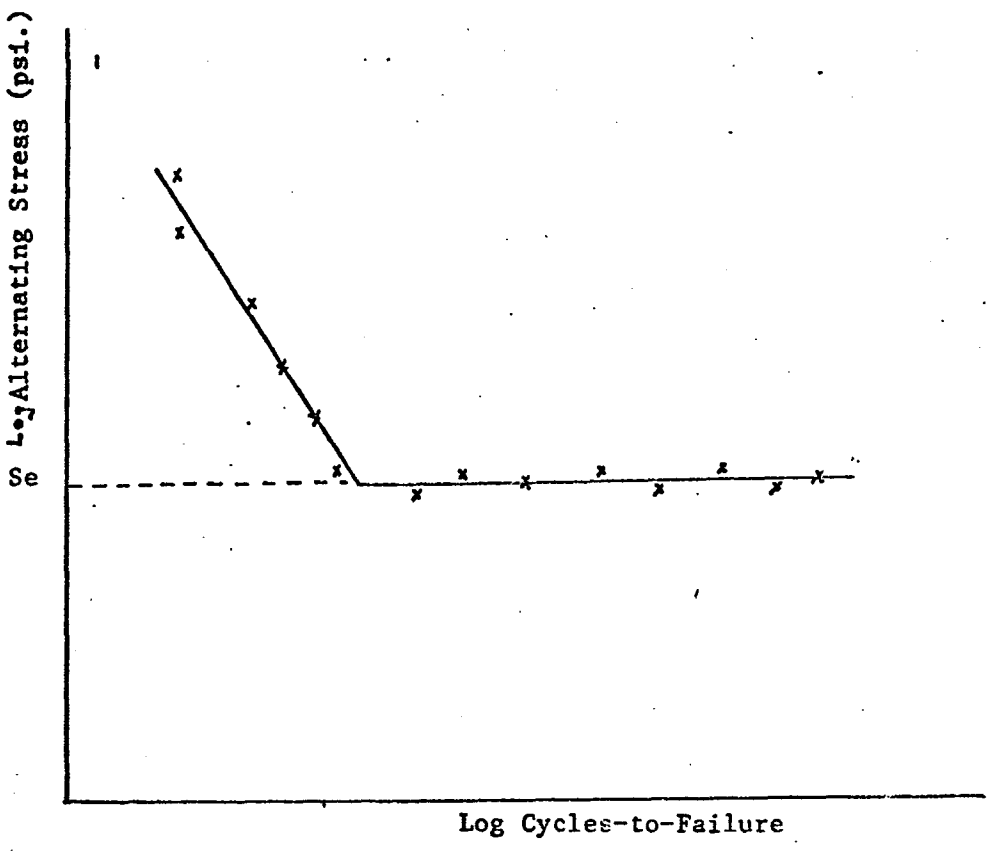

Fig. 1.1 Conventional Alternating Stress Cycles To Failure Diagram.

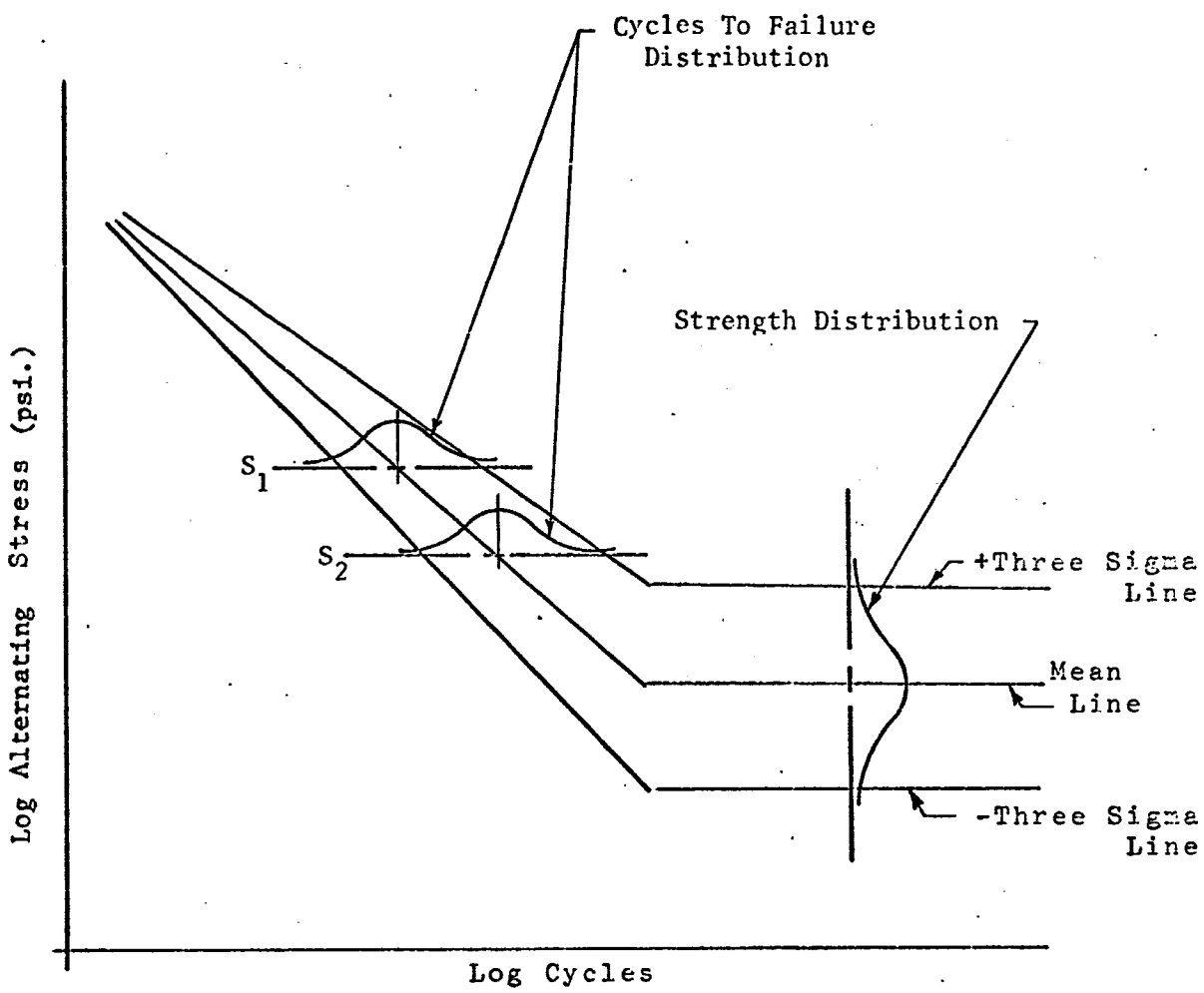

Fig. 1.2 Statistical S-N Diagram

It is possible through such statistical techniques as the use of probability plotting paper, the Chi-Squared and Kolmogorov-Smirnoff goodness of fit tests, and the computation of the four statistical moments to determine the best failure distribution probability density function. The probability density functions usually considered in such an analysis are the normal, lognormal, and Weibull distributions. The Weibull, because it is a three parameter distribution can take on many different shapes, from the exponential to the lognormal, by varying the three parameters. The Weibull probability density function, because of this flexibility is the most flexible of the three distributions mentioned.

The concept of failure distributions and strength distributions should be discussed briefly in order to avoid confusion in the later sections of this report. A failure distribution is derived directly from cycle to failure data. At a given stress level specimens will fail at particular values of cycle life. Even under the tightest controlled test conditions there will be variability in the cycle life of the individual test specimens. The failure distributions represent this variability in the test specimen's cycle to failure data. It is possible to form a histogram of the test specimen's cycle to failure data from which a failure distribution can be determined which adequately described the data. An example of such a histogram and distribution is given in Figure 1.3. Specifying the type

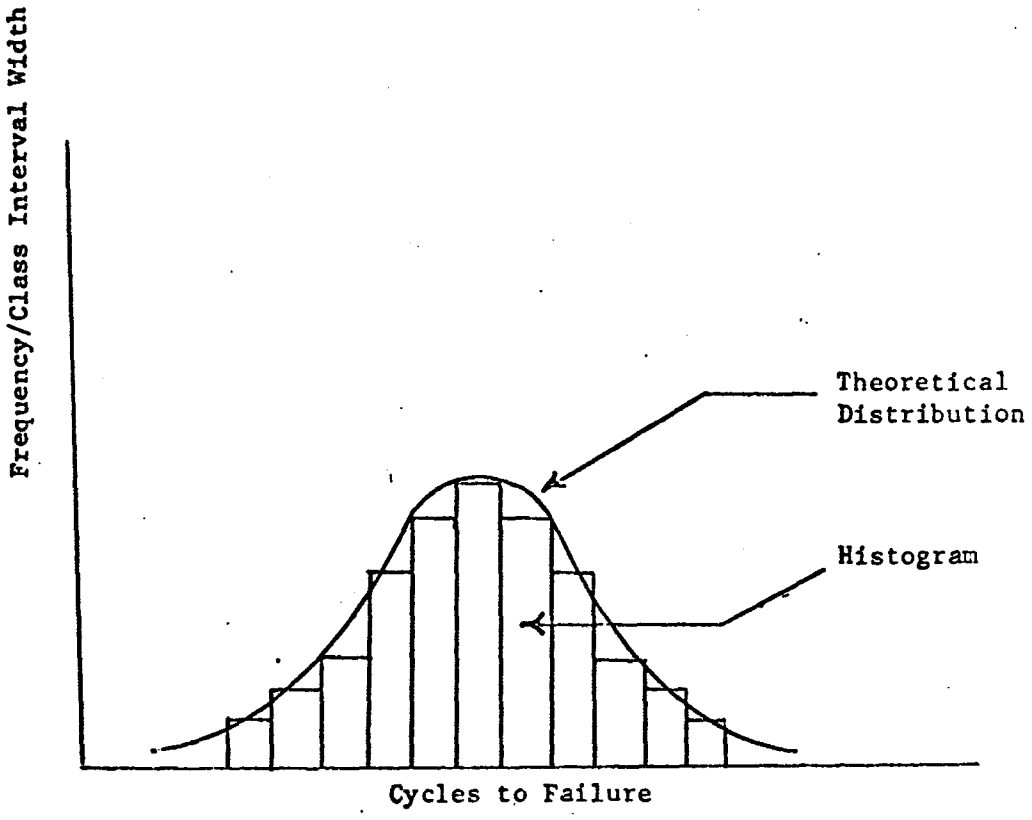

Fig. 1.3 An example of a Cycle to Failure Histogram and Distribution.

of distribution, normal, lognormal or Weibull, and the distribution parameters, uniquely describes the cycles-to-failure data.

A strength distribution is similar to a failure distribution in that it is described by a distributional type and the corresponding distributional parameters. When a specimen fails it means that the stress has exceeded the value of the strength of the specimen. Cycles-to-failure data reveals the percentage of specimens which have a strength less than the applied stress. It is possible to transform the cycles-to-failure distributions to strength distributions. A strength distribution describes the variability of the strength of a specimen at a specific value of cycle life and may be derived from a cycles to failure distribution.

The discussion of transforming cycles-to-failure distributions to strength distributions should be preceded by a discussion of some of the basic assumptions and restrictions which govern the generation of meaningful failure distribution data. Of primary concern is that all test specimens be uniform in geometry and metallurgical properties. This is important since subsequent calculations of the strength distributions will assume that specimens tested at various stress levels came from a homogeneous population. In addition the number of test specimens should be dependent upon the variability of the data generated. The statistical significance of the desired data is dependent upon the number of test specimens which are run,

the more data points generated the more positive the experimenter can be of his theoretical distribution. It has been found that at lower stress levels the variability of the data increases which indicates that an increase in test specimens is warranted at these lower stress levels.

The strength distribution may be oriented along the stress ratio axis of a distributional Goodman diagram. The ordinate axis of such a diagram presents values of alternating stress while the abscissa presents mean stress values. The strength distributions which are placed along axes where the ratio of mean stress to alternating stress is a constant form distributional surfaces. These surfaces are formed when the strength distributions are connected by a mean line and plus and minus three sigma limit lines. (see Figure 1.4). The Goodman surfaces are of vast importance in reliability engineering where the interference of a stress distribution with the corresponding strength distribution is used to calculate the designed-in reliability of a mechanical part.

The objective of this report is to clearly present the methodology of generating distributional Goodman diagrams. The accomplishment of this objective requires that the following subject areas be investigated: Chapters II and III explain methods of converting cycles to failure data to strength distributions; Chapters IV and V develop methods of generating finite life Goodman diagrams and surfaces; Chapter VII directs it's attention to resolving the question of static strength

Fig. 1.4 Goodman Surface Formed By Strength Distributions

distributions to be used on the finite life Goodman diagram. In Chapter VIII empirical mathematical models of the Goodman diagram are discussed. Chapter IX explains the theoretical strength theories associated with the combined stress condition of alternating bending stress and mean shear stress. Chapter X recommends an empirical mathematical model of the Goodman diagram and an associated theoretical strength theory. Chapter XII suggests two methods of reducing the amount of experimental data needed to generate finite life Goodman diagrams as well as methods of obtaining cycles to failure distributions from these Goodman diagrams with a minimum amount of actual fatigue testing.

The discussion of these subject areas requires that actual fatigue data be used in support of this effort. This investigator was extremely fortunate to have access to the complex fatigue data generated under National Aeronautical and Space Administration Grant No. 03-002-044 at The University of Arizona under the direction of Dr. Dimitri B. Kececiglu. The Combined stress condition under which this data was generated was that of an alternating bending stress and a constant, mean shear stress. Although the discussions in this report often apply themselves to this data, the concepts presented are applicable to the area of combined bending and shear stresses and in general to the broader area of any combined stresses in fatigue.

CHAPTER II

NASA METHOD OF GENERATING POLYGONS AND DISTRIBUTIONS

2.1 Theory

Mr. Richard E. Smith, Aerospace and Mechanical Engineering Department, The University of Arizona, in his master's report of August 1965, used data from Dr. H. T. Corten, Department of Theoretical and Applied Mechanics, University of Illinois, to present a method of transforming theoretical cycle to failure distributions to cumulative strength polygons. The following is a summary of the methodology of that effort (2, p. III).

The theoretical cycle to failure distribution is first determined. Because goodness of fit tests allow only for the rejection of a distribution, it is possible that more than one of the three major fatigue probability density functions, normal, lognormal, and Weibull, will be accepted. It then becomes necessary for the investigator to choose which one fits the data best, at all of the various stress levels. Once this has been determined, the failure data is uniquely described by the theoretical failure distribution probability density function rather than the failure histogram of the sample data. This probability density function is symbolized by f(x). At each

of the j stress levels pictured in Figure 2.1.1, there is a theoretical normal, lognormal, or Weibull distribution which represents the failure data.

The cumulative failure probability, up to the x'th cycle, for the j stress level is given by

$$F_j(x) = \int_0^x f(x)\,dx \qquad (2.1.1)$$

Of interest to the designer is the strength distribution for a specified cycle life. Once this cycle life is specified a series of cumulative failure distributions can be calculated for each stress level. In essence, the calculation of $F_j(x)$ is equal to calculating the area bound by the theoretical failure probability density function and the cycle line N (see Figure 2.1.2). Note the cumulative area in percent for each failure distribution to the right of the graph. Here it is important that the failure distributions are known for the full strength range in order that a cumulative failure probability of zero to one hundred percent is obtained (2, p. 23).

The physical significance of the cumulative failure distribution is the percent of specimens in which the stress has exceeded the strength. The percentage of specimens at a given stress and cycle life with a strength equal to or less than the stress is now a known quantity. A plot, as shown in Figure 2.1.3 can then be made of the cumulative failures in percent versus stress level, and is known as the cumulative strength

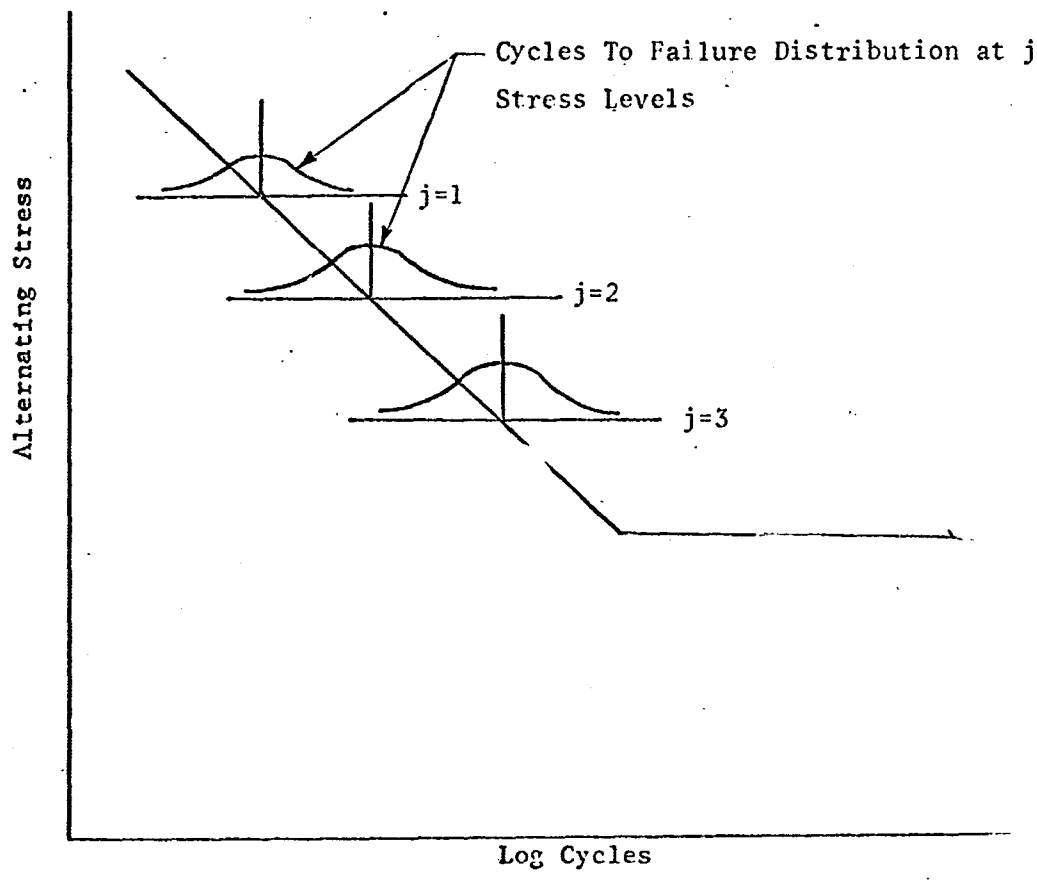

Fig. 2.1.1 Theoretical Cycles to Failure Distributions

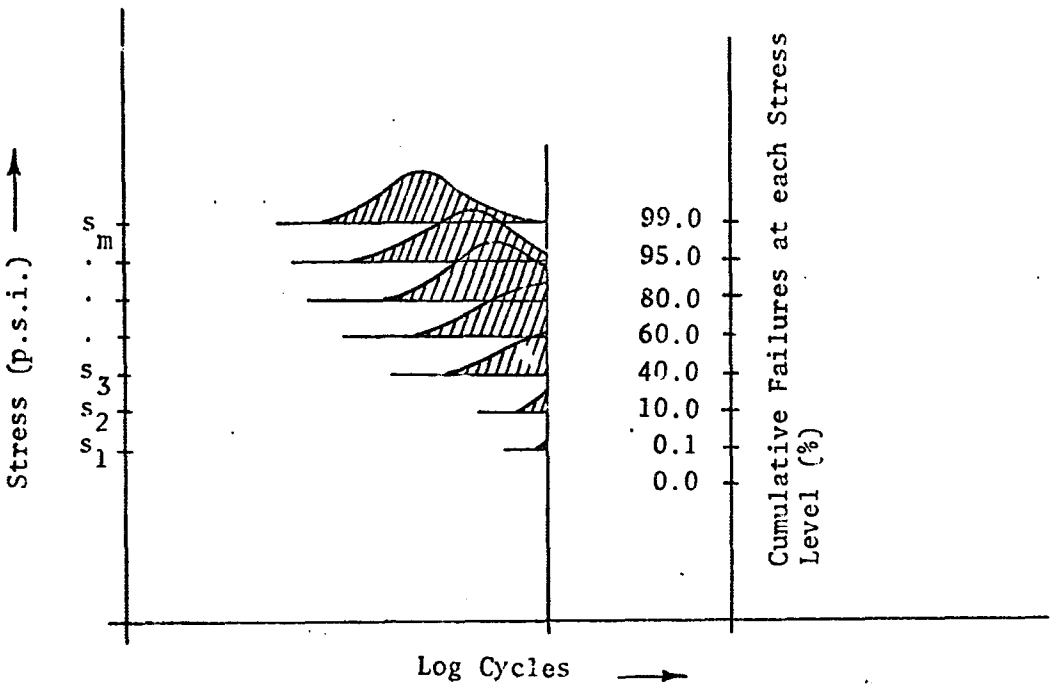

Fig. 2.1.2 - Cumulative Failure Technique for Strength Distribution Determination (2, p. 25).

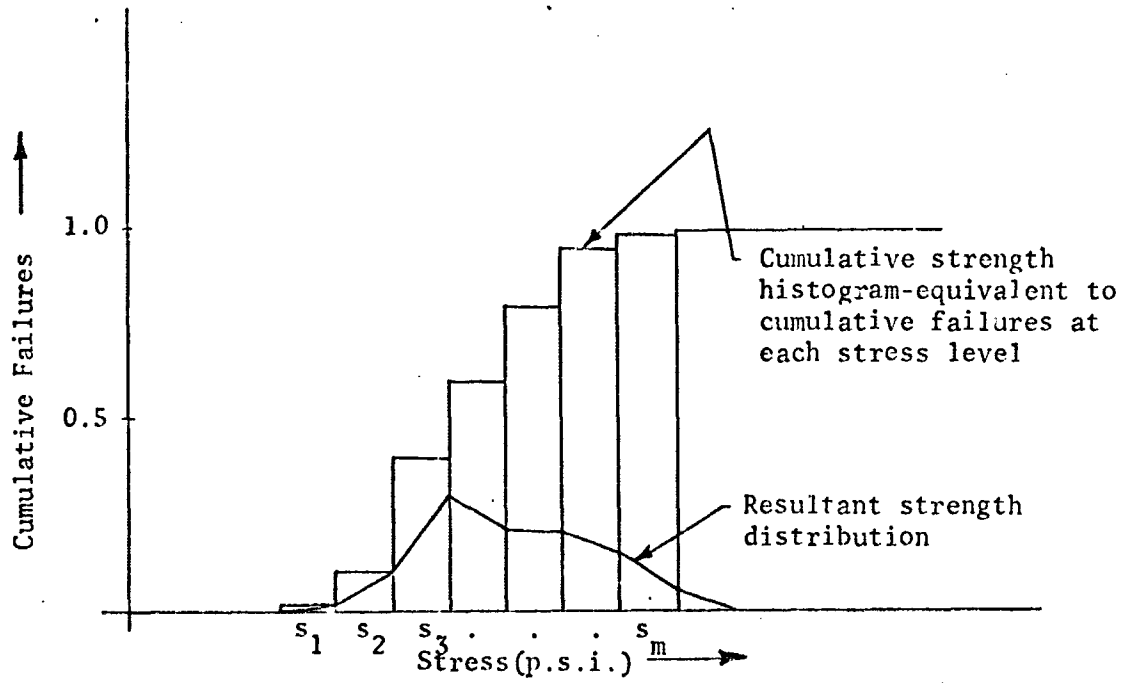

Fig. 2.1.3 - Strength Histogram (2, p. 25).

histogram. From this cumulative strength histogram it is possible to calculate the strength frequency histogram. The strength frequency histogram for the i'th cycle life is given by

$$f_i(s) = (F_{j+1}(x)-F_j(x))$$

where F_j and F_{j+1} are given by Equation 2.1.1 and where there are M different stress levels to be considered. Since the above calculation for the strength frequency histogram is based upon inferences drawn from several stress levels it is imperative that the specimens used in all stress levels be from the same statistical population and that uniform test conditions are maintained from stress level to stress level.

Upon the determination of the strength frequency histogram, $f_i(s)$, the statistical operation for goodness of fit, in this case the Chi-Squared test, can be conducted to insure that a theoretical distribution can be fitted to the histogram. For specific cycle of life values a theoretical strength distribution is specified by one of the three theoretical distributions, specifically either the normal, lognormal or Weibull distribution. It is of major importance to note that this method is capable of determining the strength distribution in either the fatigue life or infinite life portion of the S-N curve (refer to Figure 2.1.1).

This makes it unnecessary to conduct a Probit analysis or staircase test to determine the strength distribution (2, p. 31).

Beyond the endurance limit, area to the right of the knee where the S-N curve is horizontal, the failure distributions are independent of time, previously expressed in cycles. However, at some stress levels it will be impossible to achieve a cumulative failures of one hundred percent because the test will be terminated at a pre-determined time before the specimen has failed. Fortunately the cumulative failure distribution is known up until the test termination which allows one to calculate the strength distribution in an identical manner as previously discussed (2, p. 31).

The result of the strength distribution calculations allows the construction of a statistical S-N diagram, as illustrated in Figure 2.1.4.

An adequate range of stress levels is necessary so that a complete failure histogram from zero to one hundred percent can be developed. Within this range a sufficient number of failure distributions must be known at different stress levels so that there will be enough class intervals, governed by Sturges' rule, in the strength histogram. Time and economic considerations limit the number of stress levels, and consequently the number of failure distributions generated to from five to eight such levels and distributions. The use of this limited number of distributions would not give enough class intervals for an accurate strength distribution calculation. It is necessary to develop a digital computer program which will interpolate many stress-to-failure distributions from the

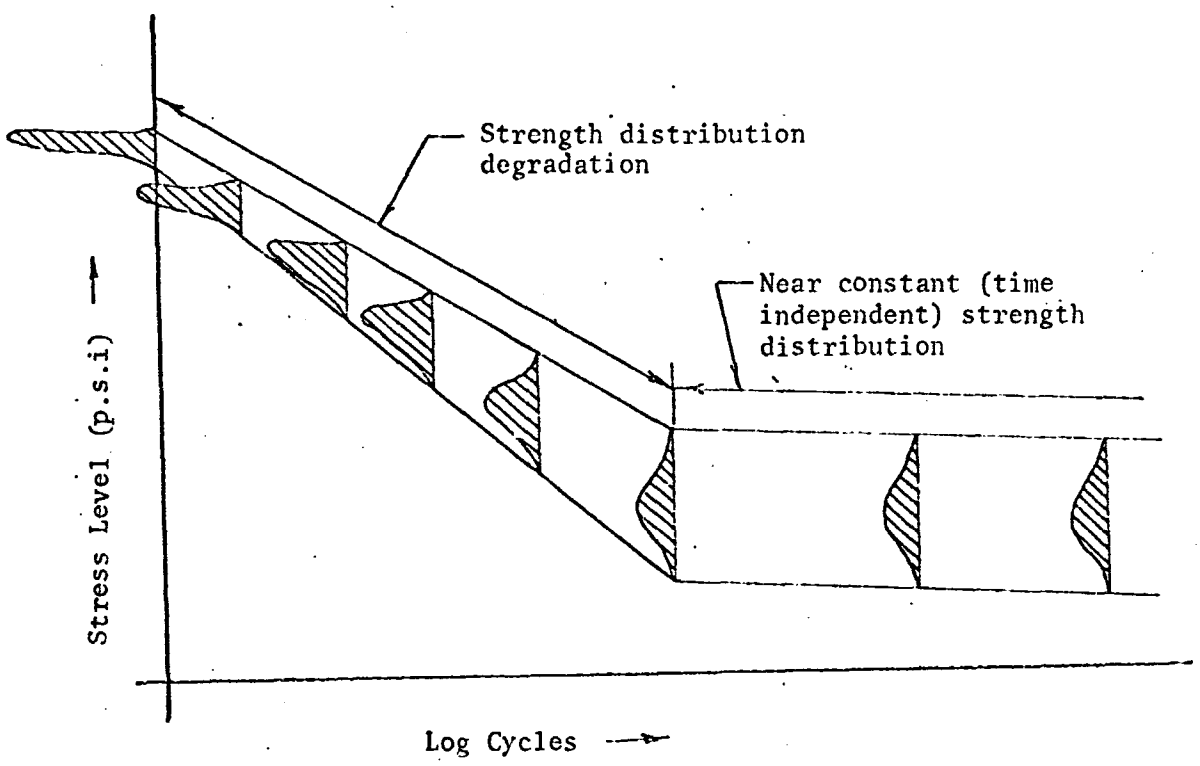

Fig. 2.1.4 - Strength Distribution Versus Cycles To Failure (2, p. 33).

limited number available from experimental data (2, p. 27). It is possible to have this program accomplish these interpolations and perform the methodology discussed for the transformation of cycles to failure distributions to strength distributions as well as accomplish all required statistical operations.

2.2 Computer Method

Two computer programs were developed in order that the strength distributions could be calculated. The first reduces the cycles to failure data to failure distributions at each stress level. The second computer program transforms the failure distributions to strength distributions.

Because of the large amount of fatigue data generated, a digital computer program, in Fortran language, was used to reduce the failure data at various stress levels to failure distributions. Failure data in terms of stress level and cycle life is read into the computer. The computer is capable of calculating the following parameters: mean, standard deviation, coeffieients of kurtosis and skewness, as well as of performing a Chi-Squared goodness of fit test. The computer program will use the normal distribution approximation in calculating the expected frequency in the Chi-Squared test when the sample data points are greater than thirty and will use the Student-t distribution when the sample number of data points is less than thirty. A flow chart, variable definitions and computer listing of the program are given in Appendix A.

The second computer program is used to determine the strength distributions from the failure distributions and is also written in Fortran language. The main steps of the program are listed below. A flow chart, cariable definitions and computer list of the program are given in Appendix B.

1. For each of the experimental stress levels read into the computer the actual cycles to failure distribution parameters are developed.
2. The computer will then calculate failure distribution parameters for interpolated stress levels at 200 increments by straight line interpolation.
3. The computer will then calculate the cumulative failure distributions for each stress level and a given series of log cycle life values.
4. Next the computer will calculate the strength frequency histogram for each cycle life.
5. The computer program then calls the computer to calculate theoretical distribution parameters from the strength frequency histograms based on a normal or lognormal distribution. These parameters include mean, standard deviation, coefficients of skewness and kurtosis. A goodness of fit test, using the Chi-Squared test will then be performed to determine which of the normal of lognormal distributions fits the data best.

6. The parameters mentioned in five are then printed out in addition to the Chi-Squared values for each cycle life. This print out allows the investigators to determine which of the two distributions is a better fit.

2.3 Results

A complete description of Dr. Corten's testing progarm is found in Chapter V of Richard Smith's report, together with the analysis by Smith (2). Results of his analysis are summarized herein.

The Chi-Squared goodness of fit tests indicated that for aluminum specimens the cycles to failure distributions more closely fit a lognormal distribution; whereas distributions of steel specimens fit either the notmal and lognormal distributions equally well (2, p. 76). It was observed that as the sample size was increased, the lognormal distribution fit the data better than the normal.

The transformation of cycles to failure distributions to strength distributions was accomplished by assuming the failure data to be distributed lognormally. The computer program previously described was used to determine the strength polygons for various cycles of life. The program output included the cumulative strength polygons, the mean, standard deviation, coefficient of skewness and kurtosis, and the Chi-Squared goodness of fit values for the strength distributions.

Analysis of this data indicates that the normal distribution fit the strength data better than the lognormal distribution. Coefficient of skewness is generally negative indicating a normal distribution. Coefficient of kurtosis values, which should be 3.0 for the normal distribution, fluctuate about a value of 3.0. In addition the Chi-Squared values indicated that for both type specimens the normal distribution represented the data better than the lognormal distribution (2, p. 85).

2.4 Discussion as to Validity

The transformation of cycles-to-failure distributions to strength data which was proposed by Richard Smith was found to be appropriate and based on well founded principles. John Smith's methodology is identical in transforming cycles-to-failure data to strength distributions. Richard Smith applied the technique to Corten's data (3, p. III) and John Smith to the NASA data.

CHAPTER III

GENERATION OF STRENGTH DISTRIBUTIONS

3.1 Theory

Smith (3) did extensive work in developing cycles to failure and strength distributions. These distributions were generated from fatigue data of specimens which were subjected to an alternating bending stress and a constant, mean shear stress. Specimens were subjected to different ratios of alternating to mean stress, known as stress ratios, at specified alternating stress levels. The specimens were of SAE 4340 steel and were of a grooved geometry. A grooved and ungrooved test specimen are shown in Figure 3.1.1 and 3.1.2. A complete description of the test program, which was sponsored by the National Aeronautics and Space Administration under Grant Number 03-002-044 at The University of Arizona, and of the procedures and materials is given in NASA CR-120831 (3).

The methodology used by John Smith in developing the strength distribution was similar to that used by Richard E. Smith (discussed in Chapter II of this report) (2). Cycles to failure distributions were developed at specific alternating stress levels for the stress ratios of infinity, 3.5, 0.825, and 0.44. The lognormal distribution was

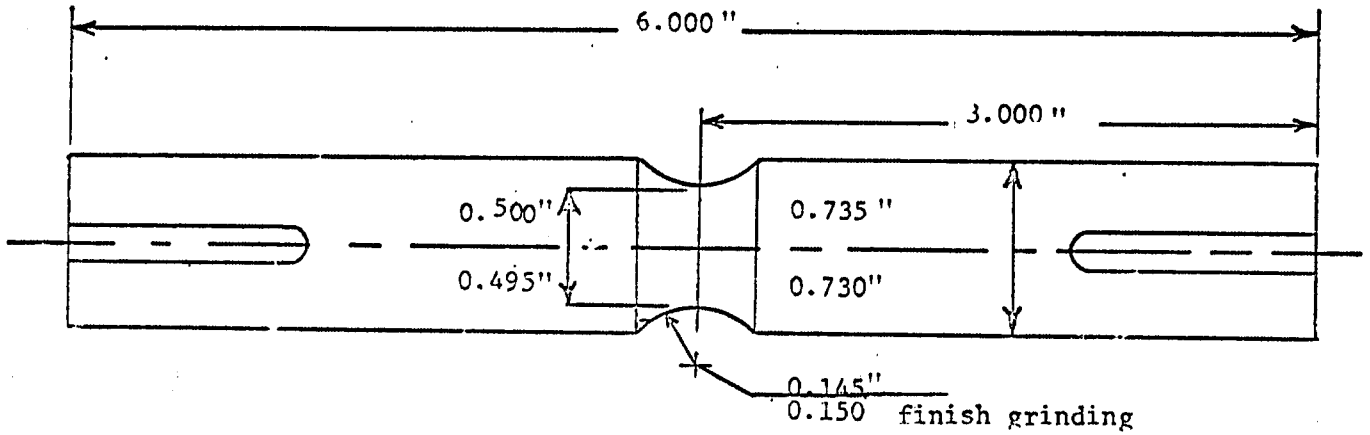

Fig. 3.1.1 Grooved Fatigue Test Specimen of 4340 SAE Steel

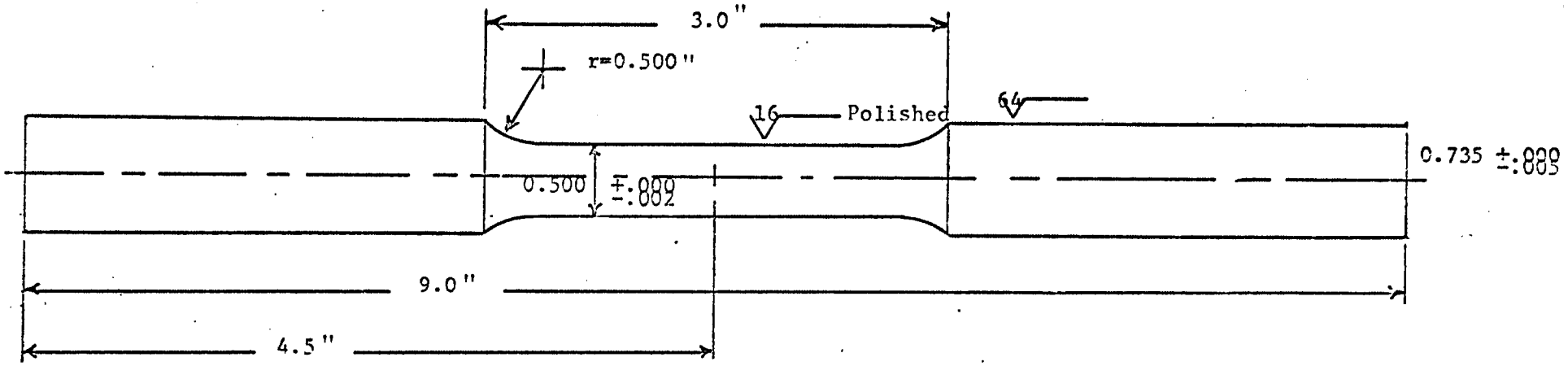

Fig. 3.1.2 Ungrooved Tensile Test Specimen of 4340 SAE Steel.

found to best describe the cycles to failure data (3, p. 47). The decision to accept the lognormal distribution over the normal distribution was based on the Kolmogorov-Smirnov test (3, p. 44).

Cycles to failure distributions for particular stress ratios at specified stress levels were plotted on S-N diagrams of alternating stress versus log cycles. This specified the mean line and $\pm 3\sigma$ (σ = standard deviation) envelope. After this was established, it was possible to interpolate many cycles-to-failure distributions at intermediate stress levels. This interpolation process made it possible to calculate strength distributions at specific cycle life values.

A review of the methodology used in the calculation of strength distributions at specific cycle life values is in order at this time. A histogram can be located along the N cycle life line in such a way that the midpoints of the cells are at the interpolated stress levels. (See Figure 3.1.3). The ordinate of each of the strength histogram cells is the area bounded by the N cycle line and the cycle to failure distributions which has been interpolated for that particular value of alternating stress. Thus if $f(N/S_i)$ is the cycle to failure distribution at a particular alternating stress level, the ordinate of the strength histogram cell at that stress level will be given by:

$$F(N/S_i) = \int_{-\infty}^{n} f(N/S_i)\, dn \qquad (3.1.1)$$

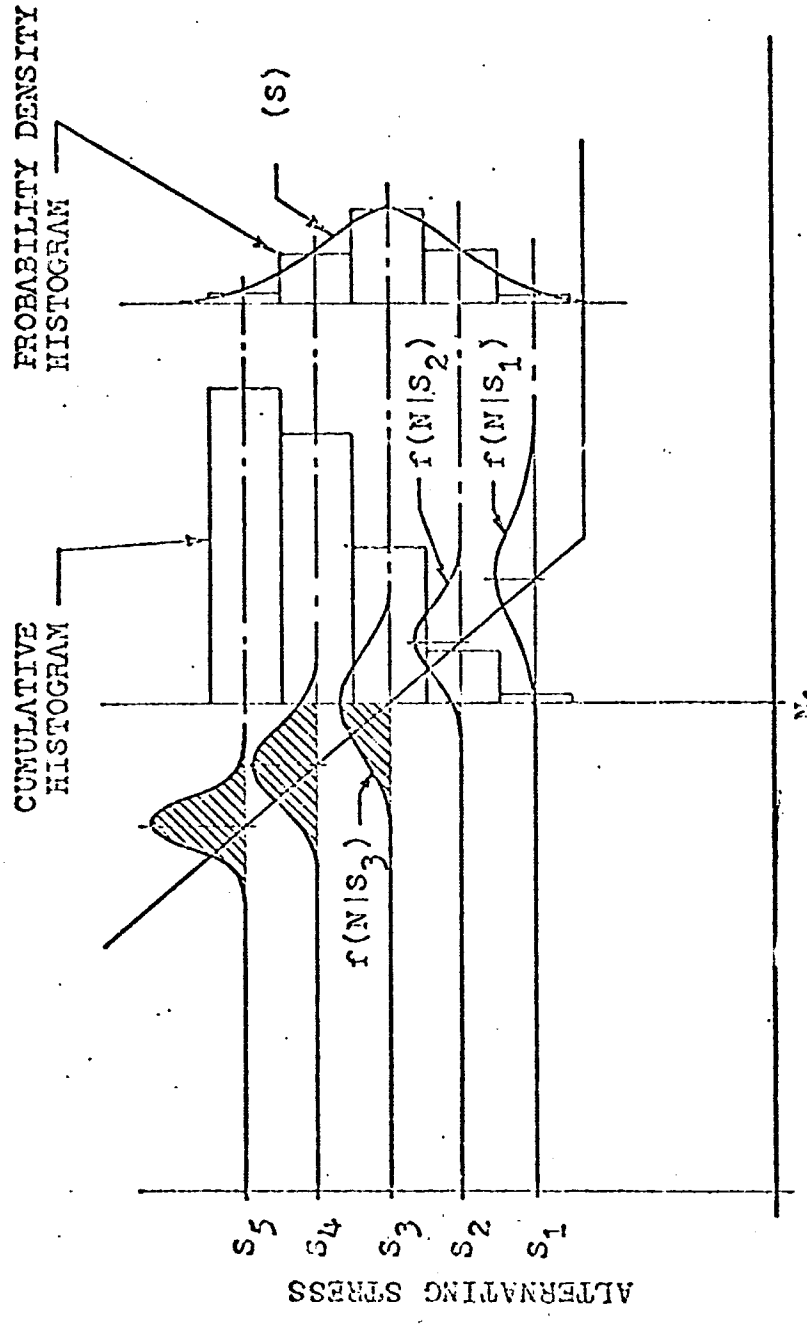

Fig. 3.1.3 Histogram Obtained From Cycles-to-Failure Distributions

The ordinate of each of the strength histogram cells will be:

$$F(N/S_i) = \int_{-\infty}^{n} f(N/S_i)\, dn \qquad (3.1.2)$$

The histogram which is developed in this way is the cumulative strength histogram of specimens failing by N cycles. If S is the strength variable along the N cycle life line, the probability density function can be developed in the following manner. The value of the i^{th} cell of the strength probability density histogram is given by:

$$f(S_i) = F(N/S_i) - F(N/S_i\text{-}1) \qquad (3.1.3)$$

The fact that there are many interpolated cycles to failure distributions on the N cycle life line insures an adequate number of class intervals in the strength histogram. A normal distribution is then fitted, by statistical methods, to the strength probability density histogram (3, p. 55).

3.2 Computer Method

John Smith developed two computer programs which were used in the strength distribution calculations. The first of which, known as CYTOFR, calculated the cycles to failure distribution parameters, mean and standard deviation as well as the coefficients of skewness and kurtosis of the normal and

lognormal distributions. It also performed the Chi-Squared and Kolmogorov-Smirnov goodness of fit tests to determine if a normal or lognormal distribution fits the data best. A flow chart, variable definition and computer listing of this modified to include a sort routine is given in Appendix C.

The program STRENG finds the normal strength distributions from the lognormal cycles to failure distribution parameters. Smith used this method because it has been found by earlier studies that the normal distribution adequately describes the strength data (2) (4). The input data of this program includes the cycles to failure data, two extrapolated lognormal distributions on either side of the experimental distributions and interpolated lognormal cycles to failure distributions between the actual experimental failure distributions. The program then calculates the mean, standard deviation, and coefficients of skewness and kurtosis for the normal strength distributions. In addition a goodness of fit test, the Kolmogorov-Smirnov test is performed on the normal strength distributions. A flow chart, variable definitiions computer listing of program STRENG given in Appendix D.

3.3 Results

The statistical S-N diagrams, which present the cycles to failure distributions for stress ratios of infinity, 3.5, 0.825 and 0.44, are given in Figures 3.3.1 through 3.3.4. The mean, standard devistions, and three sigma limits of the lognormal cycles to failure distributions are presented in Table 3.3.1.

John Smith presented only one S-N diagram which had the calculated strength distribution for a stress ratio of 3.5 and cycle life values of 10,000, 50,000, and 100,000 cycles. The normal parameters of the strength distribution which was placed on this particular S-N diagram are given in Table 3.3.2 while the S-N diagram appears as Figure 3.3.5. The completion of the stress ration tests of 0.44 allowed the calculation of strength distributions for this stress level. Table 3.3.3 presents the parameters of the normal strength distributions at three cycle life values and a stress ratio of 0.44 while these distributions were added to Figure 3.3.4.

A complete table of the normal strength distribution parameters at all stress ratios and cycle life values was inavailable and consequently recovered by use of the program STRENG. The results are presented in Table 3.3.4.

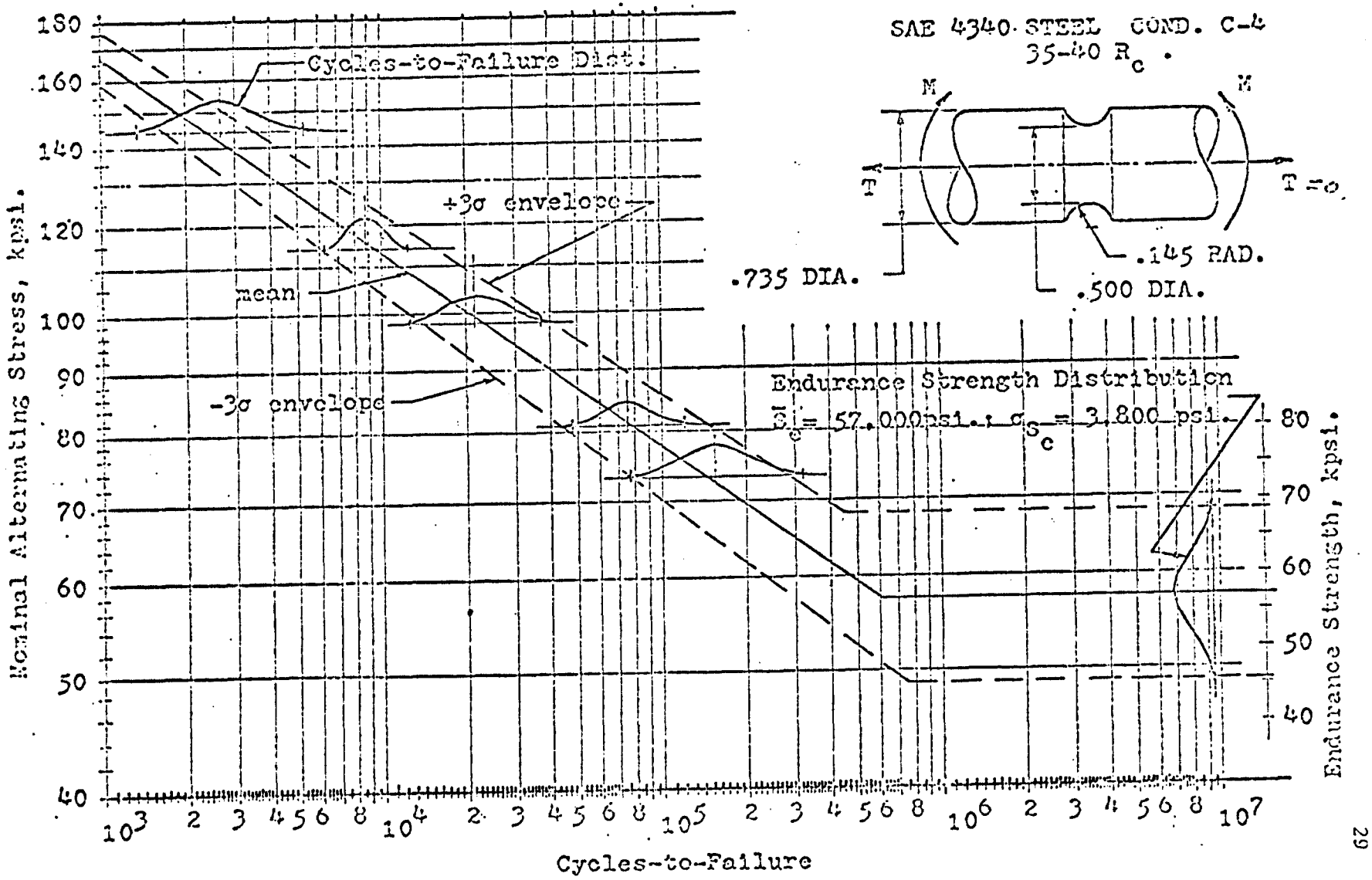

Fig. 3.3.1 Cycles-to- Failure Distributions and Endurance Strength Distribution for Stress Ratio of ∞ (3, p. 49)

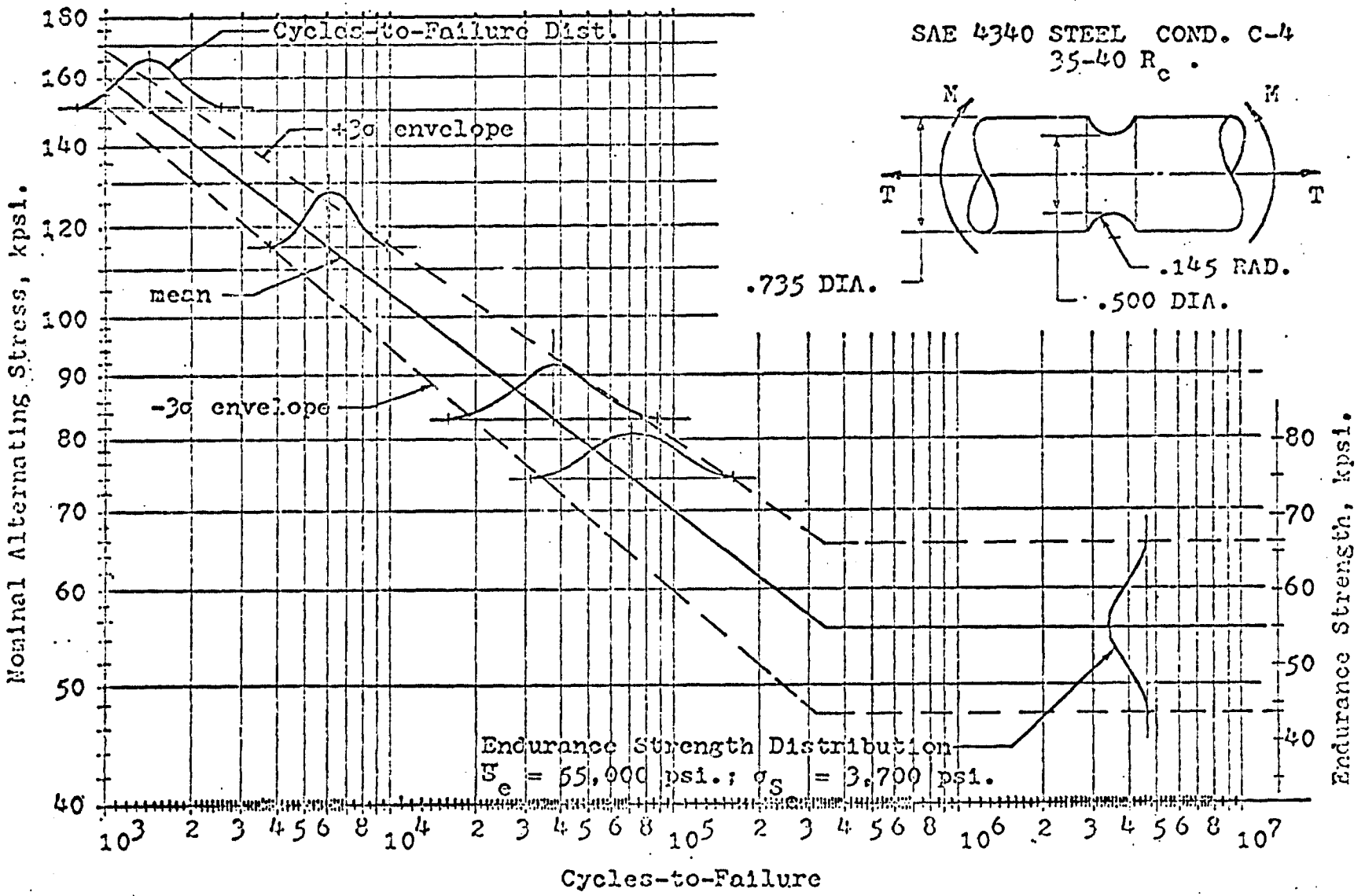

Fig. 3.3.2 Cycles-to-Failure Distributions and Endurance Strength Distribution for Stress Ratio of 3.5. (3., p.50)

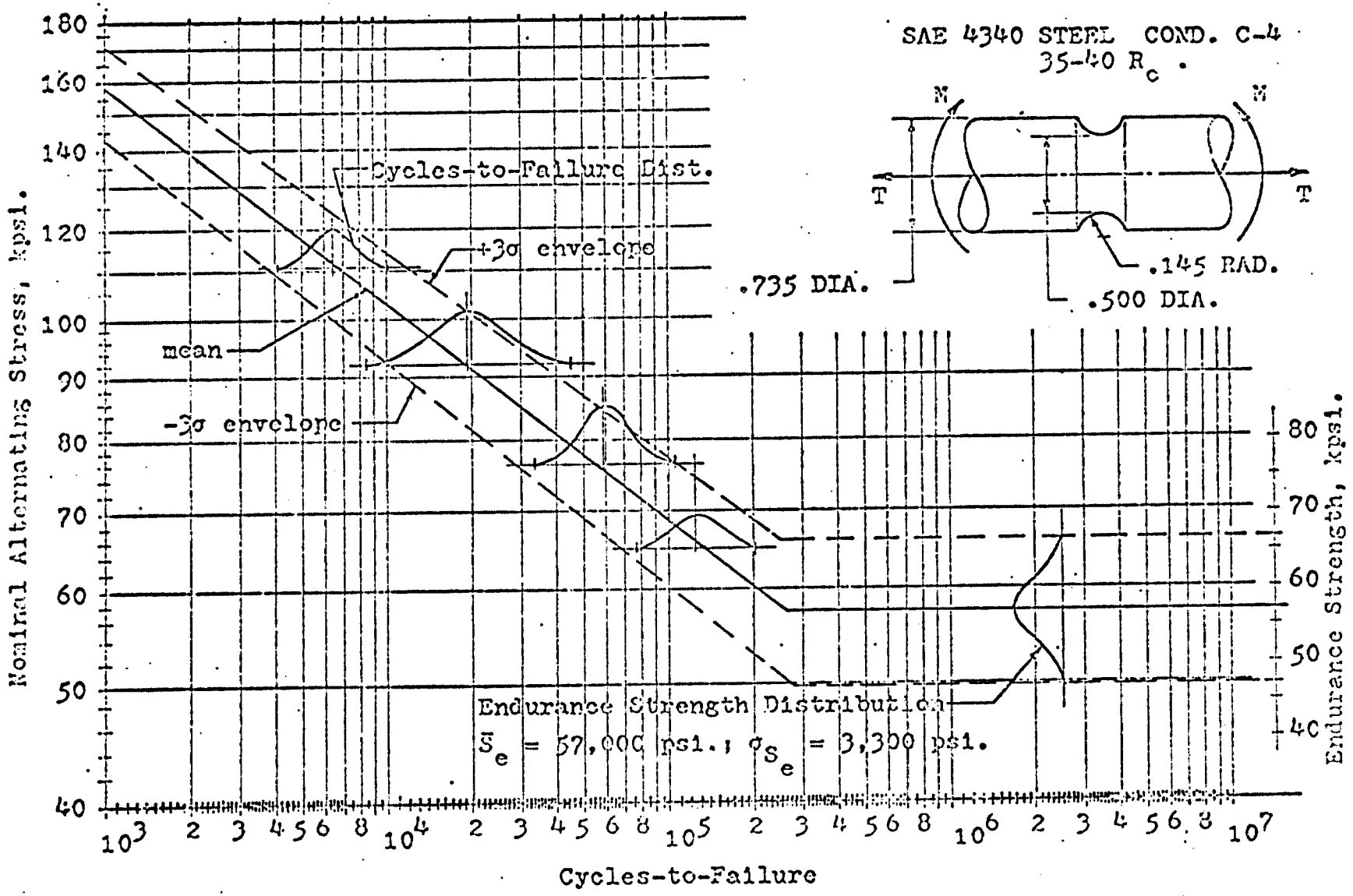

Fig. 3.3.3 Cycles-to-Failure Distributions and Endurance Strength Distribution for Stress Ratio of 0.825. (3, p. 51)

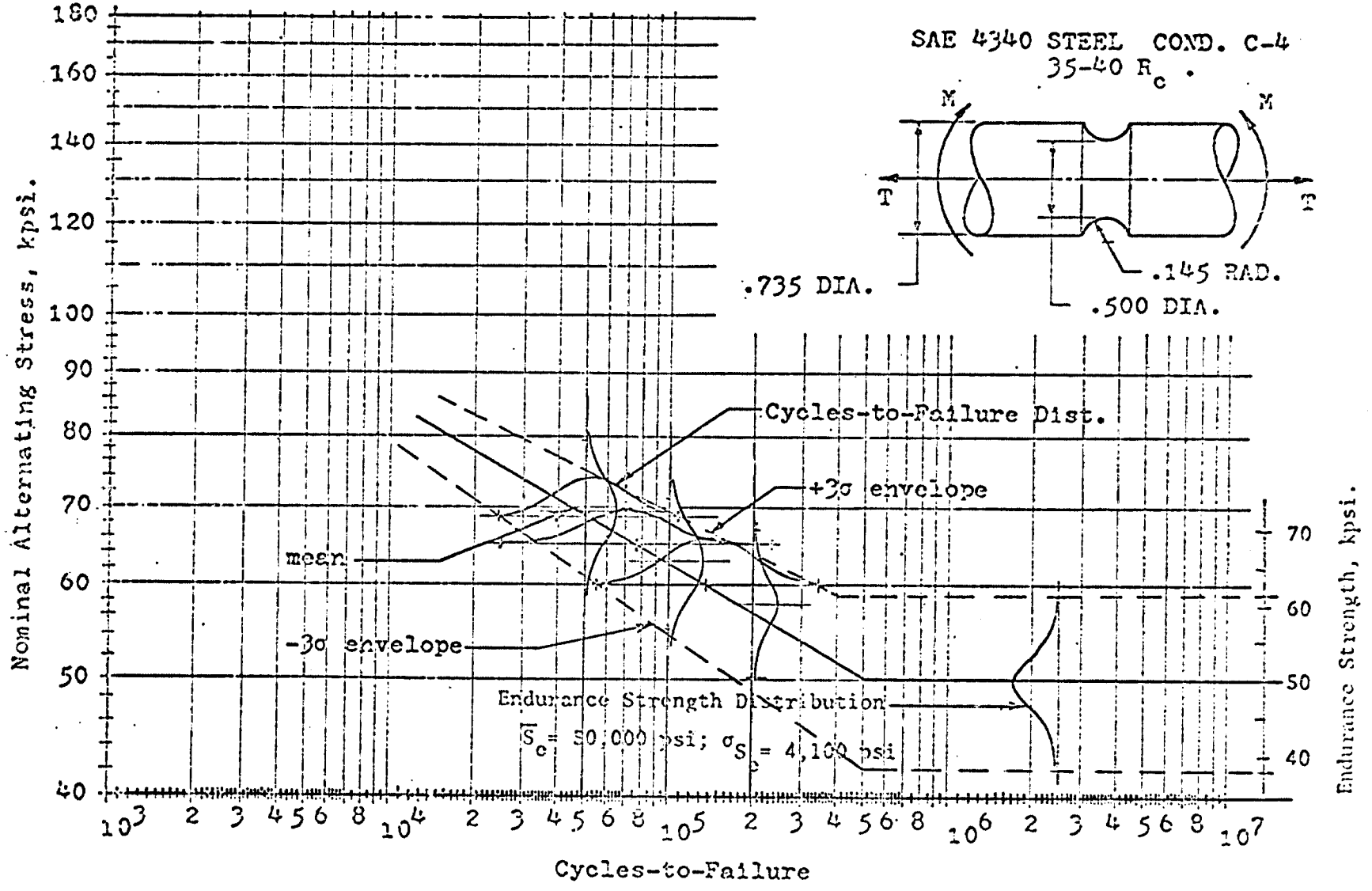

Fig. 3.3.4 Cycles-to-Failure Distributions, Strength Distributions and Endurance Strength Distribution for Stress Ratio of 0.444. (3, p. 52)

CYCLES TO FAILURE

Table 3.3.1 LOG-NORMAL DISTRIBUTION PARAMETER ESTIMATES AND MAX D-VALUES (3, p.37)

Stress Ratio	Average Alternating Stress Level (psi)	Sample Size	Log-Normal Dist. Parameters				Max. D Value*
			Mean	Standard Deviation	α_3 Skew-ness	α_4 Kurtosis	
∞	144,000	12	7.906547	.227914	-1.586	4.258	.207
	114,000	18	9.101961	.116130	-.407	2.123	.092
	98,000	18	9.992123	.176382	-.265	1.945	.094
	81,000	18	11.252667	.153954	.575	2.697	.159
	73,000	18	11.970997	.234941	-.906	2.707	.198
3.5	151,000	12	7.262676	.197789	-.435	2.006	.128
	115,000	18	8.720894	.157247	.403	2.869	.086
	83,000	18	10.545160	.286664	.686	4.407	.184
	74,000	18	11.180338	.274219	-.342	2.501	.084
0.825	111,000	12	8.777704	.145966	.742	2.295	.280
	92,000	18	9.890129	.280831	-.171	1.916	.120
	76,000	18	11.001940	.195062	-.703	2.457	.111
	65,000	18	11.743320	.167235	-.030	1.769	.147
0.44	69,000	18	10.856736	.248421	1.210	3.899	.214
	60,000	18	11.825351	.305282	-.457	3.182	.118

* Maximum D-Value From K-S Test

Table 3.3.2 Strength Distribution Parameters of the Normal Distribution at Three Cycle Life Values For A Stress Ratio of 3.5. (3, p.57)

Cycles of Life N	Parameter Estimate of Normal Distribution	
	Mean (psi)	Standard Dev. (psi)
10,000	106,639	3,256
50,000	79,021	3,253
100,000	70,972	2,313

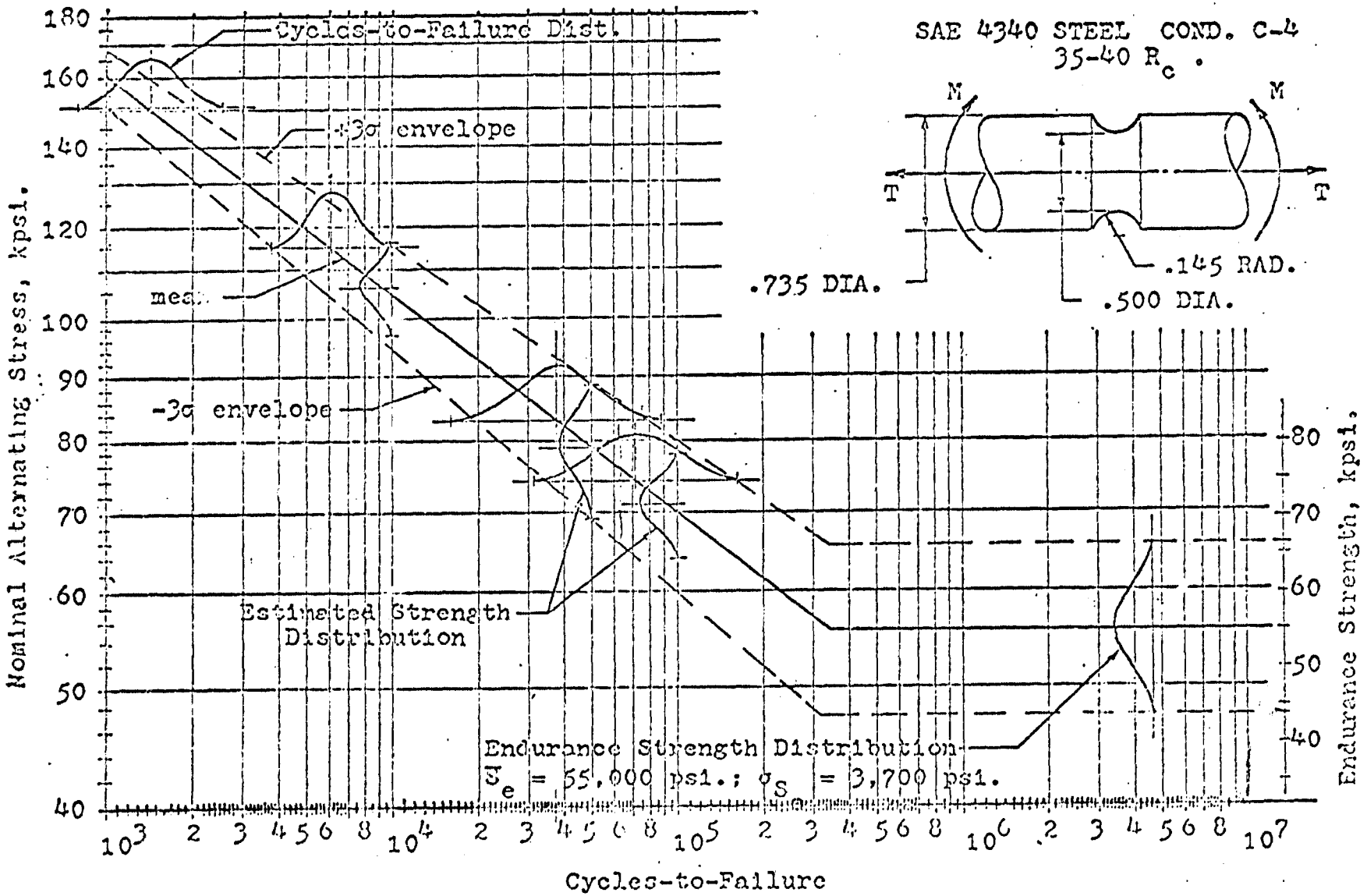

Fig. 3.3.5 Plot of Estimated Strength Distributions at Various Cycles of Life and Estimated Cycles-to-Failure Distributions at Various Stress Levels for Stress Ratio of 3.5 (3, p. 58)

Table 3.3.3. Strength Distribution Parameters of the Normal Distribution at Three Cycle Life Values for a Stress Ratio of 0.44.

Cycles of Life N	Parameter Estimates of Normal Distribution	
	Mean psi	Standard Deviation psi
10,000	103,725	3,323
50,000	77,703	3,154
1,000,000	48,686	2,394

Table 3.3.4 Parameters of Normal Strength Distribution At Specific Stress Ratios and Cycles of Life.

R = ∞				
Cycles	Mean Strength psi	Standard Deviation psi	-3 Sigma Limits psi	+3 Sigma Limits psi
1,000	164,805	1,629	159,932	169,678
3,000	139,241	2,570	131,533	146,950
3,500*	135,953	2,628	128,070	143,837
5,000	128,356	2,790	119,986	136,726
7,000	121,191	2,937	112,378	130,003
9,000*	115,926	2,907	107,205	124,647
10,000	113,844	2,801	105,441	122,246
20,000	101,523	2,772	93,206	109,840
30,000	94,972	2,559	87,296	102,648
40,000*	90,693	2,665	82,878	98,507
50,000	87,391	2,671	79,378	95,405
60,000	84,707	2,697	76,617	92,798
70,000	82,484	2,662	74,498	90,470
80,000	80,628	2,594	72,845	88,411
90,000*	79,054	2,539	71,437	86,671
150,000	72,901	2,133	66,502	79,301
200,000*	70,172	1,881	64,529	75,815
1,000,000	56,184	2,138	49,771	62,596

*Parameters used in Chapter V Finite Life Goodman Diagrams.

Table 3.3.4 Parameters of Normal Strength Distribution At Specific Stress Ratios and Cycles of Life. (Continued).

R = 3.5				
Cycles	Mean Strength psi	Standard Deviation psi	-3 Sigma Limits psi	+3 Sigma Limits psi
1,000	158,162	2,144	151,731	164,592
3,000	132,668	3,536	122,061	143,275
3,500*	128,964	3,643	118,035	139,894
5,000	120,436	3,797	109,645	131,826
7,000	113,156	3,325	103,178	123,133
9,000*	108,523	3,213	98,883	118,163
10,000	77,689	2,502		
20,000	94,273	3,611	83,440	105,106
30,000	87,100	3,701	75,998	98,203
40,000*	82,345	3,467	71,942	92,747
50,000	79,021	3,253	69,261	88,781
60,000	76,533	3,049	67,385	85,681
70,000	74,629	2,792	66,253	83,005
80,000	73,152	2,554	65,490	80,814
90,000*	71,967	2,393	64,787	79,147
100,000				
150,000	67,341	2,327	60,360	74,321
200,000*	64,792	2,400	57,593	71,991
1,000,000	50,533	2,812	42,097	58,969

*Parameters used in Chapter V Finite Life Goodman Diagrams.

Table 3.3.4 Parameters of Normal Strength Distribution at Specific Stress Ratios and Cycles of Life. (Continued).

R = 0.444				
Cycles	Mean Strength psi	Standard Deviation psi	-3 Sigma Limits psi	+3 Sigma Limits psi
1,000	121,500	200	121,439	121,560
3,000	107,185	1,141	103,761	110,605
3,500*	105,107	1,260	101,327	108,887
5,000	100,305	1,539	95,689	104,921
7,000	95,774	1,803	90,365	101,183
9,000*	92,390	2,002	86,384	98,396
10,000	90,971	2,085	84,715	97,227
20,000	81,638	2,637	73,726	89,549
30,000	76,162	3,012	67,126	85,197
40,000*	72,260	3,269	62,452	82,068
50,000	69,403	3,202	59,799	79,008
60,000	67,387	2,971	58,474	76,299
70,000	65,930	2,806	57,511	74,349
80,000	64,788	2,750	56,539	73,037
90,000*	63,821	2,753	55,562	72,079
150,000	59,657	2,608	51,832	67,482
200,000*	57,521	2,359	50,444	64,599
1,000,000	47,648	2,766	38,751	55,346

*Parameters used in Chapter V Finite Life Goodman Diagrams.

Table 3.3.4 Parameters of Normal Strength Distribution At Specific Stress Ratios and Cycles of Life. (Continued).

R = 0.825

Cycles	Mean Strength psi	Standard Deviation psi	-3 Sigma Limits psi	+3 Sigma Limits psi
1,000	154,197	2,056	148,030	160,364
3,000	130.027	3,651	119,073	140,981
3,500*	126,369	3,739	115,151	137,587
5,000	117,923	3,898	106,229	129,618
7,000	110,448	3,539	99,831	121,065
9,000*	105,645	3,308	95,722	115,569
10,000	103,725	3,323	93,756	113,694
20,000	91,498	3,243	81,769	101,227
30,000	85,248	3,148	75,805	94,691
40,000*	80,953	3,208	71,327	96,578
50,000	77,703	3,154	68,239	87,166
60,000	75,179	3,044	66,045	84,312
70,000	73,148	2,974	64,226	82,070
80,000	71,443	2,947	62,602	80,285
90,000*	69,970	2,927	61,189	78,750
150,000	64,263	2,372	57,147	71,379
200,000*	61,737	2,133	55,338	68,135
1,000,000	48,686	2,394	41,505	55,868

*Parameters used in Chapter V Finite Life Goodman Diagrams.

3.4 Discussion as to Validity

The methodology which John Smith presented was found to be well grounded and accurate. Disturbing to the original investigator was the fact that the vertical strength distributions did not completely "fill" or span the entire width of the statistical S-N diagram envelope. That is, the vertical strength distributions did not span the complete distance between the plus three sigma line and minus three sigma line of the cycles to failure distributions. This, however, was not disturbing to this investigator for the following reason.

The histogram of the vertical strength distributions was developed from the cumulative failure probabilities of a large number of cycles to failure probability density functions. Along a particular cycle life line on the statistical S-N diagram, See Figure 3.4.1, the vertical distance from the intercepted plus and minus three sigma lines is of no particular significance.

The fact that the vertical strength distribution does not span the distance between point A and B can be explained in the following manner: The cycles-to-failure distributions are lognormal while the strength distributions are normal. It must be noted that in actuality only distributions to the left of the cycle life line contribute percentile areas to the cumulative strength distribution. The two points, A and B, are then completely unrelated. The plus and minus three sigma limits, which are not necessarily points A and B, of the

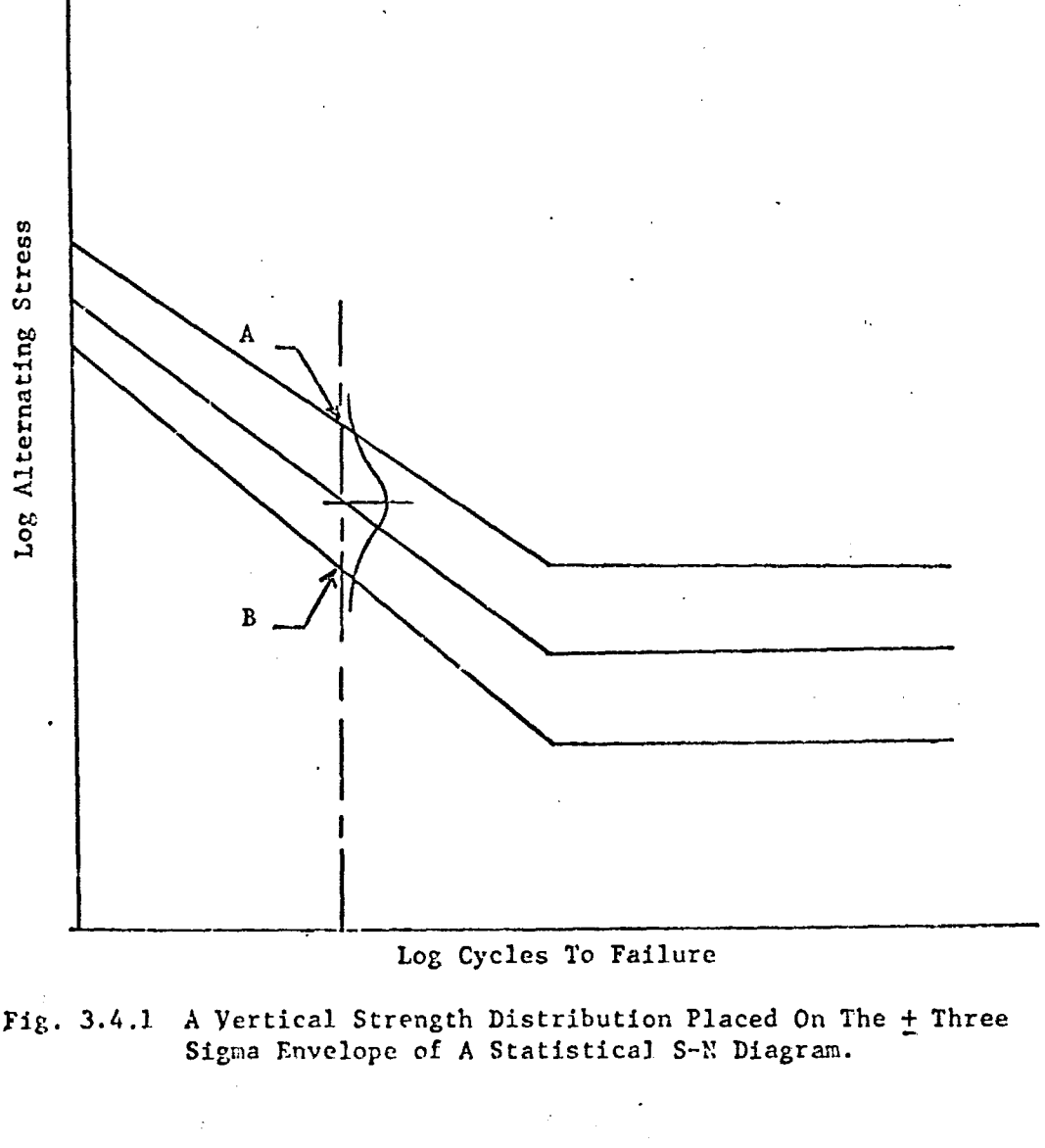

Fig. 3.4.1 A Vertical Strength Distribution Placed On The ± Three Sigma Envelope of A Statistical S-N Diagram.

vertical strength distributions are derived from the cumulative failure probabilities of the individual cycle to failure probability density functions. The plus and minus three sigma limits of the vertical strength distribution are related to the variability of the individual probability density functions of the cycles to failure data at particular stress levels intercepted by the vertical cycle life line.

CHAPTER IV

GENERATION OF FINITE LIFE GOODMAN DIAGRAMS (METHOD I)

4.1 Theory

To date most of the work done with the modified Goodman Diagram and Goodman surfaces has been concerned with the objective of presenting the relationship of alternating and mean stress for infinite periods of life. For the biaxial stress condition, where the specimen is subjected to both bending and shear stress, the Goodman diagram represents combinations of these two stresses, in the cartesian plane, where the specific combinations will not cause fracture to occur over a period of infinite life. The need for a surface to describe this relation occurs where probabilistic methods are used in reliability calculations by the interference method.

It is the purpose of the method under discussion in this Chapter to break away from the traditional concepts of using a Goodman surface to graphically represent the relation between bending and shear stresses for a period of infinite life, and present, in the cartesian plane, the relation of alternating stress to mean stress where the alternating stress is a bending stress while the mean stress is a shear stress for finite periods of life. The advantage of such an

approach is that it will graphically illustrate to a designer that it is possible to have higher combinations of bending and shear stresses for a finite life design. Hence, if a part need only fuction for a specified finite number of hours or cycles, after which its failure is not detrimental to the success of the mission, it can be subjected to combinations of bending and shear considerably higher than if it had to function in excess of 10^6 cycles.

The data which was used for this method was generated by the Reliability Research Laboratory of the Aerospace and Mechanical Engineering Department under NASA Grant 03-002-044 at The University of Arizona. Cycles to failure data was generated for rotating specimens which were subjected to an alternating bending and constant shear stress at specific stress ratios. Stress ratio is defined as the ratio of alternating bending stress, to mean normal stress from torque.

The cycles to failure data was generated from 1967 to 1970 for stress ratios, of infinity, (pure bending), 3.5, 0.8, and 0.44. The specimens which were subjected to a bending and shear stress had a grooved geometry. The material which the specimens were made of was SAE 4340 steel. A comprehensive explanation of the test program, machines, procedures and materials used can be found in NASA CR-72839 (3). The data generated by this experimental effort, which was used to construct finite life Goodman surfaces displayed in this

Chapter, included the bending and shear stress in each of the over 300 test specimens which were run to failure. The value of the cycles life at which the specimen failed was also recorded.

In the original test program twelve to eighteen test specimens were run at each stress level for each stress ratio. The lower number of specimens, twelve, occurred at higher stress levels, where variability in the cycle life data was small. The larger sample size was used at lower stress levels where variability in the data suggested a larger number of specimens be used. Referring to Figure 4.1.1, it can be seen that if the infinity stress ratio, located along the alternating stress axis, is to be bridged to a mean stress distribution at a stress ratio of zero by a Goodman surface, for the finite periods of life, there will have to be at least two other stress ratios which contain enough data points to form two strength distributions between the alternating stress distribution and the mean stress distribution and the mean stress distribution. Because of this restriction, it was necessary to screen the cycles to failure data to determine appropriate cycle life ranges. This was accomplished with the aid of Table 4.1.1. This table records the cycles to failure data for specimens at particular stress ratios. The cycle life ranges which were determined by this method are as follows:

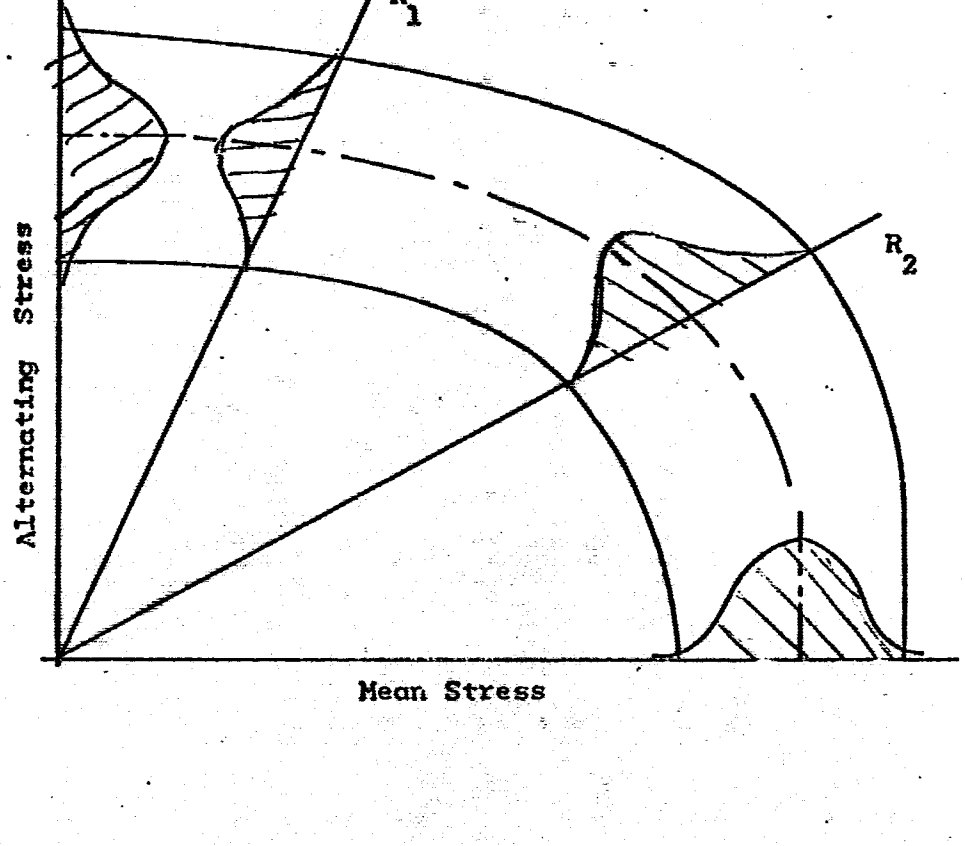

Figure 4.1.1. Finite Life Goodman Diagram Illustrating the Need of Two Additional Strength Distributions at R_1, R_2.

Table 4.1.1. Screening of Cycles-to-Failure Data to Ascertain Appropriate Cycle Life Ranges.

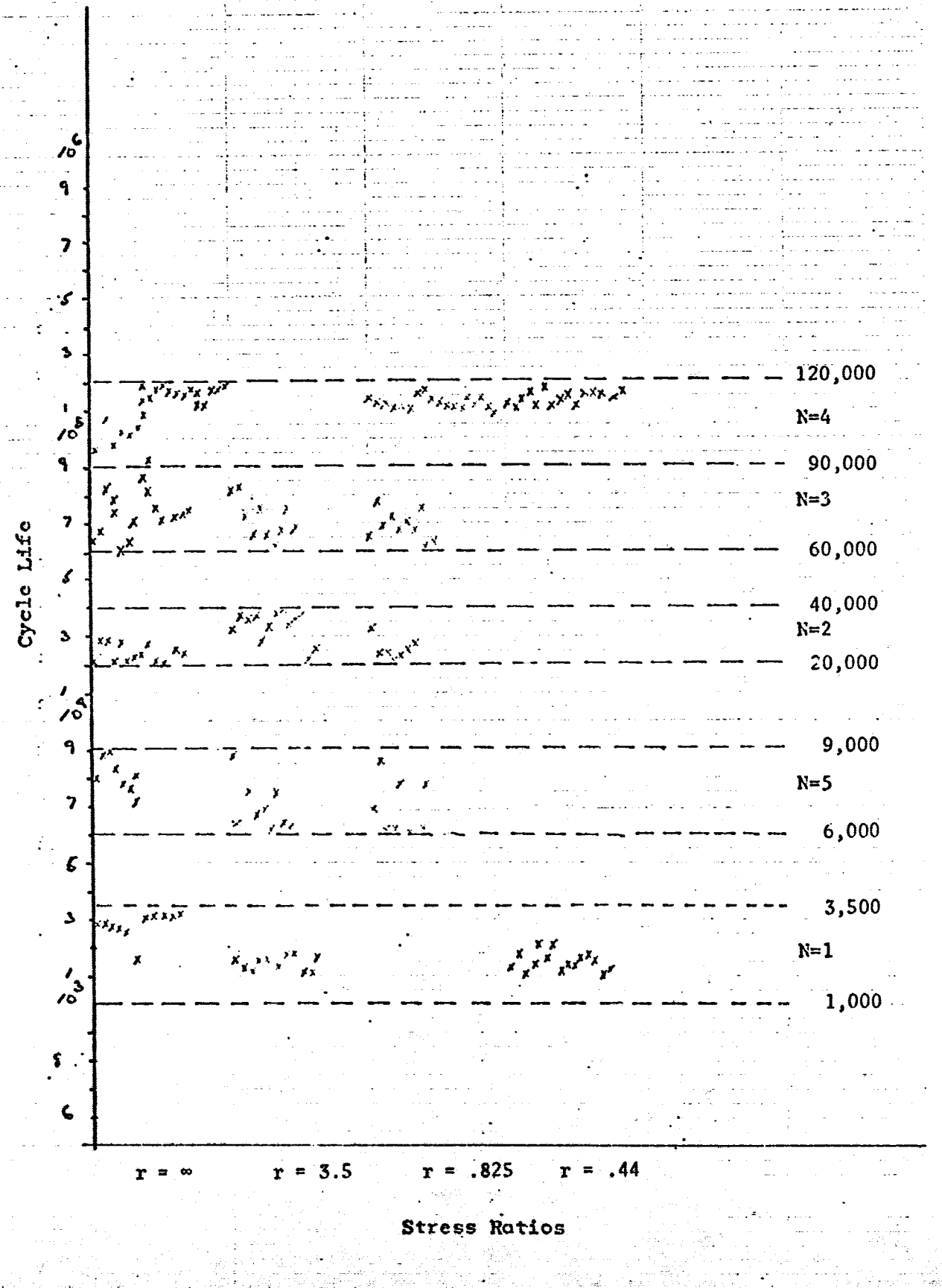

N = 1: 1,000 - 3,500 cycles to failure

N = 2: 20,000 - 40,000 cycles to failure

N = 3: 60,000 - 90,000 cycles to failure

N = 4: 90,000 - 200,000 cycles to failure

N = 5: 6,000 - 9,000 cycles to failure

It can be seen that these groups span the cycle life spectrum from low to relatively large cycle lifes. However, all five groupings are in the cycle life range to the left of the "knee" of the S-N diagram. It would have been desirable to keep the cycle life groups as small as possible, however the restriction of having enough data points within each group to form a distribution was the governing restriction in this case. The alternating stress distribution, where the shear stress or mean stress is zero, was obtained directly from the cycle to failure data of pure bending, $r = \infty$, specimens. After the cycle life groups were determined the distribution placed on the alternating stress axis for each group was specified by the bending stress recorded in each of the specimens which failed within the cycle life range of that particular group.

The distribution which was used on the mean stress axis in all cases was the ultimate strength distribution of an ungrooved tensile test specimen which had the same cross-sectional areas as the actual grooved fatigue test specimens (grooved

specimen results are used in Chapter V; see Figures 3.1.1 and 3.1.2 . The mean normal strength distribution was obtained directly from static tensile strength tests. In the case of such tensile tests, it is found that the grooved specimens have a higher ultimate strength. This is caused by a radial stress which is introduced into the specimen at the root of the groove. However, a grooved specimen which is subjected to static torque load would not experience such a radial stress. At this time in the investigation, it would, therefore, not have been correct to use the grooved specimens to determine the strength distribution for the mean stress axis (see Chapters V and VII).

After obtaining the cycle life groups the next step was to relate the shear stress in each of the specimens to the proper mean stress. This was done by using two predominant strength theories. These two theories are the Von-Mises Hencky theory and the maximum shear stress theory. A complete discussion of these two theories appears in Chapter VIII of this report.

The resultant stress vector, S_r, for each of the data points has a mean stress of $S_m = \sqrt{3}\tau$ (τ = shear stress), (3, p. 3). The resultant stress vector is a combination of mean and alternating stresses. The magnitude of the resultant vector is:

$$S_r^2 = (S_a)^2 + (S_m)^2 \qquad (4.1.1)$$

$$S_r = \left\{(S_a)^2 + (\sqrt{3}\tau)^2\right\}^{1/2} \qquad (4.1.2)$$

In the case where the Von Mises Hencky criterion is used to relate the shear stress to the mean stress the resultant stress vector is called stress vector I.

If the maximum shear stress theory is used to relate the mean stress to the torsional stress, the governing relation will be (13, p. 2):

$$S_m = 2\tau$$

The maximum shear stress theory predicts that yielding will occur when the maximum shear stress is equal to the shear stress corresponding to the shear stress produced in a simple tension test for yield strength (15, p. 152). The Mohr circle predicts that yielding will begin when (15, p. 152):

$$\tau_{max} = S_y/2 \qquad (4.1.3)$$

Hence, the mean stress is given by $S_m = 2\tau_{max}$.

Although both these failure theories are based on yielding as the failure criterion much experimental data indicates that they apply as well when fracture is the failure criterion as represented by the static ultimate strength.

For the maximum shear stress theory the resultant stress vector magnitude will be given by;

$$S_r^2 = (S_a)^2 + (S_m)^2 \qquad (4.1.4)$$

$$S_r^2 = \left\{(S_a)^2 + (2\tau)^2\right\}^{1/2} \qquad (4.1.5)$$

If the maximum shear stress theory is used to relate the shear stress to the mean stress the resultant stress vector is referred to as stress vector II.

The resultant stress vector must be described by both a magnitude and a direction. A stress ratio was previously defined as the ratio of alternating stress to mean stress. It can be seen that the stress ratio will vary with the strength theory which relates the shear stress to mean stress. Hence, for the stress vector where the Von Mises Hencky theory was used the stress ratio becomes:

$$r_1 = S_a / \sqrt{3}\,\tau \qquad (4.1.6)$$

For the second stress vector in which the maximum shear stress theory is used to relate shear stress to mean stress:

$$r_2 = S_a / 2\tau \qquad (4.1.7)$$

For both stress ratio cases the data had variability, described by the standard deviation of r (σ_r), which was quite small. The mean values of r and the corresponding standard deviation of each of the cycle life groups is given in Table 4.1.2. Because the variability of r was small in each case the resultant stress vector was assumed to lie on the stress ratio axis, defined by the average value of r. Referring to Figure 4.1.1 it can be seen that the angle Θ, along which the resultant stress vector is oriented is given by:

$$\Theta = \tan^{-1} (S_a/S_m) \qquad (4.1.8)$$

The orientation of the stress vector is thus specified by the mean stress ratio, $\bar{r}$, for each cycle life group. For each data point in a cycle life group, it was possible to use the PDP-8 Computer to perform the calculation to obtain values for S_r. After the S_r values specified by Equations (4.1.2) and (4.1.5) were obtained for each of the data points, it was possible to compute a mean $\overline{S_r}$ and a standard deviation (σ_{S_r}) which then specified a strength distribution. These were then plotted along the mean $\bar{r}$-axis. After the values of $\bar{S}_r$ and σ_{S_r} were obtained the Kolmogorov-Smirnov test was used to determine if the normal or the lognormal frequency functions could be accepted as representing the strength distributions.

Table 4.1.2 Mean and Standard Deviation of Stress Ratios.

Cycle Life Range	Mean $\bar{r}$	Standard Deviation $\sigma_{\bar{r}}$
N = 1,000-3,500		
Stress Vector I	3.514	0.1200
Stress Vector II	3.043	0.1306
N = 6,000-9,000		
Stress Vector I	3.498	0.1490
1	0.875	0.0290
Stress Vector II	3.029	0.1296
	0.757	0.0254
N = 20,000-40,000		
Stress Vector I	3.508	0.1430
	0.729	0.0890
Stress Vector II	3.043	0.1239
	0.631	0.0188
N = 60,000-90,000		
Stress Vector I	3.422	0.1720
	0.872	0.0910
Stress Vector II	2.963	0.1492
	0.755	0.0171
N = 90,000-200,000		
Stress Vector I	0.804	0.0556
	0.439	0.0710
Stress Vector II	0.696	0.0482
	0.382	0.0110

4.2 Computer Method

Three computer programs of varying complexity were used to determine the strength distributions discussed in this chapter. The first of these, a PDP-8 computer program referred to as BAR I, used an input of bending stress and shear stress to obtain a value of S_r when the Von Mises Hencky strength theory was used. For a shear stress (and alternating stress) it performs the following calculations. It first calculates a mean stress from a shear stress:

$$S_m = \sqrt{3}\tau \tag{4.2.1}$$

and then performs the operations required by Equation 4.1.2:

$$S_r = \left\{(S_a)^2 + (\sqrt{3}\tau)^2\right\}^{1/2} \tag{4.2.2}$$

The second computer program referred to as BAR II which is also a PDP-8 program, performs the calculations required by the maximum shear theory to relate the shear stress to mean stress:

$$S_m = 2\tau \tag{4.2.3}$$

BAR II then performs the calculations required by Equation 4.1.5:

$$S_r = \left\{(S_a)^2 + (2\tau)^2\right\}^{1/2} \tag{4.2.4}$$

A flow chart, variable definitions and computer listing of the PDP-8 programs BAR I and BAR II is given in Appendix E.

After the individual values for the resultant stress vector magnitudes for each specimen were computed the data was then submitted to the CDC-6400 program ASMERG which made the following calculations. The mean and standard deviation of S_r for each cycle life group and stress ratio was calculated. These values are denoted by $\bar{S}_r$ and σ_{S_r}. In addition the Kolmogorov-Smirnov goodness of fit test, for a normal and lognormal distribution, was conducted on each of the strength distributions. The coefficients of skewness and kurtosis were determined for each strength distribution. A flow chart, variable definitions and computer listing of program CYTOFR is given in Appendix C.

4.3 Results

For the two strength theories considered, Von Mises Hencky and maximum shear stress, the results of the calculations to determine the resultant stress vector magnitudes are given in Table 4.3.1. In addition these tables present the stress ratio mean for each cycle life group as well as the calculated value for the mean stress for each strength theory considered. Tables 4.3.2 and 4.3.3 present the mean and standard deviation of the resultant stress vector magnitude for each stress ratio by cycle life group. Table 4.3.4

presents the ultimate strength distribution of an ungrooved test specimen. Table 4.3.5 presents the Kolmogorov-Smirnov $/D/_{max}$ values for each cycle life group for both the Von Mises-Hencky strength theory as well as the maximum shear stress theory.

Based on the Kolmogorov-Smirnov test, in no case can the proposed distributions, normal or lognormal, for the resultant stress vector be rejected at the ninety percent confidence level. In ten out of fifteen resultant stress vector distributions the lognormal distribution had smaller $/D/_{max}$ values. For the normal and lognormal the $/D/_{max}$ difference was quite small, the difference occuring usually in the third decimal place. Because of this slight difference, it cannot be said that either the normal or lognormal distributions fit the data better, rather that both the normal and lognormal distributions fit the strength data equally well.

The third and fourth statistical moments, coefficients of skewness and kurtosis, give little insight into the nature of the underlying distribution. The "knowledge of the third moment gives almost no clue as to the shape of the distribution" (5, p. 109).

Table 4.3.1 Cycles to Failure Data, Bending and Shear Stress Data and the Resultant Stress Vector Magnitudes S_r (I) and S_r (II) for the Von Mises Hencky and the Maximum Shear Stress Theory.

r	Test #	Cycles to Failure	Bending Stress S_a	Shear Stress τ	$S_r = \sqrt{3}\tau$	S_{r_1}	$S_r = 2\tau$	S_{r_2}
∞	10	22,544	93,522					
∞	11	27,464	96,858					
∞	12	27,250	96,460					
∞	13	21,080	101,920					
∞	14	27,024	96,460					
∞	17	21,192	99,921					
∞	19	22,886	99,617					
∞	20	23,640	94,636					
∞	21	27,558	99,232					
∞	22	21,204	96,270					
∞	23	20,576	100,521					
∞	25	25,196	100,428					
∞	27	24,304	101,374					
3.820	366	32,624	84,356	12,749	22,081.9	87,198	25,498	88,125.4
2.347	368	37,089	83,254	13,905	24,084.2	86,668	27,810	87,776.0
3.393	376	36,494	83,710	14,243	24,669.6	87,269	28,486	88,424.1
3.707	435	37,298	83,012	12,921	22,392.0	85,979	25,856	86,945.5
3.565	439	27,981	83,984	13,603	23,561.1	87,226	27,206	88,280.7
3.415	440	34,797	83,789	14,167	24,538.0	87,308	28,334	88,450.1
3.470	445	38,072	82,945	13,802	23,905.8	86,321	27,604	87,417.7
3.634	453	39,054	84,081	13,360	23,140.2	38,207	26,720	88,224.6
3.456	461	34,291	81,318	13,587	23,533.4	84,655	27,174	85,738.2
3.572	463	36,673	81,651	13,189	22,844.0	84,786	26,378	85,806.1
3.520	590	37,982	82,516	13,535	23,443.3	85,782	27,070	86,842.8
3.439	592	22,176	81,171	13,626	23,600.9	84,532	27,262	85,623.6
3.248	593	25,836	83,127	14,779	25,598.0	86,979	29,558	88,225.7

Table 4.3.1 Cycles to Failure Data, Bending and Shear Stress Data and the Resultant Stress Vector Magnitudes S_r (I) and S_r (II) for the Von Mises Hencky and the Maximum Shear Stress Theory.

r	Test #	Cycles to Failure	Bending Stress S_a	Shear Stress τ	$S_m = \sqrt{3}\tau$	S_{r_1}	$S_m = 2\tau$	S_{r_2}
∞	125	2,973	144,126					
∞	126	2,973	144,982					
∞	132	2,884	145,994					
∞	134	2,765	145,405					
∞	425	2,471	143,580					
∞	426	1,584	141,357					
∞	130	3,063	142,003					
∞	131	3,033	143,727					
∞	133	3,181	145,563					
∞	135	3,181	145,141					
∞	136	3,271	145,719					
3.644	326	1,581	156,834	24,846	43,034.5	162,631	49,592	164,518
3.615	327	1,310	154,085	24,607	42,620.6	159,871	49,214	161,754
3.600	329	1,280	152,516	24,458	42,362.5	158,290	48,916	160,158
3.475	331	1,697	152,897	25,403	43,999.0	159,102	50,806	161,117
3.298	332	1,607	148,381	24,977	44,993.5	155,053	51,954	157,214
3.452	333	1,399	144,429	24,156	41,839.4	150,367	48,312	152,295
3.582	334	1,756	149,849	24,152	41,832.5	155,579	48,304	157,442
3.372	338	1,756	147,508	25,258	43,748.2	153,859	50,516	155,918
3.598	586	1,131	154,410	24,776	52,913.3	160,262	49,552	162,166
3.743	627	1,191	150,130	23,157	40,109.1	155,396	46,314	157,111
3.276	628	1,786	146,097	25,747	44,595.1	152,752	51,494	154,906

Table 4.3.1 Cycles to Failure Data, Bending and Shear Stress Data and the Resultant Stress Vector Mangitudes S_r (I) and S_r (II) for the von Mises Hencky and the Maximum Shear Stress Theory.

r	Test #	Cycles to Failure	Bending Stress S_a	Shear Stress τ	$S_m = 3\tau$	S_{r_1}	$S_m = 2\tau$	S_{r_2}
0.460	701	1.310	65,082	81,753	141,600	155,841	163,506	175,983
0.458	754	1,846	66,590	83,969	145,439	159,958	167,938	180,658
0.444	753	1,012	65,230	84,912	147,072	160,889	169,824	181,921
0.444	756	1,459	64,965	84,467	146,301	160,077	168,934	180,995
0.441	695	2,054	65,553	85,806	148,620	162,435	171,612	183,706
0.437	755	1,667	63,246	83,612	144,820	158,028	167,224	178,785
0.439	697	2,024	62,623	82,274	142,503	155,656	164,548	176,062
0.438	699	1,280	66,580	87,587	151,705	165,632	175,174	187,365
0.444	749	1,459	65,227	84,845	146,956	160,781	169,690	181,795
0.443	751	1,339	64,473	85,899	148,782	162,150	171,798	183,498
0.440	752	1,667	64,105	84,040	145,562	159,052	158,080	179,390
0.429	750	1,736	65,180	87,624	151,769	165,174	175,248	186,977
0.450	757	1,578	63,719	81,791	141,666	155,336	163,582	175,554
0.428	707	1,042	63,929	86,243	149,377	162,482	172,486	183,952
0.430	710	1,250	64,169	86,237	149,367	162,567	172,474	184,024

Table 4.3.1 Cycles to Failure Data; Bending and Shear Stress Data and the Resultant Stress Vector Magnitudes S_r (I) and S_r (II) for the von Mises Hencky and the Maximum Shear Stress Theory.

r	Test #	Cycles to Failure	Bending Stress S_a	Shear Stress τ	$S_m = \sqrt{3}\tau$	S_{r_1}	$S_m = 2\tau$	S_{r_2}
0.701	223	32,129	83,646	68,922	111,937.0	145,765	137,844	161,238
0.709	226	24,356	83,726	68,195	118,117.0	144,782	136,390	160,038
0.730	228	24,653	88,221	69,792	120,883.0	149,652	139,584	165,126
0.763	230	21,004	92,382	69,946	121,150.0	152,354	139,892	167,643
0.722	233	23,110	87,641	70,105	121,426.0	149,750	140,210	165,348
0.749	235	25,157	87,265	67,282	116,536.0	145,588	134,564	160,383
0.733	242	28,243	83,208	65,556	113,546.0	140,771	131,112	155,287

Table 4.3.1 Cycles to Failure Data, Bending and Shear Stress Data and the Resultant Stress Vector Magnitudes S_r (I) and S_r (II) for the von Mises Hencky and the Maximum Shear Stress Theory.

r	Test #	Cycles to Failure	Bending Stress S_a	Shear Stress τ	$S_m = \sqrt{3}\tau$	S_{r_1}	$S_m = 2\tau$	S_{r_2}
∞	49	64,997	81,820					
∞	50	67,757	81,282					
∞	51	83,812	81,321					
∞	52	78,352	80,421					
∞	53	50,002	82,641					
∞	54	64,857	81,027					
∞	55	71,968	80,667					
∞	56	65,349	79,201					
∞	57	72,248	81,832					
∞	58	74,690	80,031					
∞	60	75,662	80,871					
∞	61	71,166	83,112					
∞	62	71,556	82,001					
∞	63	73,089	81,224					
∞	69	74,698	81,784					
3.466	459	81,590	81,840	13,632	23,611.3	85,178	27,264	86,262
3.627	470	82,870	74,217	11,814	20,462.5	76,986.2	23,628	77,887
3.484	472	72,244	74,567	12,358	21,404.7	77,578.4	24,716	78,556
3.222	476	65,219	73,984	13,257	22,961.8	77,465.3	26,514	78,592
3.344	487	75,905	75,816	13,091	22,674.3	79,134	26,182	80,209
3.213	490	65,635	73,689	13,243	22,937.6	77,176.4	26,486	78,304
3.552	596	62,123	73,998	12,028	20,833.1	76,874.7	24,056	77,810
3.444	597	68,076	74,723	12,528	21,699.1	77,810	25,056	78,812
3.202	498	75,369	73,949	13,333	23,093.4	77,471	26,666	78,610
3.675	599	69,237	73,757	11,589	20,072.7	76,440	23,178	77,313

Table 4.3.1 Cycles to Failure Data, Bending and Shear Stress Data and the Resultant Stress Vector Magnitudes S_r (I) and S_r (II) for the von Mises Hencky and the Maximum Shear Stress Theory.

r	Test #	Cycles to Failure	Bending Stress S_a	Shear Stress τ	$S_m = \sqrt{3}\tau$	S_{r_1}	$S_m = 2\tau$	S_{r_2}
0.866	209	65,844	78,735	52,499	90,930.9	120,282	104,998	131,239
0.905	207	77,840	73,613	46,988	81,385.6	109,738	93,976	119,375
0.884	210	69,148	76,937	50,229	86,999.2	116,139	100,458	126,535
0.850	211	72,006	75,594	51,371	88,977.2	116,754	102,742	127,555
0.885	213	67,600	77,469	50,512	87,489.4	116,858	101,024	127,308
0.864	215	70,190	77,000	51,451	89,115.8	117,774	102,902	128,522
0.854	387	62,242	79,297	53,632	92,893.3	122,136	107,264	133,393

Table 4.3.1 Cycles to Failure Data, Bending and Shear Stress Data and the Resultant Stress Vector Magnitudes S_r (I) and S_r (II) for the von Mises Hencky and the Maximum Shear Stress Theory.

r	Test #	Cycles to Failures	Bending Stress S_a	Shear Stress τ	$S_m = 3\tau$	S_{r_1}	$S_m = 2\tau$	S_{r_2}
∞	65	96,004	81,423					
∞	81	107,415	81,363					
∞	68	98,468	81,363					
∞	139	125,950	73,796					
∞	140	103,413	73,886					
∞	142	145,783	70,969					
∞	143	195,824	72,029					
∞	145	93,303	71,973					
∞	146	178,192	74,341					
∞	147	196,894	73,404					
∞	148	183;306	72,572					
∞	150	177,508	74,931					
∞	152	155,178	72,925					
∞	154	172,661	75,982					
∞	155	124,137	73,647					
∞	156	127,794	72,961					
∞	157	172,572	74,629					
∞	160	172,275	68,029					
∞	163	182,860	72,164					
0.933	245	149,945	69,404	42,972	74,429.7	101,768	85,944	110,469
0.793	252	137,327	62,227	45,304	78,468.8	100,148	90,608	109,918
0.758	253	131,957	61,573	46,930	81,285.1	101,973	93,860	112,254
0.777	254	104,367	61,337	45,607	78,993.6	100,011	91,214	109,919
0.758	256	129,228	62,835	47,856	82,889.0	104;014	95,712	114,495
0.785	257	101,193	62,479	45,945	79,579.1	101,175	91,890	111,119
0.728	258	167,735	61,711	48,956	84,794.3	104,373	97,912	115,237

Table 4.3.1 Cycles to Failure Data, Bending and Shear Stress Data and the Resultant Stress Vector Magnitudes S_r (I) and S_r (II) for the von Mises Hencky and the Maximum Shear Stress Theory.

r	Test #	Cycles to Failure	Bending Stress S_a	Shear Stress τ	$S_m = \sqrt{3}\tau$	S_{r_1}	$S_m = 2\tau$	S_{r_2}
0.755	259	159,280	61,169	46,793	81,047.9	100,540	93,586	111,803
0.733	261	143,201	62,304	46,535	80,601.0	101,874	93,070	111,999
0.763	262	135,962	62,632	47,380	82,064.5	103,235	94,760	113,588
0.784	263	120,565	64,645	47,622	82,483.7	104,798	95,255	115,110
0.797	264	117,895	64,993	47,102	81,427.2	104,185	94,264	114,449
0.060	394	100,879	69,812	46,847	81,141.4	107,040	93,694	116,843
0.832	396	140,350	68,358	47,430	82,151.2	106,870	94,860	116,924
0.853	398	110,851	70,621	47,794	82,781.6	108,312	95,588	118,846
0.869	400	142,404	70,806	47,048	81,489.5	107,954	94,096	117,761
0.393	402	103,856	72,280	46,709	80,902.4	108,488	93,418	118,116
0.777	260	99,383	64,180	47,669	82,565.1	104,576	95,338	114,928
0.425	497	121,656	58,284	79,234	137,237	149,101	158,468	168,847
0.426	499	103,290	59,257	80,344	139,160	151,251	160,688	171,266
0.464	503	144,517	59,779	74,447	128,946	142,129	148,894	160,446
0.435	504	162,675	59,265	78,707	136,325	148,650	157,414	168,201
0.441	506	115,137	59,165	77,465	134,173	146,639	154,930	165,843
0.437	507	188,215	59,452	78,499	135,964	148,394	156,998	167,878
0.420	508	116,923	59,766	80,413	139,279	151,561	160,826	171,572
0.453	509	136,034	61,123	77,945	135,005	148,197	155,890	167,445
0.439	510	153,626	58,455	76,934	133,254	145,511	153,868	164,598
0.452	512	116,685	60,915	77,726	134,625	147,766	155,452	166,961
0.437	513	161,395	59,738	78,924	136,700	149,183	157,848	168,774
0.434	514	161,693	59,271	78,301	136.487	148,801	157.602	168,379

Table 4.3.1 Cycles to Failure Data, Bending and Shear Stress Data and the Resultant Stress Vector Magnitudes S_r (I) and S_r (II) for the von Mises Hencky and the Maximum Shear Stress Theory.

r	Test #	Cycles to Failure	Bending Stress S_a	Shear Stress τ	$S_m = \sqrt{3}\tau$	S_{r_1}	$S_m = 2\tau$	S_{r_2}
∞	30	8,088	113,381					
∞	36	8,860	112,017					
∞	38	8,925	113,778					
∞	39	8,376	113,778					
∞	41	7,717	113,856					
∞	43	7,622	114,975					
∞	44	7,112	114,111					
∞	47	8,015	115,003					
3.591	532	8,722	113,488	18,247	31,604.7	117,807	36,494	119,211
3.305	605	6,489	112,543	19,658	34,048.7	117,581	39,316	119,213
3.226	607	7,531	113,640	20,337	35,224.7	118,974	40,674	120,700
3.683	612	6,638	113,010	17,715	30,683.3	117,101	35,430	118,434
3.552	614	6,846	116,719	18,970	32,857.0	121,256	37,940	122,731
3.423	622	6,191	114,662	19,340	33,497.9	119,455	38,680	121,010
3.593	623	7,561	116,545	18,726	32,434.4	120,974	37,452	122,415
3.576	629	6,400	118,284	19,099	33,080.4	122,823	38,198	124,299
3.537	630	6,281	113,195	18,479	32,006.6	117,633	36,948	119,076
0.895	411	6,906	108,545	70,032	121,299	162,774	140,064	177,200
0.898	413	8,603	112,635	72,445	125,479	168,616	144,890	183,521
0.901	415	6,072	112,046	71,815	124,387	157,411	143,630	182,165
0.898	416	6,102	110,456	71,042	123,048	165,352	142,084	179,968
0.854	417	7,799	109,768	74,217	128,548	169,037	148,434	184,612
0.890	418	6,043	111,971	72,577	125,707	168,344	145,154	183,323
0.832	419	6,162	110,311	76,554	132,595	172,482	153,108	188,708
0.829	422	6,221	110,426	76,904	133,202	173,022	153,808	189,343
0.884	423	7,829	111,529	72,843	126,168	168,396	145,686	183,475

Table 4.3.2 Mean, Standard Deviations and ± 3 Limits of Resultant Stress Vector for the von Mises-Hencky Theory.

Life Range - Cycles	Mean psi	Standard Deviation psi	+3σ psi	-3σ psi
N=1,000-3,500				
r = ∞	144,327	1,538	148,934	139,710
r = 3.514	156,651	3,683	167,700	145,602
r = 0.441	150,404	3,261	170,007	150,801
N=6,000-9,000				
r = ∞	113,862	954	116,697	111,027
r = 3.498	119,228	1,999	125,225	113,231
r = 0.875	168,382	3,170	177,892	158,872
N=20,000-40,000				
r = ∞	98,247	2,683	106,300	90,196
r = 3.507	86,301	1,062	89,487	83,115
r = 0.729	146,952	3,883	158,701	135,203
N=60,000-90,000				
r = ∞	81,282	993	84,821	78,303
r = 3.422	78,211	2,550	85,861	70,561
r = 0.872	117,097	3,900	128,797	105,397
N=90,000-200,000				
r = ∞	74,336	3,556	85,004	63,668
r = 0.804	104,074	8,517	112,591	95,557
r = 0.439	148,137	2,325	155,112	141,162

The Goodman surfaces and diagrams generated by this method are presented in Figure 4.3.1 through Figure 4.3.10 for the various cycle life groups and strength theories.

4.4 Discussion as to Validity

The Goodman surfaces generated illustrate that for cycle life ranges which are well below infinite life the allowable combinations of bending and shear stress are much larger in magnitude than combinations of the same biaxial stress which could be sustained by a specimen for an infinite life range (Figure 4.4.1 is a Goodman Surface for a period of infinite life). As the cycle life groups mean value increases the corresponding combination of bending and shear stress continues to decrease toward the value which is presented in the infinite life diagram. A comparison of this surface to the surfaces generated for finite life periods, see Figure 4.3.9 illustrates the above conclusion.

The variability in the standard deviations of the resultant stress vector for stress ratios other than infinity and zero should be examined closely. This variability is larger in many cases than the variability of the bending stress and ultimate strength distributions used for the alternating and mean stress axis. In reviewing the methodology which was discussed, one finds that data used for the alternating stress distribution and the ultimate strength distribution

were taken from one series of tests. However, the data which was used to generate the strength distributions for ratios of 3.5, 0.825, and 0.44 were taken from a series of tests, each with their own variability. From the algebra of normal functions we see that when two standards deviations are added the resultant standard deviation becomes (16, p. 111):

$$\sigma_{x+y} = \sqrt{\sigma_x^2 + \sigma_y^2 + 2\rho\ \sigma_{x\ y}} \qquad (4.4.1)$$

where ρ is the correlating coefficient. If $\rho = 0$, assuming independence (16, p. 111):

$$\sigma_{x+y} = \sqrt{\sigma_x^2 + \sigma_y^2} \qquad (4.4.2)$$

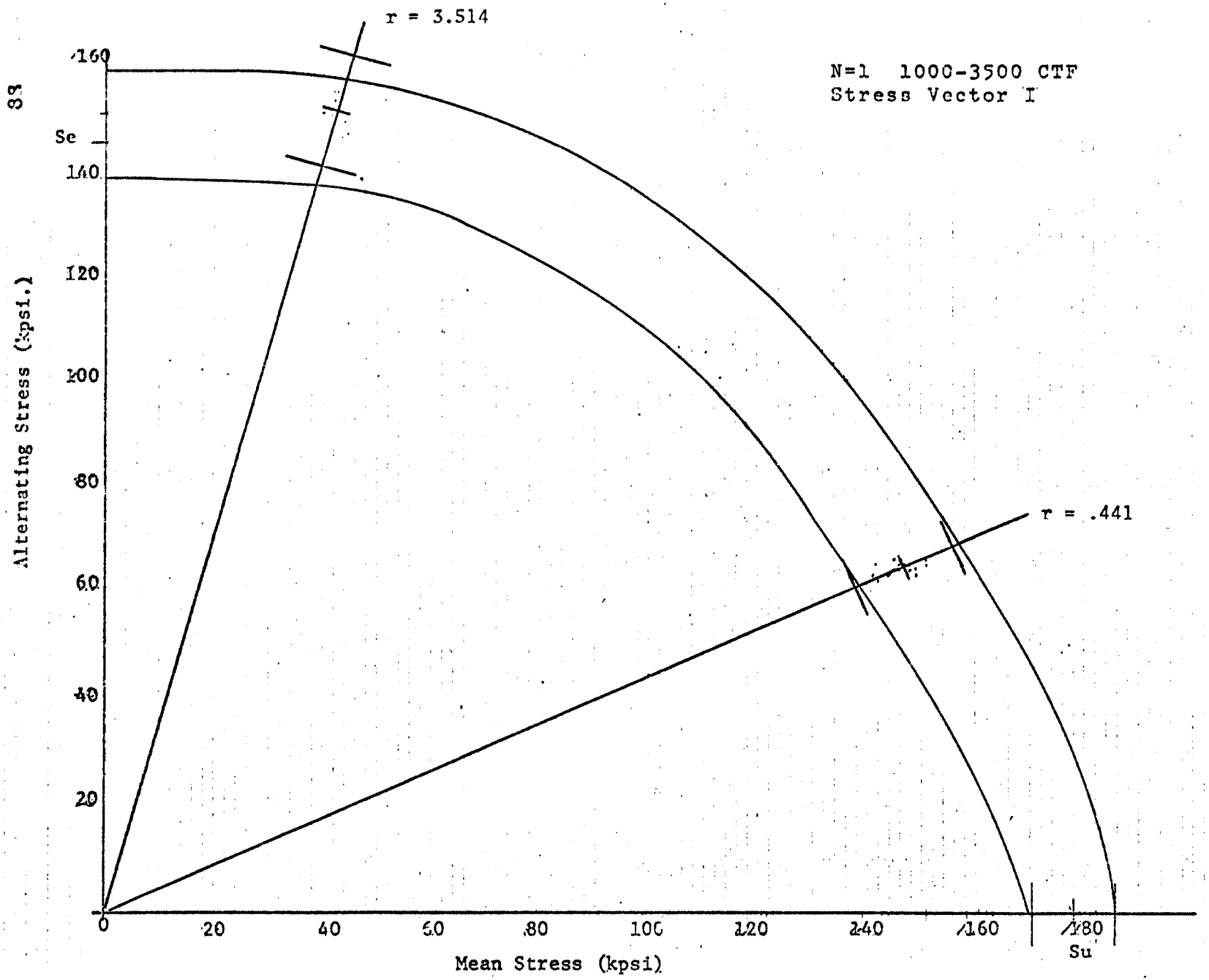

Fig. 4.3.1 Finite Life Goodman Diagram and Surface.

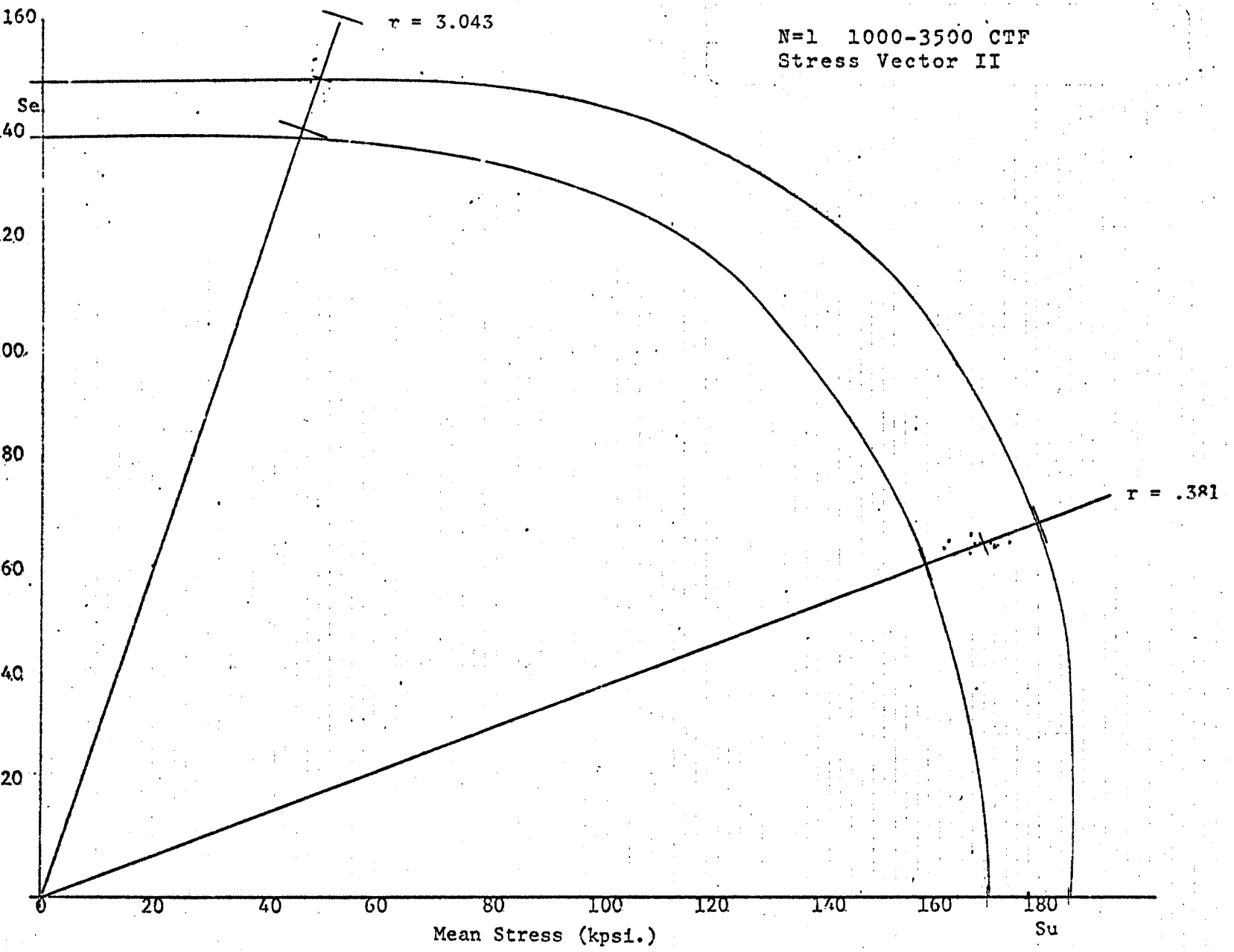

Fig. 4.3.2 Finite Life Goodman Diagram and Surface.

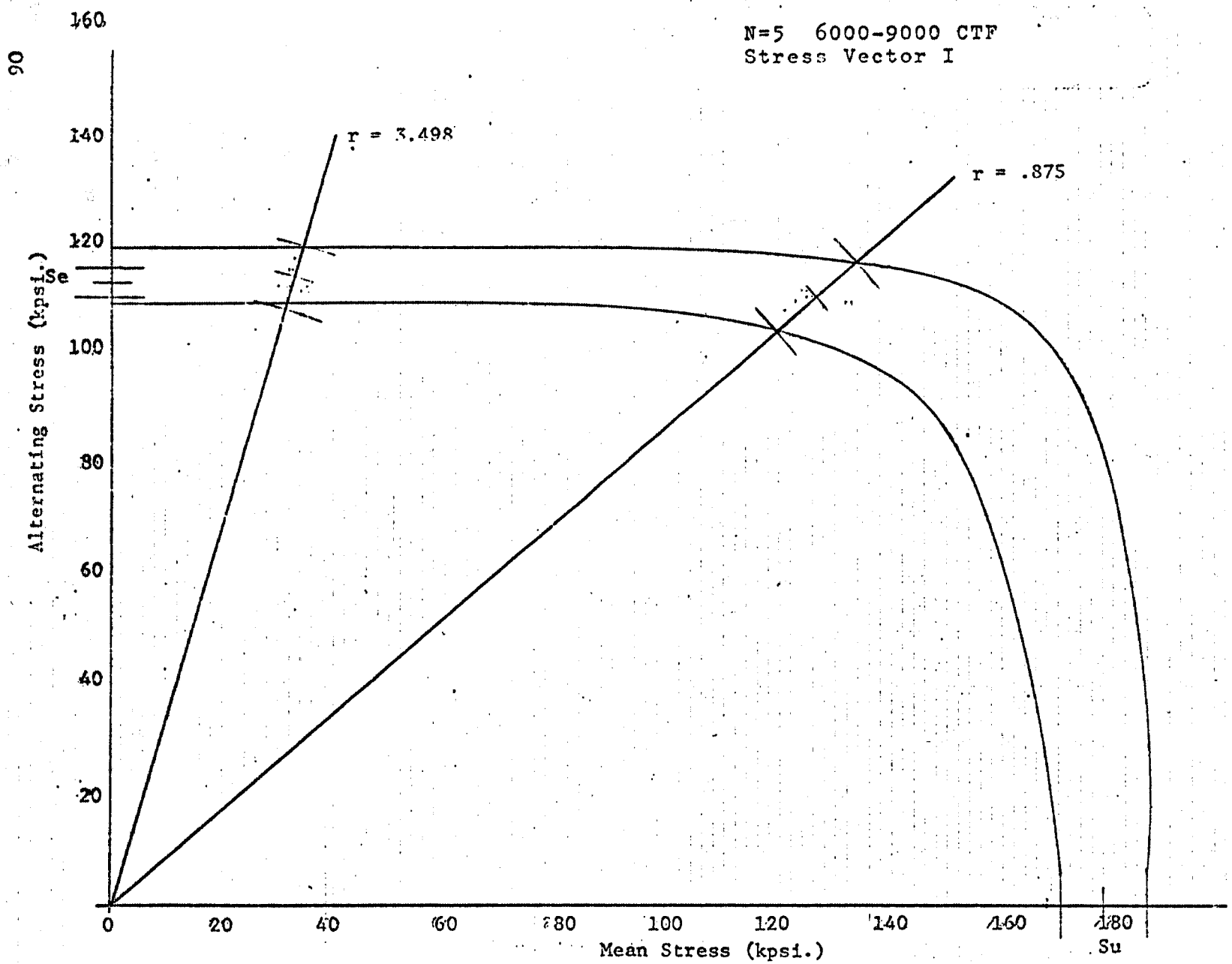

Fig. 4.3.3 Finite Life Goodman Diagram and Surface.

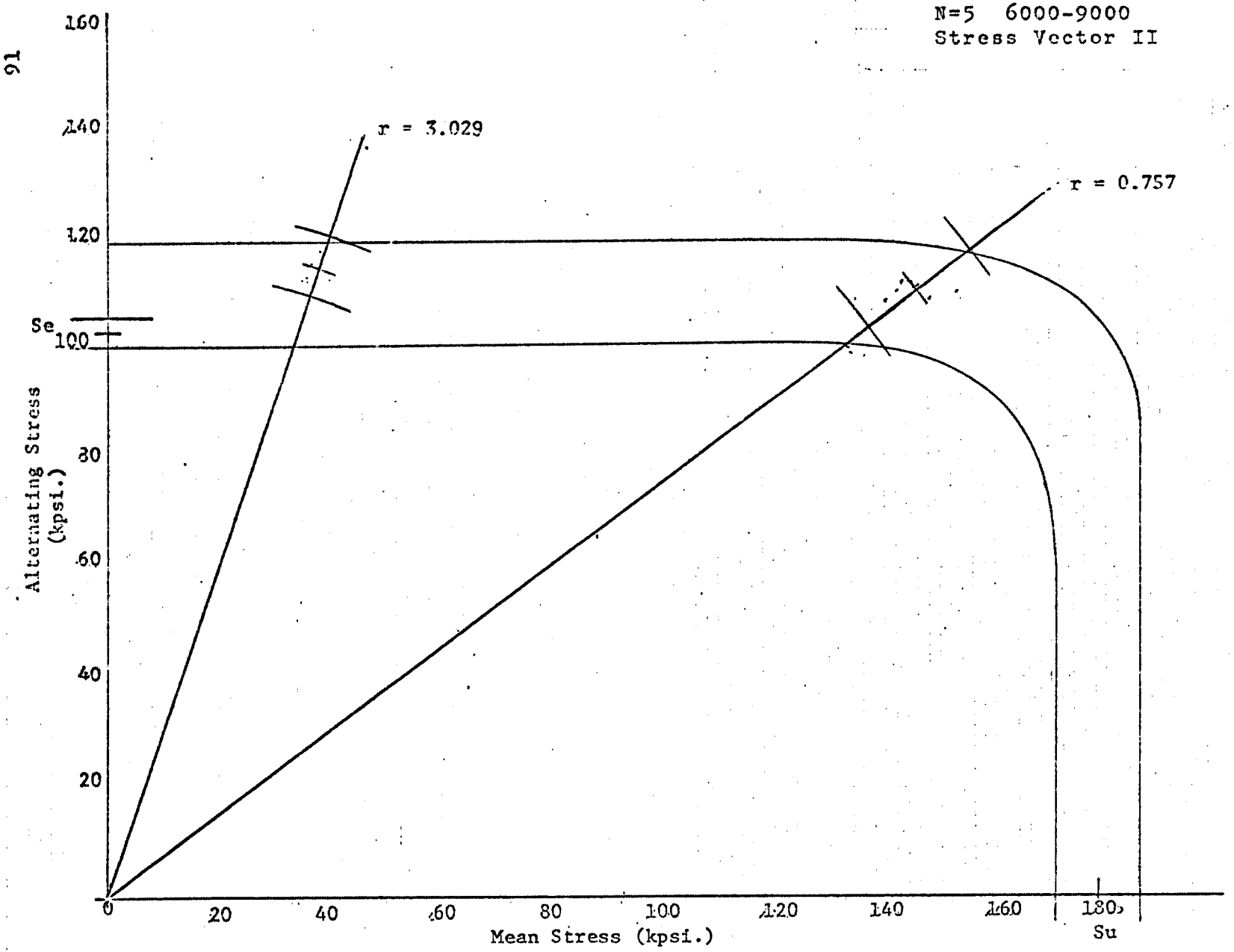

Fig. 4.3.4. Finite Life Goodman Diagram and Surface.

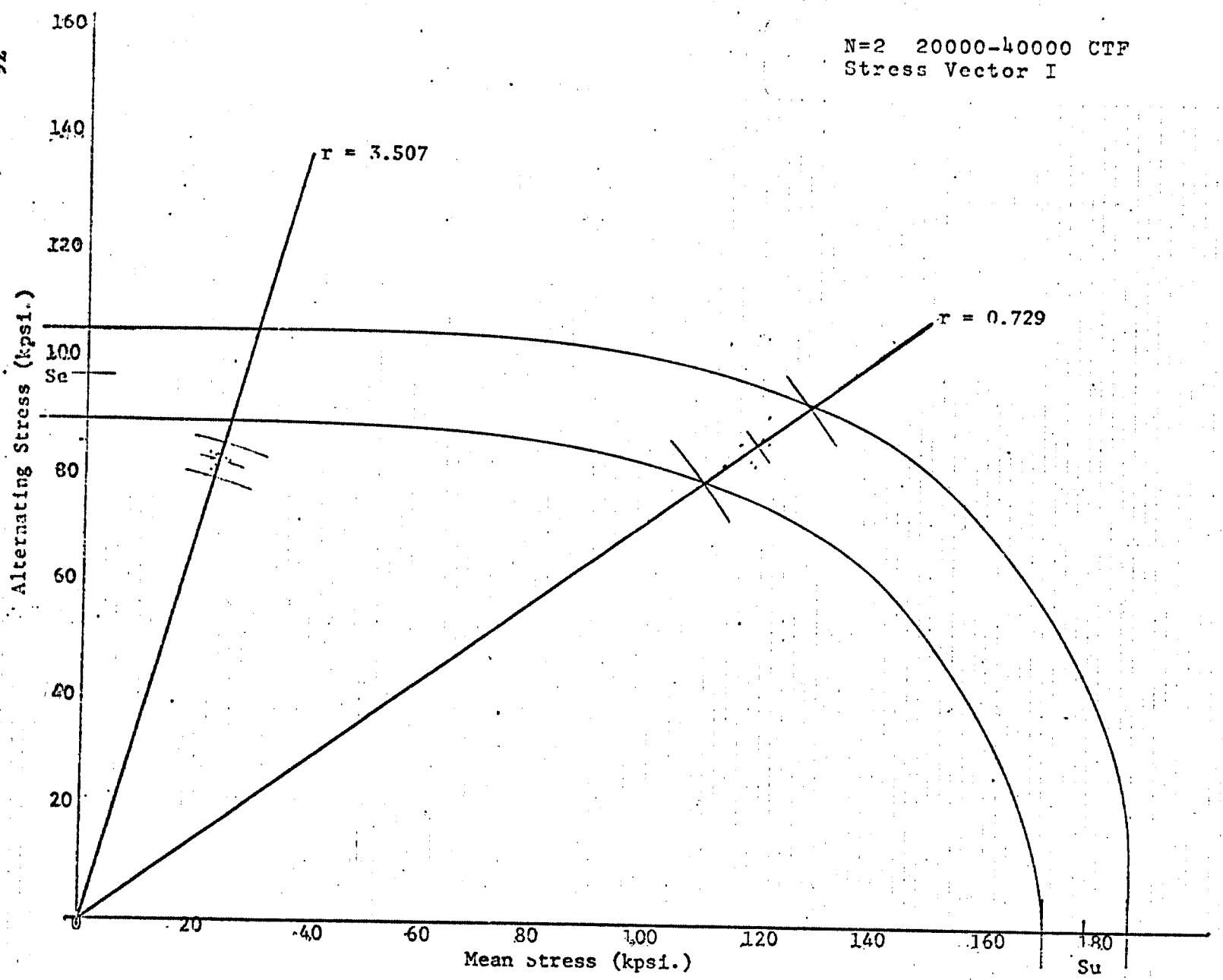

Fig. 4.3.5 Finite Life Goodman Diagram and Surface.

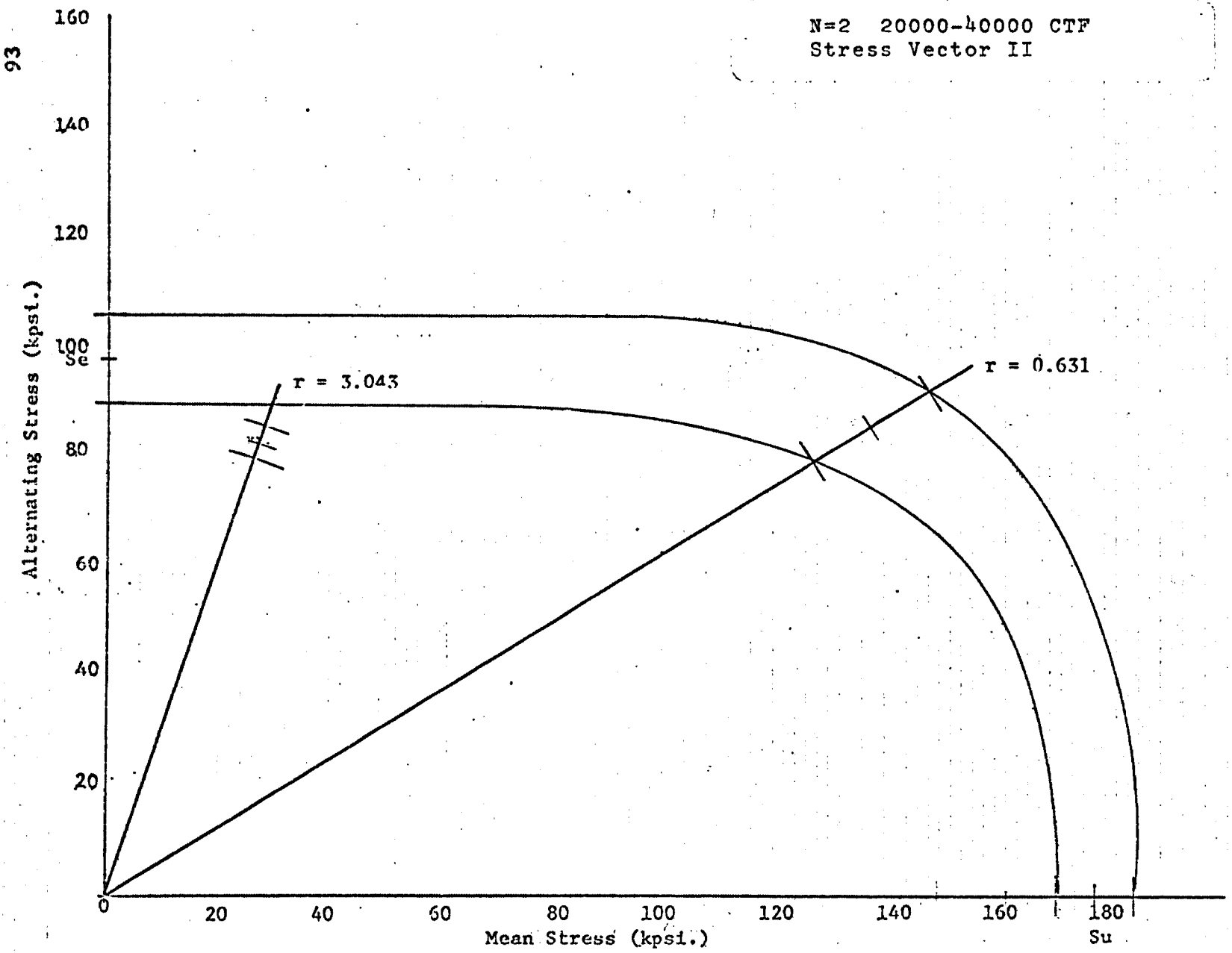

Fig. 4.3.6 Finite Life Goodman Diagram and Surface.

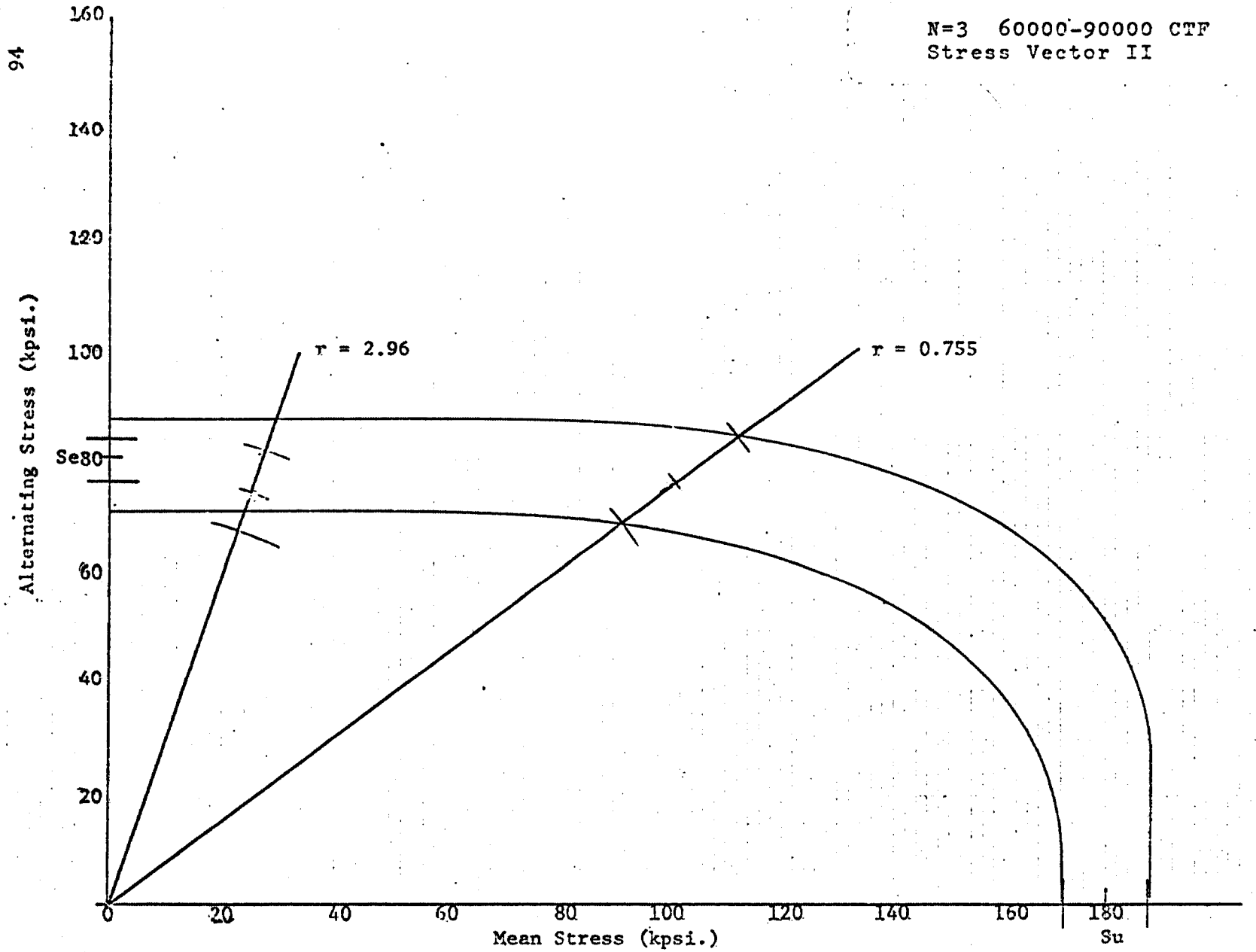

Fig. 4.3.7 Finite Life Goodman Diagram and Surface

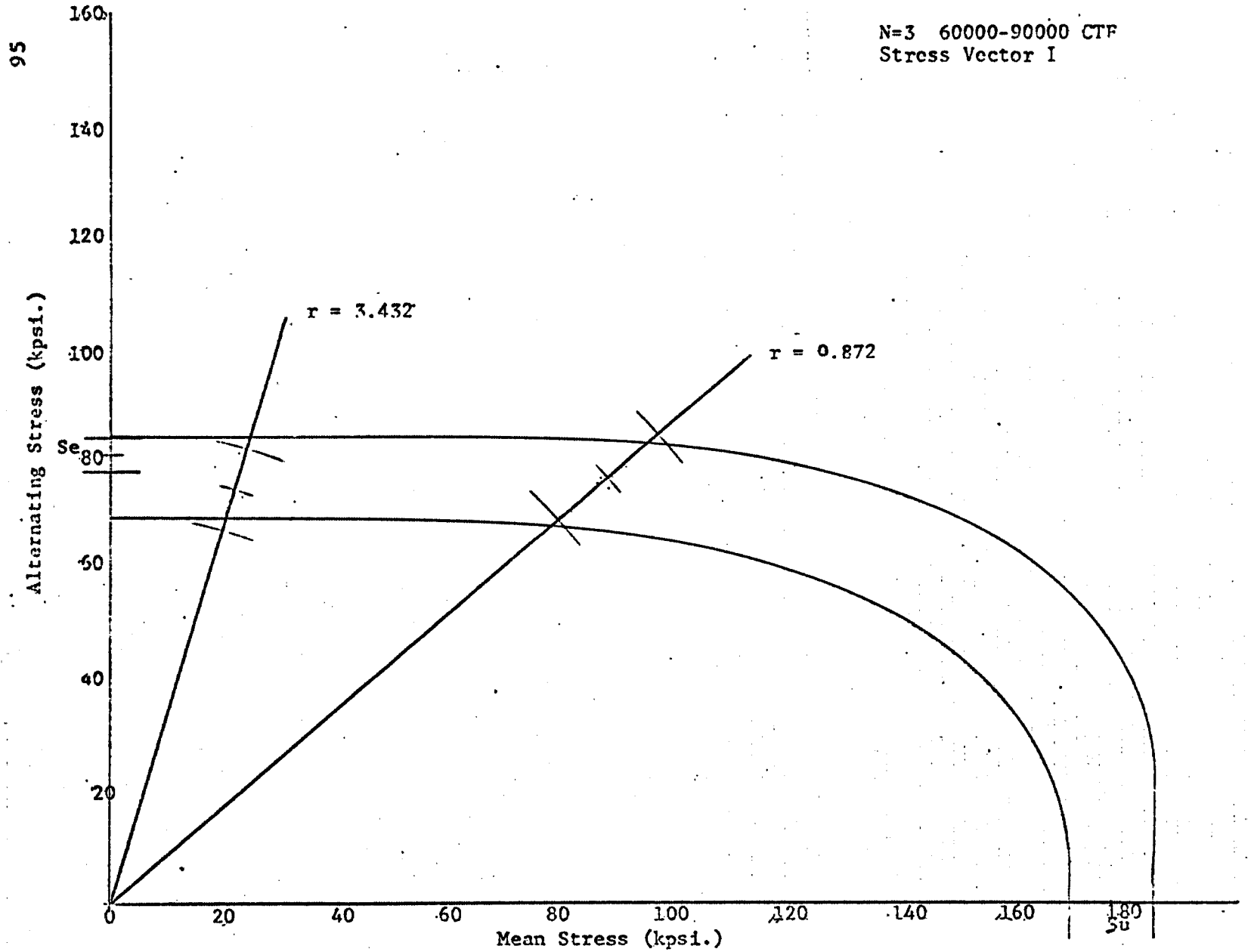

Fig. 4.3.8 Finite Life Goodman Diagram and Surface.

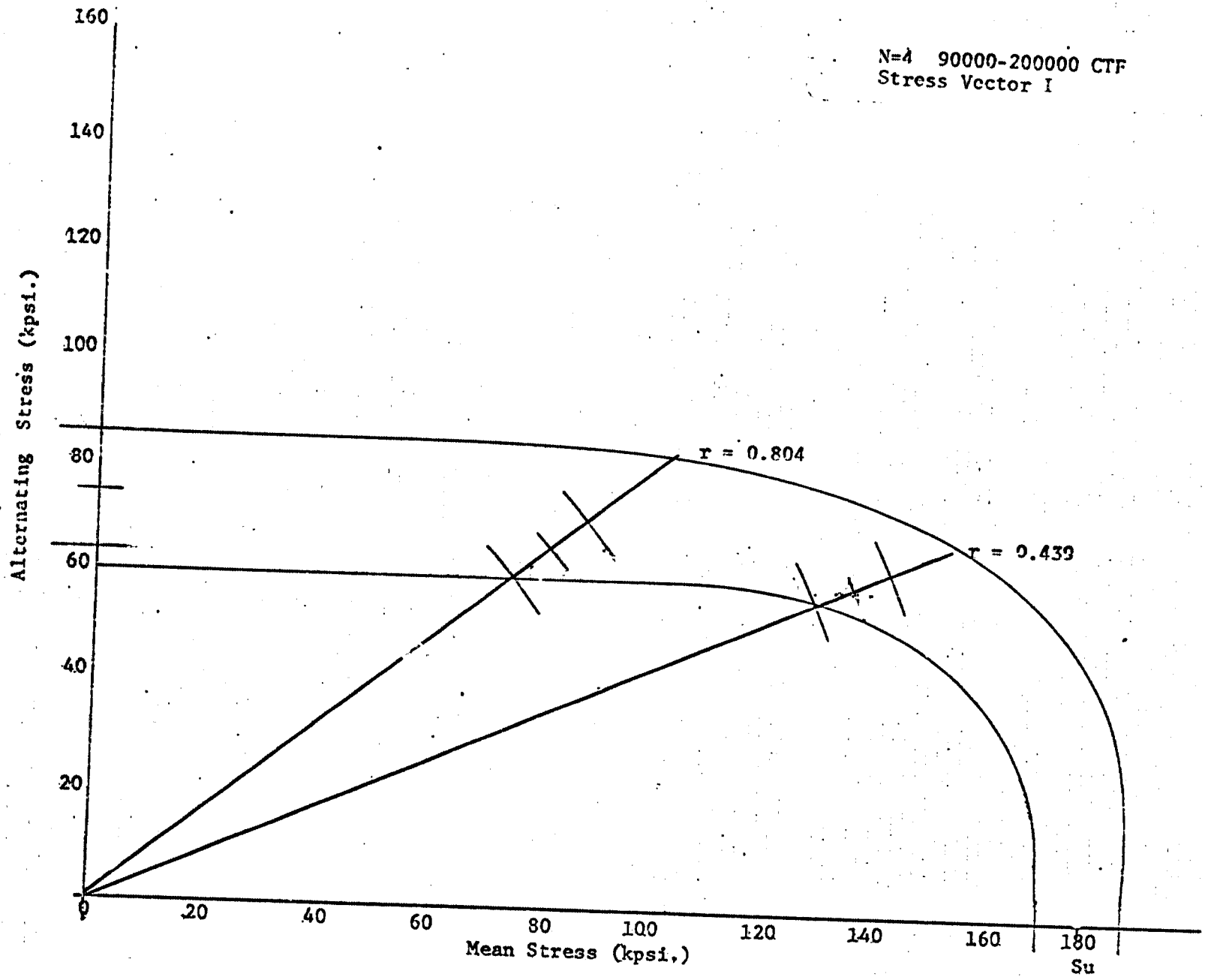

Fig. 4.3.9 Finite Life Goodman Diagram and Surface.

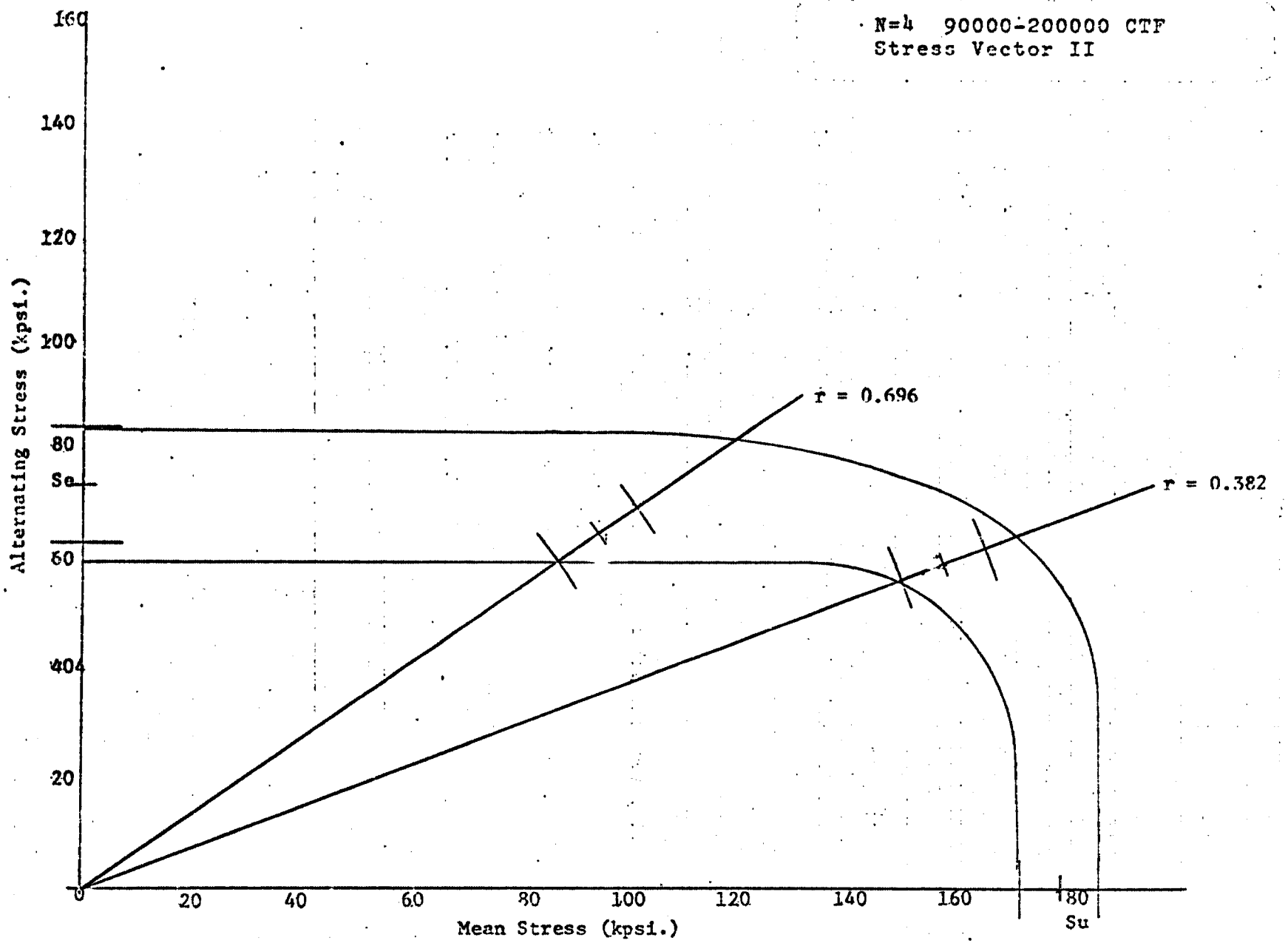

Fig. 4.3.10 Finite Life Goodman Diagram and Surface.

Table 4.3.3 Mean, Standard Deviation and ± 3 Limits of Resultant Stress Vector for the Maximum Shear Stress Equation.

Life Range - Cycles	Mean	Standard Deviation	$+3\sigma$	-3σ
	psi	psi	psi	psi
N=1,000-3,500				
r = 3.043	158,600	3,641	169,523	147,677
r = 0.381	181,411	3,704	192,523	170,299
N=6,000-9,000				
r = 3.029	120.787	2,007	126,808	114,766
r = 0.757	183,578	3,812	195,014	172,142
N=20,000-40,000				
r = 3.043	87,375	1,077	90,606	84,144
r = 0.631	162,152	4,178	174,686	149,518
N=60,000-90,000				
r = 2.960	79,236	2,586	89,994	71,478
r = 0.755	127,704	4,405	140,916	114,492
N=90,000-200,000				
r = 0.696	114,126	2,896	122,814	105,438
r = 0.382	167,554	2,742	175,780	159,328

Table 4.3.4 Ultimate Strength Distribution, Mean, Standard Deviation, and ± 3. Limits for Mean Stress Axis for Ungrooved Specimens.

	Mean	Standard Deviation	$+3\sigma$	-3σ
	psi	psi	psi	psi
r = 0	178,000	2,500	185,500	170,500

Table 4.3.4 Ultimate Strength Distribution, Mean, Standard Deviation, and ± 3 Limits for Mean Stress Axis for Ungrooved Specimens.

	Mean psi	Standard Deviation psi	$+3\sigma$ psi	-3σ psi
r = 0	178,000	2,500	185,500	170,500

Table 4.3.5 Kolmogorov-Smirnov $/D/_{max}$ Values for Stress Vectors I and II.

	Sample Size	NORMAL D-Stress Vector I	NORMAL D-Stress Vector II	LOGNORMAL D-Stress Vector I	LOGNORMAL D-Stress Vector II	D_{crit}
N = 1						
Endurance	11	0.1390	-	0.1406	-	0.35242
R = 3.514	11	0.1597	0.1703	0.1561	0.1667	0.35242
R = 0.441	15	0.1229	0.1256	0.1242	0.1270	0.30397
N = 2						
Endurance	13	0.1592	-	0.1553	-	0.32549
R = 3.508	13	0.2715	0.2738	0.2776	0.2799	0.31417
R = 0.784	7	0.1432	0.0824	0.1354	0.0748	0.35242
N = 3						
Endurance	15	0.1013	-	0.1007	-	0.30397
R = 3.422	10	0.3625	0.3650	0.3590	0.2935	0.3686
R = 0.818	7	0.1424	0.1538	0.1351	0.1464	0.3686
N = 4						
Endurance	19	0.2230	-	0.2136	-	0.27136
R = 0.805	18	0.1141	0.1299	0.1134	0.1277	0.27851
R = 0.44	15	0.1425	0.1186	0.156	0.1189	0.30397
N = 5						
Endurance	8	0.1462	-	0.1450	-	0.40962
R = 3.498	9	0.21526	0.22802	0.21538	0.22814	0.38746
R = 0.875	9	0.1958	0.1810	0.1929	0.1776	0.38746

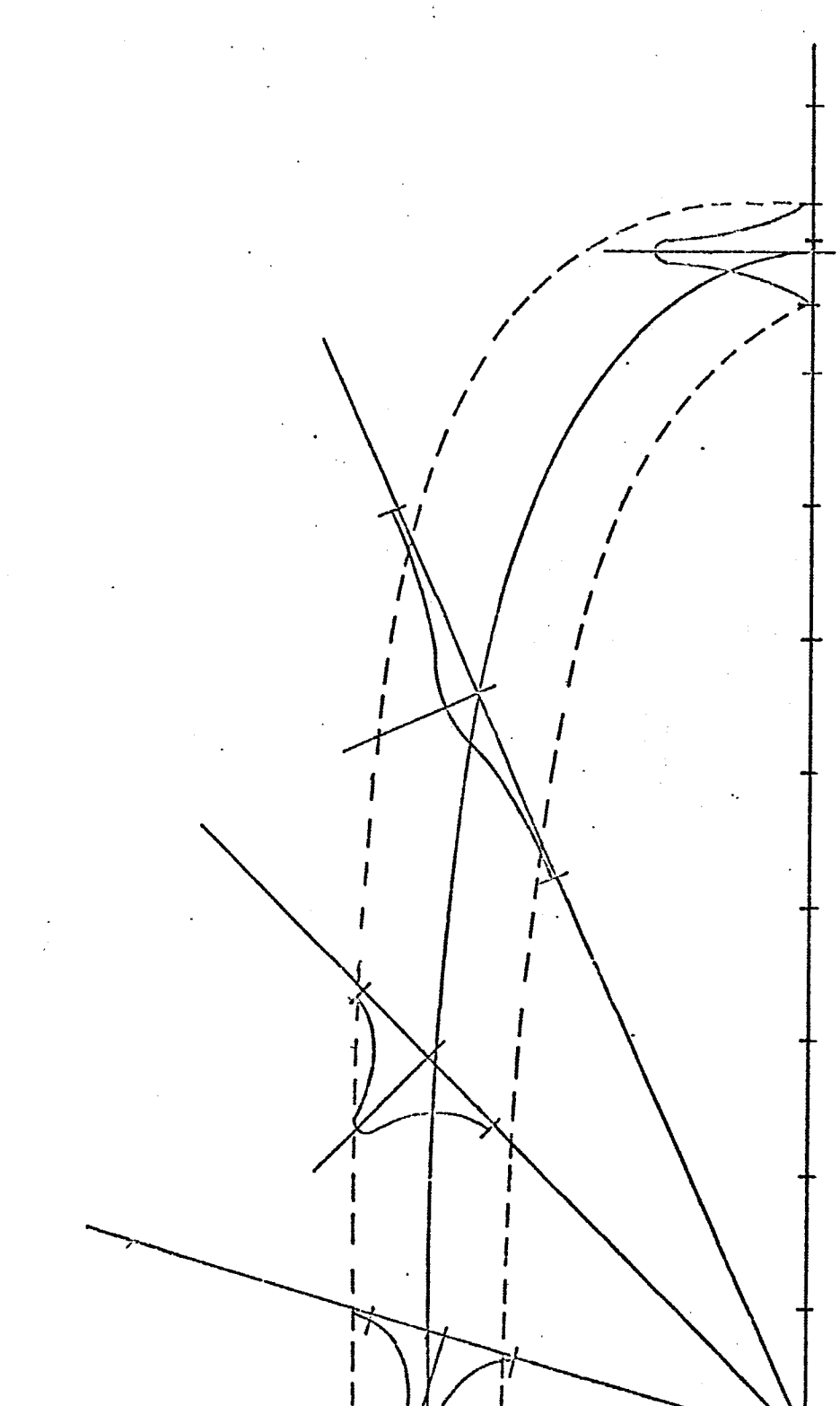

Fig. 4.4.1 Infinite Life Goodman Diagram 10^6 Cycles.

CHAPTER V

GENERATION OF FINITE LIFE GOODMAN DIAGRAM (METHOD II)

5.1 Theory

It is possible to place strength distributions which have been developed from cycles to failure distributions on statistical Goodman diagrams, as well as S-N diagrams. In Chapter III, the completed results of strength distributions developed by John Smith for the statistical S-N diagram were presented.

It is possible to place the strength distributions developed by the technique discussed in Chapter III on finite life Goodman diagrams. It is first noted that the vertical strength distributions developed in Chapter III are for a specific cycle life. This finite life Goodman diagram is then for this cycle life.

Figure 5.1.1 compares a strength distribution placed on a finite life Goodman diagram to that of the same strength distribution placed on a statistical S-N diagram. The ordinate axis of both the Goodman diagram and the statistical S-N diagram is the alternating stress level. Because of this the value of the mean of the alternating strength distribution when transformed from an S-N diagram to a finite Goodman diagram will not change. The stress ratio and alternating stress

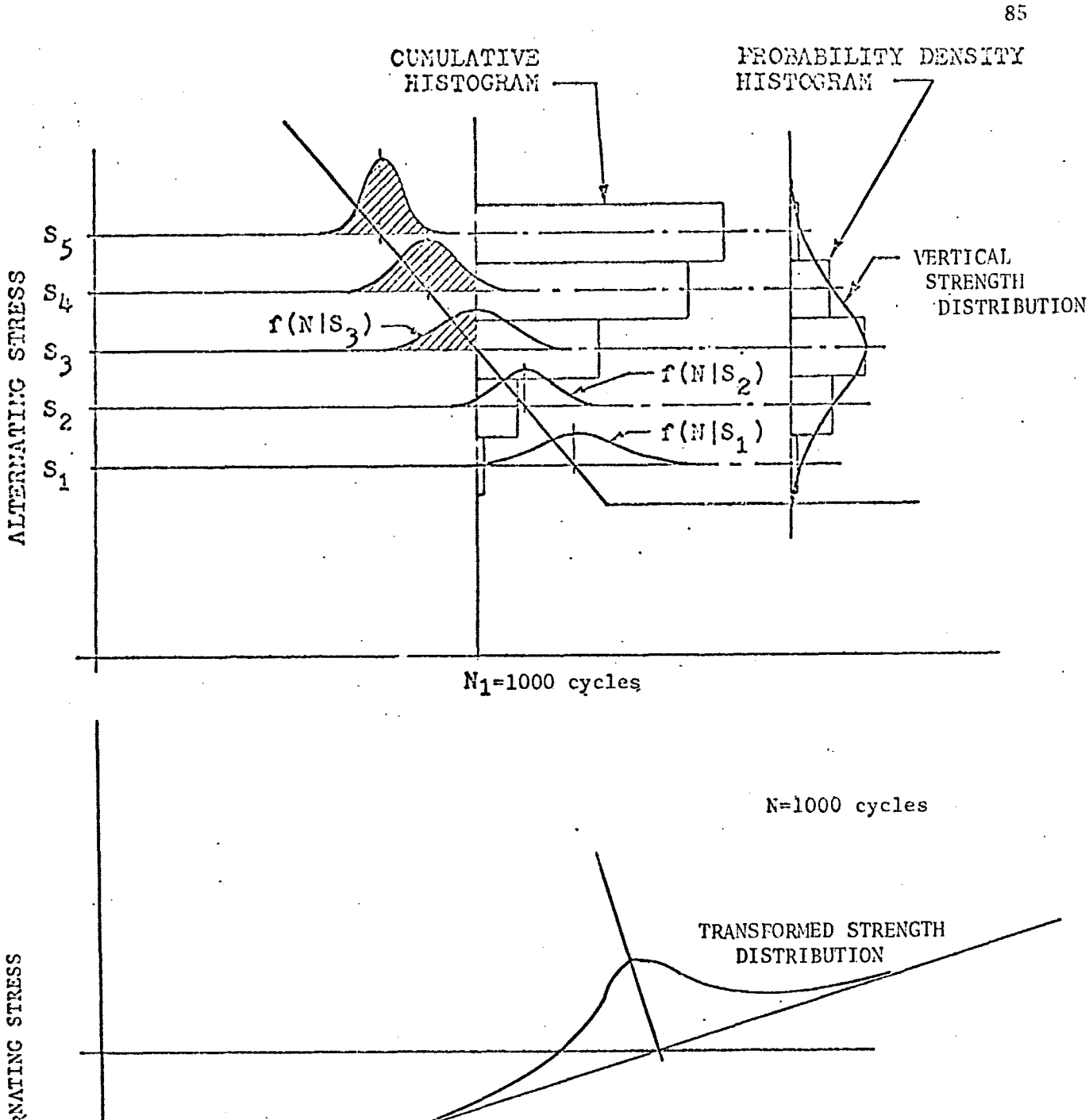

Fig 5.1.1 Comparison of Vertical Strength Distribution to A Strength Distribution Transformed to the Finite Life Goodman Diagram.

level, which are specified by the statistical S-N diagram, define the location of the mean of the strength distribution which is transformed to the finite life Goodman diagram.

The three sigma limits of the transformed strength distribution are not the same as that of the vertical strength distribution. Figure 5.1.2 depicts a strength distribution placed on the familiar coordinate axis of the Goodman diagram. The three sigma limits of the strength distribution placed on the stress ratio axis can easily be derived from the three sigma limits of the vertical strength distribution in the following manner.

Equate the upper and lower three sigma limits of the vertical strength distribution to S. The stress ratio, r, is equal to the alternating stress divided by the mean stress which referring to Figure 5.1.2 is equal to $\tan\theta$.

$$r = S_a/S_m = \tan\theta \qquad (5.1.1)$$

$$\theta = \tan^{-1}(r) \qquad (5.1.2)$$

The upper and lower three sigma limits of the transformed strength distribution are equal to S'. From Figure 5.1.2 it can be seen that:

$$\sin\theta = S_a/S' \qquad (5.1.3)$$

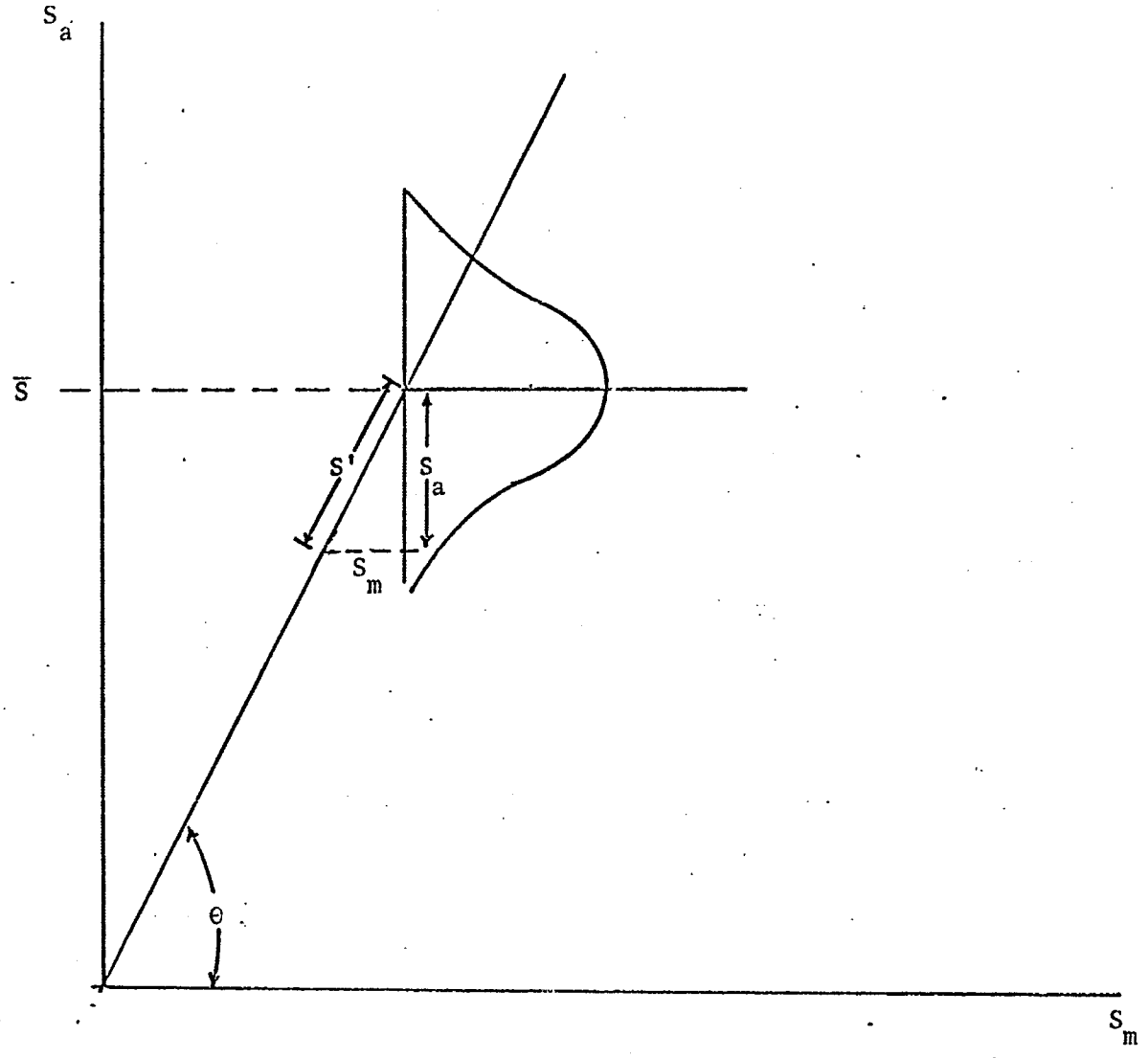

Fig. 5.1.2 Transformation of Vertical Strength Distribution's Upper and Lower Three Sigma Limits to the Stress Ratio Axis.

Solving equation 5.1.3 for S' and substituting equation 5.1.2 yields:

$$S' = S_a/\sin \epsilon \qquad (5.1.4)$$

$$S' = S_a/\sin \{ \tan^{-1}(r) \} \qquad (5.1.5)$$

If the value of r is known and the original value of the upper and lower three sigma limits are specified by the vertical strength distribution then the upper and lower three sigma limits of the transformed strength distribution can be placed along the stress ratio axis and are specified by equation 5.1.5.

Five finite life Goodman diagrams were developed by the transformation of vertical strength distribution to the stress ratio axis of the Goodman diagram. The finite life Goodman diagrams were developed for cycle lifes of 3,500, 9,000, 40,000, 90,000 and 200,000 cycles. Strength distributions placed on these finite life Goodman diagrams were at stress ratios of infinity, 3.50, 0.825, and 0.44. As discussed in Chapter VII of this report the strength distribution placed on the mean stress axis was taken to be that of the ultimate strength distribution of the grooved test specimen.

A PDP-8 computer program, ROTO, was developed to perform the calculations required by the transformation of the upper and lower three sigma limits as discissed in section 5.1. A flow chart,

variable definitions and computer listing of the ROTO program is given in Appendix E.

5.2 Results

The finite life Goodman diagrams developed by this method showing the strength surfaces for discrete cycles to failure are given in Figures 5.3.1 through 5.3.5. In Table 5.3.1 the alternating stress level of the mean of the strength distributions for each stress ratio as well as the transformed upper and lower three sigma limits of the strength distributions are given. The original parameters of the vertical strength distributions appear in Table 3.1.3 as starred quantities, as they were developed by this investigator to correspond with the cycle life values of Chapter IV. The ultimate strength distribution of the grooved and ungrooved test specimen are compared in Table 5.3.2.

5.3 Discussion as to Validity

The principle of transforming vertical strength distributions to the Goodman diagram as explained in Section 5.1 is a Straight forward procedure. The transformation is simply projection of a known distribution to a different plane which in this particular case is the stress ratio axis of the finite life Goodman diagram.

The vertical strength distributions have associated with them a cycle life value. It is possible because of this fact to develop finite life Goodman diagrams and surfaces from the valid vertical strength distributions. This method is consistent, in that the vertical strength distributions are all developed in the same manner, and hence, there is

no problem of differing variabilities caused by inconsistencies in the procedure of developing strength distributions at various stress levels. The elimination of the inconsistencies in procedure in developing strength distributions at various stress ratios is the principle advantage of rotating vertical strength distributions to the finite life Goodman diagram.

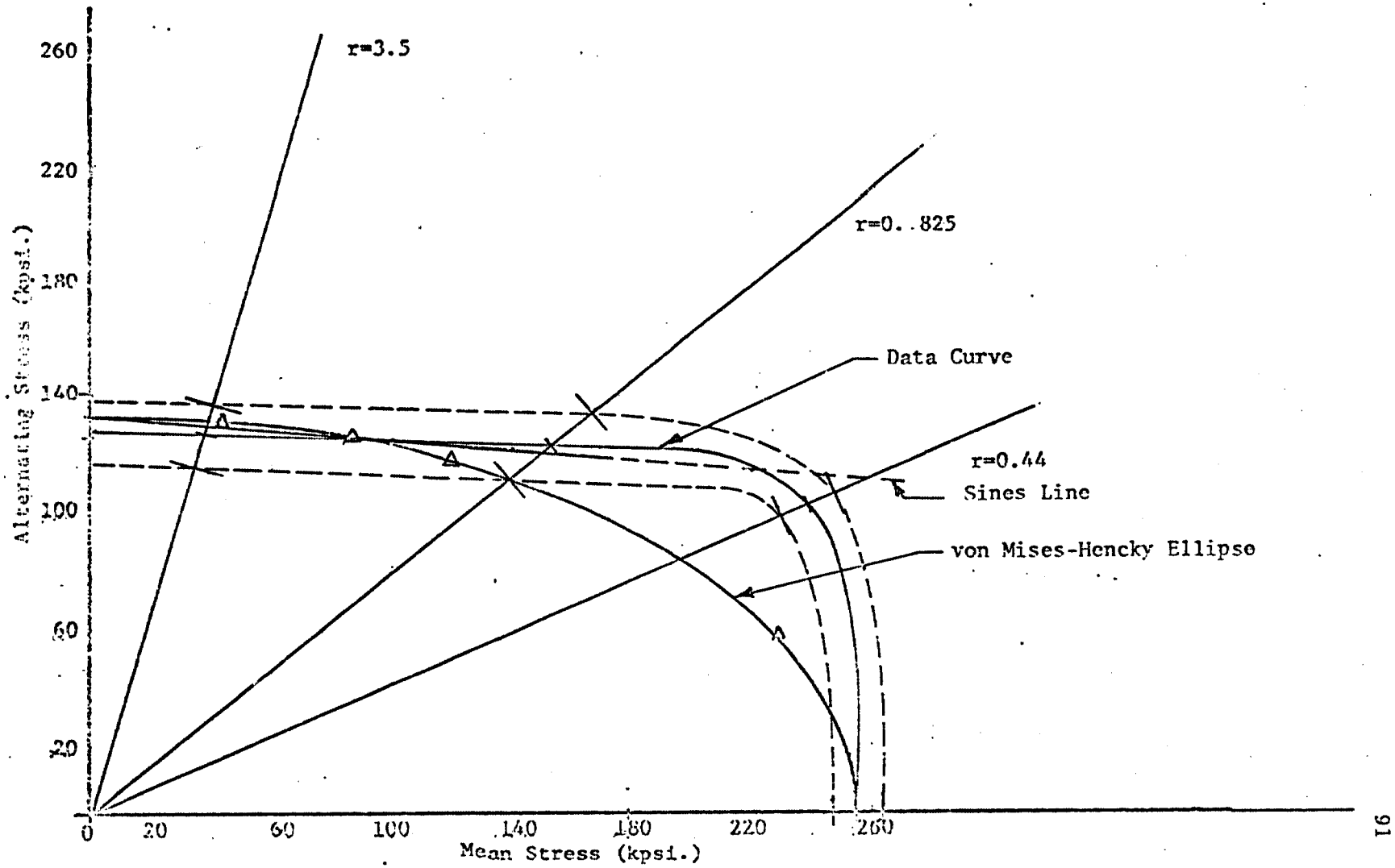

Fig. 5.3.1 Finite Life Goodman Diagram and Surface N=3500 cy.

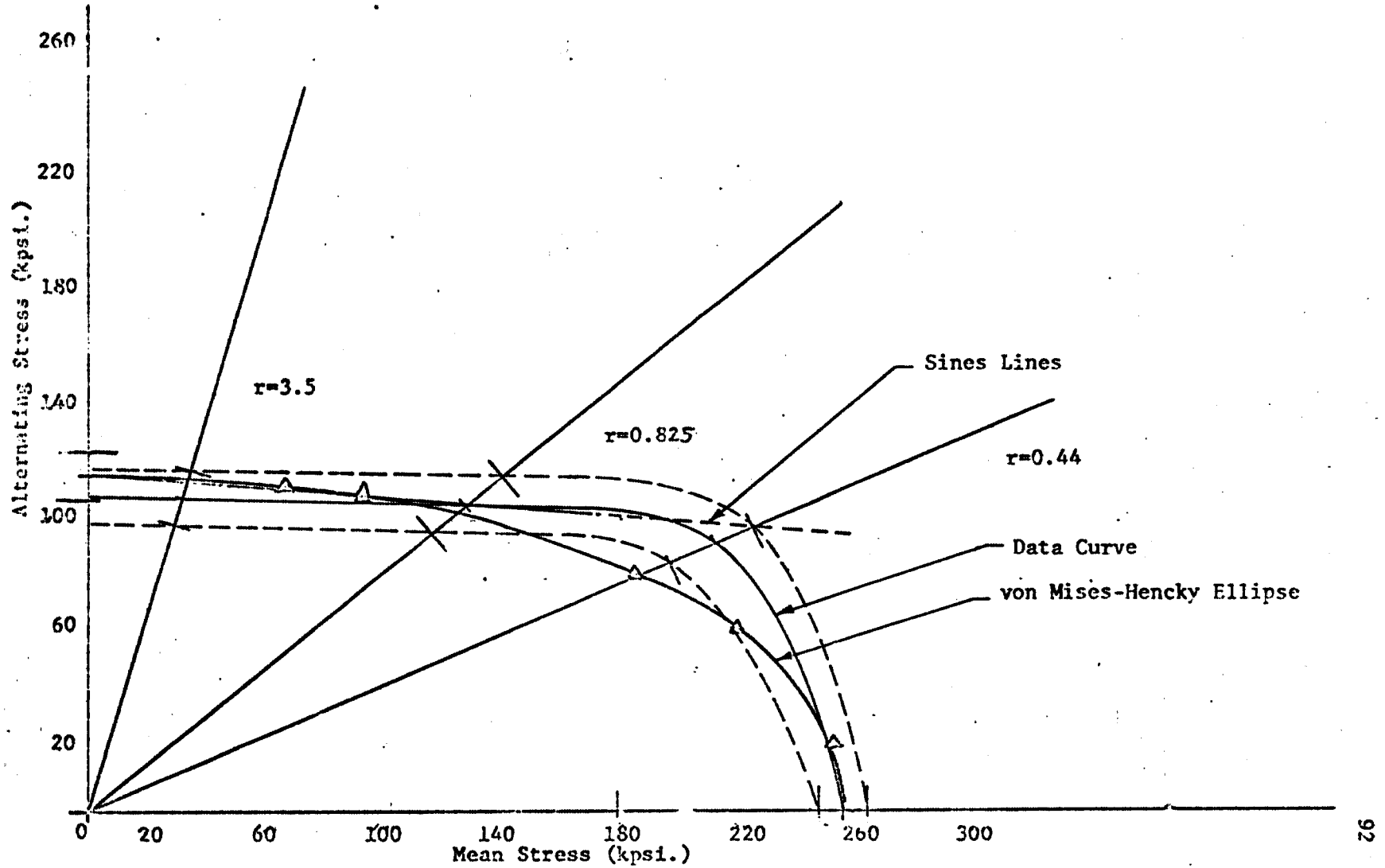

Fig. 5.3.2 Finite Life Goodman Diagram and Surface N=9,000 cy.

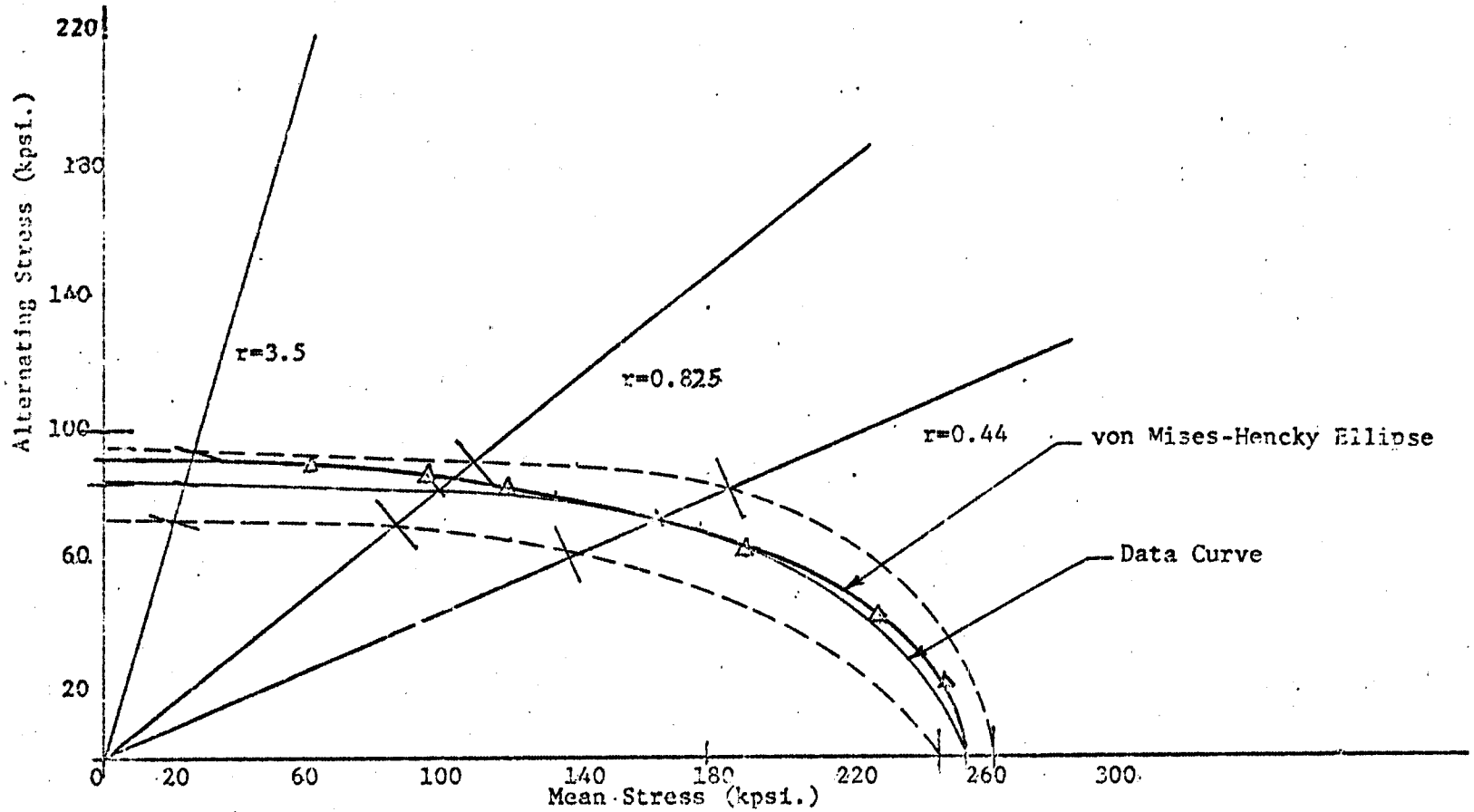

Fig. 5.3.3 Finite Life Goodman Diagram and Surface N=40,000 cy.

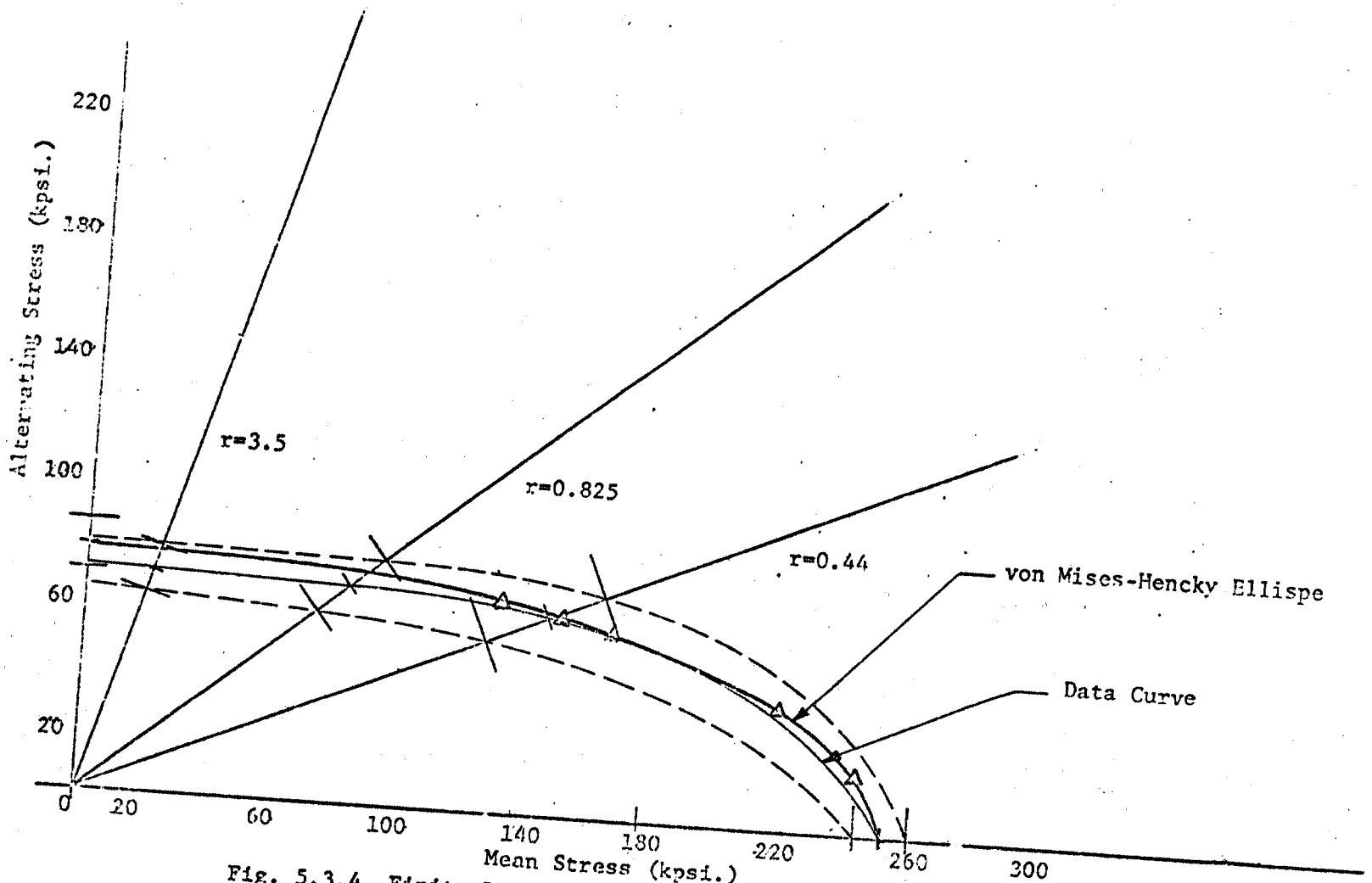

Fig. 5.3.4 Finite Life Goodman Diagram and Surface N=90,000 cy.

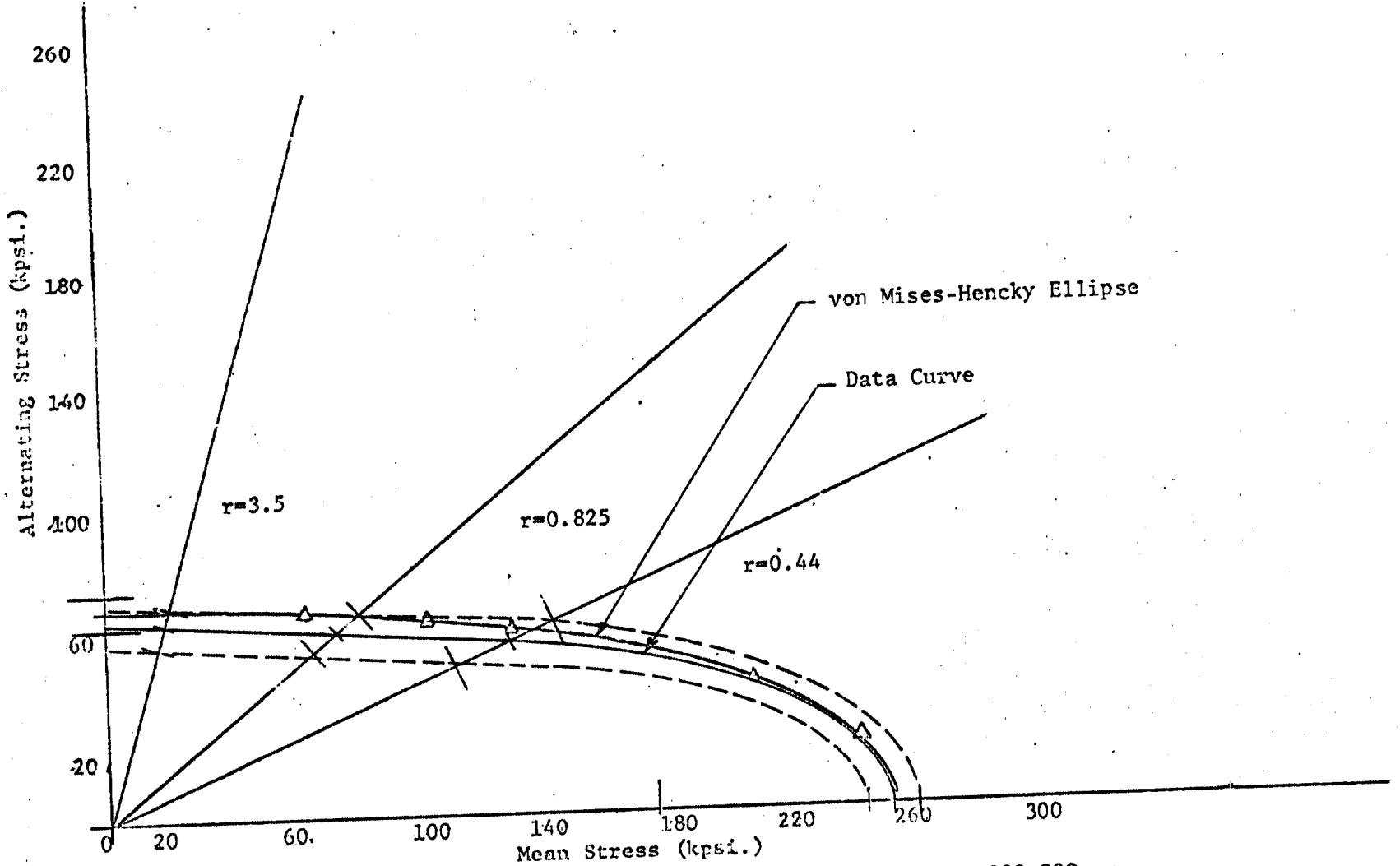

Fig. 5.3.5 Finite Life Goodman Diagram and Surface N=200,000 cy.

Table 5.3.1 Alternating Stress Level of the Mean and Standard Deviation, and ± Three Sigma Limits of Strength Distributions Placed on Stress Ratio Axes of the Finite Life Goodman Diagram.

	S_a	σ_{S_a}	-3σ	$+3\sigma$
N = 3,500				
∞	135,953	2,628	128,070	143,837
3.5	128,964	3,643	118,035	139,894
0.825	126,369	3,739	115,151	137,587
0.44	105,107	1,260	101,327	108,887
N = 9,000				
∞	115,926	2,907	107,205	124,647
3.5	108,523	3,213	98,883	118,163
0.825	105,645	3,308	95,722	115,569
0.44	92,390	2,002	86,384	98,396
N = 40,000				
∞	90,693	2,605	82,878	98,507
3.5	82,345	3,457	71,942	92,747
0.825	80,953	3,208	71,327	90,578
0.44	72,260	3,269	62,452	82,068
N = 90,000				
∞	79,054	2,539	71,437	86,671
3.5	71,967	2,393	64,787	79,147
0.825	69,970	2,927	61,189	78,750
N = 200,000				
∞	70,172	1,881	64,529	75,815
3.5	64,792	2,400	57,593	71,991
0.825	61,737	2,133	55,338	68,135
0.44	57,521			

Table 5.3.2 Comparison of Grooved and Ungrooved Specimen's Ultimate Strength Distribution.

	Mean	Standard Deviation
Grooved	255,300 psi	2,720 psi
Ungrooved	178,500 psi	2,500 psi

Table 5.3.2 Comparison of Grooved and Ungrooved Specimen's Ultimate Strength Distribution.

	Mean	Standard Deviation
Grooved	255,300 psi	2,720 psi
Ungrooved	178,500 psi	2,500 psi

CHAPTER VI

EVALUATION OF GENERATION OF FINITE LIFE GOODMAN DIAGRAMS

6.1 Evaluation of Previous Techniques in Developing Goodman Diagrams and Surfaces

The methodology which was presented in Chapters IV and V for the transformation of cycles-to-failure data to strength distributions and the resulting Goodman surfaces and diagrams will now evaluated. It appears that the method of rotating vertical strength distrinutions and placing them on the stress ratio axis of a Goodman diagram is the most uniform method of creating the Goodman surface. As discussed in Section 5.4 all distributions are created in the same manner which eliminates the problems of variability discussed in Section 4.4.

In viewing the general shape of both the finite life Goodman diagrams developed in Chapter IV and V the following conclusion can be drawn. By design each of the cycle life groups in both Chapters IV and V are similar. This was done for purposes of comparison. The curves shift progressively lower as cycle life value increase. The curves developed in both chapters are consistent in this respect. As cycle life design values decrease larger combinations of bending and shear stress are possible.

The two sets of finite life Goodman diagrams do have some inconsistencies. The ultimate strength distribution of the ungrooved test specimen was used as the static strength distribution in Chapter IV while the ultimate strength distribution of the grooved specimen was used in Chapter V. Both distributions were placed along the mean stress axis of the Goodman diagram. An explanation of these facts is in order at this time.

The method used in Chapter IV to generate the finite life Goodman diagrams and surfaces was completed in early February of 1971. At that time, there was doubt as to the geometry of the specimen to be used, consequently the conservative ultimate strength distribution of the ungrooved specimen was chosen. Although this doubt did exist the diagrams developed in Chapter IV did not seem to support the use of the higher ultimate strength of the grooved geometry specimens.

The finite life Goodman diagrams which were developed in Chapter V, in late March and early April of 1971, illustrated the critical importance of the geometry of specimen from which the static ultimate strength distribution was derived. All but the finite life Goodman diagram developed at 200,000 cycles showed the mean stress values at a stress ratio of 0.44 close to or above the ultimate strength distribution of the ungrooved test specimen. This fact, although quite alarming at first, made an investigation of the correct geometry of paramount importance and considerable effort, as exhibited in Chapter VII,

was made to resolve the question concerning the proper ultimate strength distribution to be placed along the mean stress axis.

6.2 Recommendations

The weaknesses and advantages of the two methods of generating Goodman surfaces and diagrams have been discussed. It is the opinion of this investigator that the method developed in Chapter V, that of forming vertical strength distributions from cycles to failure data and then transforming these to the stress ratio axis of a Goodman diagram, be considered as the appropriate method to be used when finite life Goodman diagrams are to be created from a large scale cycle to failure fatigue test program. Subsequently the results of Chapter V were weighted to a greater degree than those of Chapter IV in discussions dealing with the choice of geometry of test specimen used for the ultimate strength distribution in Chapter VII. This was also true in Chapters X and XI where the best empirical and theoretical math model of the Goodman diagram were sought.

In conclusion, the transformation of vertical strength distributions to the Goodman diagram is considered as the appropriate methodology to be used when large amounts of cycles-to-failure data are available. Chapter XIII considers a more efficient plan where it may be possible to generate Goodman surfaces with a minimum amount of actual fatigue testing.

CHAPTER VII

THE STATIC STRENGTH DISTRIBUTION TO BE PLACED ON THE MEAN STRESS AXIS OF FINITE LIFE GOODMAN DIAGRAMS

7.1 Introduction to Static Strength Distribution

In the previous chapters of this report, we discussed and developed several experimental methods of presenting fatigue data generated by relatively expensive and time consuming fatigue test programs. If however, this same information could be extracted from uniaxial static tests of materials the savings in time and effort would be tremendous. Chapters VIII and IX present several empirical and theoretical models of the Goodman diagram.

The development of relations, which take advantage of information obtained from static tests, to model fatigue data require that the following topics be investigated. For both the grooved and ungrooved geometry specimens which have been investigated, what are the equations which are used to determine the tensile yield, ultimate and breaking strengths? Secondly, is it possible to specify a theoretical strength distribution, such as the Gaussian normal or lognormal distribution, to each of these quantities? Of major concern in the development of the Goodman diagram for the grooved geometry specimen, subjected to the combined stress condition of alternating bending and constant shear stresses, is the determination

of the strength distribution to be used along the mean stress axis. It must be determined what strength parameter should be used along the axis and if the diagram is to model the behavior of grooved specimens, on which geometry specimen, grooved or ungrooved, should this strength parameter be based.

7.2 Calculation of Yield, Ultimate and Breaking Strengths

The calculation of static tensile strengths, is well documented throughout the literature. The yield strength is calculated by dividing the force initiating the yield by the cross-sectional area of the specimen. This cross-sectional area is based on the original diameter of the test specimen (6, p. 4). In the soft, ductile steels the yield strength is clearly marked by a yield point as shown in Figure 7.2.1a. In other materials where the yield point is less obvious, see Figure 7.2.1b, common paractice defines the yield load as the force which is required to give a 0.2 percent plastic offset (6, p. 45).

The ultimate tensile strength is defined as the maximum load sustained by a tensile test specimen divided by the "original" cross-sectional area. However, this calculation yields a parameter which is inaccurate and artificial. The load and area on which this parameter is based do not occur simultaneously. For most ductile materials the maximum load occurs after appreciable elongation which is obviously accompanied by a reduction in area. The ultimate tensile strength,

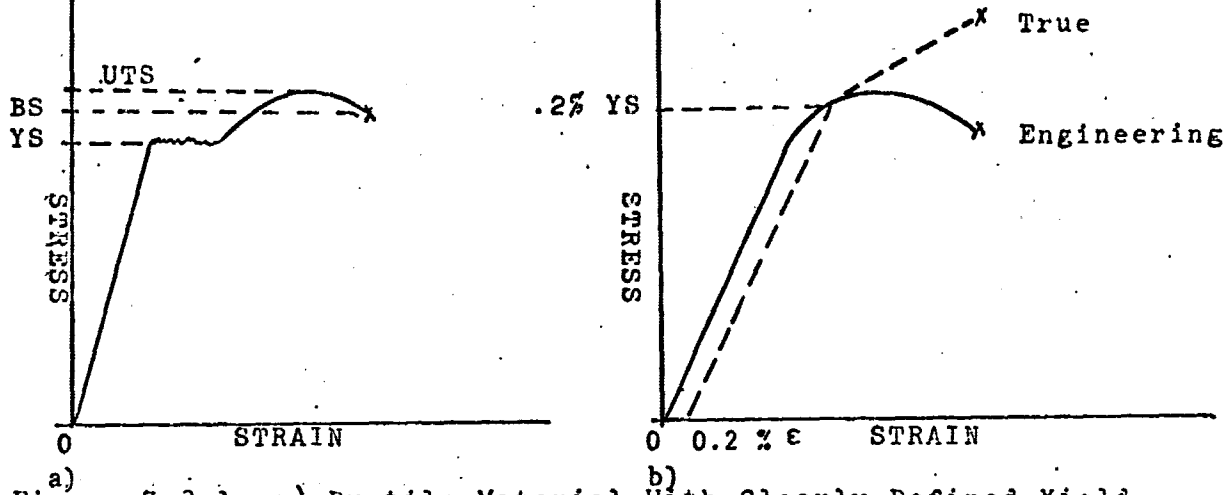

Figure 7.2.1 a) Ductile Material With Clearly Defined Yield Point. b) Ductile Material Without Marked Yield Point and Comparison of True Stress-Strain Curve versus Engineering Stress-strain Curve. (6, p. 5)

as calculated above, is, however, the most commonly sited parameter of material strength (7, p. 152).

By definition, both the ultimate and breaking strengths are based on the original cross-sectional area of the test specimen. Hence, the breaking strength is calculated by dividing the load at fracture by the original cross-sectional area. Figure 7.2.1a indicates that the breaking strength of a ductile material may be less than the ultimate tensile strength of the material. As necking and elongation occur in the test specimen the stress in the specimen continuously decreases. A more realistic measure of material strength is the tensile fracture stress. The fracture stress is determined by dividing the load just prior to fracture by the area measured just after fracture. Although the load decreases after the ultimate tensile stress is reached, the cross-sectional area decreases more rapidly which results in an increasing "true stress." Because of this the fracture stress is equal to or greater than the ultimate tensile stress (7, p. 154).

Based on the above discussion, it can be concluded that for the grooved and ungrooved specimens the ultimate and yield strength calculations should be based on the original cross-sectional area. The calculation of the breaking strength should be based on the reduced diameter measured after fracture.

7.3 Theoretical Strength Distributions of the Strength Parameters

The calculations of the strength parameters yield, ultimate and breaking strengths have been specified. The next point to be investigated is to determine if these strength parameters exhibit a known theoretical distribution. An effort to determine if the normal or lognormal distribution was favored for the three strength parameters previously discussed was initiated. This included gathering tensile test data from the research effort carried out under NASA Grant No. 03-002-044 at The University of Arizona. Tensile test data from Phase I and Phase II of the program was gathered for tensile yield, ultimate and fracture strength of both the grooved and ungrooved test specimens. This data was statistically reduced by the computer program CYTOFR, which has the ability of performing the following statistical operations; mean, standard deviation, coefficients of skewness and kurtosis, the $/D/_{max}$ value for the Kolmogorov-Smirnov goodness of fit test and the total Chi-Squared value, V_{n-1}, for the Chi-Squared goodness of fit test. The ASMERG program performs these statistical calculations for both the normal and the lognormal distributions.

Efforts to specify either the normal or lognormal distribution as favoring the yield, ultimate and breaking strengths of both the grooved and ungrooved specimens were not totally successful. The

Kolmogorov-Smirnov and Chi-Squared goodness of fit tests have the ability of only rejecting the normal and lognormal distributions as properly representing the data in question. Table 7.3.1 presents the results of the Kolmogorov-Smirnov and Chi-Squared goodness of fit test results. The mean and standard deviations of the strength parameters are given in Table 7.3.2. The breaking strength data in all but the Phase I specimens was found to be rejected as being either normally or lognormally distributed.

Previously the Kolmogorov-Smirnov test has been used as a basis in determining whether a normal or a lognormal distribution fits the data best based on which of these distributions had the smaller $/D/_{max}$ value (3, p. 47). However, because of the small difference in the maximum value of /D/ for both the normal and the lognormal distributions, the difference occuring in the second decimal place, it can not be concluded whether the normal or the lognormal distribution gives a better fit to the experimental data. It can, however, be said that neither the normal or the lognormal distribution can be rejected as distributions representing the yield, and ultimate strength of both the grooved and ungrooved specimens.

Table 7.3.1 Kolmogorov-Smirnov and Chi-Squared Test Results for Grooved and Ungrooved Test Specimens

Parameter	N	D_{crit}	V_{crit} n-r-1	Normal D	LogNor D	Normal x^2	LogNor x^2
UNGROOVED							
Yield							
Phase I	10	.3686,	-	.2135	.2104	-	-
1970	35	.2018,	42.3	.1093	.1040		
1971	35	.2018,	42.3	.1173	.1187		
Ultimate							
Phase I	10	.3686,	-	.2006	.1979	-	-
1970	34	.2047,	41.4	.1151	.1097	8.099	8.316
1971	35	.2018,	42.3	.1239	.1255	10.172	10.146
Breaking							
Phase I	10	.3686,	-	.1493	.1461	-	-
1970	33	.2077,	40.3	.2632	.2710	5.919	9.139
1971	33	.2077,	40.3	.2377	.2277	62.579	48.233
GROOVED							
Ultimate							
Phase I	10	.3686,	-	.1439	.1420	-	-
1970	33	.2077,	40.3	.0867	.0851	.788	.809
1971	32	.2108,	39.1	.0907	.0921	2.222	2.833
Breaking							
Phase I	10	.3686,	-	.1229	.1238	-	-
1970 *				-	-	-	-
1971 *				-	-	-	-

- x^2 test could not be applied due to insufficent data points.

* Breaking load not measured with sufficient accuracy to calculate strength distribution.

Table 7.3.2 Mean Values and Standard Deviations of Tensile Strength Distributions (psi)

	Mean	Standard Deviation
UNGROOVED		
Yield		
Phase I	171,150	2,779
1970	158,285	5,840
1971	155,505	1,765
Ultimate		
Phase I	177,850	2,582
1970	167,044	5,273
1971	165,108	1,521
Breaking		
Phase I	254,800	4,391
1970	255,904	12,964
1971	260,921	8,247
GROOVED		
Ultimate		
Phase I	255,300	2,720
1970	254,380	2,260
1971	269,137	2,832
Breaking		
Phase I	303,950	3,122
1970	-	-
1971	-	-

A survey of the literature clearly indicated that strength data is usually assumed to be distributed normally. The NERVA Project Report states that, "Usually the data (strength data) will be assumed to be normally distributed, however, lognormal and Weibull distributions are acceptable and can be used much the same as normal data." (8, p. 9). Hence, it can be concluded that the normal distribution is acceptable as the theoretical distribution considering the limited experimental evidence available and the fact that there is an adequate amount of documentation in the literature to support this conclusion.

7.4. Mean Stress Axis Strength Parameter

The determination of the strength parameter, and consequently, the strength distribution to be used in any fatigue data model is dependent upon the model used and the definition of the failure mode. If it has been determined that yielding is detrimental to the proper functioning of the specimen then the distribution of yield strength should be used. If only the fracture is of concern then the ultimate strength distribution should be used (10, p. 4). Chapter X describes the Goodman line in detail. The Goodman line connects the endurance strength to the ultimate tensile strength. The failure criterion of the cycles to failure data presented in this report has been fracture. The ultimate strength distribution is concluded to be the proper distribution to be placed along the mean stress axis if the failure criterion is fracture and the fatigue model is the Goodman diagram.

7.5. Least Squares Estimate of the Ultimate Tensile Strength

The final topic which remains to be discussed concerns the geometry of the tensile test specimen whose ultimate strength distribution will be placed on the mean stress axis of the Goodman diagram. There exists the possibility of using the grooved or the ungrooved ultimate strength distribution of a tensile test specimen of equal cross-sectional area.

Initially one might conclude that if the Goodman diagram is to model the behavior of a grooved specimen then the grooved ultimate strength distribution should be chosen. Mr. Carl S. Osgood, author of Fatigue Design, in response to a letter which solicated his opinion on this subject stated, "I believe it would be rather meaningless to try for a distribution on the S_m axis for both types of specimens." Robert C. Juvinall, author of Stress Strain and Strength, in a reply to the same question suggests that the static ultimate strength distribution" ... should pertain to the same notched (grooved) specimens as the S_a-S_m curve itself." Juvinall concludes that the proper static strength distribution to use is that of the ultimate strength distribution aling the S_m axis as discussed in Section 7.4 of this report.

There are, however, logical and well presented arguments supporting the use of the ungrooved specimen's ultimate strength distribution. The mean stress axis is really at a stress ratio of zero, as the stress ratio of S_a/S_m is zero at this point. Consequently, the alternating stress, S_a, must be zero. In the case of combined bending

and shear this means that the mean stress axis is the axis of pure shear. From tensile tests, it has been found that the grooved geometry test specimen has a much higher ultimate tensile strength. Reviewing the discussion found in Chapter IV of this report, this higher strength is caused by a radial stress which is introduced into the specimen at the root of the groove. However, a grooved specimen which is subjected to a static torque load would not experience such a radial stress and would fail at a torsional load equal to the load which causes an ungrooved specimen to fail. The mean stress axis in the particular case investigated can be thought of as representing the failure mode where pure shear is the cause of failure. Based on the above argument, it has been suggested that the ungrooved ultimate strength distribution be used on the mean stress axis of Goodman diagrams (3, p. 71).

In attempting to resolve these two differing opinions this investigator turned to an analytic evaluation of the problem. There are available two sets of Goodman diagrams, presented in Chapter IV and V of this report, on which to base such an analytic solution. Such an analytic solution was desired, as smooth curves can be drawn connecting the Goodman diagram data to both the grooved and ungrooved distribution of ultimate strength.

The technique used was based on the method of least squares. The conventional method of least squares, however, was not considered as being appropriate or even workable for the problem under consideration. A conventional least squares analysis requires that the equation of the expected line be completely specified. Using this knowledge the method of least squares will fit the "best" polynomial to the data.

Before proceeding further, let us pause and review the problem and the available information. We have developed Goodman diagrams for varying cycle lives including that of infinite life, which have mean values of the strength distributions specified at stress ratios of infinity, 3.5, 0.825, and 0,44. In addition, there are also several theoretical equations which are know to model the curve which should be drawn between the mean of these strength distributions. The equations include the von Mises-Hencky equation.

$$(S_a/S_e)^2 + (S_m/S_u)^2 = 1 \qquad (7.5.1)$$

and the Gerber parabola equation

$$(S_a/S_e) + (S_m/S_u)^2 = 1 \qquad (7.5.2)$$

Where S_a = alternating stress

S_m = mean stress

S_e = endurance strength

S_u = ultimate tensile strength.

In both of these equations the information available from the Goodman fatigue diagrams presented in Chapters IV and V specify all of the quantities except the ultimate strength.

A method was then sought which would give an estimate for the ultimate strength. It was assumed that the Von Mises-Hencky equation was a valid mathematical model for the fatigue data. Graybill (9, p. 111) presents a method which can be used to calculate the least squares estimator of the ultimate strength assuming that the von Mises-Hencky equation adequately models the fatigue data. The only other assumption which needs to be made is that the fatigue data to be used is not in the low cycle fatigue range, the low cycle fatigue range being below 10^4 cycles. It was expected that the ultimate strength which would be predicted in this range would be quite large. This is quite a valid

assumption as low cycle life requires a completely different mathematical model than the von Mises-Hencky equation (See Chapter XI).

The first step of the estimation process for the ultimate strength using the von Mises-Hencky equation is to transform that equation into the following form

1) $(S_a/S_e)^2+(S_m/S_u)^2=1$ (7.5.3)

2) Set $x=S_m$, $y=S_a$, and subtract $(S_a/S_n)^2$ from both sides yielding $(y/S_e)^2=1-(x/S_u)^2$ (7.5.4)

3) setting $y'=S_e^2-y^2$ (7.5.5)

$$B=S_e^2/S_u^2 \quad (7.5.6)$$

4) Substitution yields $y'=B'(x^2)$ (7.5.7)

The least squares estimate of B is given as

$$B' = [x]^T [x]^{-1} [x]^T [y] \quad (7.5.7)$$

where the brackets indicate vector quantities. Unfortunately, as Figure 7.5.1 indicates, there are only four values to be placed in the x vector. These values of the mean stress are derived from the y, or alternating stress values, in the following manner. Each of the mean stress values are related to the alternating stress value by the stress ratio r; where r equals

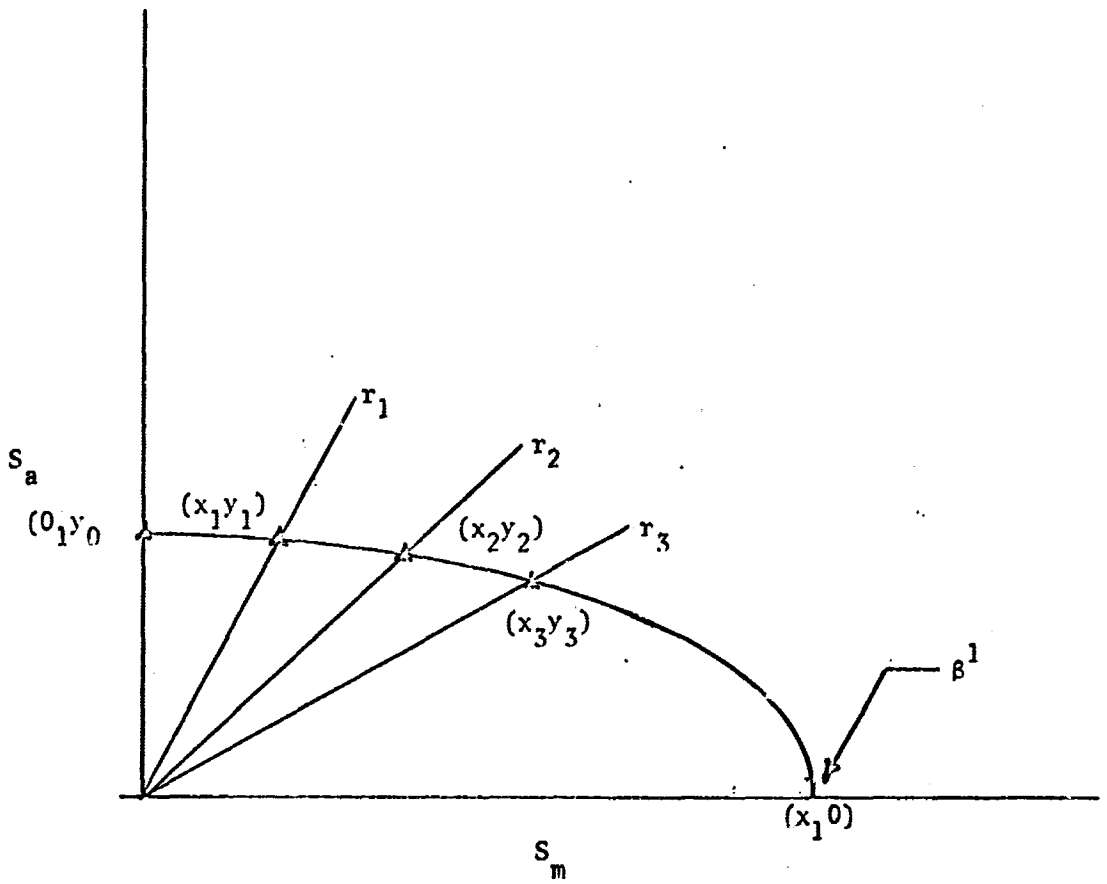

Figure 7.5.1 Goodman Diagram Illustrating Mean of Strength Distributions Used in Least Squares Estimate of Ultimate Strength. (von-Mises Hencky Equation)

$$r = S_a/S_m \qquad (7.5.8)$$

It was possible to solve for the three values of mean stress by dividing the alternating stresses by r for each Goodman diagram investigated.

Thus, the x vector was specified by three values of mean stress while the y vector was specified by the corresponding values of alternating stress. The value of B' is the least squares estimator of the X axis intercept which can then be related to the ultimate strength by Equation 7.5.6.

Rewriting equation 7.5.7 in terms of the von Mises-Hencky transfomed variables yields;

$$B' = \left[x_0^2 x_1^2 x_2^2 x_3^2\right] \begin{bmatrix} x_0^2 \\ x_1^2 \\ x_2^2 \\ x_3^2 \end{bmatrix}^{-1} \left[x_0^2, x_1^2, x_2^2 x_3^2\right] \begin{bmatrix} y_0^2 \\ y_1^2 \\ y_2^2 \\ y_3^2 \end{bmatrix} \qquad (7.5.8)$$

It can readily be seen that x_0 is zero which will cause the vector equation directly above to be reduced to;

$$B' = \begin{bmatrix} x_1^2 x_2^2 x_3^2 \end{bmatrix} \begin{bmatrix} x_1^2 \\ x_2^2 \\ x_3^2 \end{bmatrix}^{-1} \begin{bmatrix} x_1^2 x_2^2 x_3^2 \end{bmatrix} \begin{bmatrix} y_1^2 \\ y_2^2 \\ y_3^2 \end{bmatrix} \qquad (7.5.9)$$

The first two vector multiplications $[x]^T[x]$ yield a scalar. The inverse of this scalar is simply the numerical inverse. The remaining vector multiplications are straight forward.

The vector operations, after being transformed to algebraic relationships can be programmed (LSEFD) on the PDP-8 computer for the Goodman diagram data developed in Chapters IV and V of this report. A flow chart, variable definitions and computer listing of LSEFD program is given in Appendix E.

The results of the least squares estimate is given in Tables 7.5.1 for Chapter IV Goodman diagrams and Table 7.5.2 for data extracted from the Goodman diagrams of Chapter V. Cycles to failure data and the corresponding strength distributions which this data would yield above the cycle life of 200,000 cycles is unavailable at this time. It appears from Tables 7.5.1 and 7.5.2 that as cycle life increases the least squares estimate of the ultimate strength distribution decreases. Had the least squares estimate predicted consistently a value of 255,300 psi. for the measured ultimate strength of the Phase I grooved specimens, it could have been concluded that

Table 7.5.1 Chapter IV Goodman Diagram Data Used for a Least Squares Estimate of the Ultimate Strength.

Cycle Life	Least Squares Estimate of Ultimate Strength
20,000 - 40,000	238,385
60,000 - 90,000	264,662
90,000 - 200,000	222,661

Table 7.5.2 Chapter V Goodman Diagram Data Used for a Least Squares Estimate of the Ultimate Strength.

Cycle Life	Least Squares Estimate of Ultimate Strength
40,000	262,533
90,000	234,972
200,000	216,190

the grooved geometry specimen's ultimate strength distribution was the proper distribution to use along the mean stress axis. The decrease in the least squares estimate of the ultimate strength as the cycle life increases seemingly shakes the possibility that it is indeed the grooved specimens' distributions that should be used along the mean stress axis until the limiting case is investigated. This limiting case being an infinite life Goodman diagram. When the least squares estimate technique is applied to the infinite life diagram (3, p. 75), presented in Figure 4.4.1 which was developed by John Smith for the grooved specimens under discussions, the estimate of the ultimate strength is 222,661 psi. This is well above the value of the ungrooved ultimate strength of 178,000 psi. and is 87% of the ultimate strength of the grooved specimens ultimate of 255,300 psi.

It is also important to note that there is no data available for strength distributions below a stress ratio of 0.44. Because of this the least squares estimate was bassed on four points with a stress ratio greater than or equal to 0.44. It is noted that even in the Goodman diagrams of Chapter V for cycle life values of 200,000 cycles, the largest investigated alternating stress level at a stress ratio of 0.44 has only fallen 17% from the value at the stress ratio of infinity, while the mean stress value is already 76% of the ungrooved ultimate tensile strength at that particular point. The least

squares estimate would have been considerably more accurate if data below a stress ratio of 0.44 was available. It is in this region that the curve must transition to either the grooved or the ungrooved ultimate tensile strength. Perhaps if this data were available the estimates would not have fallen off to the values below the grooved ultimate strength. The analytic results, which suffered from a lack of data below a stress ratio of 0.44, show that they reach a limiting case value much greater than that of the ungrooved ultimate strength, and confirm the opinions which were solicited from noted authors on the subject of fatigue. It is the considered opinion of this investigator that the ultimate strength distribution of the grooved geometry test specimen should be used for Goodman diagrams which represent the behavior of grooved fatigue test specimens.

CHAPTER VIII

EMPIRICAL MATH MODELING OF FINITE LIFE GOODMAN DIAGRAM

8.1 Mathematical Models of the Goodman Diagram

A mathematical model of the Goodman diagram relates this alternating stress, S_A, to the mean stress S_m, by means of an algebraic equation. In most cases this equation relates a static strength parameter to the endurance strength, S_e, of the material in question. The safe design region of a Goodman diagram is conventionally defined as the area bounded by the ordinate and abscissa axes and the line of the mathematical fatigue model, or equation, under consideration. There are several mathematical models of the Goodman diagram. These include the modified Goodman line, the Gerber parabola, the von Mises-Hencky ellipse, the Soderberg line, the Sines line, and the Langer modification to the modified Goodman line. The objective of this chapter is to present these mathematical models, however the presentation of such models would be incomplete if not accompanied by a discussion of the strengths and shortcomings of each model. Figure 8.1 compares the six mathematical models discussed in this Chapter.

8.2 Modified Goodman Line

The most widely accepted theory of combined stresses is the modified Goodman line. The modified

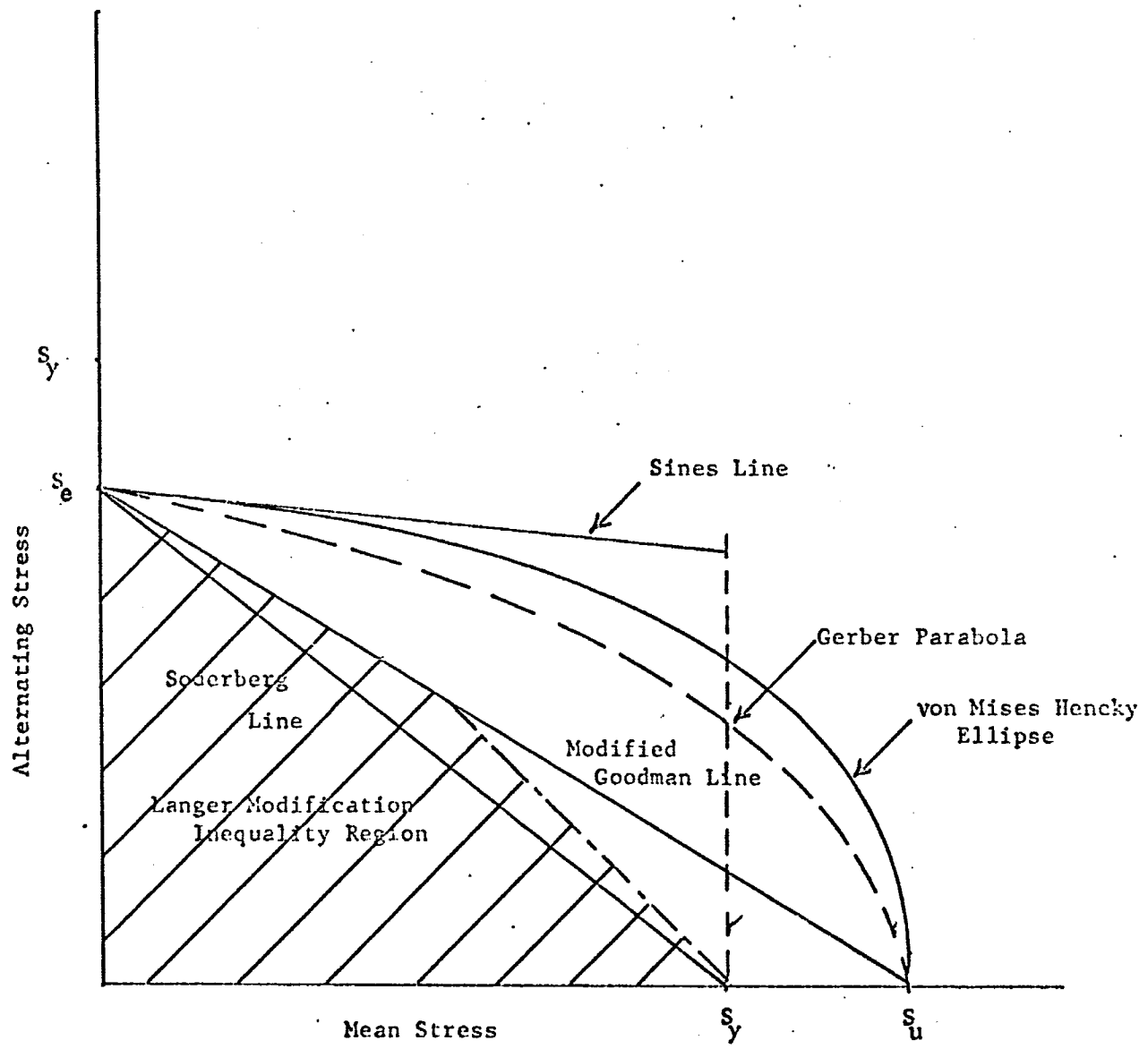

Fig. 8.1 Diagram Picturing The Six Mathematical Models of The Goodman Diagram.

Goodman line connects the endurance strength, S_e, on the ordinate axis by a straight line to the ultimate tensile strength, S_u, which is plotted on the abscissa axis, (10, p. 6).
It is important to note that the endurance strength must be defined in relation to a given number of cycles, beyond which the material is assumed to have an infinite life. A common cycle life value for the endurance strength of ductile steels is 10^6 cycles. The equation of the modified Goodman line is:

$$S_a/S_e + S_m/S_u = 1$$

A common criticism of the Goodman line is that it tends to be conservative where the stress ratios, $r = S_a/S_m$, is well above one or in the range $1 < r < \infty$.
Even though it is conservative in this range, for lower stress ratios in the range of $r = 1/10$ and less, the modified Goodman diagram may predict safe combinations of alternating and mean stress when in actuality they could cause yielding (10, p. 7).

8.3 Gerber Parabola

The Gerber Parabola was first proposed by Gerber in 1874. At this time Gerber was attempting to fit a curve to the results of Wohler's experiments with combined stresses. The parabola which Gerber proposed, known today as the Gerber parabola, joined

the ultimate tensile strength on the abscissa to the endurance strength on the ordinate axis. These two physical properties uniquely describe the shape of the Gerber parabola. The Gerber parabola requires that a parabola be drawn so as to have a vertex on the vertical axis at the value of the endurance limit and to pass through the ultimate strength which is plotted on the horizontal axis (10, p. 8). The equation of the Gerber parabola is given by

$$S_a/S_e + (S_m/S_u)^2 = 1$$

Critics of the modified Goodman line have stated that it is too conservative. The Gerber parabola was proposed to compensate for the conservatism of the modified Goodman line. In addition, it has been found that in many cases the Gerber parabola fits the experimental data far better, in the stress ratio ranges of $1 < r < \infty$, than the modified Goodman line. Unfortunately, the Gerber parabola does not give a proper representation of the fatigue data where stress ratios of one tenth and less are encountered. At these stress ratios the Gerber parabola permits an even greater amount of yielding than the modified Goodman line.

8.4 Von Mises-Hencky Ellipse

This equation, associated with the energy of distortion theory discussed in the following chapter, has been proposed for the case of combined stresses. The von Mises-Hencky equation or ellipse is given by

$$(S_a/S_e)^2 + (S_m/S_u)^2 = 1$$

This equation forms an ellipse in the first quadrant of the cartesian plane. Although this equation was originally proposed for static loads, it is commonly used as a model of combined stresses in fatigue (10, p. 10), and (it is not theoretically valid above the yield point of the material).

8.5 Soderberg Line

In 1930 Soderberg proposed his theory in the United States which was to eliminate the problem discussed previously concerning yielding in the safe design region. The Soderberg line eliminates the problem of the yield point of the material being exceeded at any combination of stress. If yielding does occur, the dimensions of the specimen are changed. Obviously, this change is of a permanent nature and the performance of the material is affected. Even though failure of the material may be considered as fracture, the maximum allowable stress level becomes the yield strength. The actual Soderberg line takes

these facts into account by specifying a straight line between the endurance strength on the ordinate axis and the yield strength S_y on the abscissa axis (11, 0.15). The equation of the Soderberg line is given by

$$S_a = S_e (1 - S_m/S_y)$$

Criticism of the Soderberg line arises because it does indeed lie below the Goodman line. Because of this fact it will be even more conservative than the modified Goodman line for stress ratios in the range of $1 < r < \infty$, the Goodman line has been shown to be conservative in this region (11, p. 15, 16, p. 18).

8.6 Sines Line

The Sines line is an empirical relationship given by

$$S_a = S_e - cS_m$$

where the constant c must be determined for the material under investigation. Because it is an empirical relation it can through the appropriate value of c, be adjusted to fit the data for a particular material. The Sines line accounts for maximum stresses up to the yield point. Consequently, the Sines line is defined only to the vertical line where the mean stress is equal to the yield strength as shown in Figure 8.1 (10, p. 9).

8.7 Langer Modification to the Modified Goodman Line

The Langer Modification to the modified Goodman line attempts to solve the problem of yielding for a different case than discussed in the Soderberg Line presentation. It will be recalled that the Soderberg line attempted to solve the problem of yield at low stress ratios. The Langer modification attempts to solve the problem of yield caused by high stress levels. At high stress levels the maximum value of the alternating and mean stress, $S_a + S_m$, which are encountered may exceed the yield strength (11, p. 16). As discussed in the Soderberg line presentation this yielding will have an adverse effect upon the fatigue characteristics of the specimen. The Langer modification excludes the area of the safe design region where the alternating stress plus the mean stress is greater than the yield strength. Hence, the safe design region becomes the area bounded by the ordinate and abscissa axes, the Goodman line and the region which satisfies the inequality $S_a + S_m < S_y$.

Criticism is again directed at the Langer modification because it is considered too conservative at stress ratios greater than one. The Langer modification does eliminate the criticism of the modified Goodman line where the yield strength is exceeded and at the same time does not demand the conservatism of the Soderberg line (11, p. 16).

CHAPTER IX

THEORETICAL STRENGTH THEORIES

9.1 Introduction to Strength Theories

The three principal stresses completely describe the stress state of any point in a structure. The need for a strength theory to describe the material behavior at a point arises when two or more of the principal stresses have a non-zero value. When one of the three principle stresses is non-zero the behavior of the material is described by the conventional tensile test. There are however, even in this relatively simple state of stress , differences between the true state of stress and the "engineering" stress-strain properties which have been previously discussed in Chapter VII of this report. The objective of a "theory of strength" is to relate a complex state of stress, i.e., when two or more of the principal stresses are non-zero, to the uniaxial properties which are obtained in a tensile test (13, p. 1).

The elastic portion of the total strain is related to stress by Hooke's Law. In the case of combined stresses initial yielding must be related to yielding in a tensile test by means of a flow theory. A flow theory relates the increments of plastic strain in each direction to the state of stress at the point under consideration. In the past there have been

several yield criteria, or strength theories, proposed but because of later experiments in hydrostatic stresses, which have conflicted with these theories, they seem now to be only of historical importance (13, p. 1). However, there are two such theories which do not have this particular fault. These two are the maximum shear stress criterion, and the energy of distortion or von Mises-Hencky criterion. The following chapter will discuss these two theories, and will present three additional modified strength theories proposed by Findley and Mathur (14). These discussions will be accompanied by comparison of these theories to the fatigue problem of combined stresses of bending and torque.

9.2 Energy of Distortion Theory

The octahedral shear stress, the energy of distrotion, or the Von Mises-Hencky theory, as this theory is often referred to, predicts yielding to occur when the elastic energy of distortion reaches a critical value. The energy of distortion is defined as the total energy minus the energy associated with a volumetric dilation. It can be shown that the energy of distorsion is proportional to the shear stress on the octahedral plane. The octahedral plane is the plane which makes equal angles with the three principle directions (13, p. 3).

Consider a cubic element of material acted upon in the three principle directions by the stresses s_1, s_2, and s_3 where $s_1 > s_2 > s_3$. For the unit cube, pictured in Figure 9.2.1,

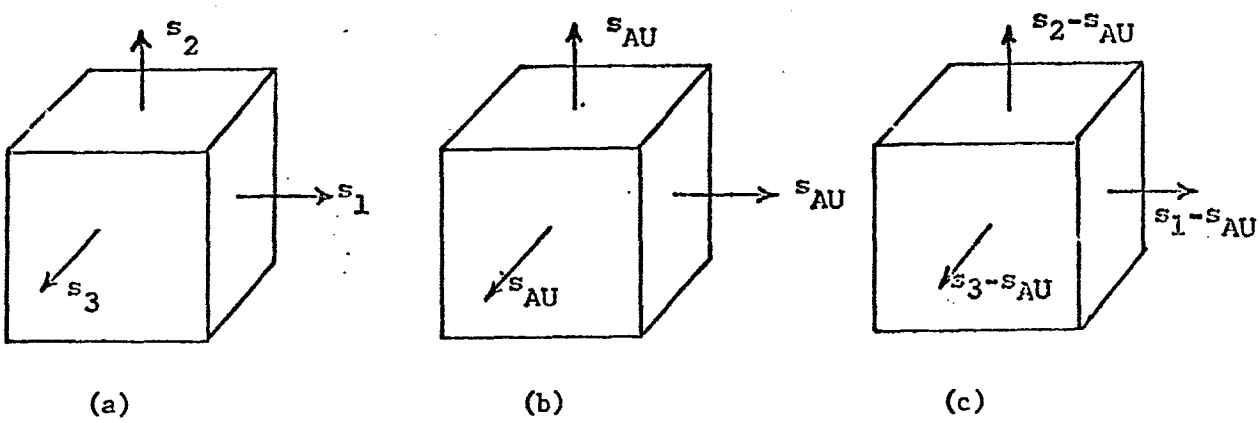

Fig. 9.2.1 (a) Element with triaxial stresses; this element undergoes both volume change and angular distortion. (b) Element under hydrostatic tension undergoes only volume change. (c) Element has angular distortion without volume change.

the work done in any principle direction is given by

$$U_n = s_n \varepsilon_n / 2 \qquad (9.2.1)$$

where ε_n are the three principle strains. Considering

$$\varepsilon_1 = s_1/E - \mu s_2/E - \mu s_3/E \qquad (9.2.2a)$$

$$\varepsilon_2 = s_2/E - \mu s_1/E - \mu s_3/E \qquad (9.2.2b)$$

$$\varepsilon_3 = s_3/E - \mu s_1/E - \mu s_2/E \qquad (9.2.2c)$$

where μ = Poissons ratio and E = Modulus of Elasticity.

The total strain energy is

$$U = U_1+U_2+U_3 = 1/2E \{s_1^2+s_2^2+s_3^2 - 2\mu(s_1s_2 + s_2s_3 + s_3s_1)\} \qquad (9.2.3)$$

Defining average stress as

$$s_{avg} = \frac{s_1 + s_2 + s_3}{3} \qquad (9.2.4)$$

which is applied to each of the principle directions of the unit cube, the remaining stresses $s_1 - s_{avg}$, $s_2 - s_{avg}$ and $s_3 - s_{avg}$, shown in Figure 9.2.1c will only produce angular distortion. If s_{avg} is substituted for s_1, s_2 and s_3 in Equation 9.2.3 the amount of strain energy which produces only change in volume is

$$U_v = \{ \frac{3s_{avg}^2 - 2\mu(3s_{avg}^2)}{2E} \} = \{3s_{avg}^2/2E\}(1-2\mu) \quad (9.2.5)$$

$$s_{avg}^2 = \{ \frac{(s_1 + s_2 + s_3)}{3} \}^2$$

If the expression for s_{avg}^2 is substituted in Equation (9.2.5) it becomes

$$U_v = \{1-2\mu/6E\}(s_1^2 + s_2^2 + s_3^2 + 2s_1s_2 + 2s_2s_3 + 2s_3s_1) \quad (9.2.6)$$

The energy of distortion is then equal to the total energy, given by Equation 9.2.3 minus the energy of the volume change given by Equation 9.2.6. The energy of distortion is thus given by

$$U_d = U - U_v = (1+\mu/3E) \frac{\{(s_1-s_2)^2+(s_2-s_3)^2+(s_3-s_1)^2\}^2}{2}$$

When a state of pure shear exists, the shearing stress at point, τ_e, is equal in magnitude to each of the principle stresses at the same point. If $s_1 = \tau$ and $s_2 = -s_1$ the energy of distortion becomes

$$U_d = (1+\mu/6E) \{(s-(-s))^2 + (s)^2 + (-s)^2\} = \{1+\mu s^2/E\} s^2$$

when $s = \tau_e$, then

$$U_d = (1+\mu/E)\tau_e^2$$

which is the energy of distortion in a torsional test specimen.

If the same unit cube is subjected to a normal stress, s_1, in one direction only, the other two principal stresses being zero as in a tensile test specimen subjected to an axial load, the energy of distortion, U_d, becomes

$$U_d = (1+\mu/6E)(s_1^2 + s_1^2) = (1+\mu/3E)s_1^2$$

Equating the energy of distortion for the case of pure shear to that of the unaxial tension condition, when yielding first occurs;

$$(1+\mu/E)\tau_e^2 = (1+\mu/3E)\, s_e^2$$

$$\tau_e = s_e/\sqrt{3}$$

The conclusion which can be reached is that yielding and eventually a ductile fracture starts when the energy of distortion reaches a critical value. The maximum shear stress, τ_e, at a point when yielding starts is $1/\sqrt{3}$ times the maximum tensile stress, s_e, at the same point. Thus the von Mises-Hencky ellipse for combined bending and shear stress is given by

$$(S_a/S_e)^2 + (S_m/S_u)^2 = 1$$

$$(S_a/S_e)^2 + (1/\sqrt{3}\,\tau/S_u)^2 = 1$$

where τ in the above equation is the constant shear stress recorded in each test specimen studied.

9.3 Maximum Shear Stress Theory

Tresca proposed in his maximum shear stress theory that yielding occurs when the maximum shear stress reaches a critical value (13, p. 2). Yielding begins when the maximum shear stress equals the shear stress corresponding to the yield strength in the simple tension test. According to Figure 9.3.1 yielding occurs when $\tau_{max} = S_y/2$ where S_y is the yield strength of the material. For a triaxial stress state three maximum shear stress may be found and are given by

$$\tau = (s_1 - s_2)/2 \qquad \tau = (s_2 - s_3)/2 \qquad \tau = (s_1 - s_3)/2$$

Yielding will begin when the largest of these shearing stresses becomes equal to one-half the tensile yield strength of a simple tension test specimen (15, p. 152).

In essence the theory predicts that the shearing yield strength is equal to one-half of the tensile yield strength. The advantages of the theory is that it is easy to use, is useful for ductile materials and is conservative in describing the behavior of brittle materials (15, p. 152).

9.4 Comparison of the Maximum Shear Stress and Energy of Distortion Theories

The maximum shear stress and energy of distortion theories can be conveniently represented in Figure 9.4.1 in the two-dimensional principal stress space.

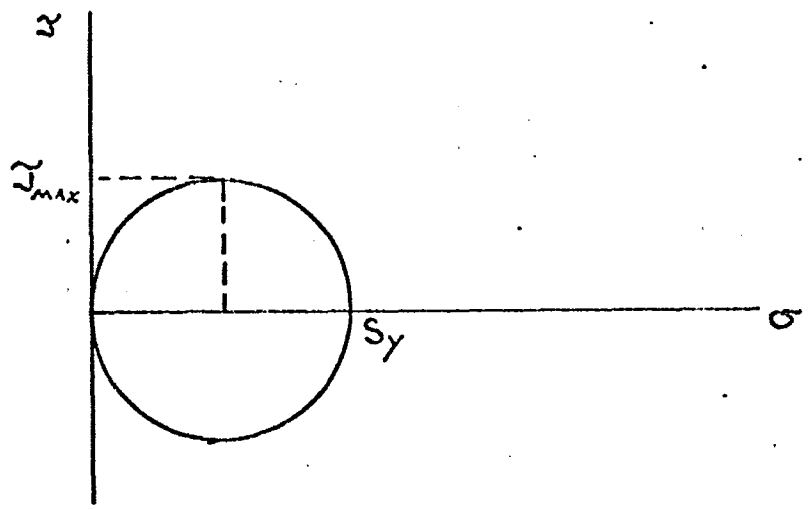

Figure 9.3.1 Mohr's Circle Showing Relation of Maximum Shearing Stress to Tensile Yield Strength (15, p. 151)

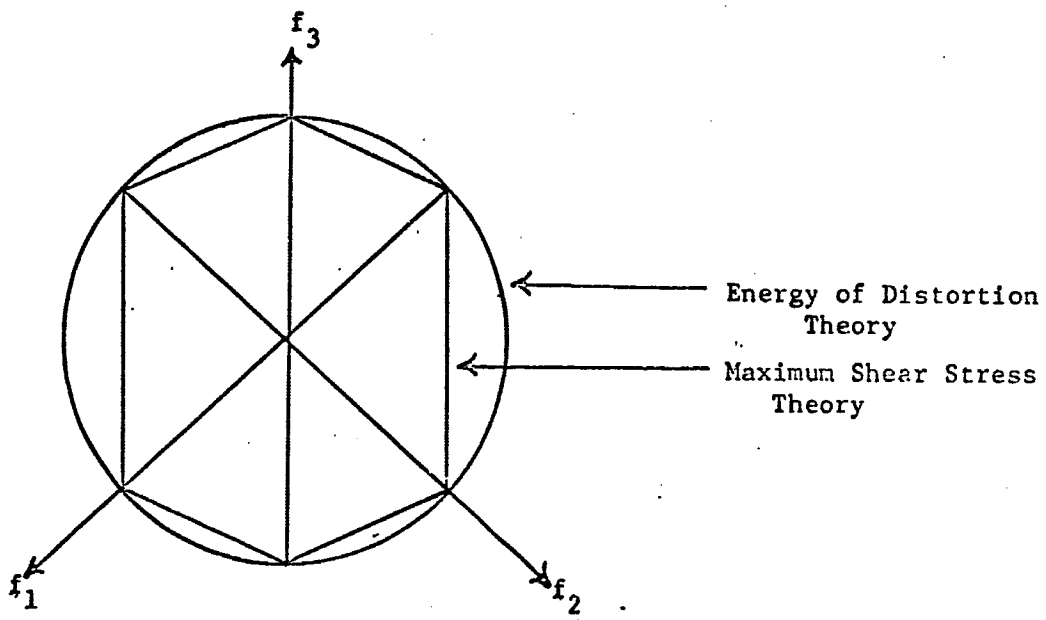

Fig. 9.41 Representation of Energy of Distortion and Maximum Shear Stress Theories in the Plane Perpendicular to the Unit Vector $(1/\sqrt{3}, 1/\sqrt{3}, 1/\sqrt{3})$. (13, p. 8)

Experimental evidence indicates that the Von Mises-Hencky or energy of distortion, criterion is more accurate than the Tresca theory for predicting the yield strength of most material under biaxial stress. In addition strain hardening and creep behavior correlate much better for most materials using the on Mises-Hencky theory. The difference between the two theories is small, the maximum difference in the two theories in any state of stress being about 16 percent. In view of this fact the Tresca theory, which is more conservative is considered satisfactory even though the von Mises-Hencky theory is more accurate (13, p. 6).

It has been stated that stress-strain properties are best correlated using the von Mises-Hencky theory. This, however, is not grounds enough to state that fatigue failures are best described by the same criterion. The energy of distortion has no directional properties and is always considered a positive quantity. This causes some serious deficiencies as a means of predicting fatigue failure. In fatigue experiments it has been found that the maximum shear stress theory will correlate results as well as the Von Mises-Hencky criterion. The problem of determining which of the theories is best is difficult because of the natural scatter of fatigue data spanning the various criteria.

Referring again to directional properties of the two criteria it is noted that the maximum shear stress changes sign

When the stresses are reversed, as during a rotating beam fatigue test, whereas, it has been previously noted that the energy of distortion is always a positive quantity. In reversed bending tests these directional properties are of critical importance. As the stresses at a point are reversed the energy of distortion goes from a positive quantity to zero and then back to a positive quantity. This means that the distortion energy theory is not reflecting a reversal in loading. Reversed loading cases are very harmful to the fatigue of any structure. It is important to recognize load reversals as adding to the range of stress and strain. It would be possible to devise methods to account for load reversals in the uniaxial case, however, in the case of combined stress the problem would be quite complex (13, p. 8).

The von Mises-Hencky theory is not free of the directional property problem in fatigue. As an example one can consider the special case where the magnitudes of the principal stresses are constant but the directions are changing with time. The energy of distortion remains constant indicating that there is no fatigue loading. However, this is not the case as the shear stress theory must also be modified for the case where the directions of the principal stresses vary with time. However, in this case one would merely use the history of maximum shear stress on a fixed plane of the material to predict the fatigue life (13, p. 9).

9.5 Modified Theories of Fatigue Failure Under Combined Stresses

Findley and Mathur (14) have developed several theories of fatigue failure under combined stresses. The following section will present the three theories which were developed by them. They state that the classical theories for the initiation of yielding under combined stresses are conflicting. The investigation of Gough and Pollard (14, p. 2) concluded that the classical theories which have been proposed are inaccurate since the ratio of fatigue strength in bending, $b = S_{S_c}$, to that in torsion fatigue strength, $t = S_u$, is not the same for all metals as required by the classical theories of yielding.

Findley and Mathur propose that the influence of the property of anisotropy, that of having different properties in different directions, and the state of combined stress are the cause of discrepencies between proposed theories of failure and results obtained from combined stress fatigue tests (4, p. 3).

The ratio of b/t varies over a considerable range for all engineering materials. Considering only metals this ratio varies from a value of 0.9 to 2.6. If, however, the metals are grouped, within each group the ratio of b/t has a much smaller range. Cast irons and its alloys have a b/t ratio which varies from 1.3 to 2.5 with a majority of these values lying between 1.5 and 2.0. This latter range is considered to be the ductile range. The b/t ratio value of notched steels was found to be considerably less than that of unnotched steels with a majority falling between 1.0 and 1.5.

It is felt that anisotropy of the material is a contributing cause to the variation of the b/t ratio. It has been suggested that fatigue failure is caused primarily by an alternating shearing stress producing repeated slip, however, the resistance of a material to this fatigue mechanism may be influenced by the magnitude and sign of the normal stress occuring on planes of maximum shearing stress. This effect may vary with the material. Differences in the effect which the normal stress may have in fatigue in a given material will cause differences in the b/t ratio (14, p. 6).

9.5.1 Correction Factors

In ductile metals the cyclic principle shear stress is the quantity most closely associated with the fatigue damage. The principle shear stress theory predicts that the bending strength should be twice the shear strength (14, p. 8). However, because of the effect of anisotropy and combined stress, Findley and Mathur suggest that the principle shear stress theory be modified to the form

$$\tau_{max} = b/2K = t \quad \text{or} \quad K = b/2t \qquad (9.5.1.1)$$

where K is the correction factor for anisotropy and the combined stress condition. The expression for modified principal shear stress theory becomes

$$\left[S_a^2/S_{S_e}\right]^2 + \left[S_m^2/S_u\right]^2 = 1 \qquad (9.5.1.2)$$

Where S_a and S_m represent respectively the amplitudes of alternating bending stress and alternating torsional stress components of combined stress (14, p. 9).

It is important to note that when correction factors are applied to the octahedral shear stress, principal shear strain, energy of distortion, total energy of distortion, total energy of deformation and magnitude of state of stress vector theories the result is the same in all cases, that of Equation 9.5.1.2.

If correction factors are applied to the principle stress theory the governing equation for combined bending and torsional stress becomes

$$S_a/S_{S_E} + S_m^2/S_u^2 = 1 \qquad (9.5.1.3)$$

When the principle strain theory is modified the fatigue strength ratio b/t predicted is

$$S_{S_E}/S_u = b/t = 1 + \mu \qquad (9.5.1.4)$$

where μ is Poisson's ratio.

The expression for the modified principal strain theory as reported previously (17) is

$$\varepsilon_1 = 1+\mu/2E\left\{\sqrt{S^2 + \left(2b/t(1+\mu)\right)^2\tau} + \left(1-\mu/1+\mu\right)S\right\} \qquad (9.5.1.5)$$

For pure bending

$$\tau = 0, \quad S = b, \text{ thus } \varepsilon_1 = b/E$$

Substituting for ε_1 in equation 9.5.1.5, and simplifying the expression, the modified principal strain theory becomes

$$\mu s^2/b^2 + (1 - \mu)\, s/b + b^2/t^2 = 1 \qquad (9.5.1.6)$$

The fatigue strength ratio b/t predicted by the principal strain theory (17) is

$$b/t = 1 + \mu \qquad (9.5.1.7)$$

Substituting equation 9.5.1.7 in equation 9.5.1.6

$$(b/t - 1)\, s^2/b^2 + (2 - b/t)\, s/b + \tau^2/t^2 = 1 \qquad (9.5.1.8)$$

This equation models the combined stress state of bending and torsion for the modified principle strain theory.

A design expression has been proposed by Findley and Mathur (14) to model the fatigue failure of notched ductile metals and irons. These materials have a behavior which is intermediate between the perfectly brittle irons which have little or no slip and ductile metals which have considerable slip. The stress system which is associated with these materials may change from the principle stress theory, b/t = 1, for materials such as the brittle irons to the principle shear stress theory where b/t = 2.0 as in the ductile metals (14, p. 11).

The design expression which is suggested to model these metals under combined bending and shear is given by

$$(S_a/S_{S_E})^{b/t} + (S_m/S_u)^2 = 1 \qquad (9.5.1.9)$$

It is noted that the exponent b/t varies with the class of material. When b/t = 1 Equation 9.5.1.9 is that of the modified principal stress theory. When b/t = 2, which is the case in ductile materials the equation reduces to that of the modified shear stress theory (14, p. 11).

9.5.2 Comparison to Fatigue Data

Findley and Mahur compare their modified stress theories to actual combined bending and torsional fatigue test results. It is found that the modified shear stress theory, Equation 9.5.2.1 served as a good model for ductile metals with a b/t ratio ranging from 1.46 to 2.0. A comparison of this equation to actual fatigue tests is given in Figure 9.5.1 (14, p. 15).

The modified principles stress theory is compared to actual fatigue data of iron and iron alloys in Figure 9.5.2 and to that of notched ductile steels in the brittle range, b/t = 1.3 in Figure 9.5.3. The modified principle strain theory predicts strengths which are higher than the actual data as can be seen

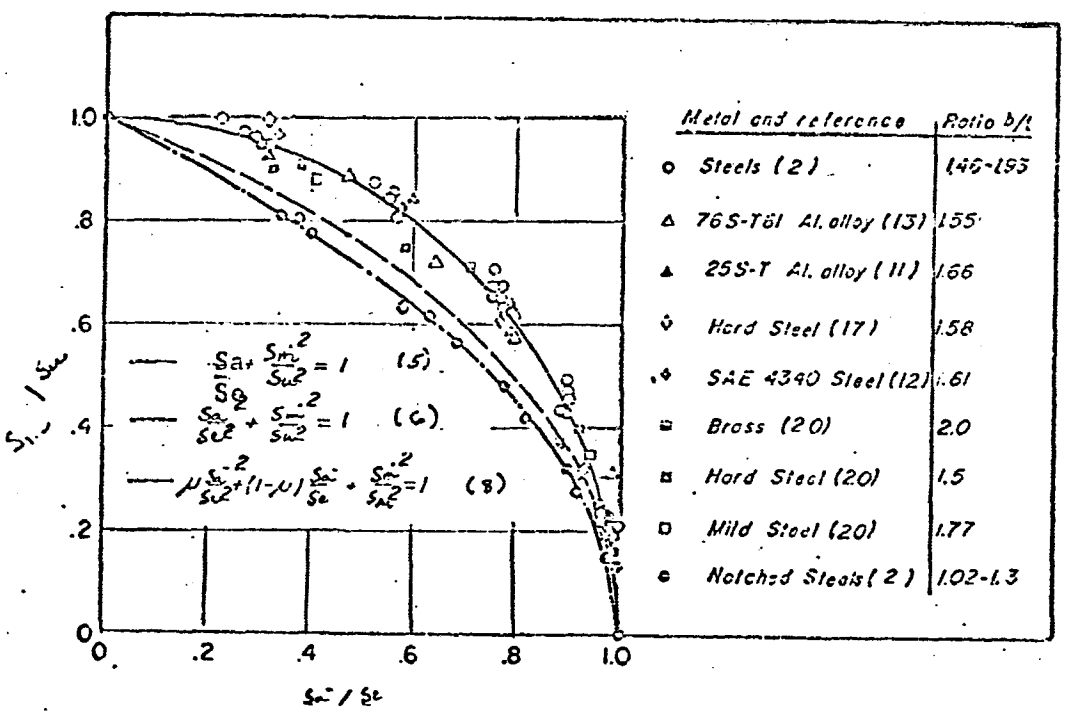

Figure 9.5.1 Comparison of Modified Stress Theories With Fatigue Data Generated Under Combined Bending and Torsional Stress (14, p. 24)

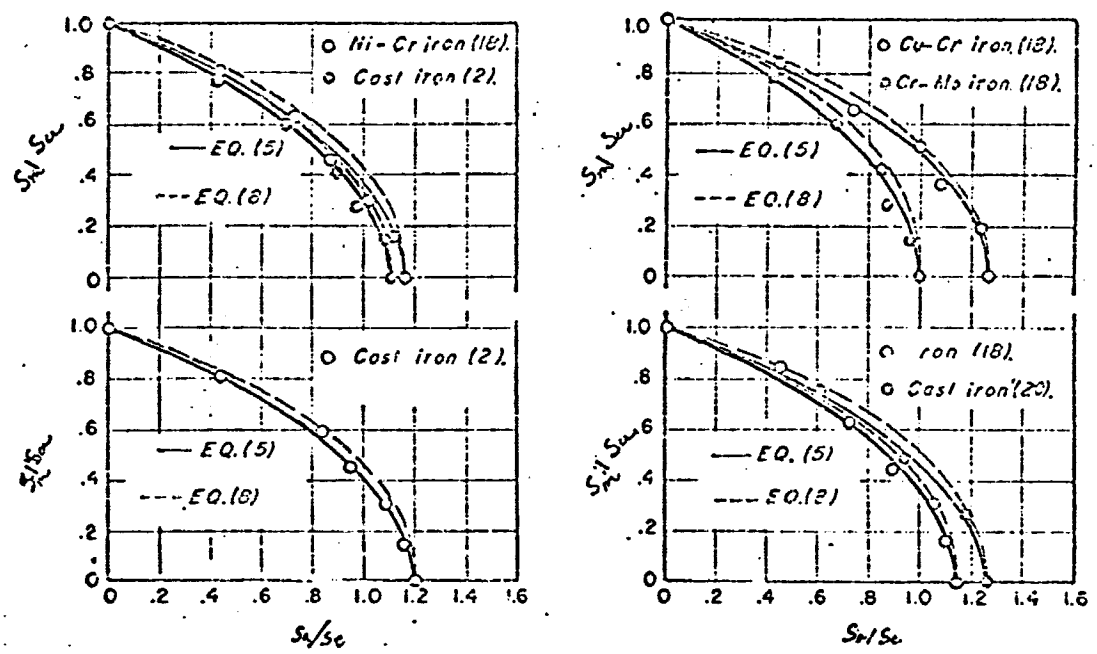

Figure 9.5.2 Comparison of The Modified Principal Stress (solid line) and Modified Principal Strain Theories (dashed line) To Fatigue Data of Iron and Iron Alloys. (14, p. 25)

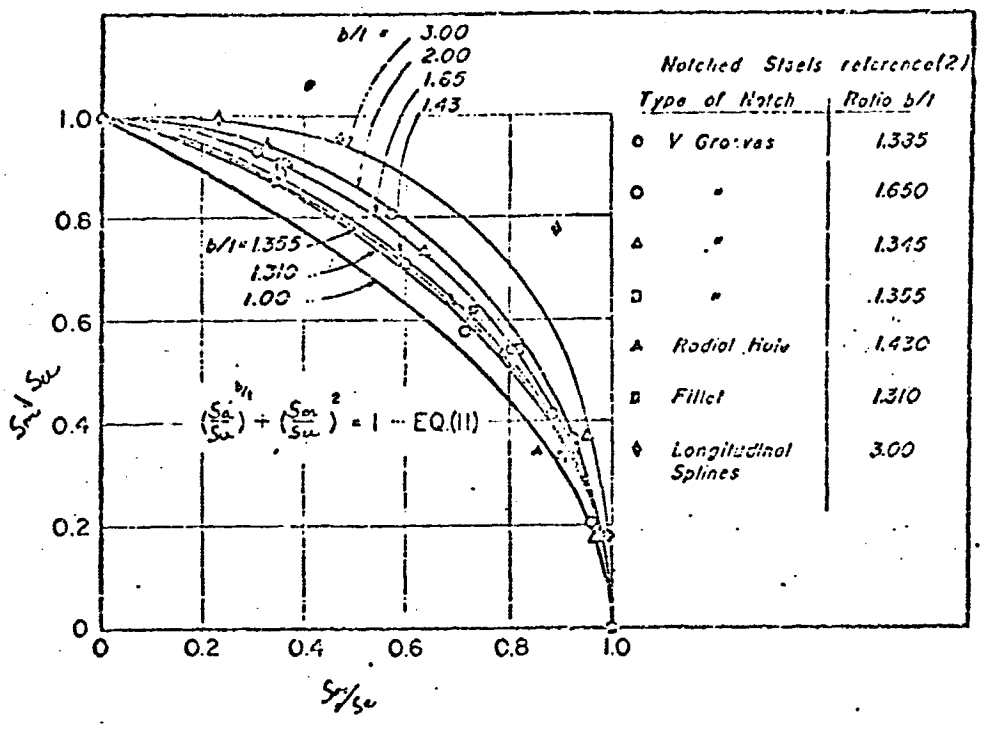

Figure 9.5.3 Comparison of Design Expression to Fatigue Data Generated Under Bending and Torsional Stress For Notched Steels Having a b/t Ratio Greater Than 1.3. (14, p. 35)

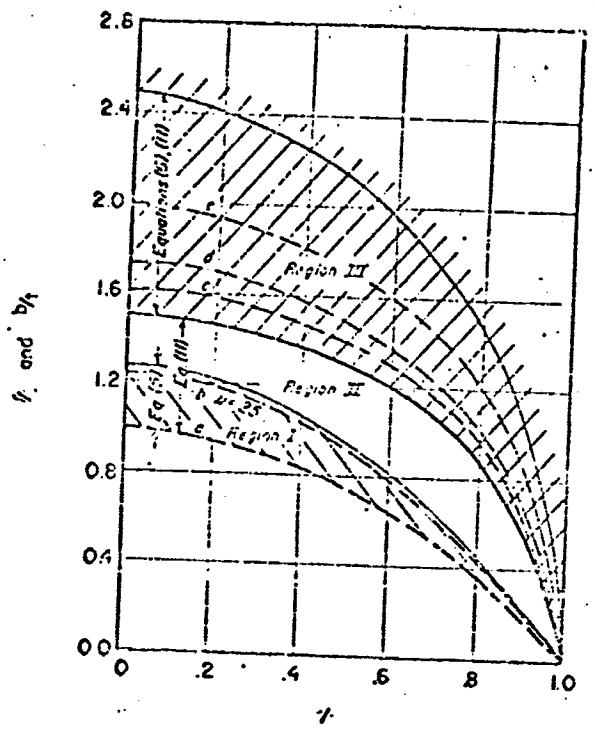

Figure 9.5.4 Position of Modified Strength Theories as Specified By b/t Ratio. (14, p. 25)

Curve A: Principle Stress Theory
Curve B: Principle Strain Theory
Curve C: Total Strain Energy Theory
Curve D: Distortion Energy Theory
Curve E: Principle Shear Stress Theory

in Figure 9.5.2 (14, p. 15).

It is found that the design expression, Equation 9.5.1.9 is in very good agreement with data of notched ductile steels, $b/t \leq 1.3$, and in good agreement with both brittle and ductile range of metals as shown in Figure 9.5.3 (9, p. 15).

Assigning the metals to regions by b/t ratio values, as discussed previously, yields the following regions:

Region I (brittle)

Region II (intermediate)

Region III (ductile)

The position of each modified strength theory within the regions described in Figure 9.5.4 is specified by the value predicted by the b/t ratio of each strength theory. Table 9.5.1 presents the value predicted by each strength theory for the ratio of b/t. The modified strength theories may be assigned to each of the regions described previously in the following descending order (9, p. 17).

Region I	Modified principal stress Design expression Modified principle strain
Region II	Design expression (notched ductile steels) (equation 9.5.1.9) Modified principal strain Modified principle stress Modified principle shear stress
Region III	Modified principle shear stress Design expression (equation 9.5.1.9)

Table 9.5.1 Values of the Ratio b/t Predicted by each Strength Theory (14, p. 17).

Principle stress theory	$b/t = 1$
Principle strain theory	$b/t = 1 + \mu$
Total strain energy theory	$b/t = \sqrt{2 + 2\mu}$
Distortion energy and octahedral shear stress theory	$b/t = \sqrt{3}$
Principle shear stress theory	$b/t = 2.0$

CHAPTER X

RECOMMENDED EMPIRICAL MATHEMATICAL MODELS OF THE FINITE LIFE GOODMAN DIAGRAM

In viewing each of the five finite life Goodman diagrams developed in Chapter V it can be seen that the equation of the mean line is generally of a quadratic nature. It is of interest to investigate if the mean line of the finite life Goodman diagrams can be described by one or more of the empirical mathematical models of the Goodman diagram discussed in Chapter VIII.

The Von Mises-Hencky ellipse was compared to the experimental finite life Goodman diagrams presented in Figure 5.3.1 through 5.3.5. The ellipse is given by

$$(S_a/S_e)^2 + (S_m/S_u)^2 = 1 \qquad (10.1)$$

The endurance strength and ultimate strength mean values specify the mean line of the Von Mises-Hencky ellipse. The endurance strengths for each of the five Von Mises-Hencky ellipses were taken from Table 5.3.1. These ellipses, superimposed upon the original experimental mean line, appear as overlays with the experimental finite life Goodman diagram in Chapter V as overlays on Figures 5.3.1 through 5.3.5 As in Chapter V the ultimate strength distribution is taken to be that of the grooved specimen. A PDP-8 program, described in Appendix E, was

used to calculate the mean stress points as specified by the ellipse for several theoretical alternating stress levels. These values are listed in Table 10.1 for each of the five finite life Goodman diagrams.

The finite life Goodman diagrams for 40,000, 90,000, and 200,000 cycles are in very close agreement with the von Mises-Hencky ellipse. The lower cycle life diagrams of 3,500 and 9,000 cycles are in very poor agreement with the von Mises-Hencky ellipse, a fact which will be investigated later in this Chapter.

Although the higher cycle life fatigue diagrams seemed to be closely approximated by the von Mises-Hencky ellipse, it was decided to determine the exponent, a, where in general the quadratic equation of interest is given by

$$(S_a/S_e)^a + (S_m/S_u)^2 = 1 \qquad (10.2)$$

This was accomplished in the following manner. Equation 10.2 can be transformed to

$$y^a + x^2 = 1 \qquad (10.3)$$

where

$$y = S_a/S_e$$

$$x = S_m/S_u$$

Table 10.1 Alternating and Mean Stress Values Predicted by the von Mises-Hencky Ellipse.

	S_a - psi	S_m - psi
N=3,500 cycles;	134,000	43,118
	128,000	86,038
S_e-135,953 psi;	120,000	119,995
	100,000	172,959
S_u=255,300 psi	60,000	229,092
	20,000	252,522
N-9,000 cycles;	112,000	65,878
	168,000	92,779
S_e=115,926	100,000	129,145
	80,000	184,145
	60,000	218,445
	20,000	251,472
N=40,000 cycles;	88,000	61,751
	84,000	96,000
S_e=90,693	80,000	120,264
	60,000	191,445
	40,000	229,128
	20,000	249,015
N=90,000 cycles;	68,000	130,204
	64,000	149,866
S_e=79,054	60,000	166,231
	40,000	220,207
	20,000	246,995
N=200,000 cycles;	68,000	63,027
	64,000	104,696
S_e=70,172	60,000	132,388
	40,000	209,761
	20,000	244,711

Solving for y^a yields

$$y^a = 1 - x^2 \tag{10.4}$$

If the natural logarithms of both sides are taken, the result is

$$a \ln y = \ln (1-x^2) \tag{10.5}$$

$$\ln y = 1/a \ln (1-x^2) \tag{10.5}$$

If this equation is plotted on ln - ln graph paper the result will be a straight line. A least squares PDP-8 program SBFE, is available which will give the slope of the best fit equation through the data as well as the correlation coefficient. The slope of this line is equal to the value of the unverse of the exponent a in Equation 10.2. A description of this program is given in Appendix E. The values derived by this method for the exponent a and ρ are given in Table 10.2

The finite life Goodman diagrams of 3,500 and 9,000 cycles as mentioned previously of not seem to be modeled by a quadratic equation. The various empirical models were reviewed and it was deterimed that the Sines Line had the greatest potential of modeling the finite life range below 10^4 cycles. The Sines Line is given by

$$S_a = S_e - cS_m \tag{10.6}$$

Table 10.2 Values of the Exponent a and Correlation Coefficient. (ρ)

Cycle Life N	Coeff. a	Correlation Coeff.(ρ)
40,000	2.3821	.9137
90,000	2.3042	.8948
200,000	1.9107	.8915

The coefficient c for the finite life Goodman diagrams of 3,500 and 9,000 cycles was found, by trial and error, to be 0.08. The Sines Line specified by c = 0.08 was placed on overlays of Figures 5.3.1 and 5.3.2. The Sines Line is valid only to the yield strength of the material. Because the yield strength of the grooved geometry specimen was not available, a dashed line was drawn beyond the yield strength of the ungrooved specimen. This is meant to signify that the yield strength of the grooved specimen is some value greater than that of the ungrooved specimen.

In conclusion, it can be said that the Von Mises-Hencky ellipse quite closely approximates the mean line of the finite life Goodman diagram, where the cycle life value is above 10^4 cycles. If the Von Mises-Hencky ellipse is modified to

$$(S_a/S_e \pm 3\sigma_{S_e})^2 + (S_m/S_u \pm 3\sigma_{S_u})^2 = 1 \qquad (10.7)$$

the Goodman surface is adequately described. This surface is shown in Figure 5.3.5. For life values below 10^4 cycles the Sines Line adequately describes the mean line of the finite life Goodman diagrams. If the Sines Line is modified as shown in overlays of Figures 5.3.1 and 5.3.2 to the form

$$S_a = (S_e \pm 3\sigma_{S_e}) - cS_m \quad , \qquad (10.8)$$

then the Goodman surface is completely modeled.

The comparison of the von Mises-Hencky ellipse with the experimental finite life diagrams, and the discussion of Section 9.3 leave little doubt that the von Mises-Hencky strength theory closely predicts the fatigue failure in steel. The discussion of Section 9.3 gives adequate documentation that the von Mises-Hencky strength theory is widely considered as a strength theory for combined stress conditions. Although the von Mises-Hencky strength theory is not free of all criticisms when considered as the criterion governing fatigue failures the very close behavior of the larger cycle finite life Goodman diagrams indicate that this criterion can be continued to be accepted as governing the fatigue data generated under National Aeronautics and Space Administration Contract NGR 03-002-044 at The University of Arizona. The material which is used in this research program is SAE 4340 steel, Rockwell C 35/40.

CHAPTER XI

TWO RECOMMENDED METHODS OF REDUCING THE QUANTITY OF EXPERIMENTAL DATA NEEDED FOR A FATIGUE DATA ACQUISITION PROGRAM

The problem of reducing the number of data points in a fatigue test program is quite complex. The nature of the fatigue mechanism requires that distributions be developed to describe the cycles to failure and strength parameters of the test specimen. To date the complex fatigue test program at The University of Arizona has performed fatigue tests on well over 650 specimens. This has been expensive but the experience gained by this pioneering program has laid the foundation to develop theoretical concepts which may possibly reduce the need for expensive fatigue acquisition programs in the future. An examination of the Goodman diagrams and surfaces developed in this paper and the application of the theories proposed by W. N. Findley (14, pp. 26) seem to offer great hope for reducing the number of test specimens required in the fatigue data acquisition program.

In reviewing the finite life Goodman diagrams developed here, it becomes evident that the distributions placed along the mean and alternating stress axes are of critical importance in determining the shape and location of the finite life Goodman diagram and surface. Currently the ultimate tensile

strength distribution which is placed along the mean stress axis is developed from the results of tensile tests. These tests include the pulling of thirty five grooved test specimens to determine the ultimate strength distribution; this method is satisfactory and should be continued.

The distribution which is placed along the alternating stress axis can be determined as it is currently being done from the stress cycles to failure data at a stress ratio of infinity. This requires the generation of cycles to failure distributions at five alternating stress levels. Currently, this would require thirty five test specimens in each of the five stress levels tested. The methods presented in Chapters III and V could then be used to place the derived strength distributions on the finite life Goodman diagrams. Considering the conclusions reached in Chapter X the development of the finite life Goodman diagrams would be possible with two hundred test specimens. To review, the endurance strength for each cycle life would be specified by the transformation of the cycles to failure distributions at a stress ratio of infinity to the vertical strength distributions on the Goodman diagram. This procedure is outlined in Chapter V. The ultimate strength distribution is specified by the tensile test of the thirty-five grooved specimens. The entire finite life Goodman diagram could be modeled, above 10^4 cycles, by the Von Mises-Hencky ellipse as specified by;

$$(S_a/S_e \pm 3\sigma_{S_e})^2 + (S_m/S_u \pm 3\sigma_{S_u})^2 = 1 \qquad (11.1)$$

The necessary data would amount to a maximum of two hundred test specimens which would include a staircase analysis of the endurance strength at 10^6 cycles, at a stress ratio of infinity.

The required number of test specimens can be reduced significantly if the cycle life values for the finite life Goodman diagrams are determined prior to the start of the test program. If for instance, three finite life Goodman diagrams are required then the required endurance strengths can be determined by the staircase method for each cycle life.

This method would reduce the number of specimens to one hundred twenty five to one hundred fifty depending upon the number of required diagrams. Each staircase method should have a sample size of thirty five while the ultimate strength distribution of the grooved specimen should also be specified by thirty five specimens.

By drawing a desired stress ratio lines on the finite life Goodman diagram, as specified by the above equation, it would be possible to develop the vertical strength distributions which would be placed on the statistical S-N diagram by following the reverse of the procedure developed in Chapter V. That is by drawing the stress ratio line on the finite life Goodman diagrams, the alternating stress level and standard deviation, in actuality the three sigma limits, of the rotated vertical

strength distributions would be obtained. It would, by the reverse of the method discussed in Chapter V, be possible to create the vertical strength distributions which would be placed on the statistical S-N diagram. This at least suggests that it may be possible to continue one step further back to determine the cycles to failure distributions. This method eliminates the need of generating cycles to failure distributions at the intermediate stress ratios between zero and infinity. Currently such investigations require slightly more than four hundred specimens. This number considers thirty five specimens to a cycles to failure distribution.

In an attempt to reduce the need for experimental data beyond that discussed above it appears that the theories proposed by Findley (14) in Chapter X offer an alternative to the expensive fatigue data acquisition program. Considering that the mean line of the finite life Goodman diagram follows the equation

$$(S_a/S_e)^a + (S_m/S_u)^2 = 1 \qquad (11.2)$$

The exponent a, which has previously been discussed in Chapter X also appeared in the design expression of Equation 9.5.1.9 proposed by Findley for notched ductile steels.

$$(S_a/S_e)^{b/t} + S_m^2/S_u^2$$

Although the equations 9.5.1.9 and 12.2 are not exactly identical, differing in the denominators of the terms on the left hand side of the equations, they do attempt to relate quantities of bending and torsional stress. Comparing the two equations, it can be seen that b is actually S_e and t is S_u. The exponent a is the ratio of bending strength to torsional strength, and could be determined experimentally. It would have to be determined if this ratio should be found from static tests or dynamic fatigue tests. In either event, facilities at The University of Arizona, including the NASA complex fatigue machines, would be adequate to determine this ratio. Findley Coleman, and Hanley site the value of b/t = 1.78 for an SAE 4340 steel, Rockwell C 35 (13, p. 153); however, the dimensions of the test specimen are not the same as that undergoing tests at The University of Arizona. In addition the specimen which Findley, et. al., used in their studies is of the ungrooved geometry. It seems that the exponent a is in actuality Findley's exponent b/t. It would be possible to experimentally determine this value with no more than the number of specimens required by the static ultimate strength tests, or thirty five specimens.

Once the mean line is specified the standard deviation along this line could quite possibly be approximated by dividing the standard deviation of the endurance strength which is placed along the alternating stress axis by $\sin\Theta$, where Θ is specified

by the ratio of alternating stress to mean stress (3, p. 73). Hence, the standard deviation along the stress ratio axis, s_{S_r}, is given by

$$\sigma_{S_r} = \sigma_{S_e} / \sin \Theta \qquad (11.3)$$

This then would give an approximation of the standard deviation of the Goodman surface.

The two methods presented in this chapter, to reduce to a minimum the required number of test specimens, are not meant to be finalized proposals for a fatigue test program. They do seem to this investigator to be valid means of reducing the need of large quantities of experimental data. The later method discussed would require only the number of specimens needed to experimentally determine the ratio of b/t, quite possibly no more than 35 - 40 specimens. The method formerly discussed would require approximately 200 test specimens. Further investigation of these two methods seems prudent.

CHAPTER XII

OVERALL CONCLUSIONS

Methodologies for developing finite life Goodman diagrams and surfaces have beer presented in this report. The finite life Goodman diagram presents allowable combinations of alternating and mean stress for the combined stress condition of alternating bending and constant torsional stresses for specific periods of design life. The actual Goodman surface, which is developed using two to five strength distributions at specified stress ratios, can be used to construct strength distributions at any desired stress ratio. The strength distributions are distributed normally. The technique of constructing a strength distribution at any specified stress ratio is initiated by construction of the desired stress ratio line on the Goodman diagram. The intercept of this line with the Goodman surface specifies the mean and the standard deviation, in terms of the three sigma limits, of the strength distribution at that stress ratio. The alternating stress level of the mean of the strength distribution can be read directly from the finite life Goodman diagram. This procedure is particularly valuable where the strength distribution at a specific stress ratio is required by the interference technique used in probabilistic design.

In conclusion the finite life Goodman diagrams and surfaces developed in this paper indicate that as the cycle life decreases the allowable combinations of bending and shear stress magnitudes increase. The strength distribution to be placed on the mean stress axis of the finite life Goodman diagram is concluded to be that of the same geometry test specimen as underwent fatigue tests. The grooved geometry test specimen is concluded to be the test specimen which specifies the ultimate strength distribution which is placed on the mean stress axis of the finite life Goodman diagram. The von Mises-Hencky strength theory and ellipse have been shown to adequately model the behavior of SAE 4340 steel, above the cycle life of 10^4 cycles, under combined alternating bending and constant torsional stresses.

CHAPTER XIII

OVERALL RECOMMENDATIONS

The following recommendations are offered by this investigator:

1. As additional cycles to failure data becomes available from Phase II of the National Aeronautics and Space Administration Grant No. 03-002-044 at The University of Arizona the methods proposed in Chapter XII to reduce the required number of test specimens should be further investigated. The recovery of cycles to failure data from the finite life Goodman diagram, should be investigated as proposed in Chapter XII , using both Phase I and Phase II data.
2. A comprehensive literature search should be undertaken to obtain the complete set of papers authored by Professor W. N. Findley of Brown University. These works would be a valuable aid to the research program being conducted at The University of Arizona for the National Aeronautics and Space Administration.
3. Additional fatigue and static strength data, beyond that supplied by Phase II of the National Aeronautics and Space Administration research effort, should be acquired through computer search facilities. These

facilities utilize high speed computers to selectively retrieve and display requested information. This would be particularly helpful in determining the best theoretical distribution to be assigned to the static strength parameters. The additional data supplied by these search facilities would compliment data acquired through the experimental test programs. These search facilities include the Mechanical Properties Data Center in Traverse City, Michigan and the Defense Metals Information in Columbus, Ohio.

APPENDIX A

FORTRAN Computer Program To Reduce Cycles To Failure Data

A-1. Flow Chart

A-2. Definition of Variables

A-3. Program Listing

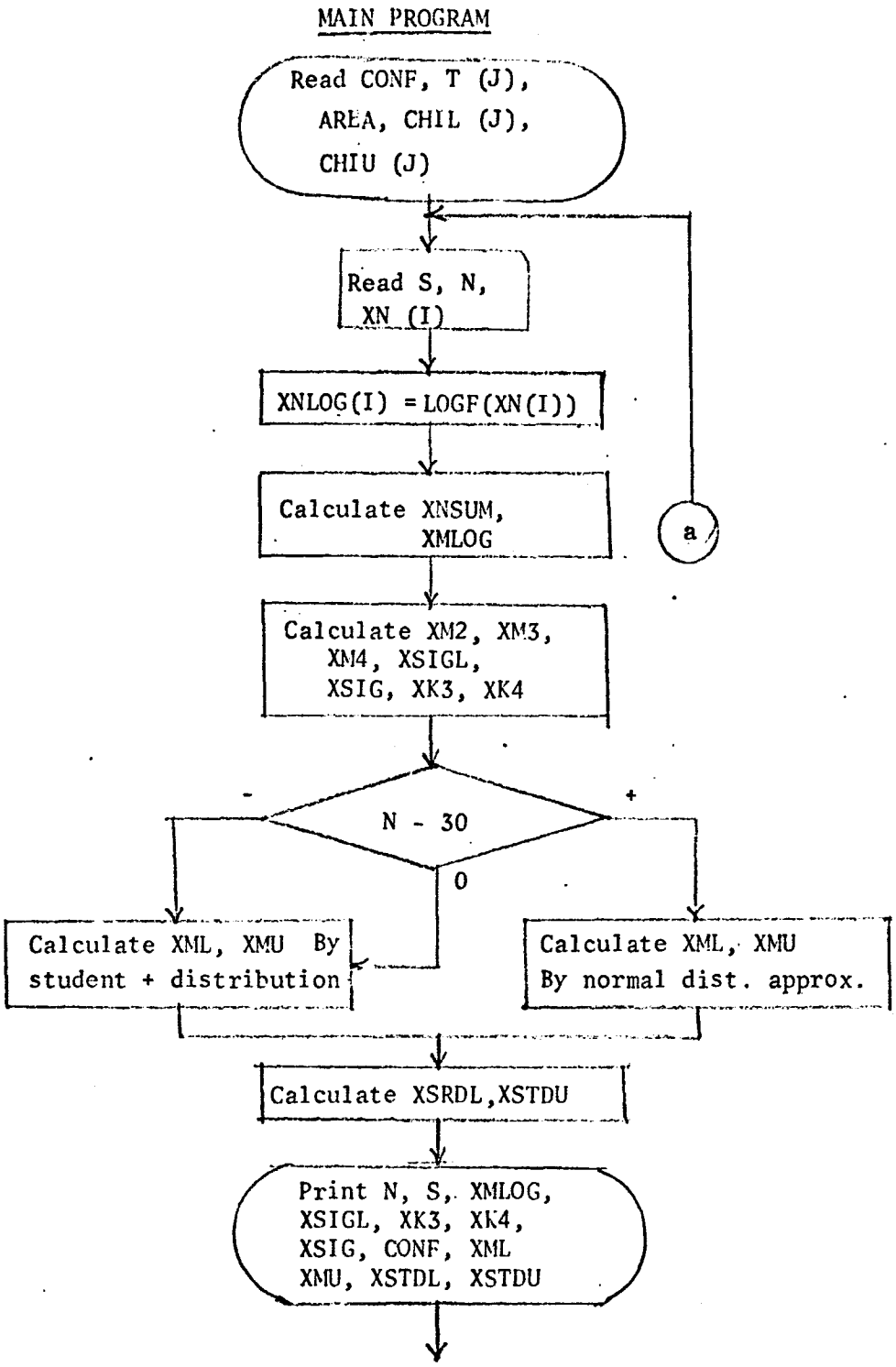

Figure A-1. Flow Chart for Failure Data Distribution Determination Computer Program.

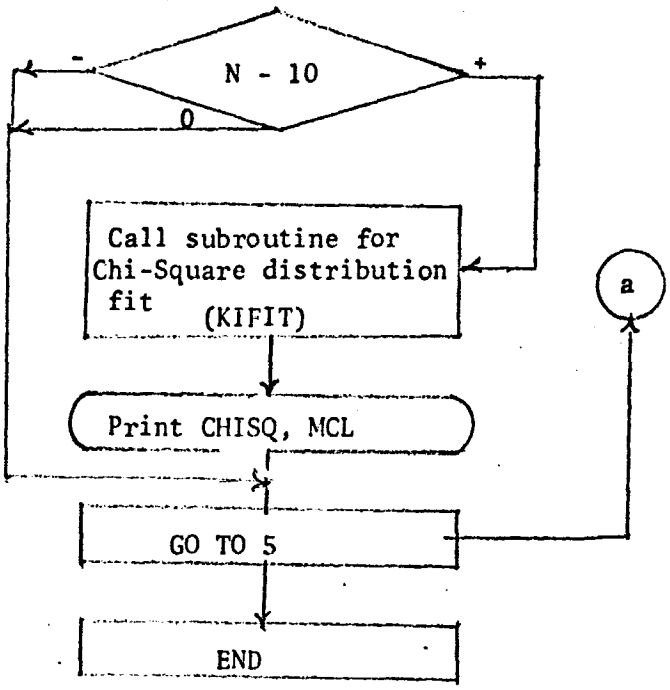

SUBROUTINE PROGRAM

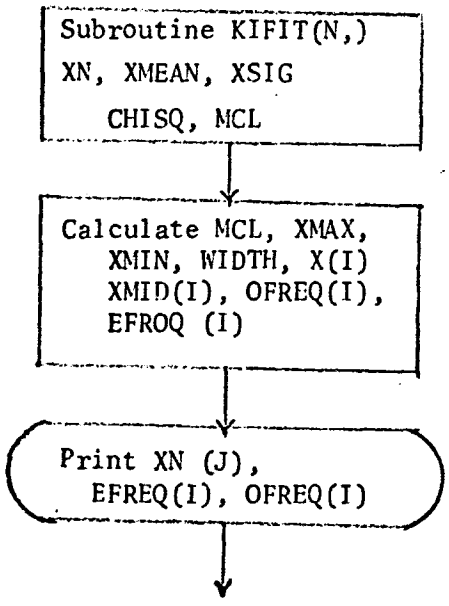

Figure A-1 (Cont'd) .

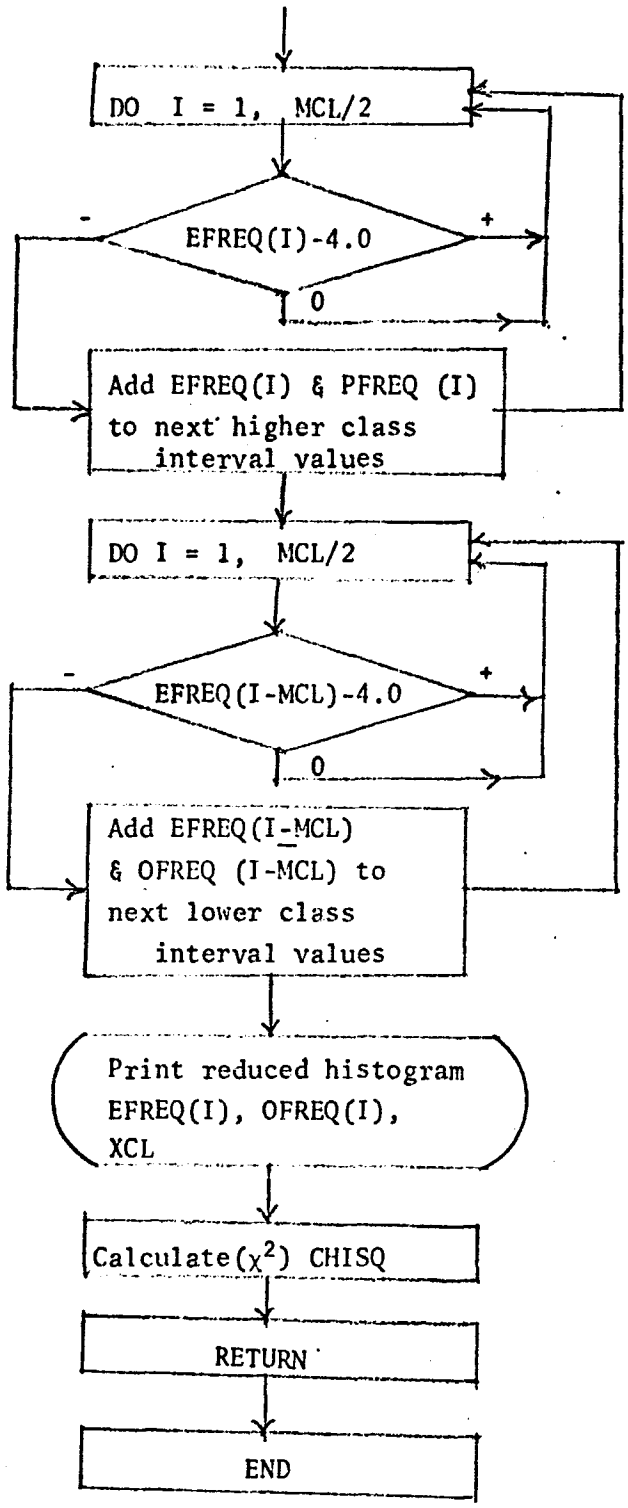

Figure A-1 (Cont'd).

```
CONF = TWO SIDED CONFIDENCE LEVEL
T = STUDENT T FOR DESIRED CONFIDENCE M AND DEGREE
   OF FREEDOM N
AREA = ABSISSA VALUE OF NORMAL DISTRIBUTION FOR
   SPECIFIED CONFIDENCE
CHIU,CHIL = CHI SQUARE FOR CONFIDENCE M AND DEGREE
   OF FREEDOM N
S = STRESS LEVEL OF TESTED SPECIMENS
N = NUMBER OF SPECIMENS
XN(I) = CYCLES TO FAILURE OF SPECIMENS
XNLOG(I) = LOG CYCLES TO FAILURE OF SPECIMENS
XNSUM = SUMMATION OF XNLOG(I)
XMLOG = MEAN LOG CYCLES AT STRENGTH, S
XSIGL = STANDARD DEVIATION IN LOG CYCLES AT STRENGTH
XSIG = SQRTF WITH N-1 DEGREES OF FREEDOM
XM2,XM3,XM4 = 2ND, 3RD, 4TH MOMENTS OF LOG CYCLES
XK3= COEFFICIENT OF SKEWNESS
XK4= COEFFICIENT OF KURTOSIS
XML,XMU = MEAN LOWER AND UPPER CONFIDENCE LIMITS OF
   MEAN LOG VALUE
XSTDL,XSTDU = STANDARD DEVIATION LOWER AND UPPER
   CONFIDENCE LIMITS OF LOG VALUE
CHISQ = VALUE OF CHI SQUARE FIT OF DATA HISTOGRAM TO
   NORMAL DISTRIBUTION DATA
MCL = NUMBER OF HISTOGRAM CLASSES FOR CHI SQUARE FIT
ADDITIONAL SUBROUTINE VARIABLES
N = NUMBER OF DATA POINTS
XN(I) = DATA POINT VALUES
XMEAN, XSIG = MEAN AND STANDARD DEVIATION OF DATA
   VALUES
XMAX = MAXIMUM FAILURE VALUE
XMIN = MINIMUM FAILURE VALUE
WIDTH = CLASS INTERVAL WIDTH
X(I) = CLASS BEGINNING POINT
XMID(I) = CLASS MID-POINT
OFREQ(I) = OBSERVED FREQUENCY OF OCCURRENCE IN CLASS
   INTERVAL I
EFREQ(I) = EXPECTED FREQUENCY OF OCCURRENCE
```

Figure A-2 - Definition of Variables for Failure Data Distribution Determination Computer Program.

```
***  SMITH,RE
*    COMPILE FORTRAN,EXECUTE FORTRAN

      SUBROUTINE KIFIT(N, XN, XMEAN, XSIG, CHISQ,MCL)
C     CHI SQUARED FIT OF DATA POINTS TO A NORMAL DIST
   46 FORMAT(1X,11HEXPONENT = ,F5.0,18H CLASS MIDPOINT = ,
     1   F5.0)
   47 FORMAT (18H DATA POINT VALUES/(1X,F11.3,9F12.3))
   48 FORMAT (1)1X,10H EXPECTED ,10X,10H OBSERVED ,10X,
     1   7H  CLASS/14X,10HCLASS FREQ,10X,10HCLASS FREQ,
     2   8X,12HBEGINNING PT/(1X,F20.8,F20.1,F20.8))
      DIMENSION XN(120), X(15), XMID(14), OFREQ(15),
     1   EFREQ(15)
      AN = N
      CLASS = 2.0+3.3*LOGF(AN)
      MCL = CLASS
      XMAX = XN(1)
      XMIN = XN(1)
      DO 60 I=2,N
      IF(XN(I)-XMIN) 52,54,54
   52 XMIN = XN(I)
      GO TO 58
   54 IF(XN(I)-XMAX) 58,58,56
   56 XMAX = XN(I)
   58 CONTINUE
   60 CONTINUE
      RANGE = XMAX-XMIN
      XCL = MCL
      WIDTH = RANGE/XCL
      MCL = CLASS+1.0
      X(1) = XMIN
      DO 70 I=2,MCL
      IM1 = I-1
      X(I) = X(IM1)+WIDTH
      XMID(IM1) = X(IM1)+WIDTH/2.0
   70 CONTINUE
      DO 80 I=2,MCL
      IM1 = I-1
      OFREQ(IM1) = 0.0
      DO 76 J=1,N
      IF(XN(J)-X(IM1)) 76,72,72
   72 IF(XN(J)-X(I)) 74,76,76
   74 OFREQ(IM1) = OFREQ(IM1)+1.0
   76 CONTINUE
   80 CONTINUE
      OFREQ(MCL) = OFREQ(MCL)+1.0
      DO 83 I=1,MCL
      EXP = ((XMID(I)-XMEAN)*(XMID(I)-XMEAN))/(2.0*XSIG*XSIG)
      IF (EXP-100.) 82,82,81
```

Figure A-3 - 7072 Computer Program Listing for Failure Data Distribution Determination.

```
   81 EFREQ(I) = 0.0
      PRINT 46, EXP,XMID(I)
      GO TO 83
   82 CONTINUE
      EFREQ(I) = AN*0.3989423/XSIG*EXPDF(-EXP)*WIDTH
   83 CONTINUE
      PRINT 47,(XM(I),I=1,N)
      PRINT 48, (EFREQ(I),OFREQ(I),X(I),I=1,MCL)
      M = MCL/2
      J = 1
      DO 84 I=1,M
      IF (EFREQ(I)-4.0) 77,84,84
   77 IF (I-M) 79,84,84
   79 J=J+1
      IP1 = I+1
      EFREQ(IP1) = EFREQ(I)+EFREQ(IP1)
      OFREQ(IP1) = OFREQ(I)+OFREQ(IP1)
   84 CONTINUE
      K = MCL
      MCTR = MCL-M+1
      DO 87 I=1,M
      MMI = MCL-I+1
      IF (EFREQ(MMI)-4.0) 85,87,87
   85 IF (MM-MCTR) 87,87,86
   86 K = MCL-I
      MMI = MMI-1
      EFREQ(MMI) = EFREQ(MMI)+EFREQ(MMI+1)
      OFREQ(MMI) = OFREQ(MMI)+OFREQ(MMI+1)
   87 CONTINUE
      PRINT 49, (EFREQ(I),OFREQ(I),X(I),I=J,K)
      MCL = K-J
      CHISQ = 0.0
      DO 88 I=J,K
      CHISQ = CHISQ+((OFREQ(I)-EFREQ(I))*(OFREQ(I)-EFREQ(I)
     1    ))/EFREQ(I)
   88 CONTINUE
      RETURN
      END

C     PROGRAM FOR FINDING THE MEAN, STANDARD DEVIATION
C       AND CONFIDENCE LIMITS OF RANDOM VARIABLES FROM
C       ASSUMED NORMAL DISTRIBUTIONS
      CONF = 90.
    3 FORMAT (I5)
    5 FORMAT (F10.0)
    6 FORMAT ((8F10.0))
   10 FORMAT (F10.3,I5/(8F10.0))
   12 FORMAT (1H0// 10H SPECIMENS, 7X,9HSTRENGTH, 12X,
     1    8HLOG MEAN,12X,12HLOG STD DEV,7X,8HSKEWNESS,7X,
```

Figure A-3 (Cont'd)

```
     2   8HKURTOSIS/1X,I10,F15.2,F20.8,10H  WITH N =,
     3   F20.8,2F15.8)
  13 FORMAT (1X,  20HCONFIDENCE LIMITS OF,I3,
     1   17H PERCENT ARE USED)
  14 FORMAT (1X, 17HCONFIDENCE LIMITS,10HMEAN LOWER,5X,
     1   10HMEAN UPPER,5X,13HSTD DEV LOWER,5X,
     2   13HSTD DEV UPPER/8X,F20.8,F15.4,F15.8,F18.8)
  15 FORMAT (41X, 10HWITH N-1 =,F20.8)
  16 FORMAT (1X, 32H CHI SQUARE FIT TO NORMAL DIST =, F14.8,
     1   5X,20HDEGREE OF FREEDOM = ,I3)
     DIMENSION XN(120),XNLOG(120),CHIL(100),CHIU(100),T(100)
     READ 3,CONF
     READ 6,(T(I),I=1,30)
     READ 5,  AREA
     READ 6, (CHIL(I),I=1,100)
     READ 6, (CHIU(I),I=1,100)
  16 READ 10, S,N,(XN(I),I=1,N)
     DO 20 I=1,N
     XNLOG(I) = LOGF(XN(I))
  20 CONTINUE
     XNSUM = 0.0
     DO 25 I=1,N
     XNSUM = XNSUM + XNLOG(I)
  25 CONTINUE
     TN = N
     AN = N
     XNLOG = XNSUM/AN
     XM2 = 0.0
     XM3 = 0.0
     XM4 = 0.0
     DO 30 I=1,N
     XSQ = (XNLOG(I)-XNLOG)*(XNLOG(I)-XNLOG)
     XM2 = XM2+XSQ
     XM3 =XM3 + XSQ*(XNLOG(I)-XNLOG)
     XM4 = XM4+XSQ*XSQ
  30 CONTINUE
     XSIG = SQRTF(XM2/(AN-1.0))
     XM2 = XM2/AN
     XM3 = XM3/AN
     XM4 = XM4/AN
     XSIGL = SQRTF(XM2)
     XK3 = XM3/(XSIGL*XM2)
     XK4 = XM4/(XM2*XM2)
     A = SQRTF(AN)
     IF (N-30) 34,34,36
  34 XNL = XNLOG - T(N-1)*XSIGL/A
     XNU = XNLOG+T(N-1)*XSIGL/A
     GO TO 38
  36 XNL = XNLOG-AREA*XSIGL/A
```

Figure A-3 (Cont'd)

```
      XMU = XMLOG+AREA*XSIGL/A
      IF (N-100) 37,37,35
   35 N = 100
      AN = N
   37 CONTINUE
   38 XSTDL = XSIGL*SQRTF((AN-1.0)/CHIL(N-1))
      XSTDU = XSIGL*SQRTF((AN-1.0)/CHIU(N-1))
      N = IN
      PRINT 12, N,S,XMLOG,XSIGL, XK3,XK4
      PRINT 15, XSIG
      PRINT 13, CONF
      PRINT 14, XML,XMU,XSTDL,XSTDU
      IF (N-10) 40,40,39
   39 CONTINUE
      CALL KIFIT(N,XMLOG,XMLOG,XSIGL,CHISQ,MCL)
      PRINT 16,CHISQ,MCL
   40 CONTINUE
      GO TO 18
      END
```

Figure A-3 (Cont'd)

APPENDIX B

FORTRAN Computer Program To Determine Time Dependent Strength Distribution parameters

B-1. Flow Chart

B-2. Definition of Program Variables

B-3. Computer Program Listing

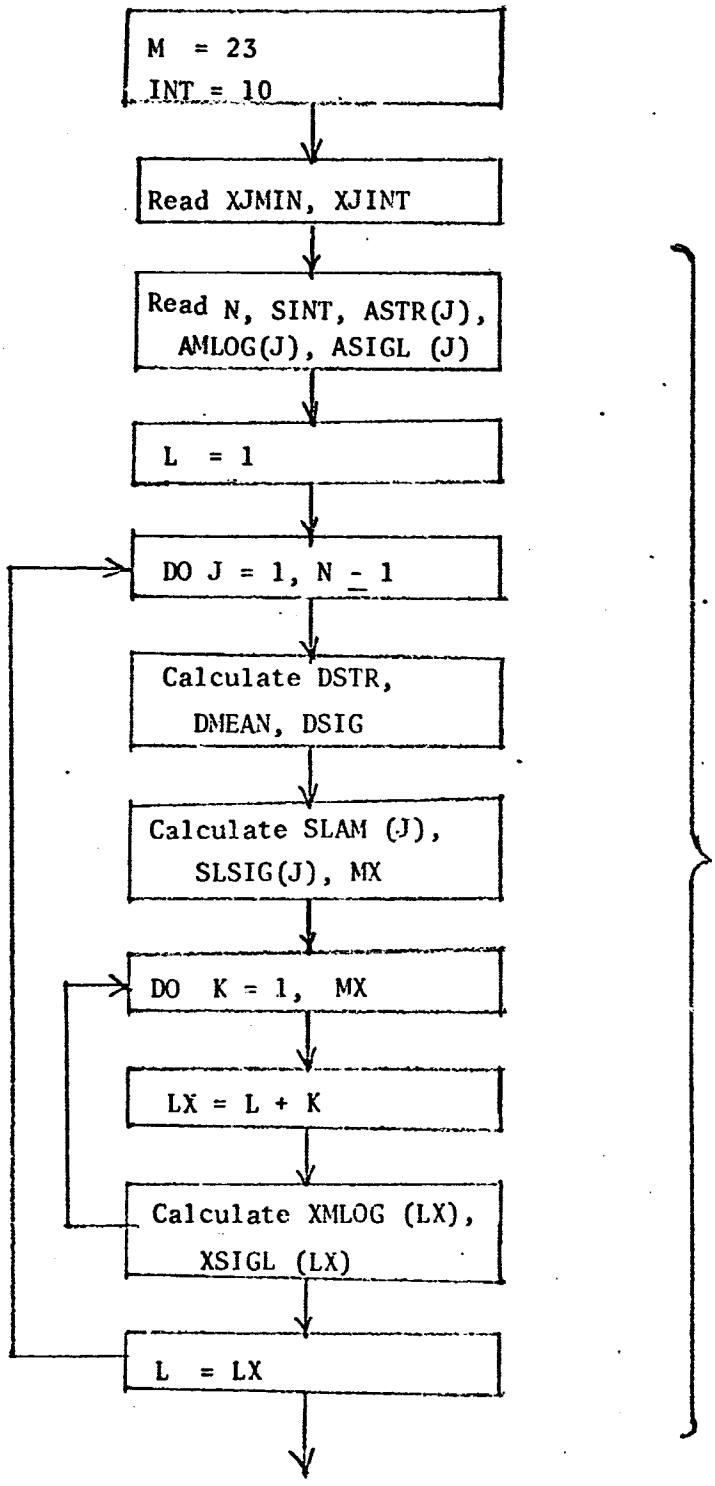

Figure B-1 - Flow Chart for Time Dependent Strength Distribution Generation from Failure Distribution Parameters.

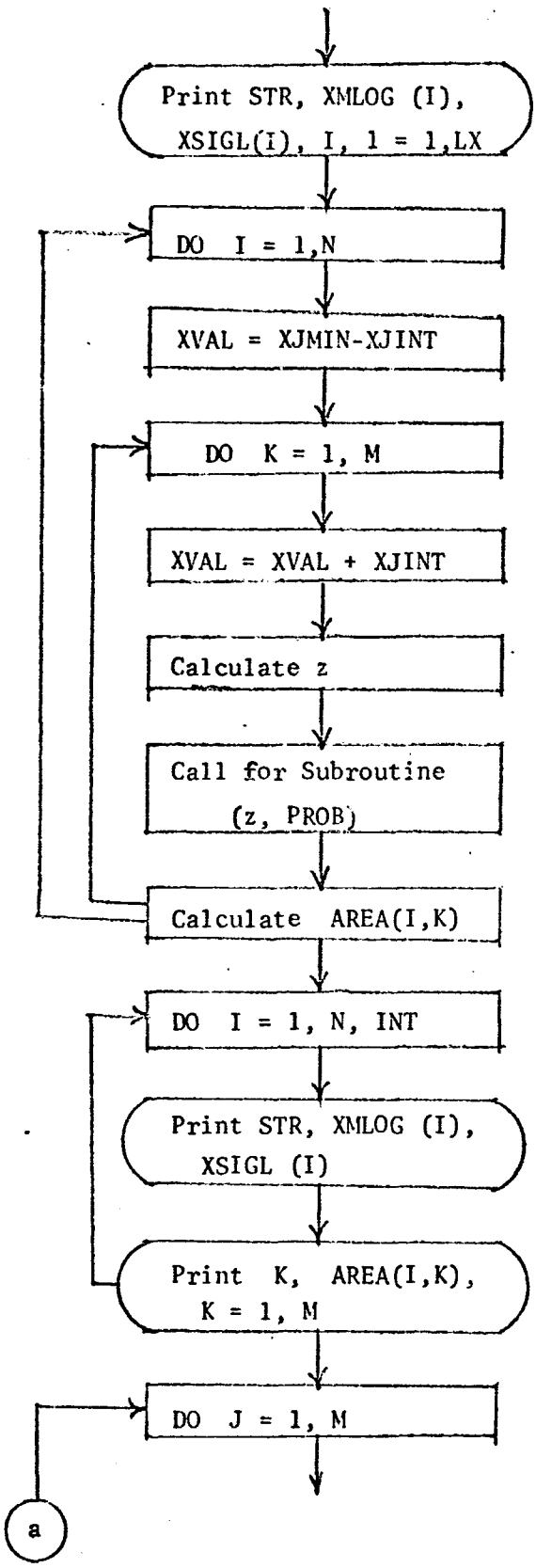

Cummulative lognormal failure distribution at N=LK stress levels from failure distributio parameters.

Figure B.1 (Cont'd).

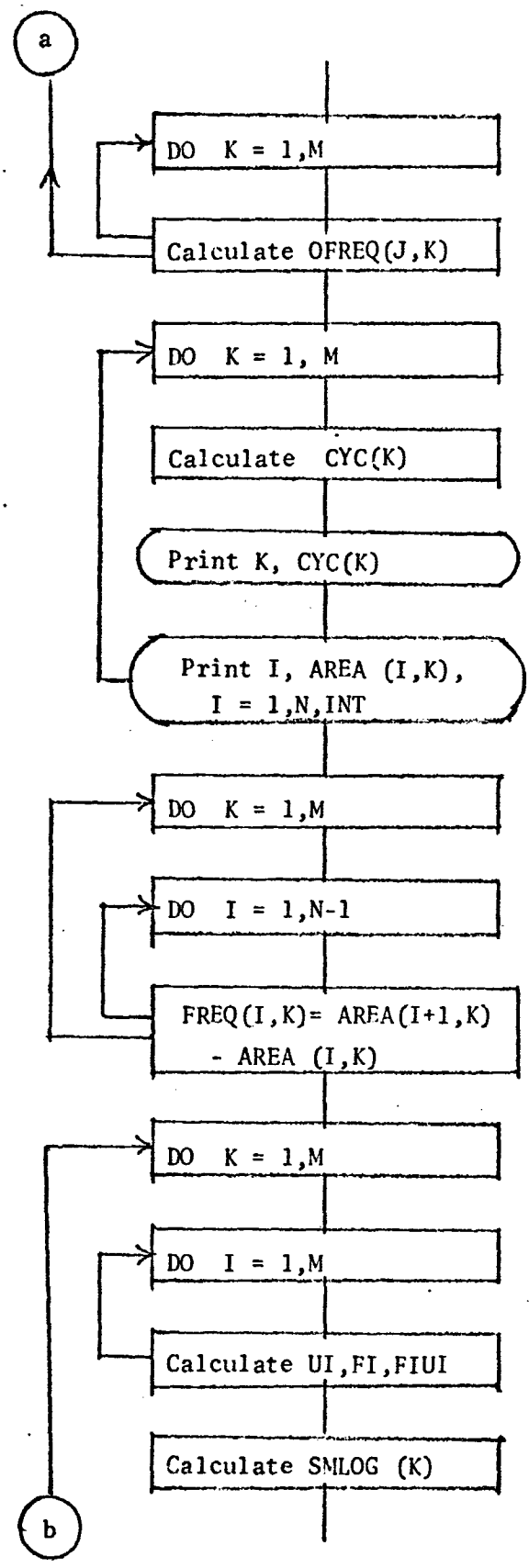

Strength frequency distributions for various log cycles of life.

Parameter calculations for normal distribution fit to strength distributions.

Figure B-1 (Cont'd)

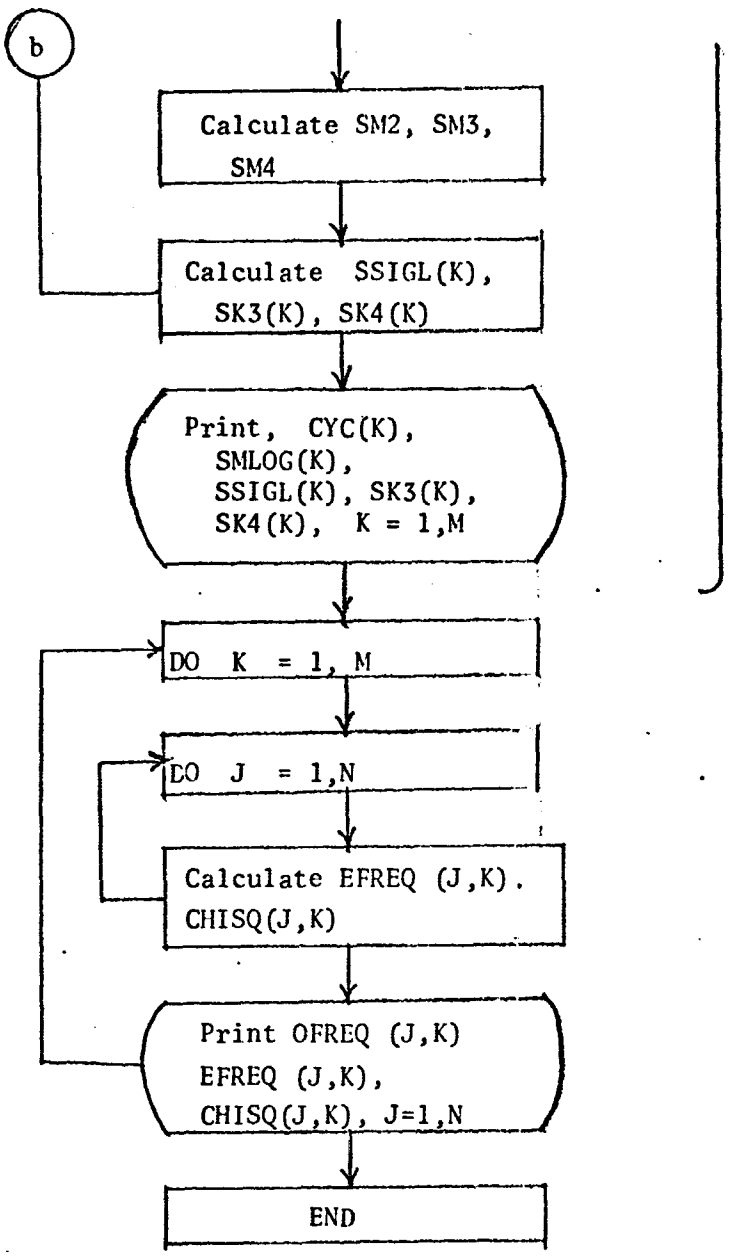

Figure B-1 (Cont'd).

```
M = TOTAL NUMBER OF GENERATED STRENGTH DIST.
INT = NO. OF VALUES OMITTED BETWEEN PRINTOUT
XJMIN = MINIMUM LOG CYCLE VALUE FOR STRENGTH DIST.
XJINT = INTERVALS BETWEEN LOG CYCLE VALUES FOR
   STRENGTH DISTRIBUTION S
N = NUMBER OF FAILURE DISTRIBUTIONS
SINT = MINIMUN STRESS INTERVAL BETWEEN INTERPOLATED
   FAILURE DISTRIBUTIONS
ASTR(J) = STRESS LEVEL FOR EXPERIMENTAL FAILURE
   DISTRIBUTION
AMLOG(J) = EXPERIMENTAL FAILURE DISTRIBUTION MEAN IN
   LOG CYCLES AT STRESS ASTR
ASIGL(J) = EXPERIMENTAL FAILURE DISTRIBUTION
   STANDARD DEVIATION IN LOG CYCLES
DSTR = DIFFERENCE BETWEEN TWO CONSECUTIVE
   EXPERIMENTAL STRESS LEVELS
DMEAN = DIFFERENCE BETWEEN TWO CONSECTIVE EXPERIMENTAL
   FAILURE DISTRIBUTION MEANS
DSIG  = DIFFERENCE BETWEEN TWO CONSECTIVE EXPERIMENTAL
   FAILURE DIST. STANDARD DEVIATIONS
SLAM(J) = SLOPE BETWEEN TWO CONSECUTIVE EXPERIMENTAL
   FAILURE DISTRIBUTION MEANS
SLSIG(J) = SLOPE BETWEEN TWO CONSECUTIVE EXPERIMENTAL
   FAILURE DISTRIBUTION STANDARD DEVIATIONS
L = COUNTER FOR INTERPOLATED FAILURE DISTRIBUTIONS
MX = DSTR/SINT
LX = SEQUENTIAL NUMBERING OF SAMPLE FAILURE
   PARAMETERS AND INTERPOLATED PARAMETERS
STR = STRESS LEVEL FOR I TH FAILURE DIST. PARAMETERS
XMLOG(I) = FAILURE MEAN IN LOG CYCLES FOR
   EXPERIMENTAL AND INTERPOLATED VALUES
XSIGL(I) = FAILURE STANDARD DEVIATION IN LOG CYCLES
   FOR SAMPLE AND INTERPOLATED VALUES
N = LX = NUMBER OF GENERATED FAILURE DISTRIBUTIONS
   BY INTERPOLATION
XVAL = LOG CYCLE VALUES FROM XJMIN TO XJMIN + M*XJINT
   FOR M STRENGTH DISTRIBUTIONS
Z = STANDARDIZED DISTANCE FOR LOG CYCLE FAILURE
   DISTRIBUTION AT I TH STRESS LEVEL FOR K TH LOG CYCLES
PROB = NORMALIZED PROBABILITY DENSITY UNDER LOGNORMAL
   DISTRIBUTION FROM -Z TO Z
AREA(I,K) = CUMMULATIVE NORMALIZED AREA OF LOGNORMAL
   FAILURE DISTRIBUTION FROM ZERO TO Z
TSTR(INO)=STRENGTH LEVELS PRINTED OUT
NINT(INO) = INTERGER REPRESENTATION OF TSTR(INO)
CYC(K) = LOG-CYCLE VALUE CORRESPONDING TO K S
```

Figure B-2. Definition of Program Vatiables.

```
FREQ(1,K) = FAILURE PROBABILITY FROM CUMMULATIVE LOG-
   NORMAL FAILURE DISTRIBUTION AT LOG CYCLES CYC
   BETWEEN STRENGTHS I(A) AND I(B)
UI = ABSCISSA VALUE OF STRENGTH HISTOGRAM CLASS
   INTERVAL
FI = FREQUENCY OF OCCURRENCE IN STRENGTH HISTOGRAM
   CLASS INTERVAL
FIUI = FI TIMES UI
SMLOG(K) = MEAN STRENGTH AT SET LOG CYCLES
SM2,SM3,SM4 = 2ND,3RD, AND 4TH MOMENTS OF
   STRENGTH DISTRIBUTION
SSIGL(K) = STANDARD DEVIATION FOR STRENGTH AT SET
   LOG CYCLES
SK3(K)=COEFFICIENT OF SKEWNESS FOR STRENGTH AT SET
   LOG CYCLES
SK4(K) = COEFFICIENT OF KURTOSIS FOR STRENGTH AT SET
   LOG CYCLES
TOTAL NUMBER OF INO S = N/NINT WHERE N = LX MAX.
TOTAL NUMBER OF J S = N SAMPLE FAILURE DIST.
TOTAL NUMBER OF I S = N WHERE N = LX MAX.
TOTAL NUMBER OF K S = M
```

Figure B-2. (Cont'd).

```
***  SMITH,RE
*    COMPILE FORTRAN,EXECUTE FORTRAN

      SUBROUTINE PROB(Z,PROB)
C     PROB = THE AREA UNDER NORMAL DISTRIBUTION BETWEEN
C        PLUS AND MINUS Z STANDARD DEVIATIONS
      IF(Z-1.2) 1000,1000,1010
 1000 ZSQ = Z*Z
      PROB = 0.79788455*Z*(0.99999774-ZSQ*(0.16659433
     1  -ZSQ*(0.024638810 - ZSQ*0.002397486?)))
      GO TO 1070
 1010 IF(Z-2.9) 1020,1060,1060
 1020 ZSQ = Z*Z
      PROB = 1.0
      PTERM = 1.0
      FACT = 1.0
      ODDIN = 3.0
 1030 PTERM = -PTERM*ZSQ/(2.0*FACT)
      TERM = PTERM/ODDIN
      PROB = PROB + TERM
      IF (ABSF(TERM) - 0.00007) 1050,1040,1040
 1040 FACT = FACT + 1.0
      ODDIN = ODDIN + 2.0
      GO TO 1030
 1050 PROB = 0.79788455*Z*PROB
      GO TO 1070
 1060 REC = 1./(Z*2)
      PROB = 1.-0.79788453*EXPEF(-Z*Z/2.0)/Z*
     1   (1. - REC*(1. - REC*(3. - REC*(15.-REC*105.))))
 1070 CONTINUE
      RETURN
      END

      M = 23
      INT = 10
      DIMENSION ASTR(10), AMLOG(10), ASIGL(10), SLAM(9),
     1   XMLOG(251), XSIGL(25)), AREA(251,23), FREQ(251,23),
     2   CYC(23), SMLOG(23), SSIGL(23), SK3(23), SK4(23),
     3 NUM(10),IADEX(10),OFREQ(10,23),GFREQ(10,23),
     4   CHISQ(10,23),ST(10),SLSIG(9), EFREQ(10,23)
      EQUIVALENCE (AREA,FREQ),
     1   (XSIGL,SSIGL), (XMLOG,OFREQ), (AREA(500),EFREQ),
     2   (AREA,CHISQ), (AREA(250),GFREQ)
    5 READ10,XMIN,XJINT
   10 FORMAT(2F10.0)
C     FAILURE DISTRIBUTION VALUES ARE READ IN FROM
C        LOWEST TO HIGHEST STRESS AND STRESSES ARE
C        INTEGER VALUES OF SINT
      READ 20
```

Figure B-3. 7072 Computer Program Listing for Time Dependent Strength Distribution Generation.

```
   20 FORMAT (50H                    BLANK
      READ 30, N,SINT,(ASTR(J),AMLOG(J),ASIGL(J),J=1,N)
   30 FORMAT (I5,F5.0/(3F10.0))
      READ32,(NUM(J),J=1,N)
   32 FORMAT ((5I10))
      NM1 = N-1
      L = 1
      INDEX(1) = 1
      DO 85 J=1,NM1
      DSTR = ASTR(J+1)-ASTR(J)
      DMEAN = AMLOG(J+1)-AMLOG(J)
      DSIG = ASIGL(J+1)-ASIGL(J)
      SLAM(J) = DSTR/DMEAN
      IF(DSIG) 40,50,40
   40 SLSIG(J) = DSTR/DSIG
   50 CONTINUE
      JP1 = J+1
      MX = DSTR/SINT
      INDEX(JP1) = L+MX
      SMIN = ASTR(1)
      XMLOG(1) = AMLOG(1)
      XSIGL(1) = ASIGL(1)
      DO 80 K=1,MX
      LX = L + K
      XMLOG(LX) = XMLOG(LX-1)+SINT/SLAM(J)
      IF(DSIG) 70,60,70
   60 XSIGL(LX) = XSIGL(LX-1)
      GO TO 80
   70 XSIGL(LX) = XSIGL(LX-1)+SINT/SLSIG(J)
   80 CONTINUE
      L = LX
   85 CONTINUE
      PRINT 90
   90 FORMAT (1H1, 8X,12HSTRENGTH-PSI,11X,8HLOG MEAN, 9X,
     1    11HLOG STD DEV,9X,11HINTEGER (I))
      XINT = INT
      STR = SMIN
      DO110 I=1,LX,INT
      PRINT100,STR,XMLOG(I),XSIGL(I),I
  100 FORMAT ((3F20.8,I20))
      STR = STR+SINT*XINT
  110 CONTINUE
      NOLD = N
      N = LX
C     CONVERTING LOGNORMAL FAILURE DIST. PARAMETERS AT N
C        STRESS LEVELS TO CUMMULATIVE LOGNORMAL FAILURE
C        DISTRIBUTION
      DO 180 I=1,N
      XVAL = XMLOG(I)-XMIN
```

Figure B-3 (Cont'd)

```
      DO 180 J=1,M
      XVAL = XVAL+XJINT
      Z = (XVAL-XMLOG(I))/XSIGL(I)
      IF(Z) 120,140,140
  120 IF(Z+3.5)160,130,130
  130 Z = -Z
      CALL PROB(Z,PROB)
      AREA(I,J) = (1.0-PROB)/2.0
      GO TO 180
  140 IF(Z-3.5) 150,150,170
  150 CALL PROB(Z,PROB)
      AREA(I,J) = PROB/2.0+0.5
      GO TO 180
  160 AREA(I,J) = 0.0
      GO TO 180
  170 AREA(I,J) = 1.0
  180 CONTINUE
      INT2 = INT*4
      STR = SMIN
      DO 220 I=1,N,INT2
      PRINT 190,STR,XMLOG(I),XSIGL(I)
  190 FORMAT(1H0,5X,11HSTRENGTH = ,F13.6,5X, 9HLOG MEAN ,
     1   9HCYCLES = ,F8.6,5X,20HLOG STD DEVIATION = ,F8.6)
      PRINT 200
  200  FORMAT (1X, 33HDATA BELOW IS J, AND CUMMULATIVE ,
     1   13HDIST UP TO J.)
      PRINT 210, (J, AREA(I,J),J=1,M)
  210 FORMAT     ((1X,I3,F9.6,I3,F9.6,I3,F9.6,I3,F9.6,
     1  I3,F9.6,I3,F9.6,I3,F9.6,I3,F9.6,I3,F9.6))
      STR = STR+SINT*XINT*4.
  220 CONTINUE
      DO 222 J=1,NOLD
      I = INDEX(J)
      XNUM = NUM(J)
      DO 224 K=1,M
      OFREQ(J,K) = XNUM*AREA(I,K)
  224 CONTINUE
  222 CONTINUE
C     FREQUENCY DIST AND NORMAL DISTRIBUTION PARAMETERS
      XJMIN = XJMIN-XJINT
      DO 240 J=1,M
      XJ = J
      CYC(J) = XJ*XJINT+XJMIN
      PRINT 240, J, CYC(J)
  240 FORMAT (1H0,3HJ = ,I3 ,5X,13HLOG CYCLES = ,F6.3)
      PRINT 250, (I,AREA(I,J),I=1,N,INT)
  250 FORMAT (2X,3H(I),1X,9HFREQUENCY/(1X,I3,F10.6,I5,F10.6
     1   ,I5,F10.6,I5,F10.6,I5,F10.6,I5,F10.6,I5,F10.6,I5,F10.6))
  260 CONTINUE
```

Figure B-3 (Cont'd).

```
      NM1 = N-1
      DO 270 J=1,M
      DO 270 I=1,NM1
      IP1 = I+1
      FREQ(I,J) = AREA(IP1,J) -AREA(I,J)
  270 CONTINUE
      N = NM1
C     MEAN AND NORMAL DISTRIBUTION PARAMETERS OF HISTOGRAM
      DO 300 J=1,M
      FI = 0.
      FIUI = 0.
      UI = SMIN-SINT*0.5
      DO 280 I=1,N
      UI = UI+SINT
      FI = FI+FREQ(I,J)
      FIUI = FIUI+FREQ(I,J)*UI
  280 CONTINUE
      SMLOG(J) = FIUI/FI
      SM2 = 0.
      SM3 = 0.
      SM4 = 0.0
      UI = SMIN-SINT*0.5
      DO 290 I=1,N
      UI = UI+SINT
      SQ = (UI-SMLOG(J))*(UI-SMLOG(J))
      SM2 = SM2 + SQ*FREQ(I,J)
      SM3 = SM3 + FREQ(I,J)*(UI-SMLOG(J))*SQ
      SM4 = SM4+SQ*SQ*FREQ(I,J)
  290 CONTINUE
      SM2 = SM2/FI
      SM3 = SM3/FI
      SM4 = SM4/FI
      SSIGL(J) = SQRTF(SM2)
      SK3(J) = SM3/(SSIGL(J)*SM2)
      SK4(J) = SM4/(SM2*SM2)
  300 CONTINUE
      PRINT 20
      PRINT 310
  310 FORMAT (10H  NUMBER  ,10HLOG CYCLES,5X,
     1    15H  MEAN STRENGTH,5X,15H STD. DEVIATION,10X,
     2    10H  SKEWNESS,10X,10H  KURTOSIS)
      PRINT 320, (J, CYC(J), SMLOG(J), SSIGL(J), SK3(J),
     1    SK4(J), J=1,M)
      PRINT 320, (J, CYC(J), SMLOG(J), SSIGL(J), SK3(J), SK4(J),
  320 FORMAT ((I8,F9.2,3F24.4,2F20.8))
      PRINT 325,(NO-(J),INDEX(J),J=1,NOLD)
  325 FORMAT ( 15X, 15HOBSERVED NUMBER, 9X, 1)HINTEGER (I)/
     1    (10X,2I20))
      DO 500 K=1,M
```

Figure B-3 (Cont'd)

```
      DO 480 J=1,NOLD
      X = INDEX(J)
      ST(J)  = SMIN+SINT*X -SINT
      Z = (ST(J)-SMLOG(K))/SSIGL(K)
      IF(Z) 330,350,350
  330 Z = -Z
      IF (Z-3.5) 340,340,360
  340 CALL PROB(Z,PROB)
      PROBA = 0.5-PROB*0.5
      GO TO 370
  350 IF(Z-3.5) 355,355,365
  355 CALL PROB(Z,PROB)
      PROBA = PROB*0.5+0.5
      GO TO 370
  360 PROBA = 0.0
      GO TO 370
  365 PROBA = 1.0
  370 OFREQ(J,K) = PROBA
      XNUM = NUM(J)
      EFREQ(J,K) = OFREQ(J,K)*XNUM
      CHISQ(J,K) = (OFREQ(J,K)-EFREQ(J,K))*(OFREQ(J,K)
     1    -EFREQ(J,K))/EFREQ(J,K)
  480 CONTINUE
      PRINT 490,K
  490 FORMAT (1H0,3H K=,I3)
      PRINT 495,(ST(J),OFREQ(J,K),OFREQ(J,K),EFREQ(J,K),
     1    CHISQ(J,K),J=1,NOLD)
  495 FORMAT(16X,14HSTRENGTH LEVEL, 9X,11HNORMAL FREQ, 7X,
     1    13HOBSERVED FREQ, 7X,13HEXPECTED FREQ, 4X,
     2    16HCHI SQUARE VALUE/ (10X,4E20.6))
  500 CONTINUE
      GO TO 5
      END
```

Figure B-3. (Cont'd).

APPENDIX C

Listing of Fortran Computer Program CYTOFR Used To Determine Cycles To Failure Distributions

C-1. Flow Chart

C-2. Definition of Variables

C-3. Fortran Program Listing

Program to Calculate Parameter Estimates for the Normal and Log-Normal Distributions and Conduct Goodness-of-Fit Tests

MAIN PROGRAM (CYTOFR)

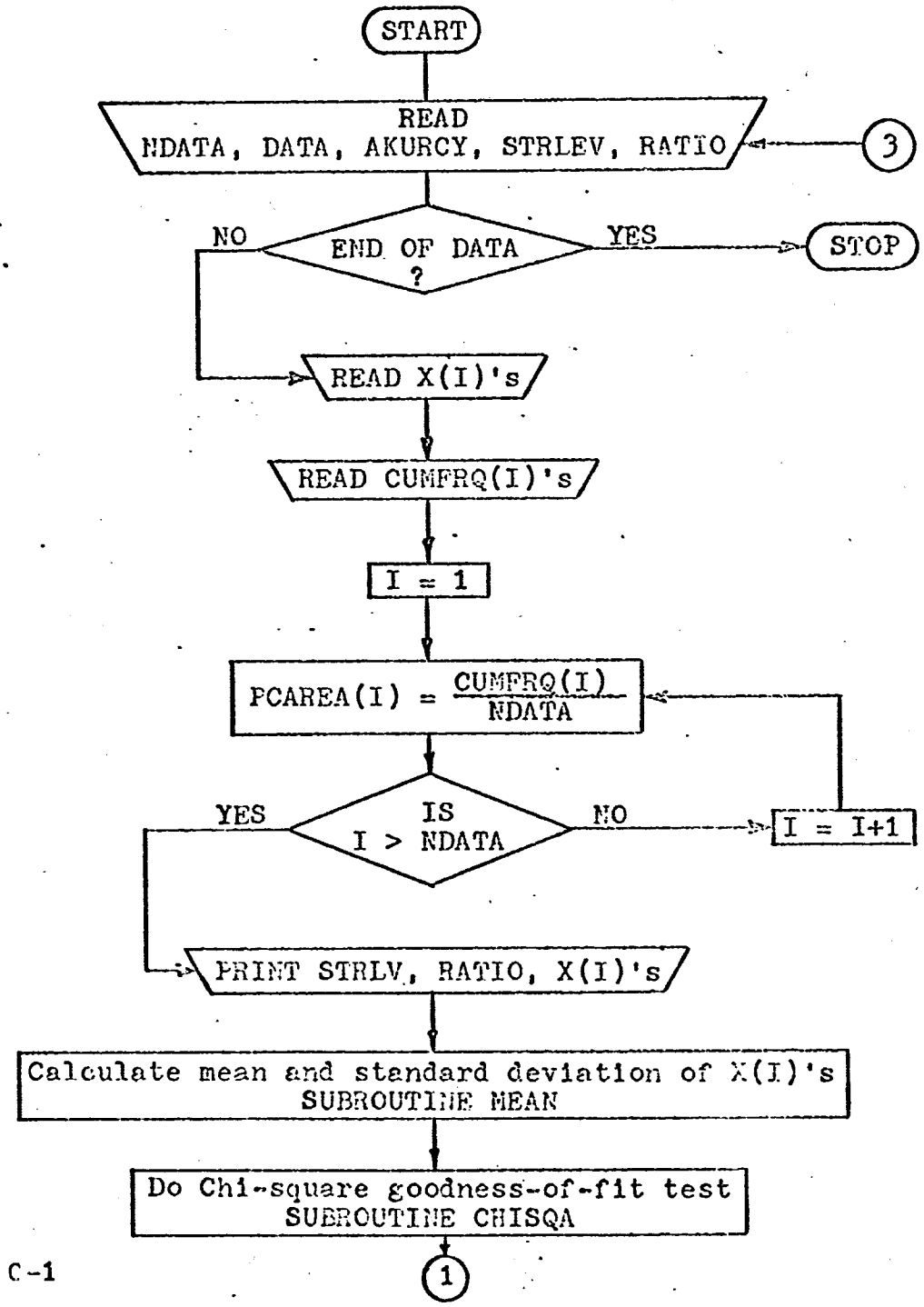

Fig. C-1

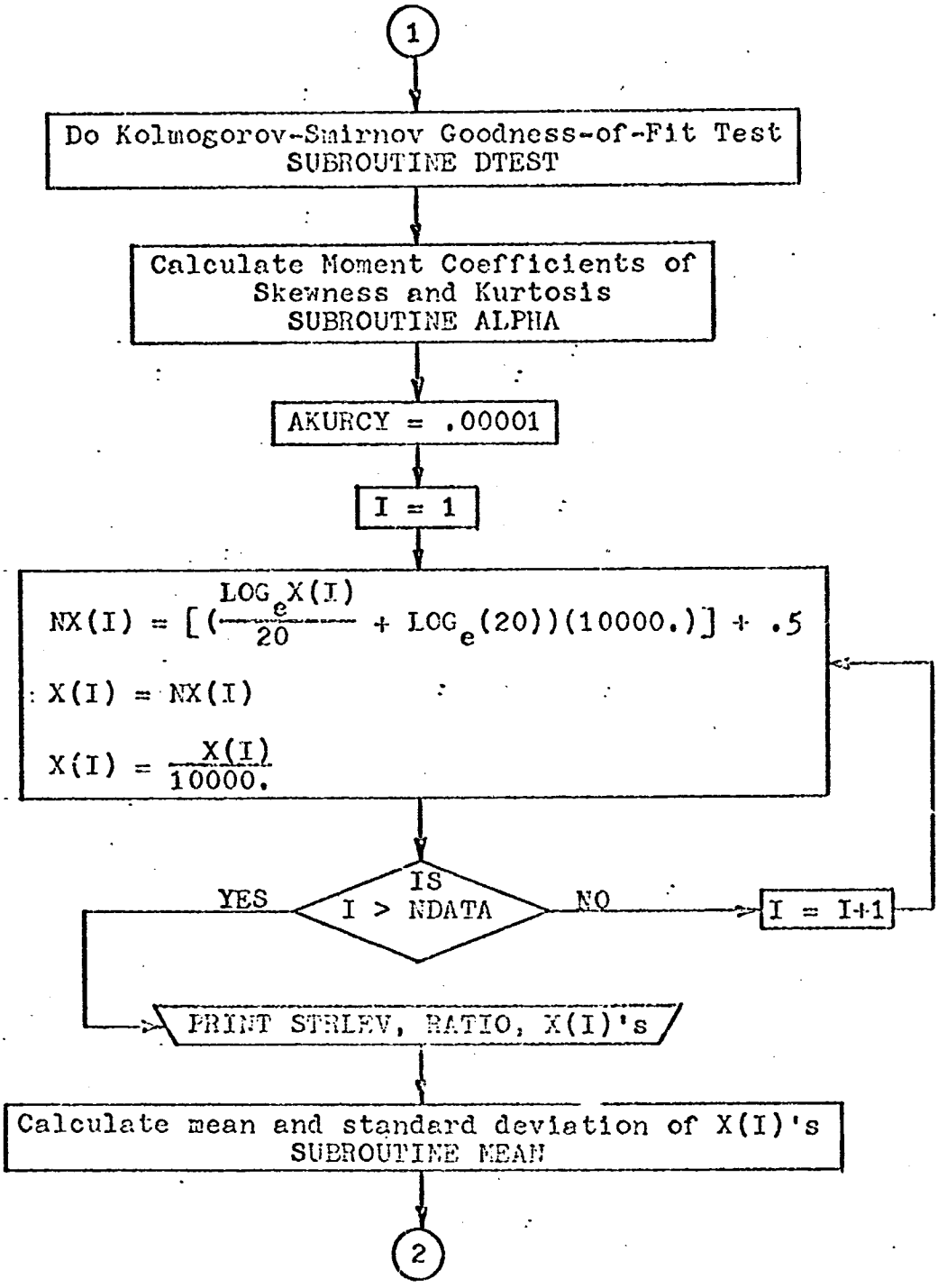

Fig. C-1 (continued)

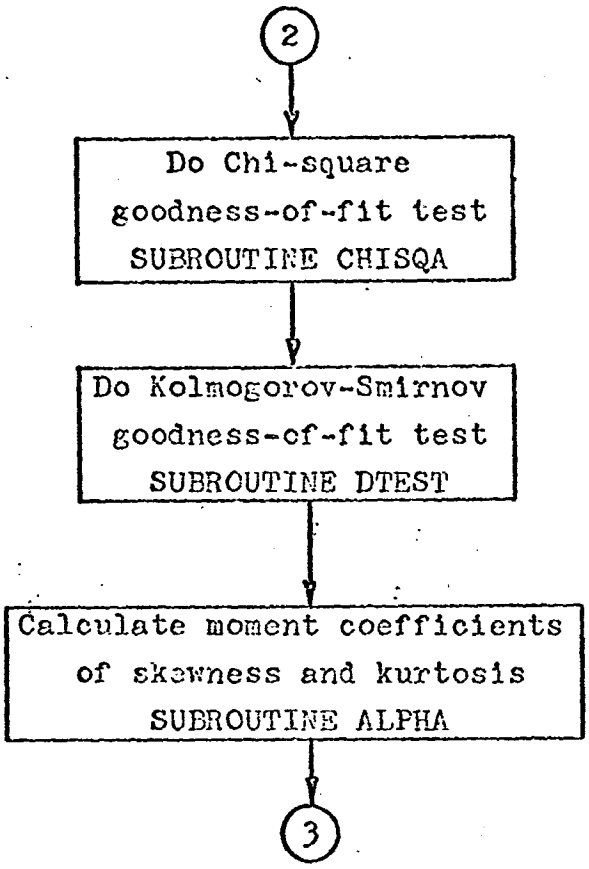

Fig. C-1 (continued)

Subroutine to Find Mean and Standard Deviation

SUBROUTINE MEAN

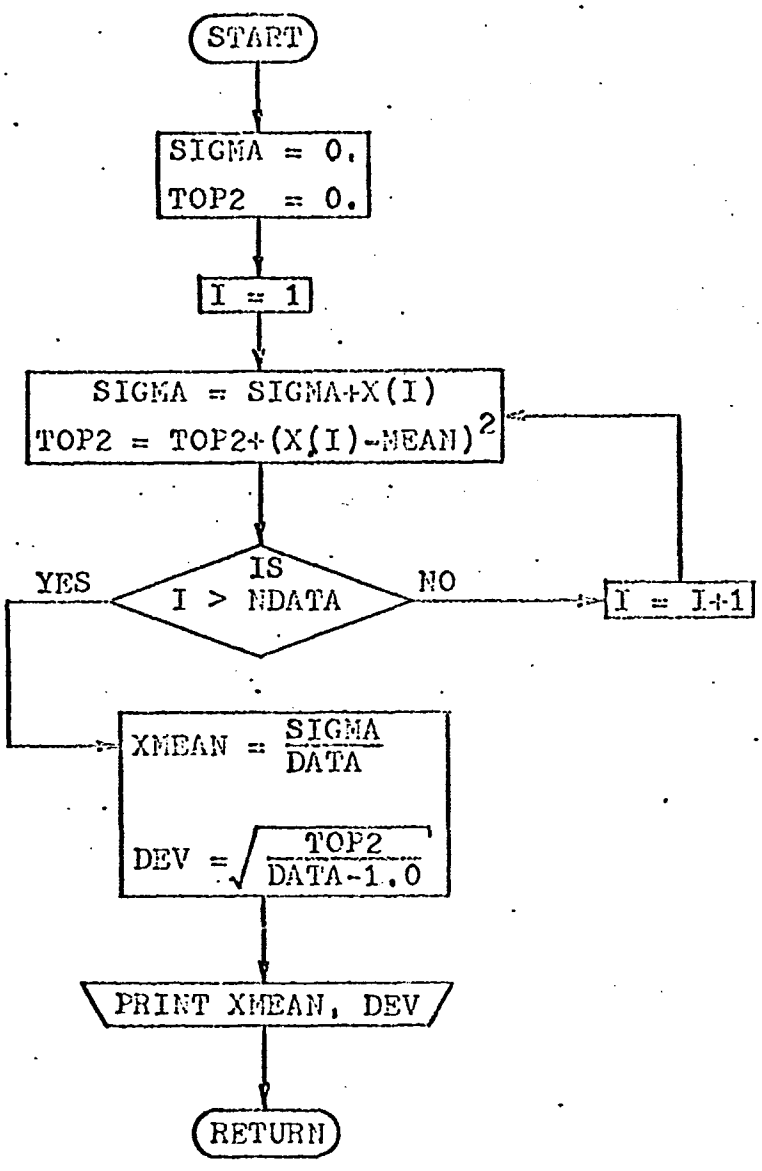

Fig. C-1 (continued)

Subroutine to Find Area Under Standard Normal Curve

FUNCTION PROB(X)

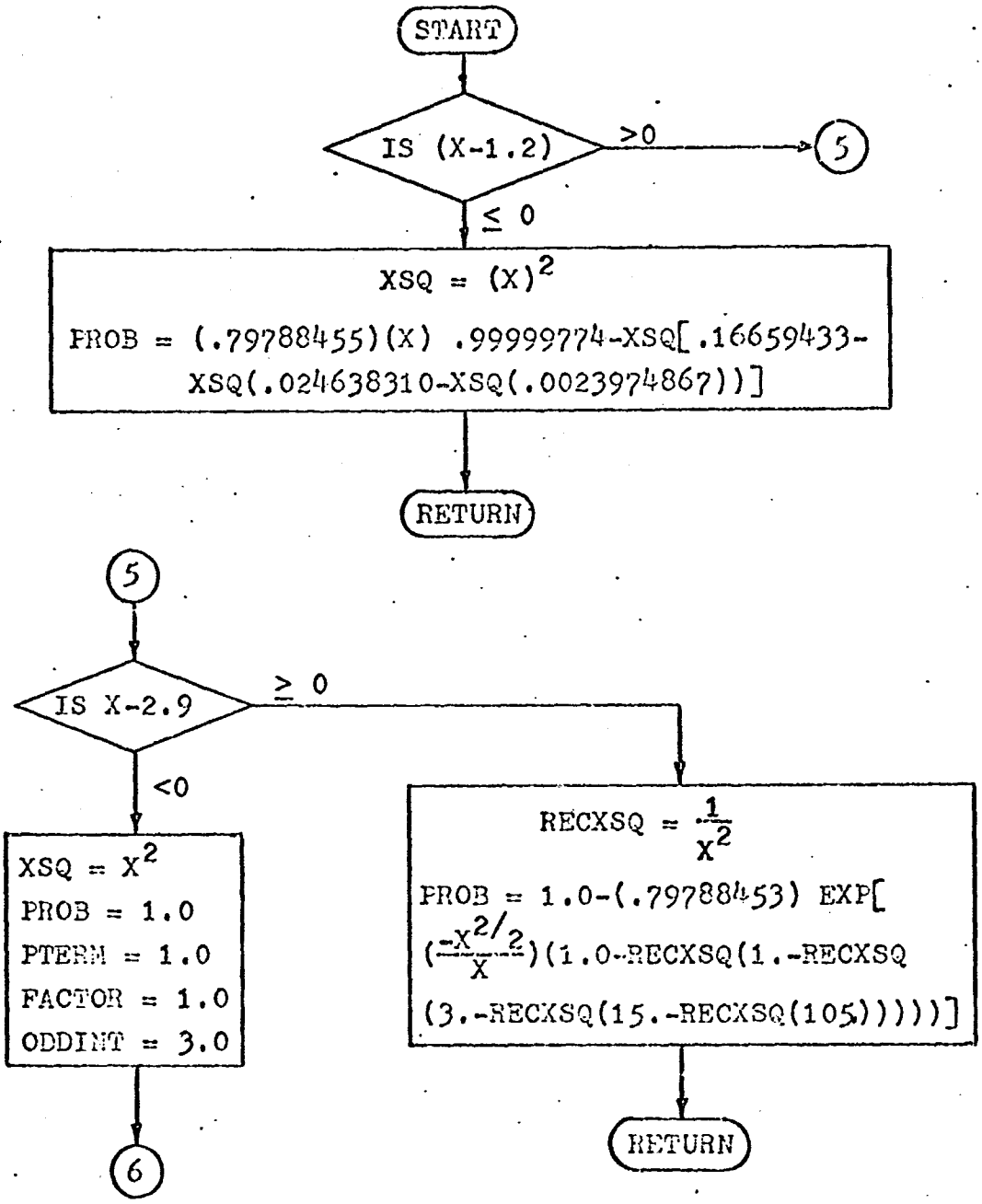

Fig. C -1 (continued)

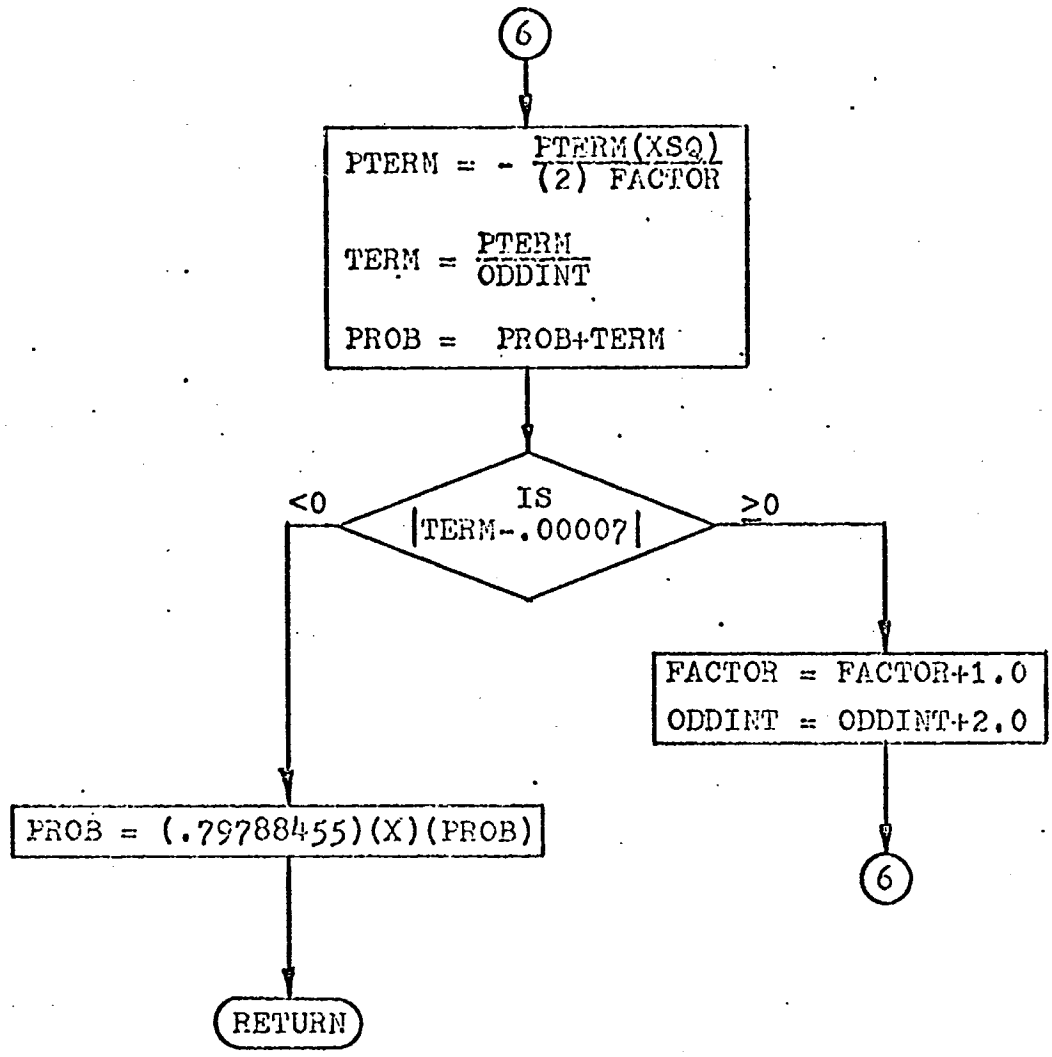

Fig. C-1 (continued)

Subroutine to Conduct Chi-Square Goodness-of-Fit Test

SUBROUTINE CHISQA

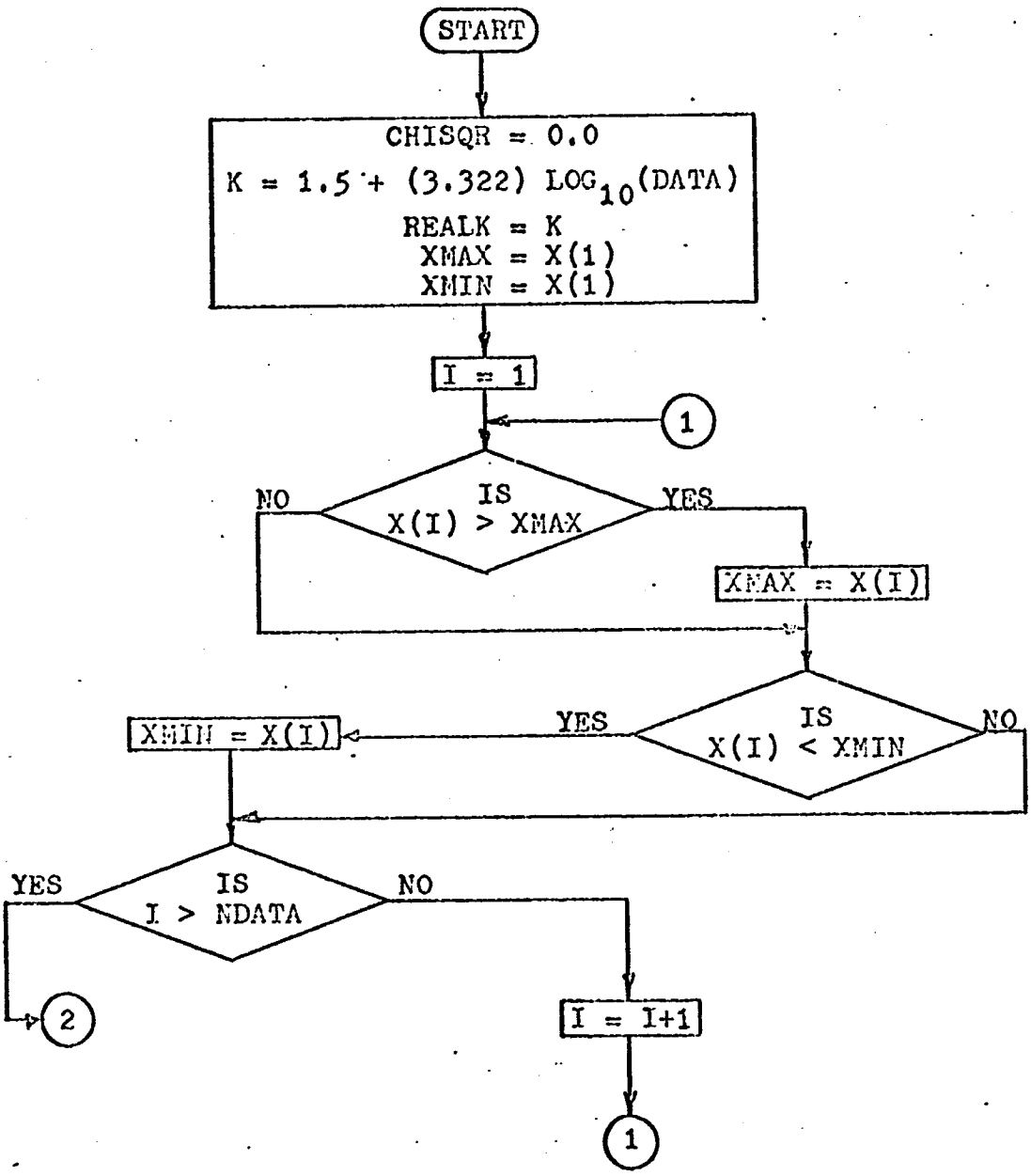

Fig. C-1 (continued)

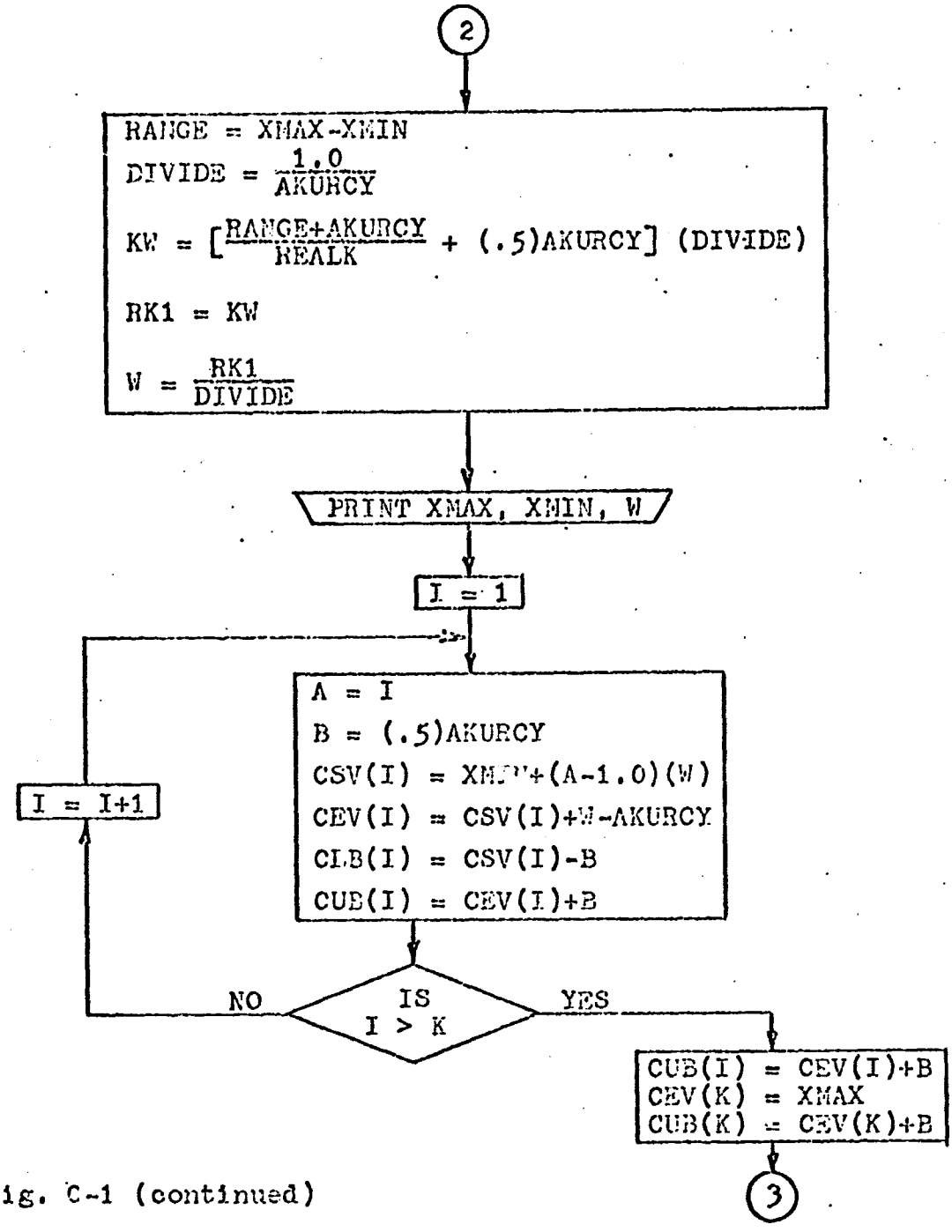

Fig. C-1 (continued)

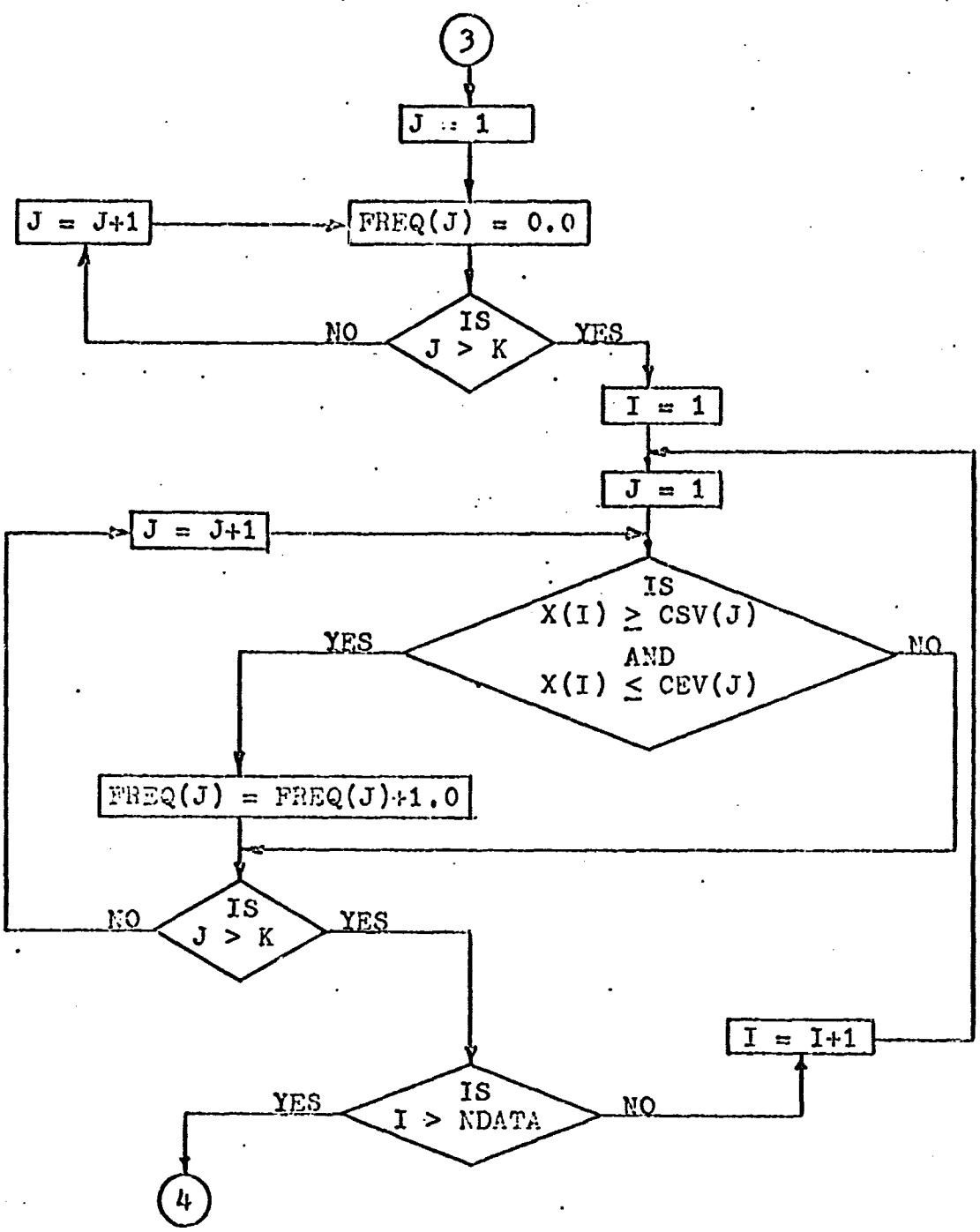

Fig. C-1 (continued)

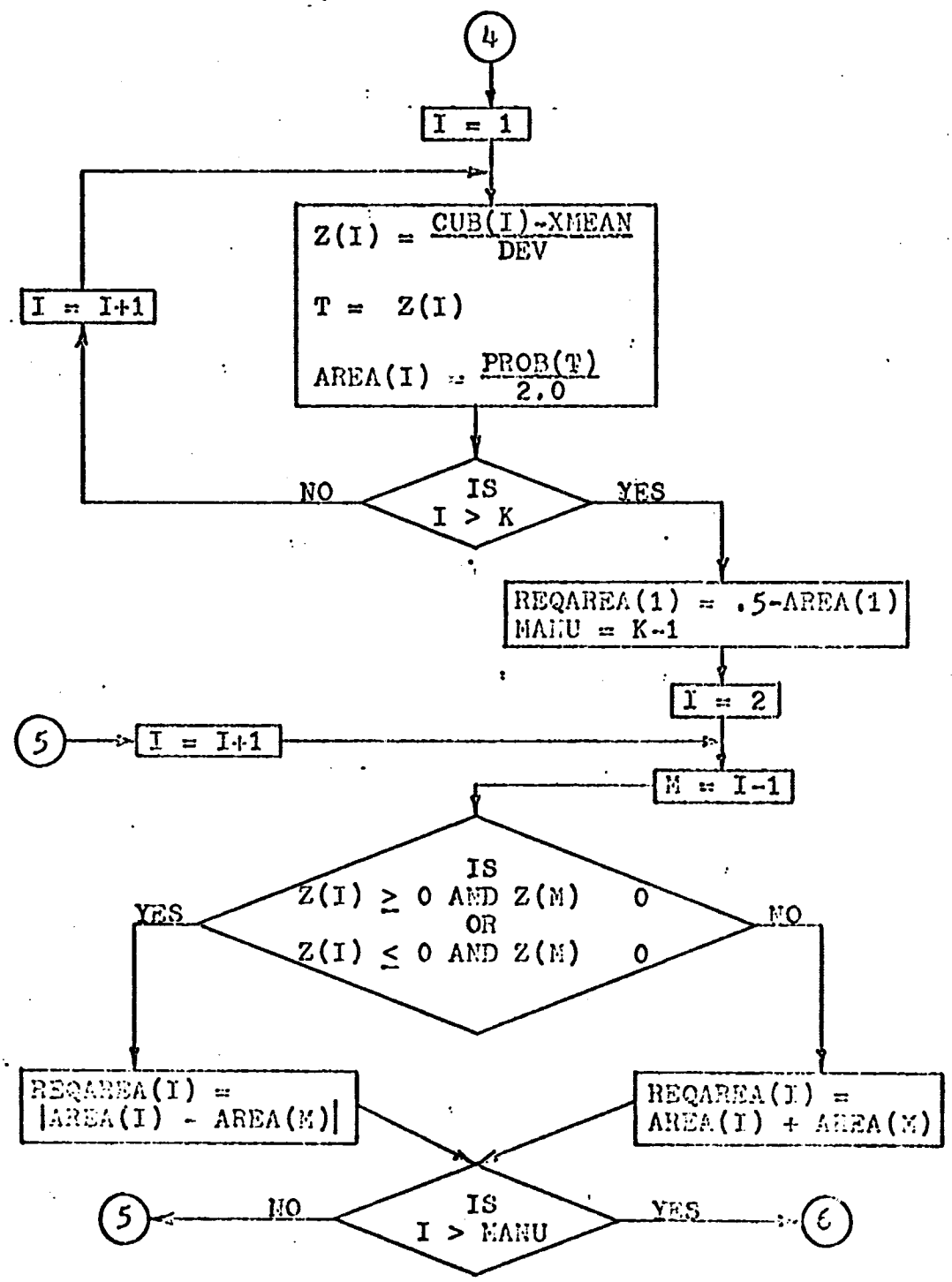

Fig. C-1 (continued)

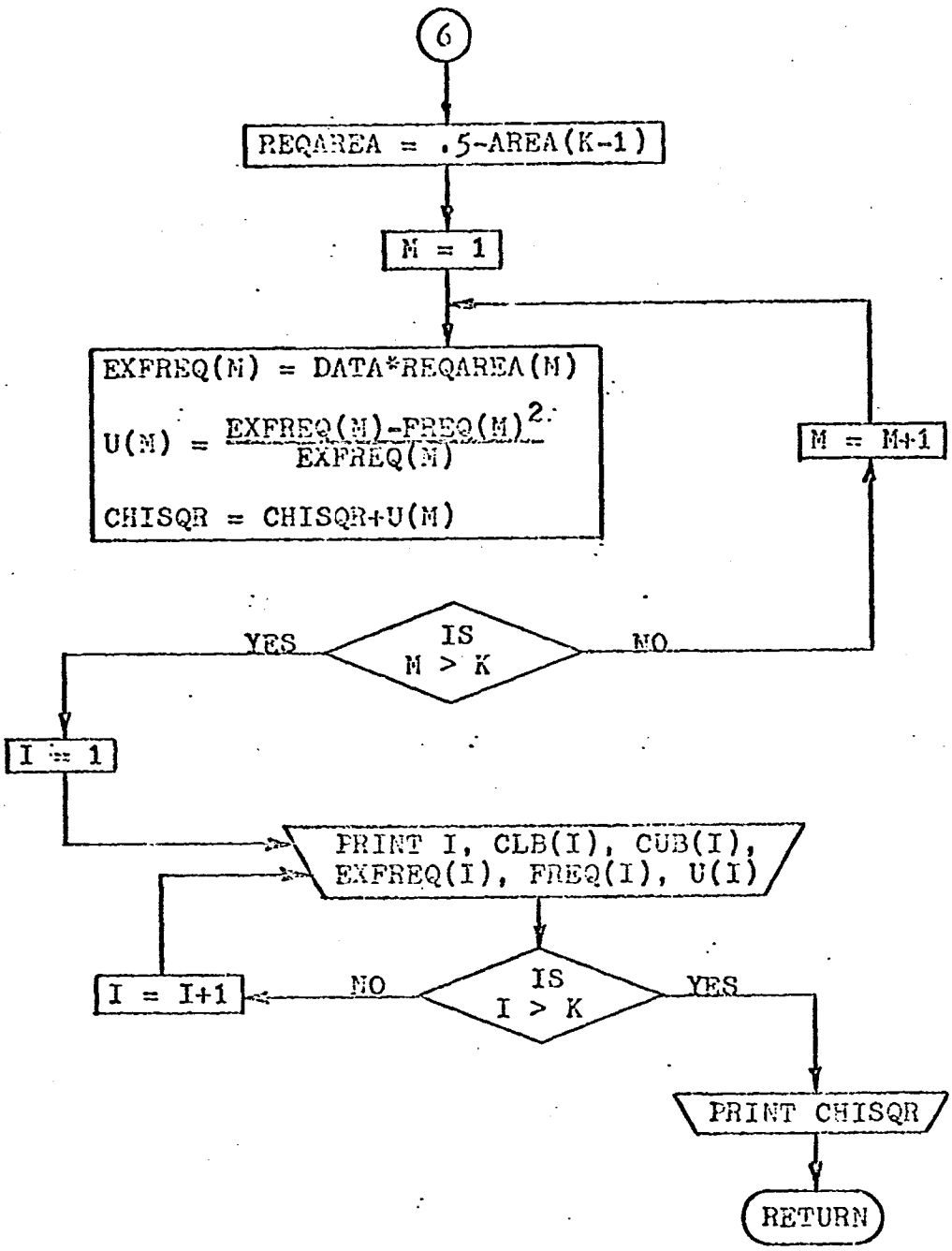

Fig. C-1 (continued)

Subroutine to Conduct Kolmogorov-Smirnov Goodness-of-Fit Test

SUBROUTINE DTEST

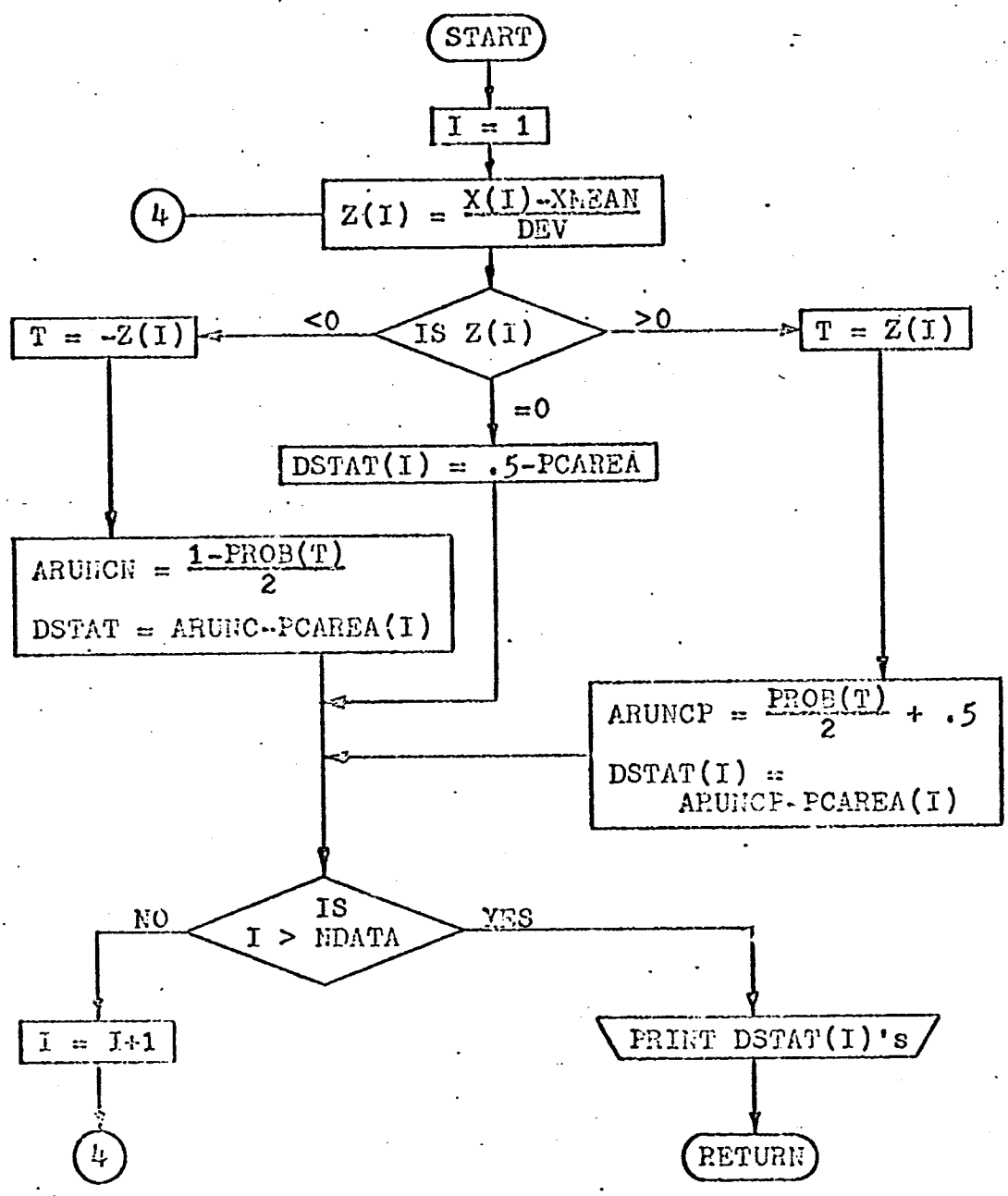

Fig. C-1 (continued)

Subroutine to Find the Moment Coefficients of Skewness and Kurtosis

SUBROUTINE ALPHA

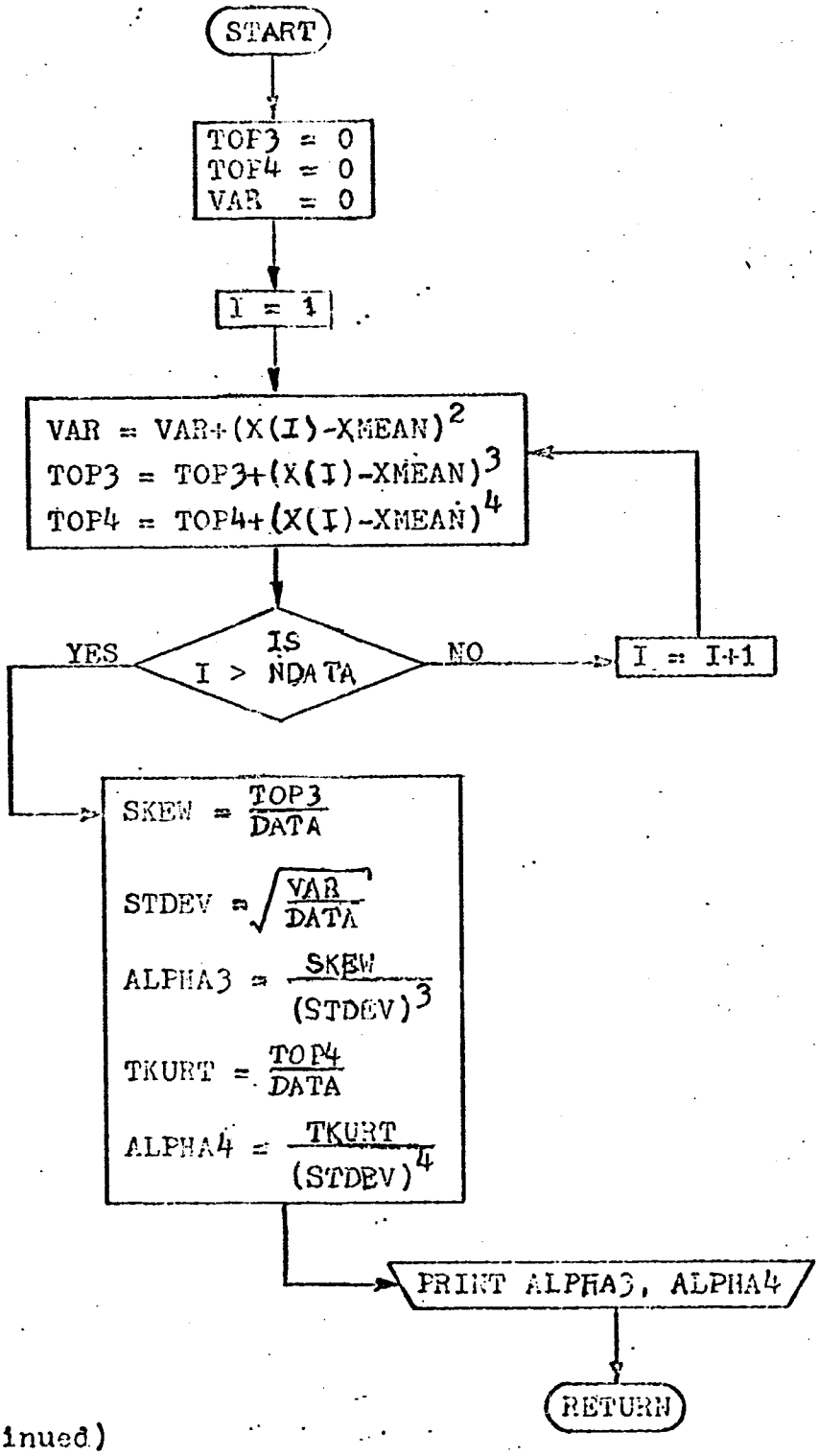

Fig. C-1 (continued)

List of Definitions for Program to Fit Normal and Log-Normal Distributions to Cycles-to-Failure Data (PROGRAM CYTOFR)

Main Program:

NDATA = DATA = number of observations.

STRLV = stress level in psi.

AKURCY = accuracy to which cycles-to-failure data are known.

RATIO = stress ratio

X(I) = cycles-to-failure data

CUMFRQ(I) = cumulative frequency of each X(I); ie, number of X's less than or equal to X(I).

PCAREA(I) = CUMFRQ(I)/NDATA

Subroutine to calculate the mean and standard deviation of the cycles-to-failure data (SUBROUTINE MEAN)

SIGMA = sum of the X(I)'s

XMEAN = average of the X(I)'s

TOP2 = $\sum_{i=1}^{n} (X(I)-XMEAN)^2$

DEV = standard deviation of the X(I)'s

Function subroutine to find the area under the normal curve (FUNCTION PROB(X)).

X = abscissa value for which corresponding area is desired.

PROB = desired area.

C-2. Definition of Variables

Subroutine for Chi-square goodness-of-fit test (SUBROUTINE CHISQA).

K	=	number cells.
XMAX	=	largest value of cycles-to-failure.
XMIN	=	smallest value of cycles-to-failure.
CSV	=	cell starting value.
CEV	=	cell end value.
CLB	=	cell lower bound.
CUB	=	cell upper bound.
FREQ(J)	=	number of observations in J^{th} cell.
REQAREA(J)	=	expected value of J^{th} cell.
CHISQR	=	total Chi-square value.
U(I)	=	Chi-square value of I^{th} cell.

Subroutine for Kolmogorov-Smirnov test (SUBROUTINE DTEST).

Z(I)	=	abscissa value on standard normal curve for a given X(I).
ARUNCN	=	area under standard normal curve from - to Z(I).
DSTAT(I)	=	absolute difference between the data cumulative frequency and the hypothesized cumulative frequency.
XMEAN	=	average of the X(I)'s.
DEV	=	standard deviation of the X(I)'s
PROB(T)	=	area under the standard normal curve from -T to +T.

C-2. (Cont'd).

Subroutine to calculate the moment coefficients of skewness and kurtosis (SUBROUTINE ALPHA).

ALPHA3 = moment coefficient of skewness.

ALPHA4 = moment coefficient of skewness.

VAR = $\sum_{i=1}^{n} (X(I)-\underline{X})^2$

TOP3 = $\sum_{i=1}^{n} (X(I)-\underline{X})^3$

SKEW = third moment of the data.

STDEV = biased estimator for standard deviation.

TOP4 = $\sum_{i=1}^{n} (X(I)-\underline{X})^4$

TKURT = fourth moment of the data.

C-2. (Cont'd).

```
      PROGRAM CYTOFR (INPUT,OUTPUT,TAPE1=INPUT)
C-----PROGRAM TO FIT NORMAL AND LOG-NORMAL CURVE TO DATA AND CHECK
C-----GOODNESS OF FIT.
0003  DIMENSION X(100),CSV(9),CEV(9),CLB(9),CUB(9),CUMFRQ(100),
     1PCAREA(100),DSTAT(100),FREQ(9),AREA(9),REQAREA(9),EXFREQ(9),U(9),
     2Z(100),NX(100),RANK(100)
003   EXTERNAL PROB
0003 710   PRINT 1
C-----NDATA=DATA=NUMBER OF OBSERVATIONS
C-----STRLV = STRESS LEVEL IN PSI.
0007  READ 6,NDATA,DATA,AKURCY,STRLEV, RATIO
C-----X= NUMBER OF CYCLES TO FAILURE
00025 6     FORMAT(I3,F5.1,F9.4,F10.1,F8.5)
0025  IF (EOF,1) 56,55
0030  55    READ 7,( X(I), I=1,NDATA)
00043 7     FORMAT(8F10.0)
      C
      C     SORT X(I) TERMS IN ASCENDING ORDER.
      C
00043 K=NDATA-1
0045  IF(K.LE.0) GO TO 30
0047  DO 20 I=1,K
00050 N=NDATA-I
00051 ISTOP=0
0053  DO 10 J=1,N
00054 IF(X(J).LE.X(J+1)) GO TO 10
00057 SAVE=X(J)
0060  X(J)=X(J+1)
0062  X(J+1)=SAVE
00063 ISTOP=ISTOP+1
0065  10 CONTINUE
070   IF(ISTOP.EQ.0) GO TO 30
0071  20 CONTINUE
      C
      C     SET CUMFRQ(I) ARRAY
      C
00073 30 DO 40 I=1,NDATA
0075  40 CUMFRQ(I) = I
C-----PCAREA = F(N) OF OBSERVATIONS
00101 DO 759 I=1, NDATA
00102 759   PCAREA(I) = CUMFRQ(I)/DATA
0106  PRINT 405
00112 405   FORMAT (40X,53HNORMAL DISTRIBUTION FITTED TO CYCLES-TO-FAILURE DAT
     1A.///)
0112  IF (RATIO.EQ.0.0) GO TO 414
0113  PRINT 402, STRLEV, RATIO
00123 402   FORMAT(29X,14H STRESS LEVEL=,F10.1,5H PSI.,16X
     1,14HSTRESS RATIO =,F6.3//)
0123  GO TO 415
00124 414   PRINT 416, STRLEV
00132 416   FORMAT(29X,14HSTRESS LEVEL=,F10.1,5H PSI.,16X
     1,23HSTRESS RATIO = INFINITY//)
00132 415   PRINT 404
00136 404   FORMAT(55X,22HCYCLES TO FAILURE DATA/)
0136  PRINT 403, (X(I),I=1,NDATA)
0151  403   FORMAT (6(10X,F10.3))
151   PRINT 3
```

C-3. Fortran Progam Listing.

```
000155    3     FORMAT (1H0)
  0155          CALL MEAN(X, DATA, NDATA, XMEAN, DEV)
  0161          CALL CHISQA(X, DATA, NDATA, PROB, AKURCY, XMEAN, DEV, Z)
000171          CALL DTEST (PCAREA,NDATA,X,DEV,DSTAT,PROB,XMEAN, Z)
  0201          CALL ALPHA(X, NDATA, DATA, XMEAN, DEV, ALPHA3, ALPHA4)
  0210          AKURCY =  .0001
000212          DO 54 I=1,NDATA
  213           NX(I) =(ALOG(X(I)/20.)+ALOG(20.))*100000.  + .5
  0226          X(I) = NX(I)
000230    54    X(I) = X(I)/100000.
000234          PRINT 1
  0240    1     FORMAT (1H1,3HASD/// )
  0240          PRINT 401
000244    401   FORMAT (38X,57HLOG-NORMAL DISTRIBUTION FITTED TO CYCLES-TO-FAILURE
                1 DATA.///)
  0244          IF (RATIO.EQ.0.0) GO TO 417
000245          PRINT 402, STRLEV, RATIO
000255          GO TO 418
  0256    417   PRINT 416, STRLEV
  0264    418   PRINT 2
000270    2     FORMAT (49X,34HLOGS OF THE CYCLES TO FAILURE DATA/)
  0270          PRINT 413, (X(I),I=1,NDATA)
  0303    413   FORMAT (6(8X,F12.5))
000303          PRINT 3
000307          CALL MEAN(X, DATA, NDATA, XMEAN, DEV)
  0313          CALL CHISQA(X, DATA, NDATA, PROB, AKURCY, XMEAN, DEV, Z)
000323          CALL DTEST (PCAREA,NDATA,X,DEV,DSTAT,PROB,XMEAN, Z)
000333          CALL ALPHA(X, NDATA, DATA, XMEAN, DEV, ALPHA3, ALPHA4)
  0342          GO TO 710
  0343    56    STOP
000345          END
```

C-3. (Cont'd).

```
                SUBROUTINE MEAN (X, DATA, NDATA, XMEAN, DEV)
              C-----SUBROUTINE TO CALCULATE THE MEAN AND STANDARD DEVIATION OF DATA.
 000010               DIMENSION X(NDATA)
 000010               SIGMA= 0.0
 000011               DO 8 I=1, NDATA                                          207
 000012     8         SIGMA=SIGMA+ X(I)
 000016               XMEAN = SIGMA/DATA
 000017               TOP2 = 0.0
 000020               DO 9 I=1,NDATA
 000021     9         TOP2 = TOP2 + (X(I) - XMEAN)**2
 000026               DEV =SQRT(TOP2/(DATA - 1.0))
 000036               PRINT 14, XMEAN
 000043               PRINT 15, DEV
 000054     14        FORMAT( 10X,  12HSAMPLE MEAN=, F17.6)
 000054     15        FORMAT( 10X,  15HSTD. DEVIATION=, F14.6)
 000054               RETURN
 000055               END
```

C-3. (Cont'd).

```
      FUNCTION PROB(X)
C-----THIS SUBROUTINE GIVES AREA UNDER NORMAL CURVE FROM -Z TO +Z
C     WITH AN ACCURACY OF 0.00005
C-----Z VALUE GIVEN BY CALLING PROGRAM MUST BE A POSITIVE NUMBER.
000003      IF (X-1.2)11,11,12
000005 11   XSQ=X*X
000006      PROB= 0.79788455*X*(0.99999774-XSQ*(0.16659433-XSQ*(0.02463810-XS
           1Q*0.0023974867)))
000016      RETURN
000017 12   IF(X-2.9) 13,14,14
000022 13   XSQ=X*X
000023      PROB=1.0
000024      PTERM=1.0
000025      FACTOR=1.0
000026      ODDINT=3.0
000030 970  PTERM=-PTERM*XSQ/(2.0*FACTOR)
000034      TERM=PTERM/ODDINT
000035      PROB=PROB+TERM
000037      IF( ABS (TERM) - 0.00007 ) 80,90,90
000042 90   FACTOR =FACTOR+1.0
000044      ODDINT=ODDINT+2.0
000046      GO TO 970
000046 80   PROB=0.79788455*X*PROB
000051      RETURN
000051 14   RECXSQ= 1.0 / (X*X)
000053      PROB= 1.0 - 0.79788453*EXP(-X*X/2.0)/X*(1.0-RECXSQ*(1. -RECXSQ*(3.
           1 - RECXSQ*(15. - RECXSQ*105. ))))
000075      RETURN
000076      END
```

C-3. (Cont'd).

```
      SUBROUTINE CHISQA (X, DATA, NDATA, PROB, AKURCY, XMEAN, DEV,Z)
C-----SUBROUTINE TO FIT A HISTOGRAM TO THE DATA AND PERFORM THE CHI-SQUARE
C-----TEST FOR THE NORMAL OR LOG-NORMAL DISTRIBUTIONS.
000013      DIMENSION X(NDATA),Z(NDATA),CSV(9),CEV(9),CLB(9),CUB(9),      209
     1REQAREA(9),AREA(9),EXFREQ(9),    FREQ(9),    U(9)
0 0013      CHISQR= .0
C-----TO DETERMINE THE NUMBER OF CLASS INTERVALS,K
000013      K= 1.5 +3.322*ALOG10(DATA)
0 0024      REALK=K
C-----IN ORDER TO DETERMINE THE RANGE,FIND X(MAX) AND X(MIN)
000025      XMAX=X(1)
000027      XMIN= X(1)
0 0030      DO 17 I=1,NDATA
000032      IF( X(I).GT.XMAX ) XMAX = X(I)
000037  17  IF(X(I).LT. XMIN) XMIN=X(I)
0 0046       RANGE=  XMAX- XMIN
C------TO DETERMINE THE CLASS INTERVAL WIDTH,W
C-----ROUTINE TO ROUND OFF CLASS WIDTH TO SAME NUMBER OF PLACES AS THE ACC
0 0050      DIVIDE = 1.0/AKURCY
0 0051      KW =(((RANGE+AKURCY)/REALK)+.5*AKURCY)*DIVIDE
000057      RK1 = KW
000060      W = RK1/DIVIDE
0 0062      PRINT 62,XMAX
000067      PRINT 63,XMIN
000075      PRINT 65,W
0 0103      DO 22 I=1,K
0 0110      A=I
000111      B = 0.5*AKURCY
000112      CSV(I)= XMIN+(A-1.0)*W
0 0117      CEV(I)= CSV(I)+W-AKURCY
000123      CLB(I)= CSV(I)-B
0 0127  22  CUB( I ) = CEV(I)+B
0 0135      CEV(K) = XMAX
000137      CUB(K) = CEV(K) +B
000143      DO 23 J=1,K
0 0144  23  FREQ(J)=0.0
0 0150      DO 24 I=1,NDATA
000152      DO 24 J=1,K
000153      IF( X(I).GE.CLB(J).AND. X(I).LE.CUB(J)  ) FREQ(J)=FREQ(J)+ 1.0
0 0172  24  CONTINUE
C-----CHI-SQUARE TEST
000177      PRINT 41
0 0202      PRINT 406
0 0206      DO 30 I=1,K
000213      Z(I)=( CUB(I)- XMEAN) / DEV
0 0220      T= ABS( Z(I) )
0 0224  30  AREA(I)= PROB(T)/2.0
000243      REQAREA(1) = 0.5 - AREA(1)
000244       MANU=K-1
0 0246      DO 32 I=2,MANU
0 0247      M=I-1
000250      IF(  (Z(I).GE.0.0.AND.Z(M).GE.0.0).OR.( Z(I).LE.0.0.AND.Z(M).LE.0.
     1 )  ) GO TO 31
0 0272      REQAREA(I)= AREA(I)+AREA(M)
000300      GO TO 32
0 0300  31  REQAREA(I) = ABS( AREA(I)-AREA(M) )
0 0310  32  CONTINUE
```

C-3. (Cont'd).

```
                DO 80 M=1,K
                EXFREQ(M)=DATA*REQAREA(M)
                U(M)=(( EXFREQ(M)-FREQ(M))**2)/EXFREQ(M)
       80       CHISQR=CHISQR+U(M)                                          210
      C-----TO PRINT THE TABLE FOR CHI-SQUARE TEST
                DO 33 I=1,K
       33       PRINT 34,I,CLB(I),CUB(I), EXFREQ(I),FREQ(I),U(I)
                PRINT 35, CHISQR
       62       FORMAT( 10X, 14HMAXIMUM VALUE=,F15.6)
       63       FORMAT( 10X, 14HMINIMUM VALUE=, F15.6)
       65       FORMAT( 10X, 12HCLASS WIDTH=, F17.6)
       41       FORMAT(1H0)
      406       FORMAT (8X,5H CELL,10X,10HLOWER CELL,11X,10HUPPER CELL,13X,8HEXPEC
                1TED,13X,8HOBSERVED,13X,11HCHI-SQUARED/8X,6HNUMBER,10X,8HBOUNDARY,
                213X, 8HBOUNDARY,13X,9HFREQUENCY,12X,9HFREQUENCY,12X,13HVALUE OF CE
                3LL/)
       34       FORMAT (10X,I2,5F21.6)
       35       FORMAT (1H0,81X,25HTOTAL CHI-SQUARED VALUE =,F10.6)
                RETURN
                END
```

C-3. (Cont'd).

```
      SUBROUTINE DTEST (PCAREA,NDATA,X,DEV,DSTAT,PROB,XMEAN,Z)
C-----SUBROUTINE TO CALCULATE THE KOLMOGOROV-SMIRNOV D-VALUES.
      DIMENSION PCAREA(NDATA),X(NDATA),Z(NDATA),DSTAT(NDATA)
      DO 706 I=1, NDATA
      Z(I) = (X(I) - XMEAN)/DEV
      IF (Z(I)) 703, 704, 705
703   T =ABS(Z(I))
C-----ARUNCN=AREA UNDER THE NORMAL CURVE TO LEFT OF Z FOR NEGATIVE Z.
      ARUNCN = (1.0-PROB(T))/2.0
      DSTAT(I) = ARUNCN - PCAREA(I)
      GO TO 706
704   DSTAT(I) = .5 - PCAREA(I)
      GO TO 706
705   T = Z(I)
C-----ARUNCP=AREA UNDER THE NORMAL CURVE TO LEFT OF Z FOR POSITIVE Z.
      ARUNCP = PROB(T)/2.0 +  .500
      DSTAT(I) =    (ARUNCP - PCAREA(I))
706   CONTINUE
      PRINT 708
      PRINT 707, (DSTAT(I),I=1,NDATA)
707   FORMAT (6(10X,F10.5))
708   FORMAT (//40X,53H D VALUES FOR KOLMOGOROV-SMIRNOV GOODNESS OF FIT
     1TEST/41X,52H(LISTED IN THE SAME ORDER AS CYCLES-TO-FAILURE DATA)/)
      RETURN
      END
```

C-3. (Cont'd).

```
                SUBROUTINE ALPHA (X, NDATA, DATA, XMEAN, DEV, ALPHA3, ALPHA4)
000012          DIMENSION X(NDATA)
              C-----SUBROUTINE TO CALCULATE THE COEFFICIENTS OF SKEWNESS AND KURTOSIS
              C-----CALCULATE THE THIRD MOMENT OF THE DATA (SKEWNESS)
000012          TOP3 = 0.0                                                    212
000012          VAR = 0.0
000014          DO 710 I =1, NDATA
000015          VAR = VAR + (X(I) - XMEAN)**2
000020    710   TOP3 = TOP3 +(X(I) - XMEAN)**3
000027          SKEW = TOP3 / DATA
000030          STDEV = SQRT(VAR/DATA)
              C-----ALPHA3 = MOMENT COEFFICIENT OF SKEWNESS.
000037          ALPHA3 = SKEW/(STDEV**3)
              C-----CALCULATE THE FOURTH MOMENT OF THE DATA (KURTOSIS).
000041          TOP4 = 0.0
000042          DO 711 I = 1, NDATA
000044    711   TOP4 = TOP4 + (X(I) - XMEAN)**4
000052          TKURT = TOP4 / DATA
              C-----ALPHA4 = MOMENT COEFFICIENT OF KURTOSIS.
000053          ALPHA4 = TKURT/(STDEV**4)
000056          PRINT 712
000062          PRINT 713
000066          PRINT 714, ALPHA3, ALPHA4
000102    712   FORMAT (///19X,39HMOMENT COEFFICIENT OF SKEWNESS (ALPHA3),18X,39HM
                1OMENT COEFFICIENT OF KURTOSIS (ALPHA4)/)
000102    713   FORMAT    (21X,34HFOR NORMAL DISTRIBUTION ALPHA3 = 0,23X,36HFOR NO
                1RMAL DISTRIBUTION ALPHA4 = 3.0/)
000102    714   FORMAT (26X,25HFOR ABOVE DATA---ALPHA3 =F6.3,26X,25HFOR ABOVE DATA
                1---ALPHA4 =,F6.3)
000102          RETURN
000103          END
```

C-3. (Cont'd).

APPENDIX D

Program STRENG (FORTRAN)

D-1. Flow Chart

D-2. Definition of Variable

D-3. Computer Listing

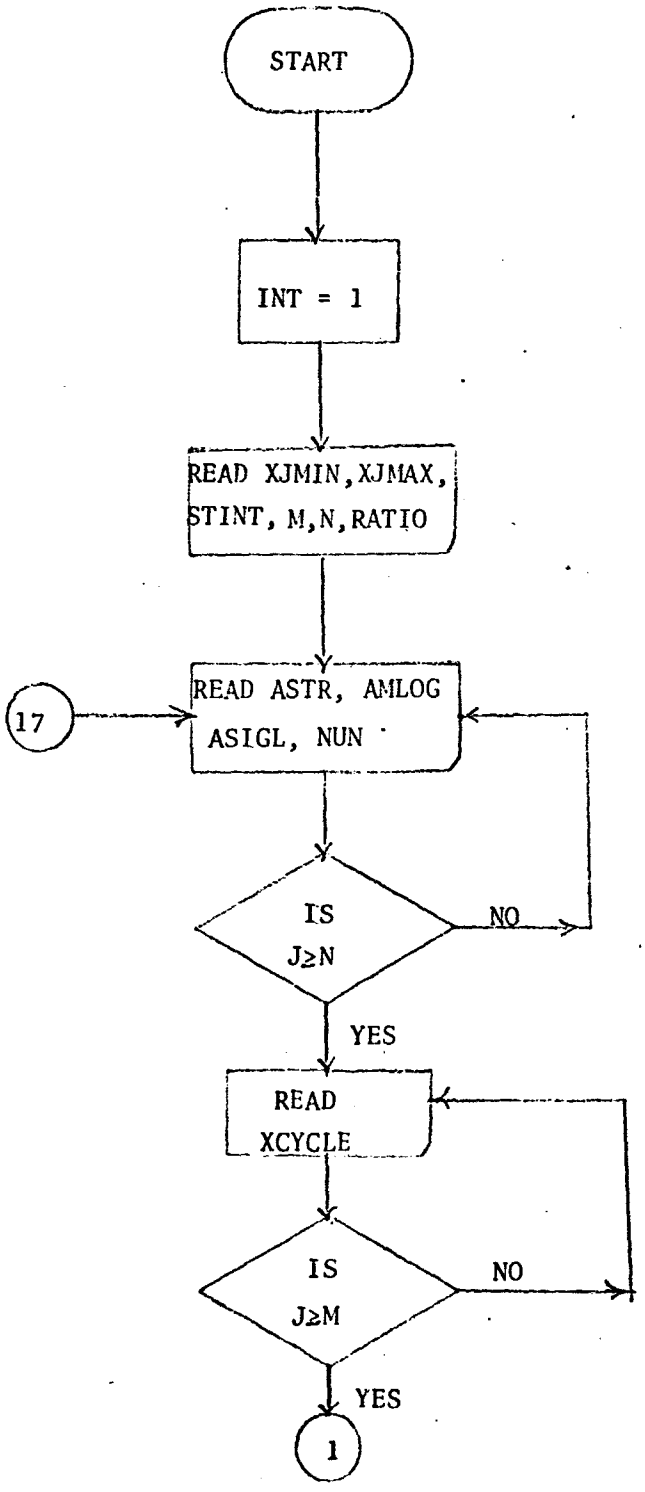

D-1. Flow Chart

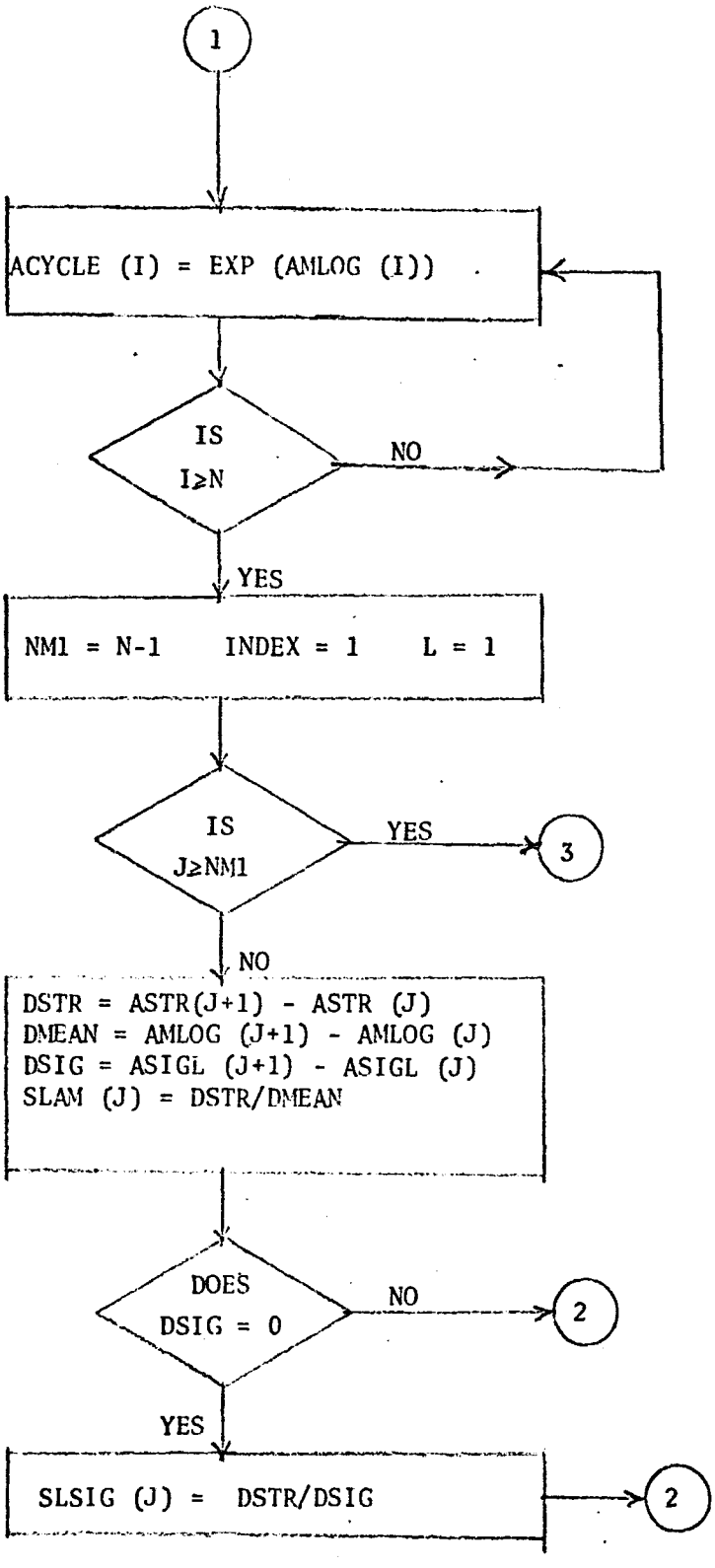

D-1. Fow Chart (Cont'd).

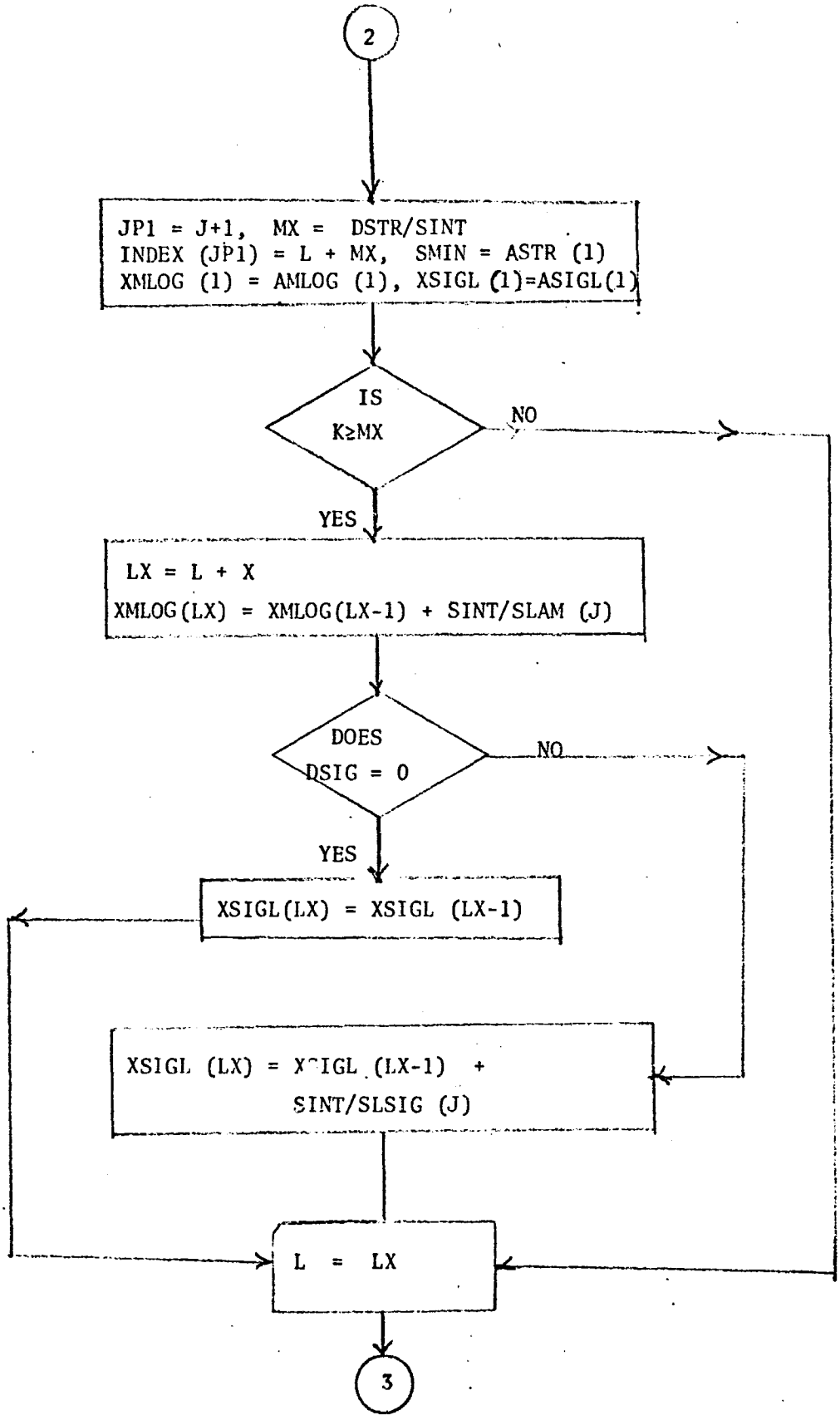

D-1. Flow Chart (Cont'd).

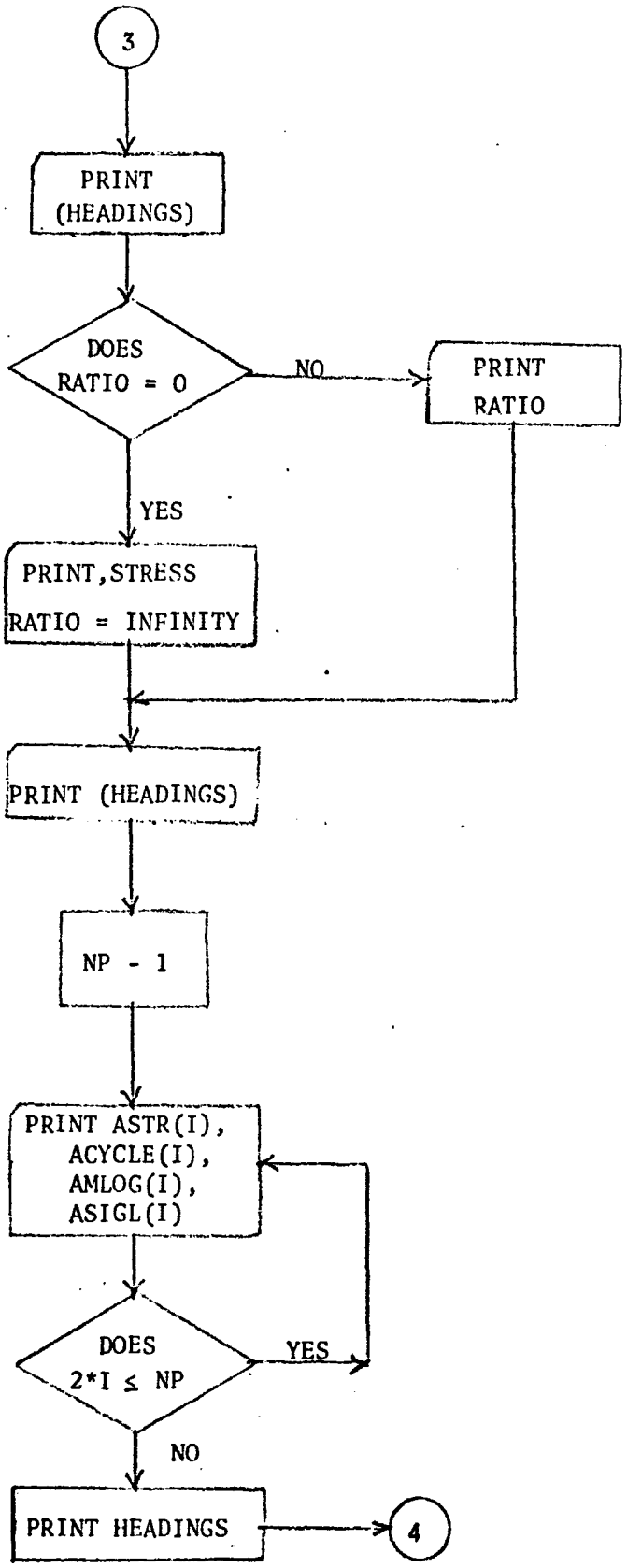

D-1. Flow Chart (Cont'd)

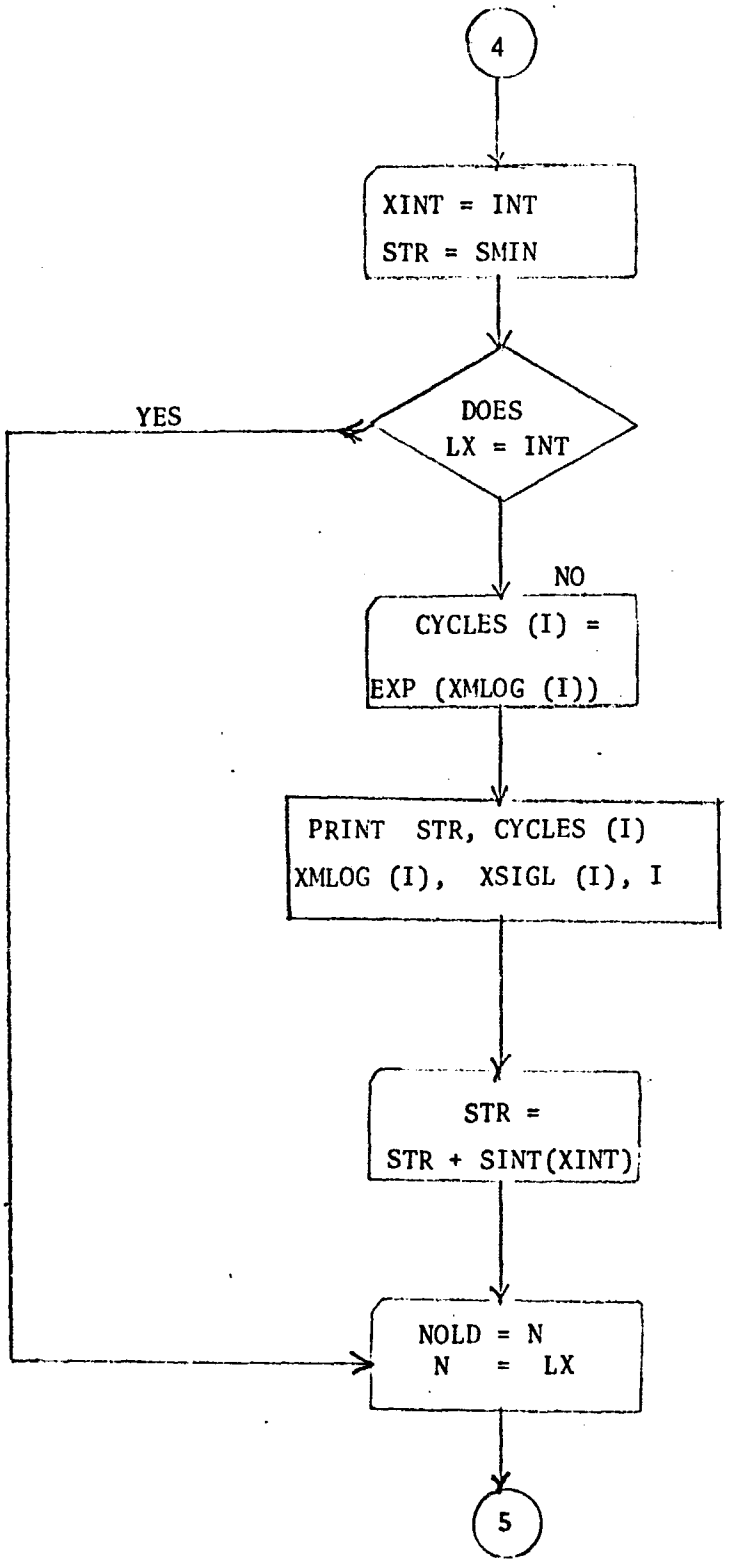

D-1. Flow Chart Cont'd).

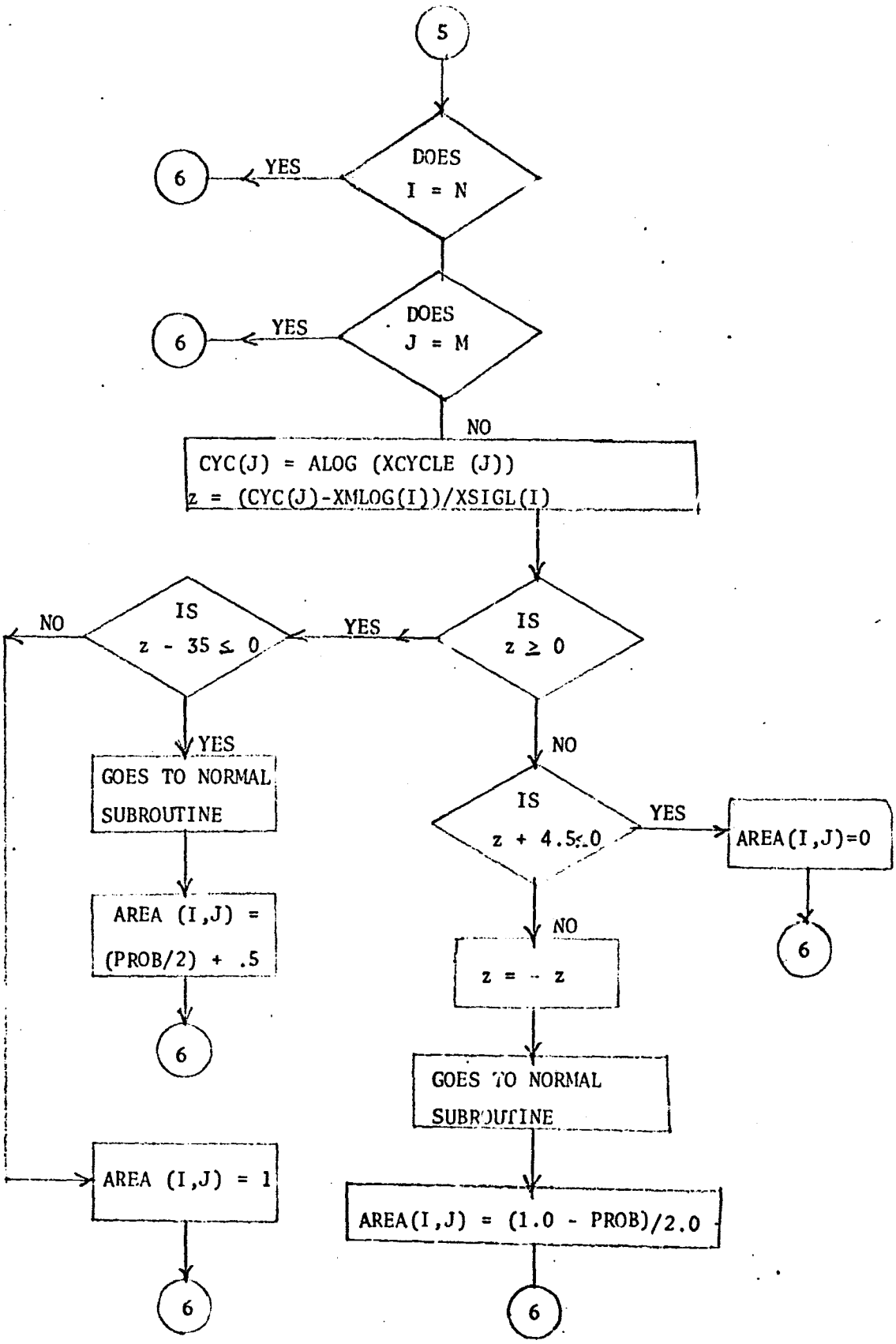

D-1. Flow Chart(Cont'd).

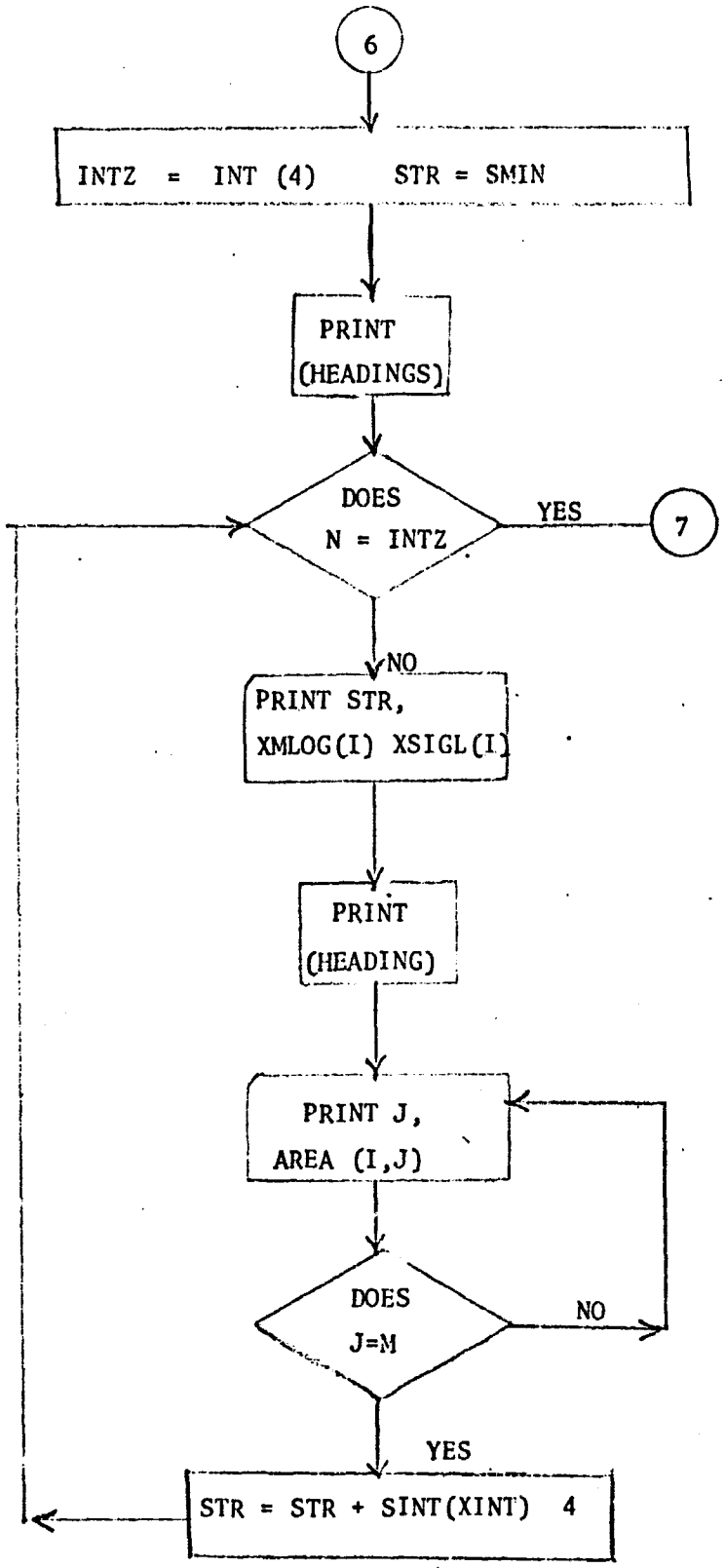

D-1. Flow Chart (Cont'd).

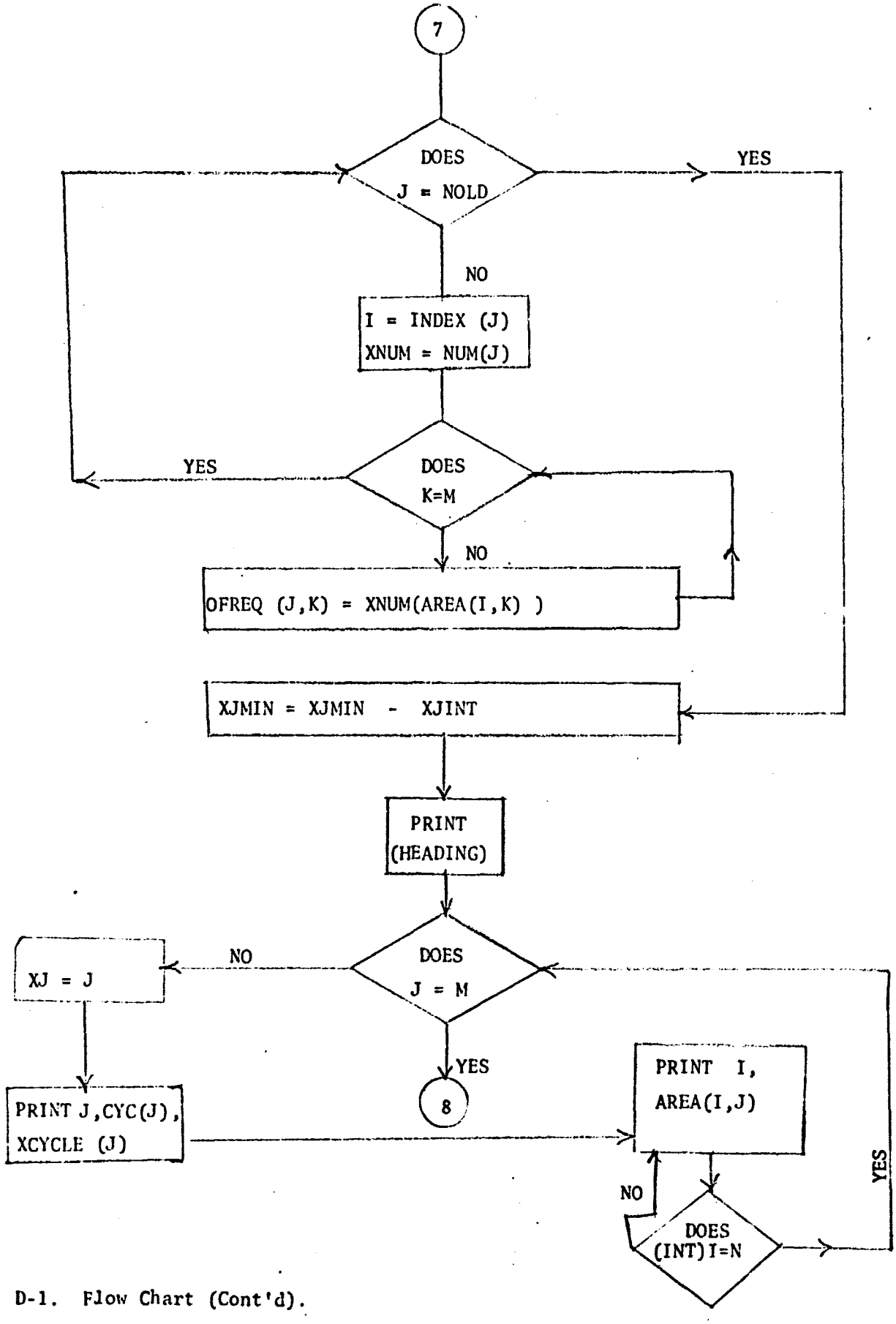

D-1. Flow Chart (Cont'd).

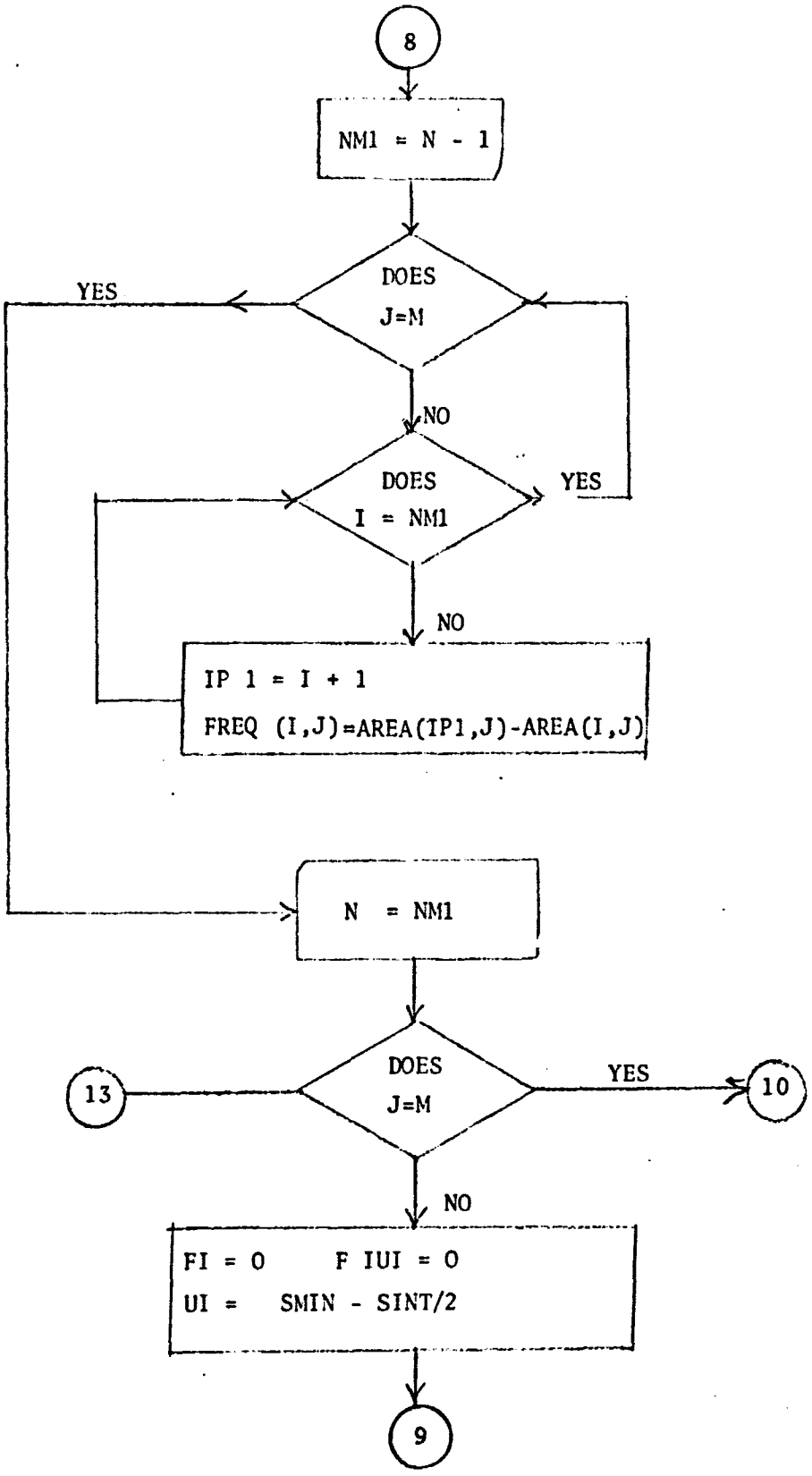

D-1. Flow Chart (Cont'd).

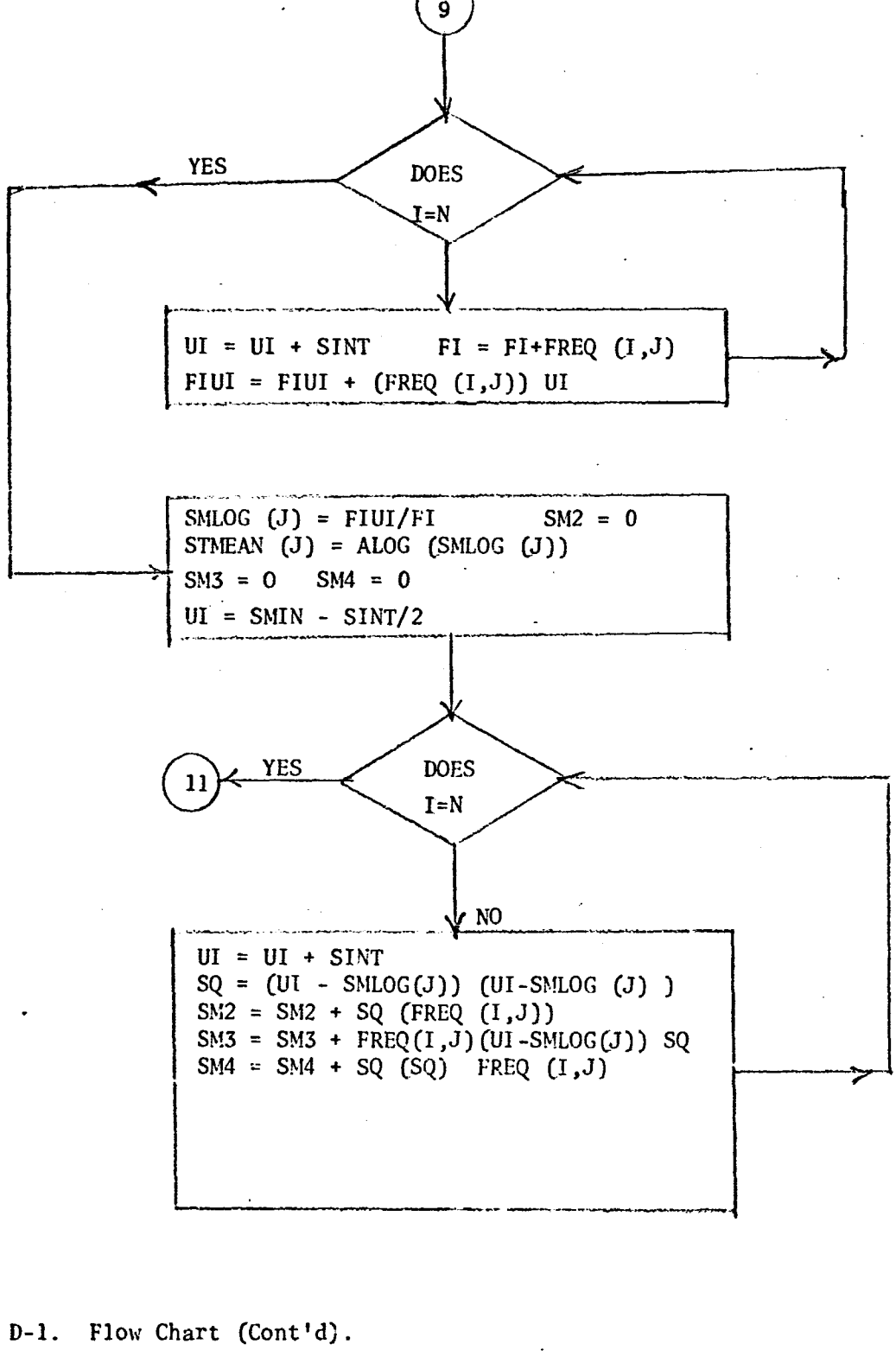

D-1. Flow Chart (Cont'd).

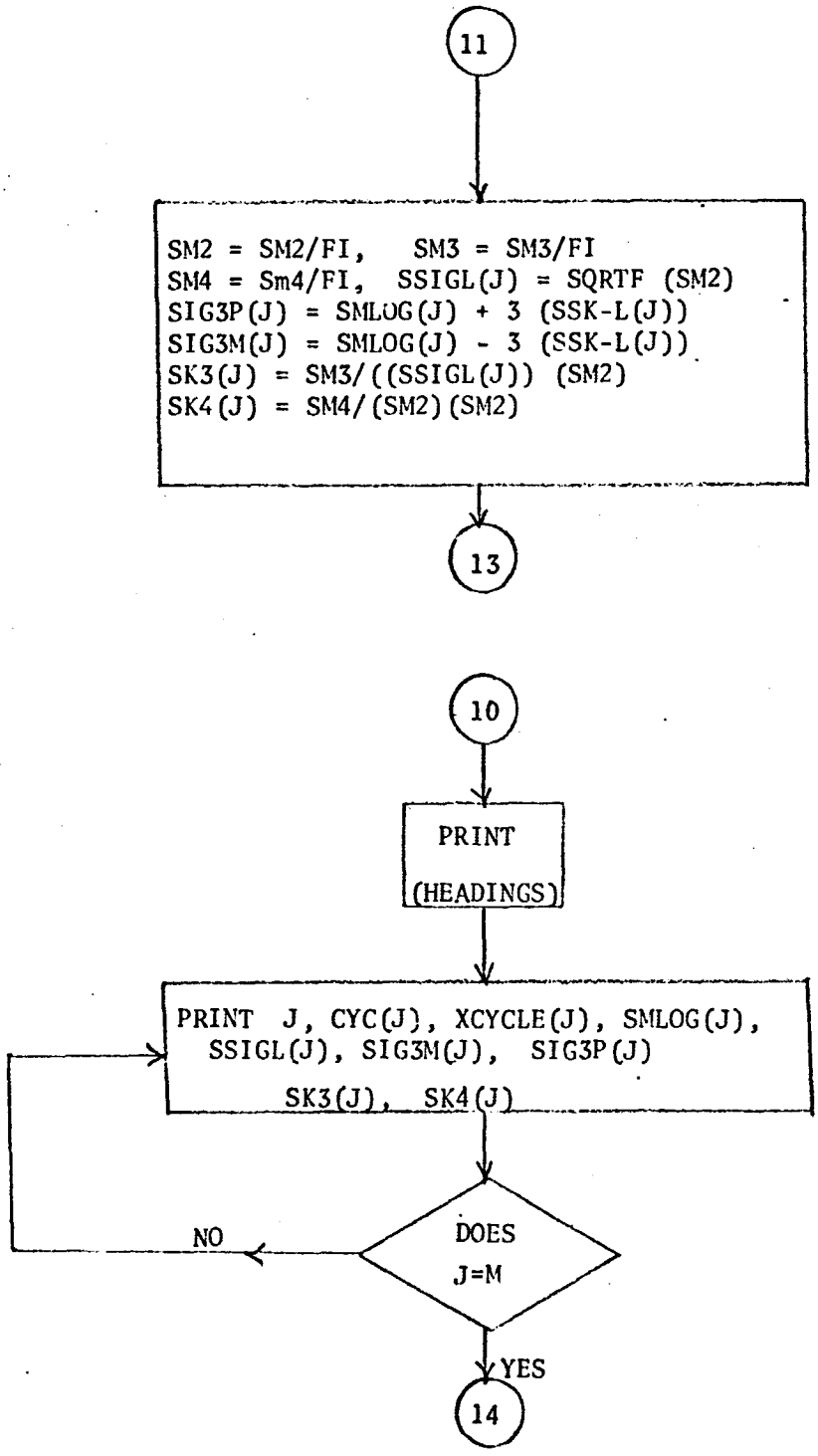

D-1. Flow Chart (Cont'd).

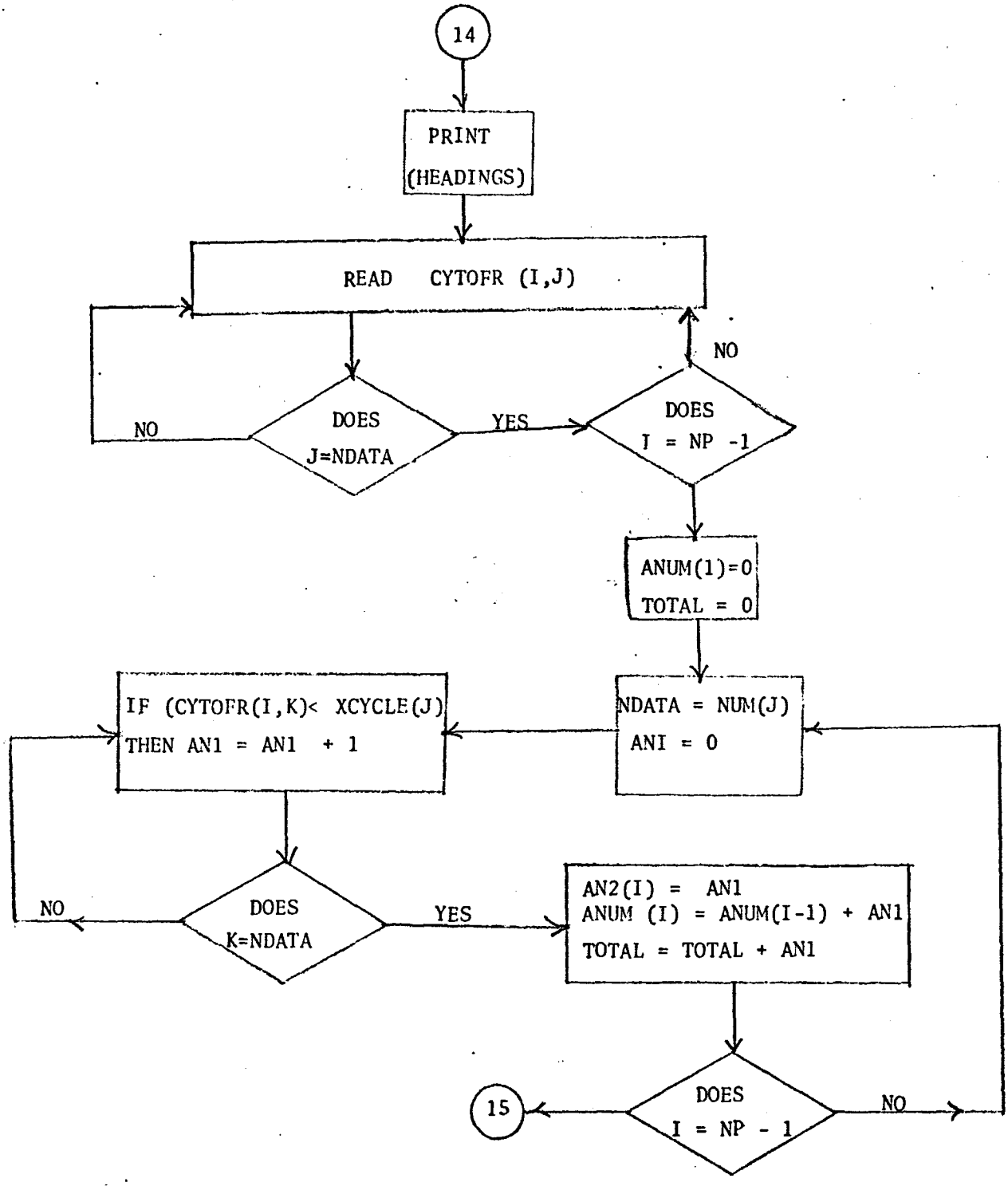

D-1. Flow Chart (Cont'd).

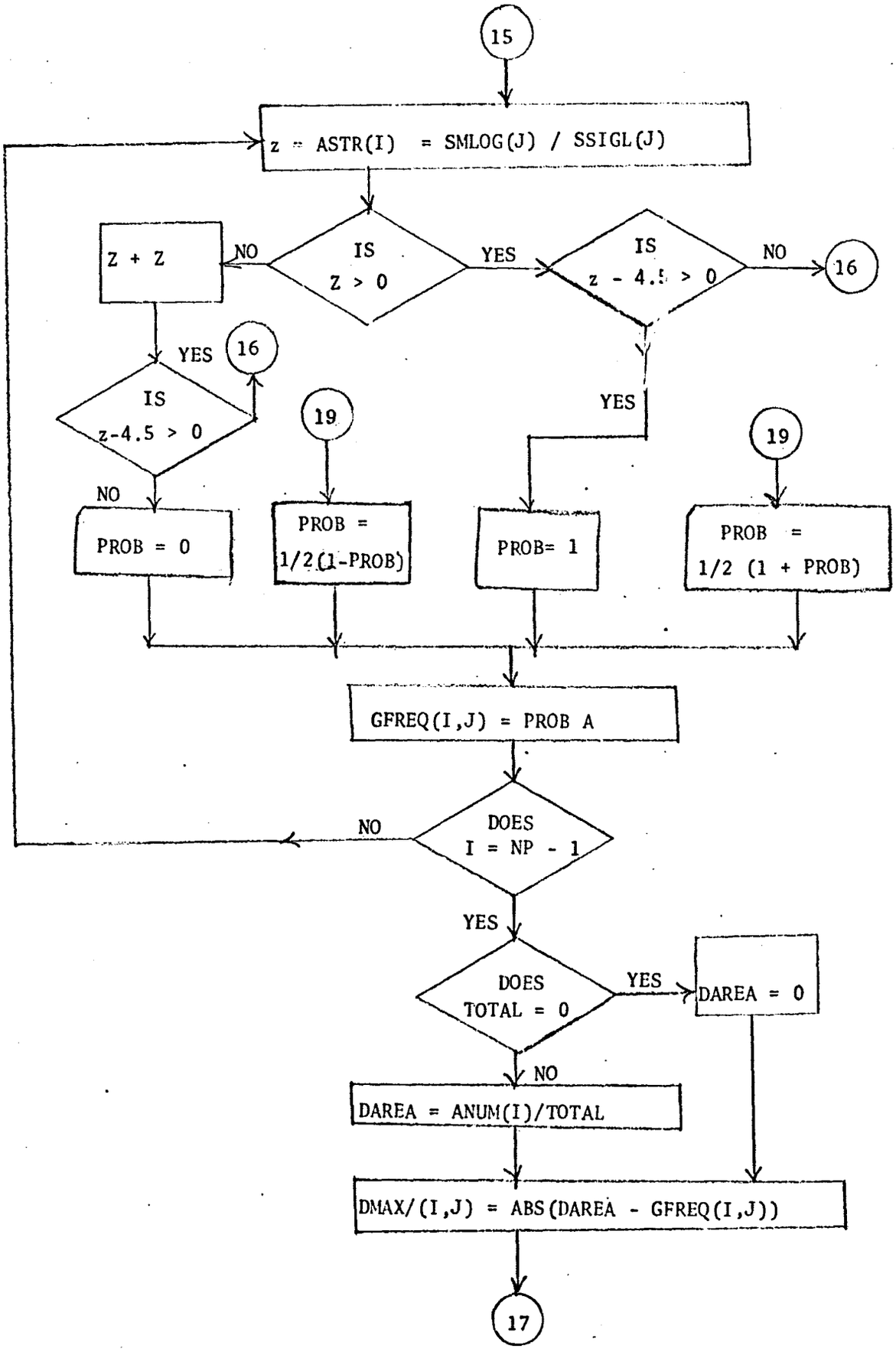

D-1. Flow Chart (Cont'd).

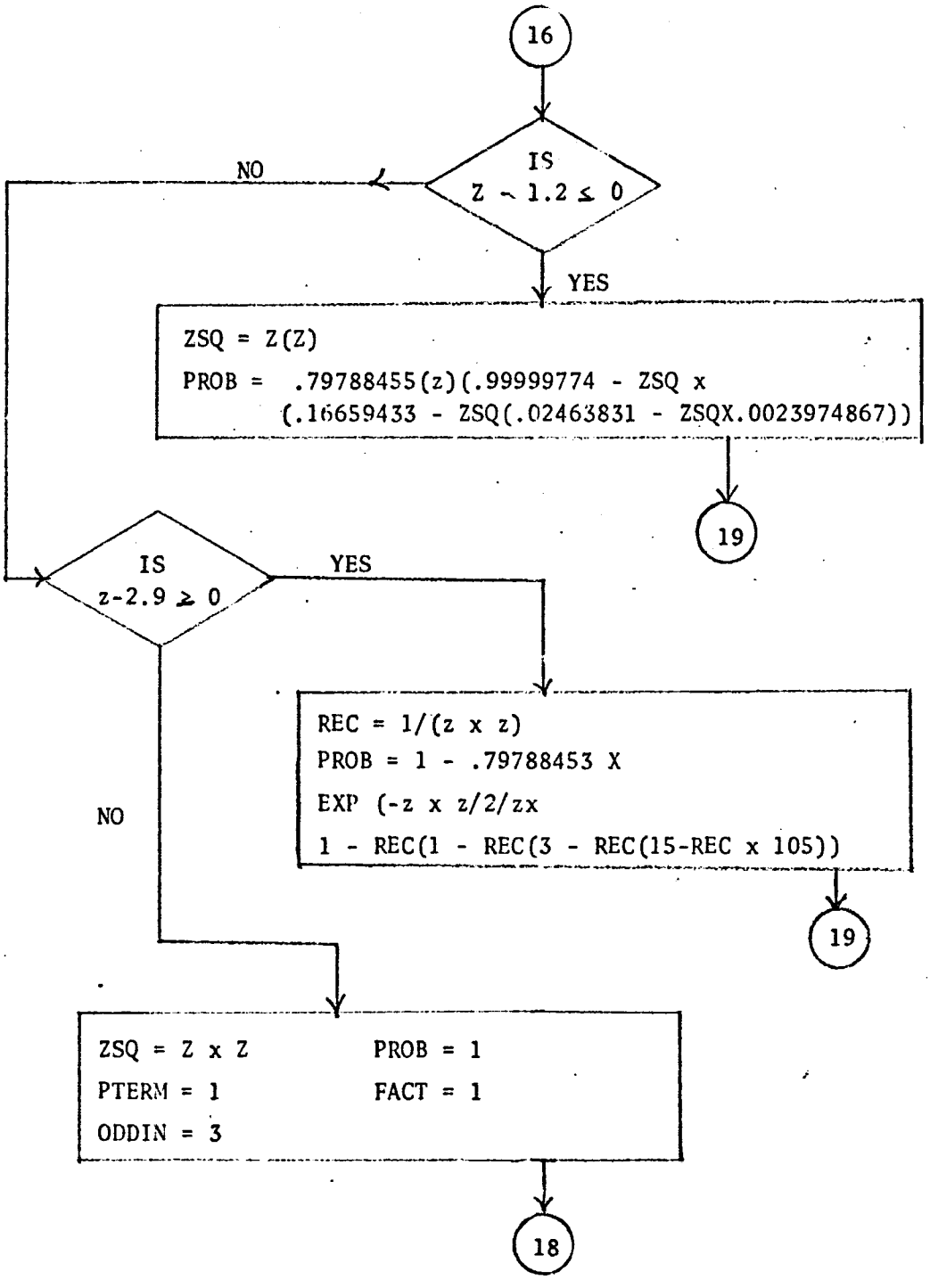

D-1. Flow Chart (Cont'd).

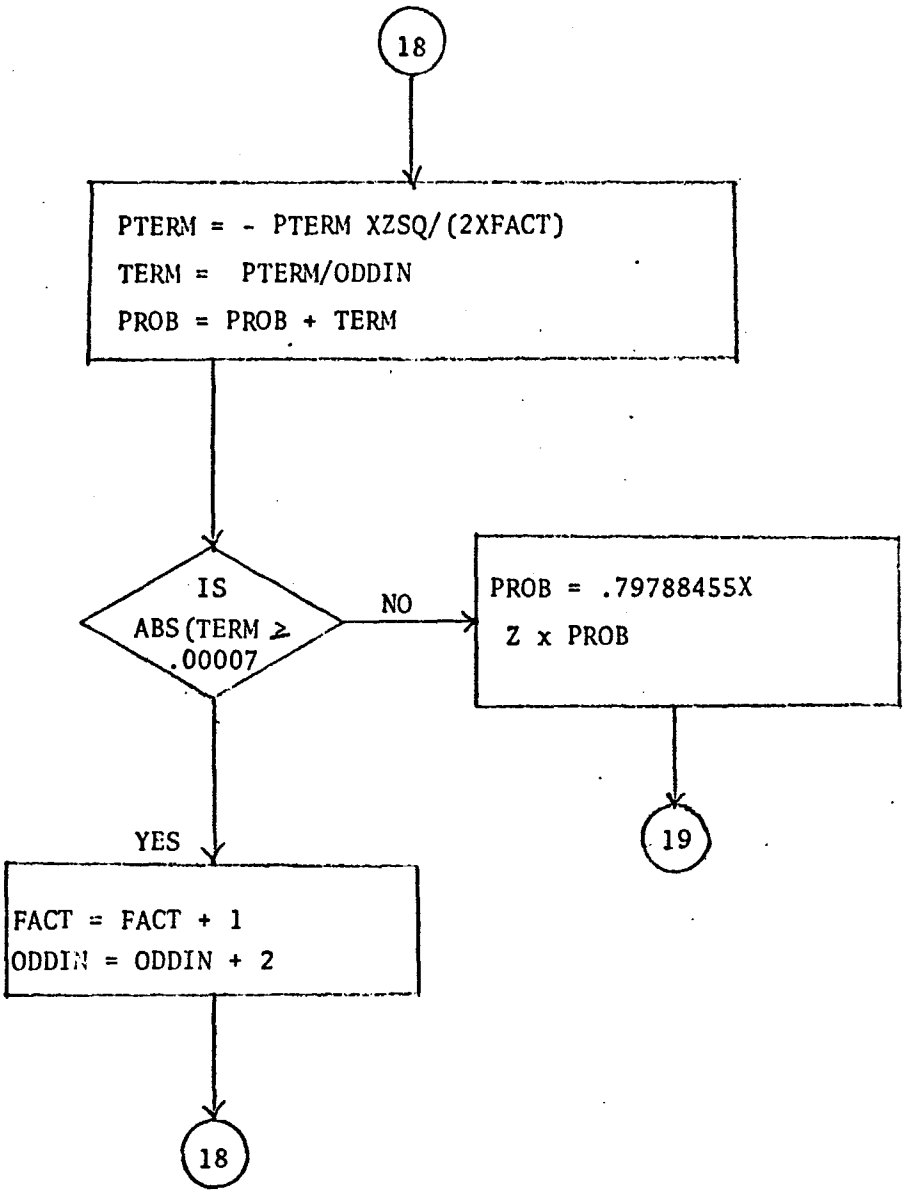

D-1. Flow Chart (Cont'd).

XJMIN = log cycles of extrapolated minimum value of M

XJMAX = log cycles of extrapolated maximum value of M

M = number of cycles (XCYCLES) of XJMIN

N = number of distributions to be used at a particular stress ratio

RATIO = stress ratio

ASTR = bending stress level in psi

AMLOG = log of bending stress level

NUM = number of cycles to failure inputs (ie. no. of XCYLCE)

XCYLCE = the actual number of cycle to failure

STINT = standard deviation of cycles to failure in log terms.

ACYCLE = number of cycles to failure or mean cycles

Interpolated stress values

- STR - ASTR
- CYCLE - ACYCLE
- XMLOG - AMLOG
- XSIGL - ASIGL

AREA (I,J) = cumulative are under log normal cycles to failure curve.

Parameters of Normal Stress Distribution at Specified Cycles-To-Failure.

- CYC = cycles in log value
- XCYCLE = cycles
- SMLOG = mean strength
- SSIGL = the standard deviation of the mean strength
- SIG3M = the minus three sigma limit
- SIG3P = the plus three sigma limit
- SK3 = the skewness value
- SK4 = the value of kurtosis

D-2. Definitions of Variables.

```
      PROGRAM STRENG (INPUT,OUTPUT,TAPE) =INPUT)
C-----PROGRAM FINDS NORMAL STRENGTH DISTRIBUTION FROM LOGNORMAL
C-----CYCLES-TO-FAILURE DISTRIBUTIONS.
0 0003      DIMENSION ASTR(10), AMLOG(10), ASIGL(10), SLAM(9),SIG3M(23),
     1   XMLOG(301), XSIGL(301), AREA(301,23), FREQ(301,23),SIG3P(23),
     2   CYC(23), SMLOG(23), SSIGL(23), SK3(23), SK4(23),CYTOFR(10,25),
     3 NUM(10),INDEX(10),OFREQ(10,23),GFREQ(10,23),DMAX(10,23),AN2(10)
     4  ,CHISQ(10,23),ST(10),SLSIG(9), EFREQ(10,23),INDEX2(10),ANUM(10)
     5,CYCLES(301),ACYCLE(25), STRLOG(10), STMEAN(23), XCYCLE(23)
0 0003      EQUIVALENCE (AREA,FREQ),
     1   (XSIGL,SSIGL), (XMLOG,OFREQ), (AREA(500),EFREQ),
     2   (AREA,CHISQ), (AREA(250),GFREQ)
0 0003      INI = 1
0 0004    5 READ10,XJMIN,XJMAX,SINT,M,N,RATIO
000024   10 FORMAT (2F10.6,F10.0,2I5,F10.5)
C       FAILURE DISTRIBUTION VALUES ARE READ IN FROM
C          LOWEST TO HIGHEST STRESS AND STRESSES ARE
C          INTEGER VALUES OF SINT
000024      IF (EOF,1) 510, 20
000027   20 READ 30, (ASTR(J),AMLOG(J),ASIGL(J),NUM(J), J=1,N)
000050   30 FORMAT (F10.0,2F10.6,I5)
000050      READ 36, (XCYCLE(J), J=1,M)
000063   36 FORMAT (8F10.0)
000063      DO 34 I=1,N
000065   34 ACYCLE(I)=EXP(AMLOG(I))
000074      NM1 = N-1
000075      L = 1
000076      INDEX(1) = 1
000077      DO 85 J=1,NM1
000101      DSTR = ASTR(J+1)-ASTR(J)
000103      DMEAN = AMLOG(J+1)-AMLOG(J)
000105      DSIG = ASIGL(J+1)-ASIGL(J)
000107      SLAM(J) = DSTR/DMEAN
000111      IF(DSIG) 40,50,40
000112   40 SLSIG(J) = DSTR/DSIG
000115   50 CONTINUE
000115      JP1 = J+1
000117      MX = DSTR/SINT
000122      INDEX(JP1) = L+MX
000124      SMIN = ASTR(1)
000126      XMLOG(1) = AMLOG(1)
000127      XSIGL(1) = ASIGL(1)
000131      DO 80 K=1,MX
000132      LX = L + K
000134      XMLOG(LX) = XMLOG(LX-1)+SINT/SLAM(J)
000140      IF(DSIG) 70,60,70
000141   60 XSIGL(LX) = XSIGL(LX-1)
000143      GO TO 80
000144   70 XSIGL(LX) = XSIGL(LX-1)+SINT/SLSIG(J)
000151   80 CONTINUE
000154      L = LX
000155   85 CONTINUE
000160      PRINT 87
000163   87 FORMAT(1H1///44X,   44HNORMAL STRENGTH DISTRIBUTIONS FROM LOGNORMA
     1L/49X,32HCYCLES TO FAILURE DISTRIBUTIONS.///)
000163      IF(RATIO.EQ.0.0) GO TO 91
000164      PRINT 89, RATIO
```

D-3. Computer Listing for Program STRENG.

```
0 0172   88    FORMAT (44X,17HEXPERIMENTAL DATA,8X,14HSTRESS RATIO =,F6.3//)
0 0172         GO TO 93
000173   91    PRINT 92
0 0177   92    FORMAT(44X,17HEXPERIMENTAL DATA,8X,23HSTRESS RATIO = INFINITY//)
0 0177   93    PRINT 94
0  03    94    FORMAT(8X,13HSTRENGTH PSI.,9X,32HMEAN-CYCLES      LOG MEAN-CYCLES,
        18X,11HLOG STD DEV/)
0 0203         NP = N-1
000205         PRINT 95, (ASTR(I), ACYCLE(I), AMLOG(I),ASIGL(I), I=2,NP)
000226   95    FORMAT(2F20.2,2F20.8)
0 0226         PRINT 96
0.0232   96    FORMAT(///54X,26HINTERPOLATED STRESS LEVELS//)
000232         PRINT 90
0 0235   90    FORMAT(8X,13HSTRENGTH PSI.,9X,32HMEAN-CYCLES      LOG MEAN-CYCLES,
        18X,11HLOG STD DEV,14X,10HINTEGER(I)/)
000236         XINT = INT
000240         STR = SMIN
0 0241         DO110 I=1,LX,INT
000243         CYCLES(I)=EXP(XMLOG(I))
000247         PRINT 100,STR,CYCLES(I),XMLOG(I), XSIGL(I),I
0 0265   100   FORMAT (2F20.2,2F20.8,120)
0 0265         STR = STR+SINT*XINT
000270     110 CONTINUE
0 0273         NOLD = N
0 0274         N = LX
         C     CONVERTING LOGNORMAL FAILURE DIST. PARAMETERS AT N
         C        STRESS LEVELS TO CUMMULATIVE LOGNORMAL FAILURE
         C        DISTRIBUTION
000275         DO 180 I=1,N
000276         DO 180 J=1,M
0  77          CYC(J) = ALOG(XCYCLE(J))
0 0303         Z= (CYC(J)-XMLOG(I))/XSIGL(I)
000307         IF(Z) 120,140,140
000310     120 IF(Z+4.5)160,130,130
0 0313     130 Z = -Z
000314         CALL NORMAL (Z,PROB)
000316         AREA(I,J) = (1.0-PROB)/2.0
0 0324         GO TO 180
0 0324     140 IF(Z-3.5) 150,150,170
000327   150   CALL NORMAL (Z,PROB)
0 0331         AREA(I,J) = PROB/2.0+0.5
0 0336         GO TO 180
000337     160 AREA(I,J) = 0.0
0 0343         GO TO 180
0 0343     170 AREA(I,J) = 1.0
000347   180   CONTINUE
000354         PRINT 225
0 0360         INT2 = INT*4
0 0362         STR = SMIN
000363         PRINT 185
0 0367   185   FORMAT(///46X,42HCUMULATIVE LOGNORMAL FAILURE DISTRIBUTIONS)
0 0367         DO 220 I=1,N,INT2
000371         PRINT 190,STR,XMLOG(I),XSIGL(I)
000402     190 FORMAT(1H0,5X,11HSTRENGTH = ,F10.0,5X, 9HLOG MEAN ,
           1    9HCYCLES = ,F9.6,5X,20HLOG STD DEVIATION = ,F9.6)
0  02          PRINT 200
00 06      200  FORMAT (1X, 33HDATA BELOW IS J, AND CUMMULATIVE ,
           )    13HDIST UP TO J.)
```

D-3. (Cont'd)

```
000406          PRINT 210, (J, AREA(I,J),J=1,M)
000424      210 FORMAT     ((1X,I3,F9.6,I3,F9.6,I3,F9.6,I3,F9.6,
               1  I3,F9.6,I3,F9.6,I3,F9.6,I3,F9.6,I3,F9.6))
000424          STR = STR+SINT*XINT*4.
000430      220 CONTINUE
000433          DO 222 J=1,NOLD
000434          I = INDEX(J)
000436          XNUM = NUM(J)
000437          DO 224 K=1,M
000441          OFREQ(J,K) = XNUM*AREA(I,K)
000451      224 CONTINUE
000454      222 CONTINUE
C             FREQUENCY DIST AND NORMAL DISTRIBUTION PARAMETERS
000456          XJMIN = XJMIN-XJINT
000460          PRINT 225
000464      225 FORMAT (1H1)
000464          PRINT 230
000470      230 FORMAT(///51X,33HCUMULATIVE STRENGTH DISTRIBUTIONS)
000470          DO 260 J=1,M
000472          XJ = J
000473          PRINT 240, J, CYC(J), XCYCLE(J)
000505      240 FORMAT (1H0,4HJ = ,I3 ,5X,13HLOG CYCLES = ,F9.6,
               15X,8HCYCLES =,F10.1)
000505          PRINT 250, (I,AREA(I,J),I=1,N,INT)
000523      250 FORMAT (2X,3H(I),1X,9HFREQUENCY/(1X,I4,F10.6,I5,F10.6
               1  ,I5,F10.6,I5,F10.6,I5,F10.6,I5,F10.6,I5,F10.6))
000523      260 CONTINUE
000526          NM1 = N-1
000530          DO 270 J=1,M
000531          DO 270 I=1,NM1
000532          IP1 = I+1
000534          FREQ(I,J) = AREA(IP1,J) -AREA(I,J)
000542      270 CONTINUE
000547          N = NM1
C             MEAN AND NORMAL DISTRIBUTION PARAMETERS OF HISTOGRAM
000551          DO 300 J=1,M
000552          FI = 0.
000553          FIUI = 0.
000554          UI = SMIN-SINT*0.5
000557          DO 280 I=1,N
000560          UI = UI+SINT
000562          FI = FI+FREQ(I,J)
000566          FIUI = FIUI+FREQ(I,J)*UI
000573      280 CONTINUE
000575          SMLOG(J) = FIUI/FI
000577          SMEAN(J) = ALOG(SMLOG(J))
000603          SM2 = 0.
000604          SM3 = 0.
000605          SM4 = 0.0
000606          UI = SMIN-SINT*0.5
000611          DO 290 I=1,N
000612          UI = UI+SINT
000614          SQ = (UI-SMLOG(J))*(UI-SMLOG(J))
000617          SM2 = SM2 + SQ*FREQ(I,J)
000624          SM3 = SM3 + FREQ(I,J)*(UI-SMLOG(J))*SQ
000632          SM4 = SM4+SQ*SQ*FREQ(I,J)
000637      290 CONTINUE
000642          SM2 = SM2/FI
```

D-3. (Cont'd)

```
000643          SM3 = SM3/FI
000644          SM4 = SM4/FI
000645          SSIGL(J) = SQRTF(SM2)
000651          SIG3P(J) = SMLOG(J) + 3.0*SSIGL(J)
000655          SIG3M(J) = SMLOG(J) - 3.0*SSIGL(J)
000660          SK3(J) = SM3/(SSIGL(J)*SM2)
000663          SK4(J) = SM4/(SM2*SM2)
000665      300 CONTINUE
000670          PRINT 225
000673          PRINT 305
000677    305   FORMAT(///30X,73HPARAMETERS OF NORMAL STRESS DISTRIBUTIONS AT SPEC
                1IFIED CYCLES TO FAILURE.//)
000677          PRINT 310
000703    310   FORMAT (83X,20H-3 SIGMA     +3 SIGMA  /3X,20HNUMBER    LOG CYCLES ,
                1 6X,6HCYCLES,10X,13HMEAN STRENGTH,10X,9HSTD. DEV.,7X,5HLIMIT  ,
                2 7X,34HLIMIT        SKEWNESS     KURTOSIS  /)
000703          PRINT 320, (J,CYC(J),XCYCLE(J),SMLOG(J), SSIGL(J),
                1 SIG3M(J),SIG3P(J),SK3(J),SK4(J), J =1,M)
000735    320   FORMAT (4X,I3,F16.6,F13.0,2F20.0,F15.0,F12.0,2F12.4)
000735          PRINT 225
000741          PRINT 322
000745    322   FORMAT (1H0)
                C-----ROUTINE FOR KOLMOGOROV-SMIRNOV GOODNESS OF FIT TEST
000745          PRINT 325
000751    325   FORMAT (//41X,52HD-VALUES FOR KOLMOGOROV-SMIRNOV GOODNESS OF FIT T
                1EST  /)
000751          DO 600 I=2,NP
000753          NDATA = NUM(I)
000755          READ 605,(CYCFR(I,J),J=1,NDATA)
000770    605   FORMAT (8F10.0)
000770    600   CONTINUE
000773          DO 500 J=1,M
000774          ANUM(1) = 0.0
000775          TOTAL = 0.0
000776          DO 665 I=2,NP
000777          NDATA = NUM(I)
001001          AN1 = 0.0
001002          DO 660 K = 1,NDATA
001003          IF (CYCFR(I,K).LE.XCYCLE(J))  AN1 = AN1 + 1.0
001012    660   CONTINUE
001015          AN2(I) = AN1
001017          ANUM(I) = ANUM(I-1) + AN1
001021          TOTAL = TOTAL + AN1
001022    665   CONTINUE
001024          DO 480 I=2,NP
001026          Z =(ASTR(I) -SMLOG(J))/SSIGL(J)
001032          IF(Z) 330,350,350
001033      330 Z = -Z
001034          IF(Z-4.5) 340,360,360
001037      340 CALL NORMAL (Z,PROB)
001041          PROBA = 0.5-PROB*0.5
001044          GO TO 370
001044    350   IF(Z-4.5)355,365,365
001047      355 CALL NORMAL (Z,PROB)
001051          PROBA = PROB*0.5+0.5
001054          GO TO 370
001054      360 PROBA = 0.0
001055          GO TO 370
```

D-3. (Cont'd)

```
001056      365 PROBA = 1.0
001060    370   GFREQ(I,J)=PROBA                                          234
001064          IF (TOTAL.EQ.0.0) GO TO 375
001065          DAREA = ANUM1(I)/TOTAL
001067          GO TO 380
001067    375   DAREA = 0.0
001070    380   DMAX(I,J) = ABS(DAREA-GFREQ(I,J))
001101    480   CONTINUE
001103          PRINT 490, XCYCLE(J),  TOTAL,(AN2(I),DMAX(I,J), I=2,NP)
001125    490   FORMAT (6X,F8.0,21H CYCLES     TOTAL N =,F3.0/(9(F9.0,F6.3)))
001125          PRINT 322
001131    500   CONTINUE
001134          GO TO 5
001134    510   STOP
001136          END
```

D-3. (Cont'd)

```
      SUBROUTINE NORMAL(Z,PROB)
C     PROB = THE AREA UNDER NORMAL DISTRIBUTION BETWEEN
C        PLUS AND MINUS Z STANDARD DEVIATIONS
      IF(Z-1.2) 1000,1000,1010
 1000 ZSQ = Z*Z
      PROB = 0.79788455*Z*(0.99999774-ZSQ*(0.16659433
     1  -ZSQ*(0.024638319 - ZSQ*0.0023974867)))
      GO TO 1070
 1010 IF(Z-2.9) 1020,1060,1060
 1020 ZSQ = Z*Z
      PROB = 1.0
      PTERM = 1.0
      FACT = 1.0
      ODDIN = 3.0
 1030 PTERM = -PTERM*ZSQ/(2.0*FACT)
      TERM = PTERM/ODDIN
      PROB = PROB + TERM
      IF ( ABS(TERM) - 0.00007) 1050,1040,1040
 1040 FACT = FACT + 1.0
      ODDIN = ODDIN + 2.0
      GO TO 1030
 1050 PROB = 0.79788455*Z*PROB
      GO TO 1070
 1060 REC = 1./(Z*Z)
      PROB = 1.-0.79788453*  EXP(-Z*Z/2.0)/Z*
     1    (1. - REC*(1. - REC*(3. - REC*(15.-REC*105.))))
 1070 CONTINUE
      RETURN
      END
```

D-3. (Cont'd)

APPENDIX E

Listing of Short PDP-8 Programs

```
01.10 A "SH" S, "SA" SA; S SM=FSQT(3)*S

02.10 S C=FSQT(SA↑2+SM↑2); T %8.1,"C" C, "SM" SM, !
02.20 GT1.1
*
*
*
```

where: SH = shear stress

SA = alternating stress

SM = mean stress

C = resultant stress vector magnitude S_r

E-1. Listing of PDP- 8 Program BAR I.

```
*E A
*W A
C-8K MODV 11-219
*01.10 A "SH" S, "SA" SA; S SM=2*S
*02.10 S C=FSQT(SA↑2+SM↑2); T %8.1, "C" C, "SM" SM, !
*02.20 GT1.1
*GO
```

where: SH = shear stress

SA = alternating stress

SM = mean stress

C = resultant stress vector magnitude S_r

E-2. Listing of PDP-8 Program Bar II.

```
*
*C-8K MODV 11-219
*
*01.10 a "R" R, "S" S; S SR=S/PSIN  FATN(R)
*
*02.10 T %8.2 "ROTATED THREE SIGMA" SR, !
*02.20 GT 1.10
**/
*
*
*
```

Where R = Stress Ratio

S = Vertical Strength Distribution's Upper and Lower Three Sigma Limits.

SR = Transformed Strength Distribution's Upper and Lower Three Sigma Limits.

E-3. Listing of PDP-8 Prgram ROTO.

```
C-FOCAL,1969

0.10 A "A" A, "B" B, "D" D, "E" E, "N" N
0.20 S XA=A/E
01.21 S XB=B/N
01.23 S YA=D↑2-A↑2
01.24 S YB=D↑2-B↑2

02.10 S E=XA↑2*YA+XB↑2*YB
02.11 S J=XA↑4+XB↑4
02.13 S K=E/J

0.10 S SU=FSQT(D↑2/K); T "SU" SU!
```

Definition of Variables

$$A = Sa_1 = y_1$$

$$B = Sa_2 = y_2$$

$$D = Sn$$

$$ya = Sm_1 = x_1$$

$$yb = Sm_2 = x_2$$

$$E = r_1$$

$$N = r_2$$

E-4. PDP-8 Program for Least Squares Estimator of the Ultimate Strength for Fatigue Data of Chapter IV.

```
*C-FOCAL,1969

*01.10 a "A" A, "B" B, "C" C, "D" D
*01.20 S XA=A/3.5
*01.21 S XB=B/.825
*01.22 S XC=C/.44
*01.23 S YA=D↑2-A↑2
*01.24 S YB=D↑2-B↑2
*01.25 S YC=D↑2-C↑2
*
*02.10 S E=XA↑2*YA+XB↑2*YB+XC↑2*YC
*02.11 S J=XA↑4+XB↑4+XC↑4
*02.13 S K=E/J
*
*03.10 S SU=FSQT(D↑2/K); T "SU" SU!
```

Definition of Variables

$$A = Sa_1 = y_1$$

$$B = Sa_2 = y_2$$

$$C = Sa_3 = y_3$$

$$xa = Sm_1 = x_1$$

$$xB = Sm_2 = x_2$$

$$xC = Sm_3 = x_3$$

E-5. PDP-8 Program for Least Squares Estimator of the Ultimate Strength for Fatigue Data (LSEFD) of Chapter V.

```
*
*C-8K MODV 11-219
*
*01.10 a "SA" S, "SE" W; S SM-255300*FSQT(1-<S/W> ↑ 2)
*01.20 T %8.2 "MEAN STRESS" SM, !
*01.30 GT 1.10
** GO
```

E-6. Listing of PDP-8 Program Which Calculated Mean Stress Specified by the Von Mises-Hencky Ellipse

```
C-8K MODV 11-219

02.05 A "NO. OF DATA POINTS ",ND,!,!
02.10 T "  X - AXIS     Y _ AXIS",!
02.20 S XS=0
02.21 S XQ=0
02.22 S YS=0
02.23 S YQ=0
02.24 S XY=0
02.40 FOR I=1,1,ND; DO 3.0
02.49 S D=(ND*XQ-XS*XS)
02.50 S A0=(YS*XQ-XS*XY)/D
02.60 S A1=(ND*XY-XS*YS)/D
02.70 S DN=FSQT(D*(ND*YQ-YS*YS))
02.75 S R=(ND*XY-XS*YS)/DN
02.80 T %8.05 !, "SLOPE ",A1,"    Y INTERCEPT ",A0,!,!
02.90 T %6.04 "CORRELATION COEFFICIENT ",R,!
02.95 Q

03.10 A "    ",X(I),"     ",Y(I),!
03.15 S XS=XS+X(I)
03.18 S XQ=XQ+X(I)*X(I)
03.20 S YS=YS+Y(I)
03.24 S YQ=YQ+Y(I)*Y(I)
03.26 S XY=XY+X(I)*Y(I)
*GO
```

E-7. Listing of PDP-8 Program which Calculates Slope of Best Fit Equation (10.5).

LIST OF REFERENCES

1. A Guide for Fatigue Testing and the Statistical Analysis of Fatigue Data, Second edition ASTM Special Technical Publication No. 19-A, 1963, 83 pp.

2. Smith, Richard E., "Time Dependent Reliability of Components Subjected to Simple Fatigue", The University of Arizona, Tucson Arizona, 1965, 150 pp.

3. Kececioglu, Dimitri, and Smith, John L., "Statistical Complex Fatigue Data for SAE 4340 Steel, and Its Use in Design by Reliability", The University of Arizona, NASA CR-72835, 175 pp., (1970).

4. Kececioglu, Dimitri, and Broome, H. Wilson, "Probabilistic-Graphical Phenomenological Analysis of Combined Bending-Torsion Fatigue Reliability Data", The University of Arizona, NASA CR-72839, 79 pp., (1969).

5. Mood, A.M., and Graybill, F. A., Introduction to the Theory of Statistics, New York, McGraw-Hill Book Company, 1963, Second edition, 443 pp.

6. Von Vlock, Lawrence H., Elements of Material Science, Addison-Wesley Publishing Company, Palo Alto, 1967, 455 pp.

7. Manson, S. S., Thermal Stress and Low Cycle Fatigue, San Francisco, McGraw-Hill Book Company, 1966, 404 pp.

8. Simplified Pre-PDR Technique for Assessing Component Reliability, NERVA, 1970, Document R101-NRP-403. 58 pp.

9. Graybill, Franklin, An Introduction to Linear Statistical Models, Volume I, New York, McGraw-Hill Book Company, 1961, 462 pp.

10. Hritz, John A. "Re-definition of Endurance Life Design Criteria by Statistical Methods", The University of Arizona, Tucson, Arizona, 1969, 85 pp.

11. Dvorak, Roy F., "Analytic and Experimental Definition of the Goodman Envelope and Mean Locus Value for SAE 4130 Steel", The University of Arizona, Tucson, Arizona, 1970, 54 pp.

12. Findley, W. N., "Combined Stress Fatigue of 76S-T61 Alluminum Alloy with Superimposed Mean Stresses and Correction for Yielding", NACA, No. 2924, (1953), 65 pp.

LIST OF REFERENCES (Continued).

13. O'Donnell, W. J., "Strength Criteria for Selected Failure Modes", Pre-PDR Technique for Assessing Component Reliability, NERVA, 1970, 36 pp.

14. Findley, W. N., and Mathur, P. N., "Modified Theories of Fatigue Failure Under Combined Stress", Technical Report No. 5 to Office of Ordiance Corp Department of the Army. on Contract No. DA-11-022-ORD-995, Urbana, Illinois, 1954, 26 pp.

15. Shigley, J. E., Mechanical Engineering Design, San Francisco, McGraw-Hill Book Company, 1963, 631 pp.

16. Haugen, Edward B., Probabilistic Approaches to Design, New York, John Wiley and Sons, 1968, 323 pp.

DISTRIBUTION LIST

NASA Lewis Research Center (3)
Program Manager
21000 Brookpark Road
Cleveland, Ohio 44135
Attention: V. P. Lalli, M.S. 54-1

NASA Lewis Research Center (1)
Procurement Manager
21000 Brookpark Road
Cleveland, Ohio 44135
Attention: F. H. Stickney, M.S. 500-203

NASA Lewis Research Center (1)
Patent Counsel
21000 Brookpark Road
Cleveland, Ohio 44135
Attention: Norman T. Musial, M.S. 500-311

NASA Scientific and Technical (3)
Information Facility
NASA Headquarters
Box 5700
Bethesda, Md. [illegible]
Attention: NASA Representative

NASA Lewis Research Center (2)
Lewis Library
21000 Brookpark Road
Cleveland, Ohio 44135
Attention: Library

NASA Lewis Research Center (1)
Lewis Technical Information
Division
21000 Brookpark Road
Cleveland, Ohio 44135
Attention: Report Control Office

U. S. Atomic Energy Commission (1)
Technical Reports Library
Washington, D. C. 20545

U. S. Atomic Energy Commission (3)
Technical Information Service
Extension
P. O. Box 62
Oak Ridge, Tenn. 37830

DISTRIBUTION LIST CONTINUED

National Aeronautics and Space Administration (3)
NASA Headquarters Program Office
Washington, D. C. 20546
Attention: KR/D. E. Negola
RNP/F. Scholman
Y/F. B. Smith Forward to

NASA Lewis Research Center (2)
Lewis Research Center Staff Members
21000 Brookpark Road
Cleveland, Ohio 44135
Attention: C. R. Ensign, M.S. 49-1
J. P. Gyekenyesi, M.S. 21-4

NASA Lewis Research Center (1)
Lewis Office of Reliability and Quality Control
21000 Brookpark Road
Cleveland, Ohio 44135
Attention: S. M. Perrone, M.S. 500-111

NASA Ames Research Center (1)
Ames Research Center
Moffett Field, California 94035
Attention: Library

NASA Flight Research Center (1)
Flight Research Center
P. O. Box 273
Edwards, California 93523
Attention: Library

NASA Goddard Space Flight Center (1)
Goddard Space Flight Center
Greenbelt, Md. 20771
Attention: Library

Jet Propulsion Laboratory (1)
4800 Oak Groove Dr.
Pasadena, California 91103
Attention: Library

NASA Langley Research Center (1)
Langley Station
Hampton, Va. 23365
Attention: Library

DISTRIBUTION LIST CONTINUED

NASA Manned Spacecraft Center (1)
Houston, Texas 77001
Attention: Library

NASA Marshall Space Flight Center (1)
Huntsville, Ala. 35812
Attention: Library

NASA Western Operations (1)
150 Pico Blvd.
Santa Monica, Califorina 90406
Attention: Library